JGR Solid Earth

RESEARCH ARTICLE
10.1029/2018JB017199

# Jurassic Monster Polar Shift Confirmed by Sequential Paleopoles From Adria, Promontory of Africa

**G. Muttoni[1] and D.V. Kent[2,3]**

[1]Dipartimento di Scienze della Terra 'Ardito Desio', Università degli Studi di Milano, Milan, Italy, [2]Earth and Planetary Sciences, Rutgers University, Piscataway, NJ, USA, [3]Lamont-Doherty Earth Observatory, Columbia University, Palisades, NY, USA

**Key Points:**
- We review the status of the Jurassic apparent polar wander path, which has long been controversial
- We show with new data that the widely used paleomagnetic poles from the Morrison Formation of the Colorado Plateau are overprinted
- We provide paleomagnetic poles from Adria, promontory of Africa, that confirm the Jurassic monster shift, a major candidate for true polar wander

**Supporting Information:**
- Supporting Information S1

**Correspondence to:**
G. Muttoni,
giovanni.muttoni1@unimi.it

**Citation:**
Muttoni, G., & Kent, D. V. (2019). Jurassic monster polar shift confirmed by sequential paleopoles from Adria, promontory of Africa. *Journal of Geophysical Research: Solid Earth*, *124*. https://doi.org/10.1029/2018JB017199

Received 19 DEC 2018
Accepted 4 MAR 2019
Accepted article online 7 MAR 2019



**Abstract** Jurassic paleomagnetic data from North America have long been contentious, generating ambiguities in the shape of the global-composite apparent polar wander path. Here we show from a restudy of two subdivisions of the Late Jurassic Morrison Formation at the classic locality at Norwood on the Colorado Plateau that the derived paleopoles reflect variable overprinting probably in the Cretaceous and are of limited value for apparent polar wander determination. We instead assembled an updated set of Jurassic paleopoles from parauthocthonous Adria, the African promontory, using primary paleomagnetic component directions derived from stratigraphically superposed intervals and corrected for sedimentary inclination error. These paleopoles are found to be in superb agreement with independent igneous paleopoles from the literature across the so-called Jurassic monster polar shift, which in North American coordinates is a jump of ~30° arc distance from the 190- to 160-Ma stillstand pole at 79.5°N 104.8°E to a 148 ± 3.5-Ma pole at 60.8°N 200.6°E defined by four Adria sedimentary paleopoles and the published Ithaca, Hinlopenstretet, and Swartsruggens-Bumbeni igneous paleopoles. The implied high rate of polar motion of ~2.5°/Myr across the monster shift is compatible with maximum theoretical estimates for true polar wander. We include a critique of published Jurassic paleomagnetic data that have been variably used in reference APWPs but that as a result of their low quality muted the real magnitude of the Jurassic monster shift. Finally, we provide paleocontinental reconstructions to describe examples of the bold signature that the monster polar shift left in the distribution of climate-sensitive sedimentary facies worldwide.

## 1. Introduction and Historical Perspective on Jurassic Polar Wander

The Jurassic apparent polar wander path (APWP) has long been controversial (Courtillot et al., 1994; Hagstrum, 1993; Kent & Irving, 2010), introducing critical uncertainties in the paleogeography of the major continents and relative movements of tectonic terranes. Here we first present a brief updated historical overview of data used in reference APWPs and describe a desultory restudy of the Late Jurassic Morrison Formation (Fm.), a prominent source of Late Jurassic data for North America. We follow with an analysis of data from Adria, the promontory of Africa (Channell, 1996), and make the case that these independent data strongly bolster a new course in the understanding of Jurassic polar wander.

The late Paleozoic through Cenozoic APWP for North America of Irving and Irving (1982), obtained using a sliding window average of 30-Myr duration that was incremented in 10-Myr steps (Figure 1), was erected for the Jurassic (nominally 200 to 140 Ma) on 10 paleo poles (henceforth referred to simply as poles) screened for minimum reliability, including three poles from sedimentary rocks on the Colorado Plateau (lower and upper Morrison Fm.; Steiner & Helsley, 1975; and the Summerville Fm.; Steiner, 1978). May and Butler (1986) subsequently applied the less agnostic paleomagnetic Euler pole (PEP) analysis technique (Gordon et al., 1984) and fit a small-circle track to seven poles comprised between an Early Jurassic cusp (J1), represented by the Wingate Fm. pole (cited by Gordon et al., 1984 from a PhD thesis by Reeve, 1975), and a Late Jurassic cusp (J2), represented by the lower Morrison pole (Steiner & Helsley, 1975; Figure 1). This J1-J2 segment was followed by a barely constrained Late Jurassic-Cretaceous small-circle track from the lower Morrison (J2 cusp) through the upper Morrison pole of Steiner and Helsley (1975) and to an average Cretaceous stillstand pole (KA). A total of six Jurassic poles, including those from the lower and upper Morrison Fm. in common with Irving and Irving (1982), was from the Colorado Plateau and adjusted by May and Butler (1986) for its tectonic rotation (although not by Irving & Irving, 1982).

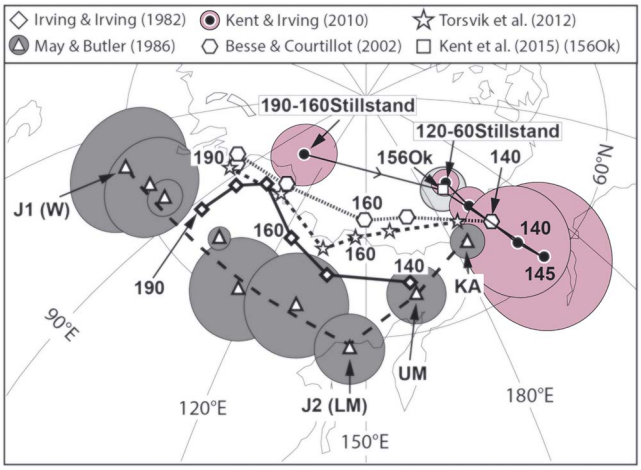


**Figure 1.** Comparison of some published reference APWPs in North American coordinates straddling the Jurassic-Cretaceous. For the *May and Butler* (1986) APWP, poles J1(W), J2(LM), UM, and KA, are, respectively, the J1 (Wingate) cusp pole, the J2 (lower Morrison) cusp pole, the upper Morrison pole, and the Cretaceous average pole; the lower and upper Morrison poles are those of Steiner and Helsley (1975) corrected for 3.8° clockwise rotation of the Colorado Plateau (as for other poles from the Colorado Plateau used in May & Butler, 1986). The Kent and Irving (2010) APWP occupies the northernmost latitudes over Siberia in the Early Jurassic (190- to 160-Ma Stillstand pole) and shows a prominent polar shift through the Ontario kimberlites pole (156Ok; Kent et al., 2015) and ending in a cusp over western Alaska at 145 Ma, in turn followed by a return shift to the Cretaceous 120- to 60-Ma Stillstand pole. See text for discussion.

Seemingly small differences between the Jurassic APWPs for North America of Irving and Irving (1982) and May and Butler (1986) had important tectonic consequences. For example, because the Jurassic APWP of May and Butler (1986) placed North America at lower latitudes than the APWP of Irving and Irving (1982), this had the effect of decreasing sometimes to statistical insignificance estimates of latitudinal displacement of Cordilleran terranes (Irving & Wynne, 1990).

Following the pioneering methodology introduced by Phillips and Forsyth (1972), Besse and Courtillot (1991) compiled data from all major continents into a master global-composite APWP using established independent plate reconstructions for 200 Ma to Present. In the critical 170- to 140-Ma time interval, their updated (Besse & Courtillot, 2002) global-composite APWP (Figure 1) is dominated by data from sediments from central Europe (eight entries from 142 to 168 Ma from France, Switzerland, Poland: Aubourg & Rochette, 1992; Gehring et al., 1991; Gose & Kyle, 1993; Heller, 1977, 1978; Johnson et al., 1984; Kądziałko-Hofmokl & Kruczyk, 1987; Kruczyk & Kądziałko-Hofmokl, 1988); see discussion below in section 4 and in supporting information S1). Although used in the earlier version of their APWP (Besse & Courtillot, 1991), neither data from the Colorado Plateau (e.g., Morrison Fm.) nor data more generally used by *May and Butler* (1986) in their PEP analysis were adopted in their updated version (Besse & Courtillot, 2002). The resulting 170- to 140-Ma portion of the Besse and Courtillot (2002) APWP in North American coordinates was found to lie somewhat to the north of the Irving and Irving (1982) and May and Butler (1986) APWPs (Figure 1).

Paleomagnetic directions in igneous rocks with known paleohorizontal can generally record the field in which they were acquired more accurately than sedimentary rocks, which are prone to have inclinations shallower than the ambient field. This is inclination error: *I* error, which has become much more widely recognized in sedimentary rocks using the elongation/inclination (*E*/*I*) statistical method (Tauxe & Kent, 2004). Accordingly, Kent and Irving (2010) constructed a global-composite APWP using poles from all major continents preferentially from reasonably well-dated igneous rocks and only those sedimentary units corrected directly for *I* error using the *E*/*I* method of Tauxe and Kent (2004). Jurassic sedimentary data from central Europe and from the Colorado Plateau, including the lower and upper Morrison poles of Steiner and Helsley (1975), were thus not included in the final pole compilation.

The scenario thus obtained by Kent and Irving (2010) for the Jurassic is characterized by a high-latitude stillstand of poles in North American coordinates over northern Siberia from 190 to 160 Ma (Figure 1). This implies that the North American continent was steady relative to lines of latitude and did not experience significant rotation relative to meridians. For example, averaging items #42–53 in Table 5 of Kent and Irving (2010) results in a well grouped 190- to 160-Ma mean pole at 79.5°N, 104.8°E, A95 = 4.0° (Table 1, entry #1; Figure 1). This 190- to 160-Ma stillstand pole would not substantially change upon exclusion of item #45 of Kent and Irving (2010), the 169-Ma Moat Volcanics pole (Van Fossen & Kent, 1990), which according to a recent U-Pb zircon dating study of some White Mountain plutonic rocks (Amidon et al., 2016), could be somewhat older than originally assumed.

This 190- to 160-Ma stillstand is followed by a prominent jump termed the Jurassic monster polar shift to a well-grouped mean pole at 145 Ma that falls off western Alaska (Figure 1). The jump is partially captured by the intermediate 156.1 ± 1.6 Ma Ontario kimberlites pole 156Ok of Kent et al. (2015) based on averaging data from the Peddie kimberlite and Triple B kimberlite with high-precision U-Pb perovskite dates of 154.9 ± 1.1 and 157.5 ± 1.2 Ma, respectively (Table 1, entry #2; Figure 1). Kent et al. (2015) regarded the stable remanent magnetization retrieved in these kimberlites as a thermochemical magnetization associated with late stage magmatic crystallization of magnetite or magnetite growth during deuteric serpentinization, and in conjunction with the observation that this magnetite carries magnetic component directions of opposite polarity acquired at distinctly different times, they suggested that the process of magnetization acquisition

**Table 1**
*Paleomagnetic Poles Relevant to Jurassic Monster Shift From Adria and Elsewhere*

| Item#, pole name and Chron | | Age (Ma/relative) | N/n | f | Long NW Africa | Lat NW Africa | A95 α95 | K k | Long N America | Lat N America | R |
|---|---|---|---|---|---|---|---|---|---|---|---|
| (1) | 190–160Stillstand | 190–160 | 12 | n. a. | | | 4.0 | 122 | 104.8 | 79.5 | |
| (2) | 156Ok | 154.9 ± 1.1 and 157.5 ± 1.2 | 2/34 | n. a. | | | 2.8 | | 189.5 | 75.5 | |
| (3) | 145K&I (mean of (4)–(6)) | 145 ± 2 | 3 | n. a. | | | 9.0 | 189 | 200.2 | 61.2 | |
| (4) | 146Ik | 146.4 ± 1.4 | 7 | n. a. | | | 3.8 | | 203.1 | 58.0 | |
| (5) | 145SB | 145.0 ± 0.4 and 145.8 ± 1.3 | 6 | n. a. | | | 6.3 | | 209.6 | 63.1 | |
| (6) | 144Hi | 144 ± 5 | 17 | n. a. | | | 7.5 | | 188.0 | 61.5 | |
| (7) | 120–60Stillstand | 120–60 | 4 | n. a. | | | 1.7 | 2938 | 192.8 | 75.9 | |
| (8) | 238Dol | 238 ± 3/Ladinian-Carnian | 4 | 0.6–0.9 | 213.0 | 59.4 | 10.3 | 81 | 98.4 | 53.9 | a |
| (9) | 158Bomb pre-CM30 | ~158/Callovian | 1/54 | 0.7 | 266.5 | 56.8 | 4.3 | 21 | 164.7 | 77.5 | b |
| (10) | 158Foz pre-CM30 | ~158/Callovian | 1/100 | 0.6 | 254.9 | 64.8 | 3.7 | 16 | 119.7 | 76.8 | b |
| (11) | 154Vig CM25–CM30 | 154 ± 2/Oxfordian | 1/74 | 0.8 | 267.5 | 38.1 | 2.9 | 33 | 195.8 | 60.9 | c |
| (12) | 150Branch CM22–CM25 | 150 ± 3/Kimmeridgian | 1/54 | 0.7 | 275.1 | 34.7 | 3.5 | 32 | 209.0 | 58.7 | c |
| (13) | 150Sci CM22–CM25 | 150 ± 3/Kimmeridgian | 1/45 | 0.9 | 270.3 | 38.5 | 3.4 | 41 | 200.0 | 61.8 | c |
| (14) | 147VFF CM22 | 147 ± 1/Early Tithonian | 3 | 1.0 | 265.4 | 37.6 | 4.1 | 895 | 198.1 | 60.3 | d |
| (15) | 150Adria (mean of (11)–(14)) | 150 ± 6 | 4 | | 269.6 | 37.3 | 4.3 | 459 | 200.9 | 60.5 | |
| (16) | 143BVFF CM17–CM21 | 143 ± 3/Mid Tithon.–Berrias. | 6 | 0.8–1.0 | 263.5 | 45.3 | 3.1 | 463 | 190.4 | 67.4 | d |
| (17) | 128Mai CM1–CM11 | 128 ± 7/Hauteriv.-Barrem. | 5 | 0.6–0.9 | 260.0 | 51.2 | 9.2 | 70 | 190.4 | 71.3 | e |
| (18) | 50Sca C17–C29 | 50 ± 15/Paleocene–Eocene | 3 | 0.4–0.6 | 210.1 | 74.5 | 3.7 | 1113 | 181.5 | 75.8 | f |
| (19) | 148Cusp (mean of (4)–(6) and (11)–(14)) | 148 ± 3.5/Oxfordian-Tithonian | 7 | | | | 3.1 | 392 | 200.6 | | |

*Note*. Chron = chron attribution of mean pole; age = numerical (Ma) and/or relative age of mean pole; $N$ = number of independent poles used to calculate the mean pole; if $N = 1$ and $N = 2$, the mean pole is calculated on the $n$ paleomagnetic directions; f = flattening factor calculated using the elongation/inclination ($E/I$) statistical method of Tauxe and Kent (2004) using software of Tauxe et al. (2016); n. a. = flattening correction not applicable); Long, Lat NW Africa = longitude (°E) and latitude (°N) of mean pole in Northwest African (Adria) coordinates; A95/$\alpha$95 = radius of 95% confidence circle (A95 when $N \geq 3$, $\alpha$95 when $N = 1$ and $N = 2$); $K/k$ = Fisher precision parameter ($K$ when $N \geq 3$, $k$ when $N = 1$ and $N = 2$); Long, Lat N America = longitude (°E) and latitude (°N) of pole in North American coordinates; $R$ = Northwest African (Adria) to North America rotation parameters (see below). (1) Pole calculated by averaging poles #42–53 in Table 5 of Kent and Irving (2010). (2) Ontario kimberlite pole of Kent et al. (2015). (3) The 145-Ma pole of Kent and Irving (2010) obtained by averaging the following items 4–6. (4) Ithaca kimberlite pole (Van Fossen & Kent, 1993) with updated U-Pb perovskite age (Kent et al., 2015). (5) Swartruggen-Bumbeni pole (Hargraves et al., 1997) rotated to North America by Kent and Irving (2010) using Roest et al. (1992). (6) Hinlopentretet dikes pole, Svalbard (Halvorsen, 1989) rotated to North America by Kent and Irving (2010). (7) Mean pole calculated by averaging poles of Kent and Irving (2010) at 60, 80, 100, and 120 Ma in North American coordinates. (8) Pole based on unflattened ($E/I$ corrected) data of entries #21–24 of Table 1 of Muttoni et al. (2013) from the Belvedere (Brack & Muttoni, 2000), Froetschbach (Muttoni et al., 1997), Margon (Gialanella et al., 2001), and Stuores (Broglio Loriga et al., 1999) sections of Ladinian-Early Carnian age. This mean pole differs by 0.6° from the Ladinian-Early Carnian mean pole of Table 2 of Muttoni et al. (2013) that includes also one entry from Al-Azizia and Kaf Bates sediments from Libya (#25 of Table 1 of Muttoni et al., 2013). (9) Pole from this study obtained by unflattening ($E/I$ correcting) data of Channell et al. (2010) from the pre–*C. wiedmanni* LO interval of the Bombatierle section. (10) Pole from this study obtained by unflattening ($E/I$ correcting) data of Channell et al. (2010) from the pre–*C. wiedmanni* LO interval of the Foza section. (11) Pole from this study obtained by unflattening ($E/I$ correcting) data of Channell et al. (2010) from the pre–*F. multicolumnatus* FO interval of the Colme di Vignola section. (12) Pole based on unflattened ($E/I$ corrected) data of entry #43 of Table 1 of Muttoni et al. (2013) from the approximately post–*F. multicolumnatus* FO and pre–*C. mexicana minor* FO interval of the Passo del Branchetto section of Channell et al. (2010). (13) Pole from this study obtained by unflattening ($E/I$ correcting) data of Channell et al. (2010) from the post–*F. multicolumnatus* FO and pre–*C. mexicana minor* FO interval of the Sciapala section. (14) Pole based on unflattened ($E/I$ corrected) data of entries #44–46 of Table 1 of Muttoni et al. (2013) from the CM22 interval of the Colme di Vignola, Foza, and Frisoni sections of Channell et al. (2010). (16) Pole based on unflattened ($E/I$ corrected) data of entries #47–52 of Table 1 of Muttoni et al. (2013) from the CM17–CM19 and CM20–CM21 intervals of the Torre de' Busi, Colme di Vignola, Foza, and Frisoni sections of Channell et al. (2010). This pole is equivalent to the Early Tithonian mean pole of Table 2 of Muttoni et al. (2013). (17) Pole based on unflattened ($E/I$ corrected) data of entries #55–59 of Table 1 of Muttoni et al. (2013) from the approximately CM11–CM1 interval at Capriolo (Channell et al., 1987), Cismon (Channell et al., 2000), Polaveno and San Giovanni (Channell & Erba, 1992), and Val del Mis (Channell et al., 1993) sections straddling the Maiolica Limestone. This mean pole differs by 1.6° from the Hauterivian-Barremian mean pole of Table 2 of Muttoni et al. (2013) that includes also entries from Africa (#60–61 of Table 1 of Muttoni et al., 2013). (18) Pole based on unflattened ($E/I$ corrected) data of entries #68–70 of Table 1 of Muttoni et al. (2013) from the approximately C17–C29 interval at South Ardo (Dallanave et al., 2012), Cicogna (Dallanave et al., 2009), and Alano di Piave (Agnini et al., 2011) sections straddling the Scaglia Formation. This mean pole differs by 2.1° from the Paleocene-Eocene mean pole of Table 2 of Muttoni et al. (2013) that includes also entries from Africa (#71–72 of Table 1 of Muttoni et al., 2013).
R:
[a]= Lottes and Rowley (1990) at Pangea fit: Lat. = 66.4°N, Long. = 345.9°E, Rot. = −75.1°. [b]= Euler pole at Lat. = 66.8°N, Long. = 344.9°E, Rot. = −67°, interpolated between Roest et al. (1992) at anomaly M25 and Klitgord and Schouten (1986) at Blake Spur Magnetic Anomaly. [c]= Roest et al. (1992) at anomaly M25: Lat. = 66.7°N, Long. = 344.1°E, Rot. = −64.9°. [d]= Roest et al. (1992) at anomaly M21: Lat. = 66.2°N, Long. = 341.7°E, Rot. = −62.1°. [e]= Euler pole at Lat. = 66°N, Long. = 341°E, Rot. = −56°, interpolated between poles at anomalies M0 and M11 (Roest et al., 1992). [f]= Muller et al. (1993) at anomaly 21 (Africa to Hot spot + Hot spot to North America = Africa to North America: Lat. = 75.70°N, Long. = 356.26°E, Rot. = −15.49°).

may have been sufficiently long to average out geomagnetic secular variation. The 145-Ma mean pole of Kent and Irving (2010; Table 1, entry #3) was originally defined by three igneous poles from three different continents: the Ithaca kimberlite pole 146Ik from North America (Van Fossen & Kent, 1993), with an updated U-Pb perovskite age of 146.4 ± 1.4 Ma (Kent et al., 2015; Table 1, entry #4); the combined Swartruggen-Bumbeni pole 145SB from southern Africa (Hargraves et al., 1997), which we assign a nominal age of

145.4 ± 1.4 Ma based on an Ar/Ar date for the Swartruggens kimberlite of 145.0 ± 0.4 (Phillips, 1991) and an Ar/Ar date of 145.8 ± 1.3 on the Bumbeni syenite (Hargraves et al., 1997; Table 1, entry #5); and the 144 ± 5-Ma (K/Ar) Hinlopenstretet dikes pole 144Hi from Svalbard (Halvorsen, 1989; Table 1, entry #6). Finally, this cluster of three poles defining the reference 145-Ma pole of Kent and Irving (2010) is followed by a smaller return shift to the oft-documented stillstand of poles for North America in the Cretaceous as calculated by averaging mean poles of Kent and Irving (2010) at 60, 80, 100, and 120 Ma (Table 1, entry #7; Figure 1).

Torsvik et al. (2012) elaborated on a previous pole compilation (Torsvik et al., 2008) to generate a global-composite APWP using data from all major continents. The critical 170- to 140-Ma portion of their APWP is based chiefly on data from sediments from the Colorado Plateau, including the lower and upper Morrison poles (Steiner & Helsley, 1975) and other entries used in May and Butler (1986) all corrected by 5.4° to account for the clockwise rotation of the Colorado Plateau citing Bryan and Gordon (1990; who actually estimated the rotation was 5° +2.4°/−2.3°), in conjunction with entries from sediments from central Europe similar to those used by Besse and Courtillot (2002): Aubourg & Rochette, 1992; Bucker et al., 1986; Hagstrum, 1994; Johnson et al., 1984; Kądziałko-Hofmokl & Kruczyk, 1987; & Kądziałko-Hofmokl et al., 1988; Kluth et al., 1982; Nairn et al., 1981; (see discussion below in section 4 and in supporting information S1). Acknowledging the necessity to do something about $I$ error with the general unavailability of sample or site level data from often vintage publications, Torsvik et al. (2012) assumed for selected (but hardly all) sedimentary entries a nominal correction factor, $f = 0.6$.

The overall result was that the APWP of Torsvik et al. (2012) tends to lie slightly to the south of Besse and Courtillot (2002) and even more to the south of Kent and Irving (2010; Figure 1). A notable feature is for around 145 Ma where the constituent poles of Kent and Irving (2010) occupy the easternmost longitudes of all considered APWPs. Torsvik et al. (2012) included only one pole (Ithaca kimberlites of New York; Van Fossen & Kent, 1993) and Besse and Courtillot (2002) two poles (Ithaca pole and a pole from Hinlopentretet dikes of Svalbard; Halvorsen, 1989) of the three poles used by Kent and Irving (2010) to define the 145-Ma cusp (Ithaca, Hinlopentretet, and Swartruggens-Bumbeni. But by averaging these three poles with other data in a broad 20-Myr moving time window, the APWPs of Besse and Courtillot (2002) and Torsvik et al. (2012) show an attenuated cusp compared to the hybrid APWP of Kent and Irving (2010), which also used a 20-Myr moving time average for temporally well distributed selected data as in the Late Triassic and Early to Middle Jurassic (230 to 160 Ma), but a discrete nonoverlapping time average (such as had been sometimes more generally used for APWP construction, e.g., by Van der Voo, 1993) for the more spatiotemporally isolated poles defining the 145-Ma mean pole.

As pointed out by Torsvik et al. (2012), the Kent and Irving (2010) hybrid APWP for the Jurassic differs strongly from their and most other published paths APWPs (e.g., Besse & Courtillot, 2002), which was attributed to the small number of poles used by Kent and Irving (2010) that were also not averaged in a 20-Myr window over the cusp interval. However, including for the sake of averaging larger numbers of poles that are likely to be variably biased by undiagnosed errors and possibly by overprinting from earlier and less adequate laboratory procedures (see discussion below and in supporting information S1) will tend to attenuate and obscure the full expression of important features of APW such as the Jurassic monster polar shift. Nevertheless, it is obviously critical that such features are tested with new data. With this in mind, we attempted a renewed study of a key unit for the Jurassic APWP of North America, the Late Jurassic age Morrison Fm., at the same locale where it had been studied by Steiner and Helsley (1975). We then proceed to describe a much more fruitful and independent source of Late Jurassic data from Adria, the promontory of Africa, that has largely been ignored in global-composite APWPs. We review poles obtained from magnetobiostratigraphic sections from the literature that have been already corrected for sedimentary inclination shallowing and provide a new set of poles for Adria from existing magnetobiostratigraphic sections that we corrected for inclination shallowing, in order to provide better insights into Late Jurassic polar motion.

## 2. The Morrison Conundrum

A key example of the broad influence of biased poles on APWP construction is provided by the classic lower and upper Morrison poles from North America (Steiner & Helsley, 1975), which have been used widely since Irving and Irving (1982), are critical to the PEP analysis of May and Butler (1986), and are included in the

recent global-composite APWP of Torsvik et al. (2012). The lower Morrison is composed of the basal Tidwell Member, dominated by siltstones and gray limestone beds with occasional ash layers, overlain by the Salt Wash Member, which is a fluviatile unit dominated by channel sandstones. The upper Morrison is comprised of the Brushy Basin Member, a unit dominated by floodplain mudstones with volcanic ash layers. Ar/Ar ages on sanidine crystals extracted from the ash layers allowed dating of the basal Tidwell Member to 155 Ma and the base and top of the Brushy Basin Member to 150 and 148 Ma, respectively (Kowallis et al., 1998).

Steiner and Helsley (1975) sampled the lower and upper Morrison Fm. in the Norwood area on the Colorado Plateau (Figure 2a) and obtained poles (Figure 3, S&H75) that were not corrected for Colorado Plateau rotation, which was not recognized before Hamilton (1981). May and Butler (1986) corrected these poles (Steiner & Helsley, 1975) by 3.8° to account for the then-estimated clockwise rotation of the Colorado Plateau (Bryan & Gordon, 1986) and used the lower Morrison pole (Figure 3, M&B86) to define their critical J2 cusp (Figure 1) and along with the upper Morrison pole to help define the ensuing J2-KA PEP track (Figure 1). Bazard and Butler (1994) produced a pole (Figure 3, B&B94) from the upper Morrison Fm. (Brushy Basin Member) from Montezuma Creek, Utah, that is virtually undistinguishable from the upper Morrison pole of Steiner and Helsley (1975) from Norwood, Colorado, that is also on the Colorado Plateau and subject to correction for its tectonic rotation.

Kent and Irving (2010) attempted to reconcile these lower and upper Morrison poles with their global-composite APWP by applying to the Steiner and Helsley (1975) data an assumed inclination flattening correction of $f = 0.55$ and a much larger (13°) restorative counterclockwise Colorado Plateau rotation relative to cratonic North America (Kent & Witte, 1993; Steiner, 1986; Steiner, 1988). The thus doubly "corrected" upper Morrison (149 Ma) pole was found to lie encouragingly close to the 145-Ma mean pole at the terminus of the Jurassic monster shift (Figure 3, K&I10); however, the doubly corrected lower Morrison (155 Ma) pole was found to still lie off any beaten APW track (Figure 3, K&I10).

Another set of data from the Morrison Fm. was reported from the Front Range east of the Colorado Plateau (Van Fossen & Kent, 1992; Figure 2a). The Front Range Morrison (its type locality) is thought to be stratigraphically equivalent to the Brushy Basin Member of the upper Morrison Fm. from the Colorado Plateau localities, according to Bazard and Butler (1994), but gave a pole that, with some uncertainties related to differential local structural rotations of the sampled sites, was found to lie at much more northern latitudes (Figure 3, VF&K92: 83.7°N 150.4°E) than the Morrison poles from the Colorado Plateau. Nonetheless, persistent uncertainties in pole position, lack of direct $I$ error assessment, and suspicion of remagnetization led Kent and Irving (2010) to exclude all these Morrison Fm. data (Bazard & Butler, 1994; Steiner & Helsley, 1975; Van Fossen & Kent, 1992) from their composite APWP.

## 3. New Paleomagnetic Data From the Morrison Formation

In an attempt to better constrain the significance of the lower and upper Morrison poles with regard to the Jurassic monster shift in which they should temporally fall and the North American APWP in general, we revisited the classic locality near Norwood, Colorado (Steiner & Helsley, 1975) where we sampled the same flat-lying lower and upper Morrison Fm. The aim was to perform an $E/I$ test as well as the "correction-by-site" method (Tauxe & Kent, 2004) for direct assessments of the inclination flattening factor.

On roadcuts along State Highway 145 east of Norwood, we sampled the lower Morrison Fm. (Salt Wash Member) at 11 stratigraphically superposed sites (JMA-JML) and the upper Morrison Fm. (Brushy Basin Member) at 18 stratigraphically superposed sites (JBA-JBR; Figure 2b). A total of 152 (with 100 from sites JMA and JMB devoted to the correction-by-site $E/I$ test) and 37 standard (10 $cm^3$) paleomagnetic core samples from the lower and upper Morrison Fm., respectively, were subjected to progressive thermal demagnetization in an ASC Model TD48-SC thermal demagnetizer and measurement of the resulting natural remanent magnetization (NRM) with a 2G Enterprises Model 760 DC SQUID superconducting rock magnetometer, all located in a magnetically shielded room with ambient fields nominally less than 300 nT (thermal demagnetization data in supporting information S2, Table S1 for sites JMA-JML, and Table S2 for sites JBA-JBR).

After removal of spurious "A" component directions between room temperature and 100 °C, NRM demagnetization trajectories of the samples typically showed the occurrence of a pervasive "B" component up to

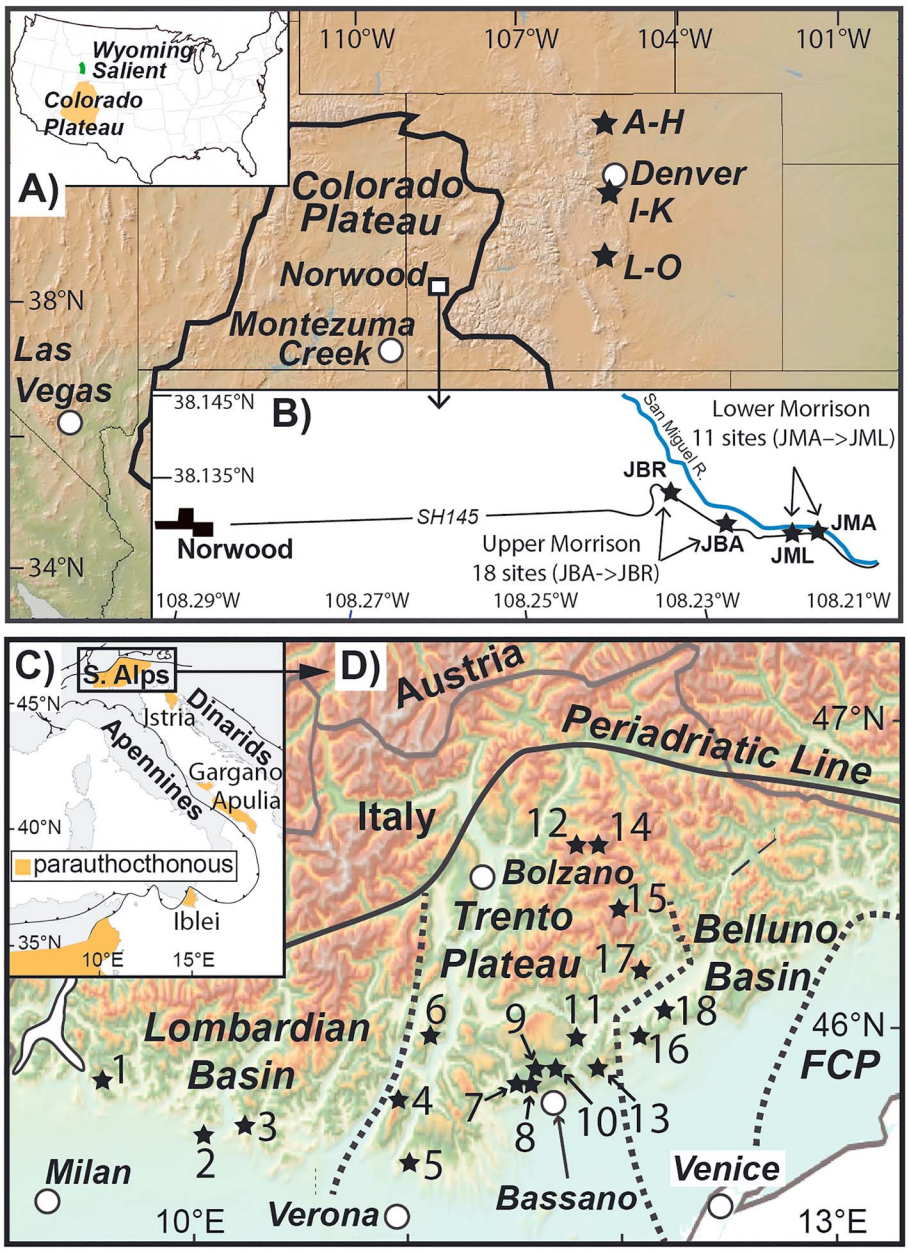


**Figure 2.** (a) Simplified elevation map of southwestern United Sates showing outline of Colorado Plateau with indication of sampling areas of Morrison Fm. of this study near Norwood, Colorado, and of Van Fossen and Kent (1992) in the Front Range off the Colorado Plateau (sites A–H, I–K, and L–O). (b) Detailed location map of the Norwood area with sites from the lower and upper Morrison Fm. sampled in this study. (c) Italian Peninsula and North Africa showing the distribution of regions that are considered essentially stable (parauthocthonous) relative to the African craton: The central eastern Southern Alps (S. Alps in the figure), Istria, Gargano, Apulia (and in general the Adriatic foreland between the Apennine and the Dinaric thrust-and-fold belts), and Iblei in Sicily. These regions constitute parauthocthonous Adria discussed in the text (as opposed to allochthonous Adria in the Apennines). (d) The central eastern Southern Alps with main paleogeographic features (Lombardian Basin, Trento Plateau, Belluno Basin, and Friuli Platform = FCP) and locations of sites considered in this study: (1) Torre de' Busi, (2) Capriolo, (3) Polaveno and San Giovanni, (4) Colme di Vignola (abbr. Vig), (5) Passo del Branchetto (abbr. Branch), (6) Margon, (7) Bombatierle (abbr. Bomb), (8) Sciapala (abbr. Sci), (9) Foza (abbr. Fo), (10) Frisoni, (11) Cismon, (12) Froetschbach, (13) Alano, (14) Stuores, (15) Belvedere, (16) South Ardo, (17) Val del Mis, and (18) Cicogna.

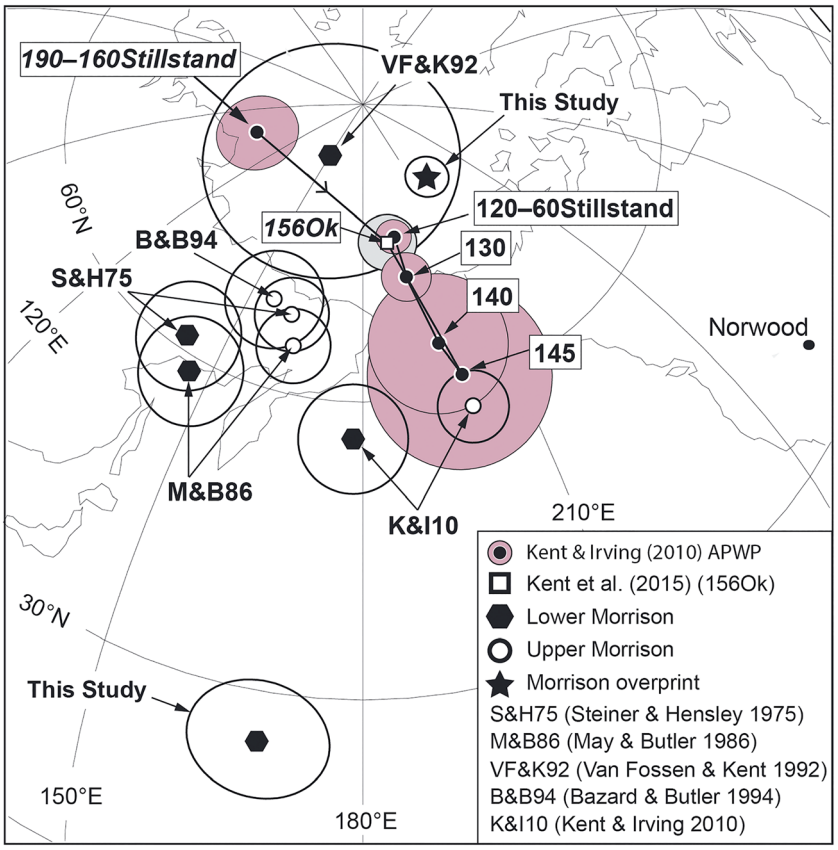


**Figure 3.** Poles from the lower and upper Morrison Fm. from the literature compared to the Kent and Irving (2010) apparent polar wander path in North American coordinates from the 190- to 160-Ma stillstand in the Early Jurassic to the 145-Ma cusp pole and the ensuing 120-60-Ma stillstand. The Ontario kimberlites pole (156Ok; Kent et al., 2015) is also indicated. Steiner and Helsley (1975) poles are without Colorado Plateau rotation. May and Butler (1986) poles are those of Steiner and Helsley (1975) corrected for 3.8° clockwise rotation of the Colorado Plateau. Kent and Irving (2010) poles are those of Steiner and Helsley (1975) but with 13° Colorado Plateau rotation and an assumed flattening factor $f = 0.55$. Van Fossen and Kent (1992) lower Morrison pole is from the Front Range near the type area of the Morrison Fm. (Peterson & Turner, 1998) but off the Colorado Plateau (and it is therefore nor corrected for Colorado Plateau rotation). The lower Morrison pole and the Morrison "B" component overprint pole of this study are also indicated before and after 13° clockwise rotation of the Colorado Plateau.

600–650 °C (Figure 4a) with directions oriented north-and-down (positive inclinations) that could be isolated in a total of 140 lower and upper Morrison samples. These B component directions (supporting information S2, Table S3) are relatively well clustered around a mean of declination, $D$ = 6.2°E, inclination, $I$ = 63.9° (radius of 95% confidence circle, $\alpha 95$ = 2.1°; Figure 4b). What are optimistically regarded as characteristic component ("Ch") directions were isolated in a very narrow temperature range from 600–650 to 680 °C, consistent with hematite as carrier of the remanence (see also Bazard & Butler, 1994), in 40 samples from the lower Morrison and only 6 in the upper Morrison (Figure 4a). These occasional Ch component directions (supporting information S2, Table S4) are commonly oriented southeast-and-up (negative inclinations) or northwest-and-down, which are interpreted as recording reverse and normal geomagnetic polarity, respectively, but are distinctively not antipodal (Figure 4b). The overall mean obtained by averaging the $n$ = 40 Ch component directions (after inverting the reverse polarity directions) from the lower Morrison is $D$ = 298.9°E, $I$ = 35.9° ($\alpha 95$ = 7°; Figure 4b). Due to the paucity of Ch component directions that could be isolated and the negative reversal test that they provided, no $E/I$ test for a direct assessment of the flattening factor could be performed.

The B component mean direction defines a high-latitude pole (81.2°N 281.1°E) that, when rotated 13° counterclockwise to account for Colorado Plateau rotation, falls at 80.2°N 219.1°E (Figure 3, solid star of "This Study"). This is in the vicinity of the 120- to 60-Ma Cretaceous stillstand pole for cratonic North

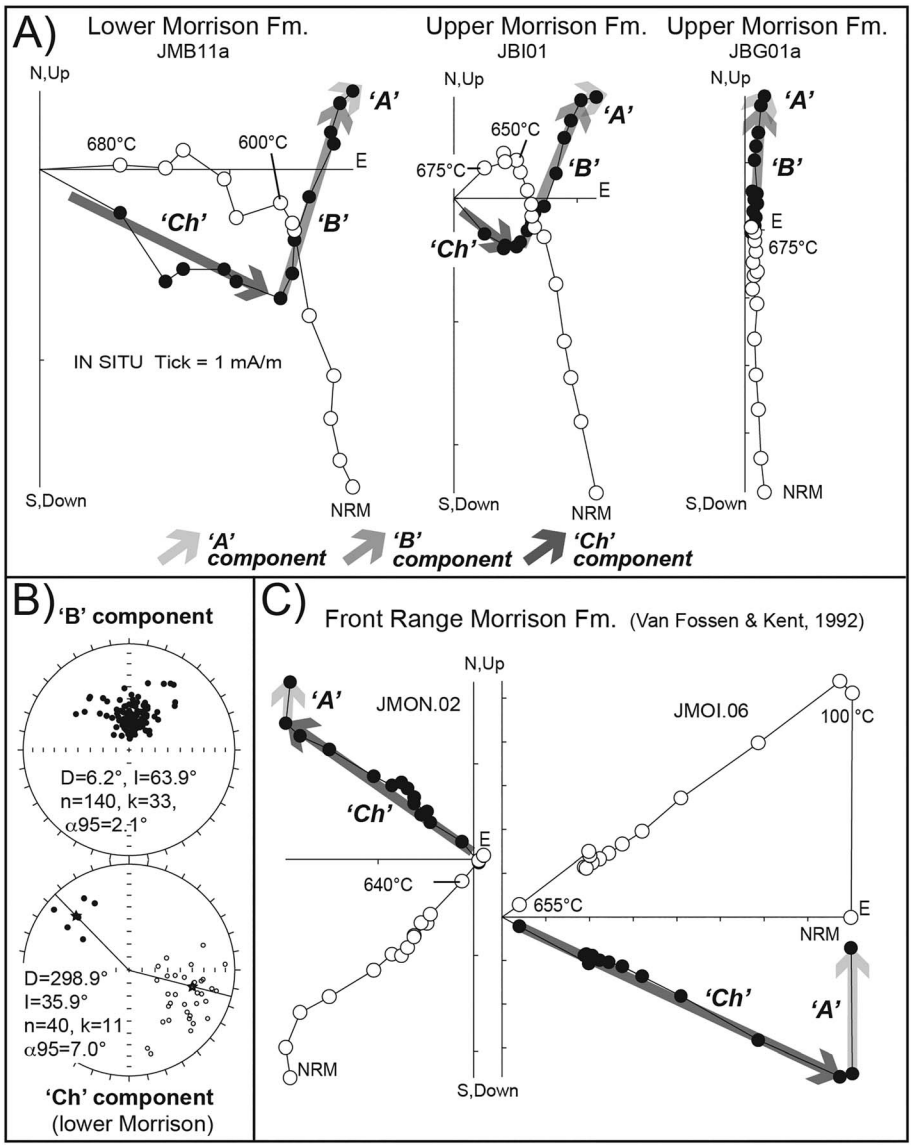


**Figure 4.** Paleomagnetic data of this study from the Morrison Fm. near Norwood on the Colorado Plateau (a, b) and of Van Fossen and Kent (1992) from the Front Range off the Colorado Plateau (c). (a) Representative vector endpoint diagrams for progressive thermal demagnetization of NRM of samples from the lower and upper Morrison Fm. (see supporting information S2, Tables S1 and S2) revealing the presence of an initial (low temperature) "A" transient component direction followed by an intermediate "B" component overprint (supporting information S2, Table S3), and an occasional high temperature "Ch" component direction trending to the origin of the demagnetization axes (supporting information S2, Table S4). (b) The $n = 140$ B component directions from lower and upper Morrison samples, and the $n = 40$ (sporadic) Ch component directions from the lower Morrison samples, are plotted on equal area stereograms with associated standard Fisher statistics (the upper Morrison yielded only six Ch component directions that are not figured but listed in supporting information S2, Table S4). (c) Representative thermal demagnetization diagrams of NRM of lower Morrison samples from the Front Range of Colorado (from Van Fossen & Kent, 1992) showing the absence of the pervasive B component overprint that tends to dominate samples from Norwood on the Colorado Plateau (see panel a).

America (Table 1, entry #7; Figure 3). Based on this correspondence, we tentatively interpret the B component as an overprint that may be associated with deep weathering at the K-1 unconformity that often truncates the top of the Morrison Fm. and that may correspond to a ~20-Myr hiatus after which the Early Cretaceous Burro Canyon and Cedar Mountain formations were deposited (Kowallis et al., 1998). Alternatively, the overprint may represent (thermo)chemical diagenetic formation of hematite from fluids

activated by the Late Cretaceous Laramide orogeny, whose remagnetization effects have been described from throughout western North America (Muttoni et al., 2001) even though other redbeds from the Colorado Plateau such as the Late Triassic Chinle Fm. (e.g., Kent et al., 2018) usually do not show such pervasive overprinting. Interestingly, McWhinnie et al. (1990) reported a paleomagnetic study on the Jurassic Twin Creek Fm. from the frontal segment of the Idaho-Wyoming Overthrust Belt, some 600 km to the NNW of Norwood and just off the Colorado Plateau ("Wyoming Salient" in upper left inset of Figure 2a), that revealed the presence of a pervasive remagnetization component carried by authigenic magnetite that yielded a pole (83°N 286°E) that is virtually undistinguishable from the B component pole of this study without correction for Colorado Plateau rotation, implying the B component was acquired after the rotation occurred.

The Ch component mean direction from the lower Morrison defines a pole (34.6°N 160.9°E) that, even when rotated 13° counterclockwise to correct for Plateau rotation as for the B pole, falls at 23.9°N 168.3°E, well to the south of any known Morrison pole from the literature (Figure 3, empty hexagon of This Study). We interpret the anomalous lower Morrison pole position as an artifact, reflecting a bias caused by a partially unremoved overprinting of the few Ch component directions of reverse polarity by the superposed northerly and steep-down B component. The unblocking temperature spectra of the Ch directions are either very narrow, limiting our confidence in component extraction (e.g., Figure 4a, sample JBI01), or they tend to partially overlap with the unblocking spectra of the pervasive B component, as revealed by the slightly curved path that magnetic directions follow during transition from B to Ch component endpoints. This curvature due to partial mixing of components, particularly visible in the inclination values, would explain the observed bias toward easterly and shallow-up Ch directions (e.g., Figure 4a, sample JMB11a). This distortion of the Ch component directions induced by the pervasive B component overprint seems to be present also in the Steiner and Helsley (1975) data: their normal and reverse polarity mean directions, even of the well-grouped sites, are almost never truly antipodal (see their Figure 6). Moreover, we suspect from our experience that some of the normal polarity directions that they assumed were primary are in fact B component overprints. Averaging various populations of heavily overprinted Ch directions and/or a mixture of Ch and B directions is bound to result in a variety of variably biased poles strung out from 60°N to less than 30°N as observed after over 40 years of research on the Morrison Fm. (Figure 3).

## 4. The Contribution of Adria

Finding that the paleomagnetic directions from the Morrison Fm. at the classic localities on the Colorado Plateau are too heavily overprinted and of scarce significance for constraining the Late Jurassic monster shift, we looked elsewhere for reliable Late Jurassic data. We scrutinized the global paleomagnetic database used in Besse and Courtillot (2002) and Torsvik et al. (2012) in search of alternative poles, struggling with entry numbers that differ from one version of the database to another. According to our analysis, described in supporting information S1 and associated Figures S1 and S2, the Late Jurassic time interval is relatively deficient in reliable poles in both of these compilations, which are dominated by relatively low-quality ($q$-factor typically only 3 out of 7) Jurassic poles from mostly sedimentary units in published work going as far back as the 1970s from central Europe, the Colorado Plateau and Louisiana, Tunisia, and Brazil, whose inclusion and averaging had the effect to smear out what we consider the real magnitude and rapidity of the Jurassic monster polar shift.

We therefore turn our attention to Adria, the promontory of Africa, that can be rotated into North America coordinates using standard Central Atlantic reconstruction parameters for northwest Africa. Paleomagnetic data from Adria (see Channell, 1996, for a first compilation) have been largely neglected in global-composite APWPs, such as by Besse and Courtillot (2002), Kent and Irving (2010), and Torsvik et al. (2012), and are therefore totally independent from them. Nevertheless, Channell et al. (2010) and Muttoni et al. (2013) have shown that Triassic and Jurassic poles from Adria map close to global-composite APWPs, a correspondence also noted by Kent et al. (2015). Here we show in detail that Jurassic data from Adria can be used to assess and refine the character of Jurassic APWP, especially the disputed Jurassic monster shift of Kent and Irving (2010).

The African affinity of parautochthonous regions of Adria is well documented since Channell and Horvath (1976) and Channell (1996). Permian to Paleogene paleomagnetic poles from the Trento Plateau (including

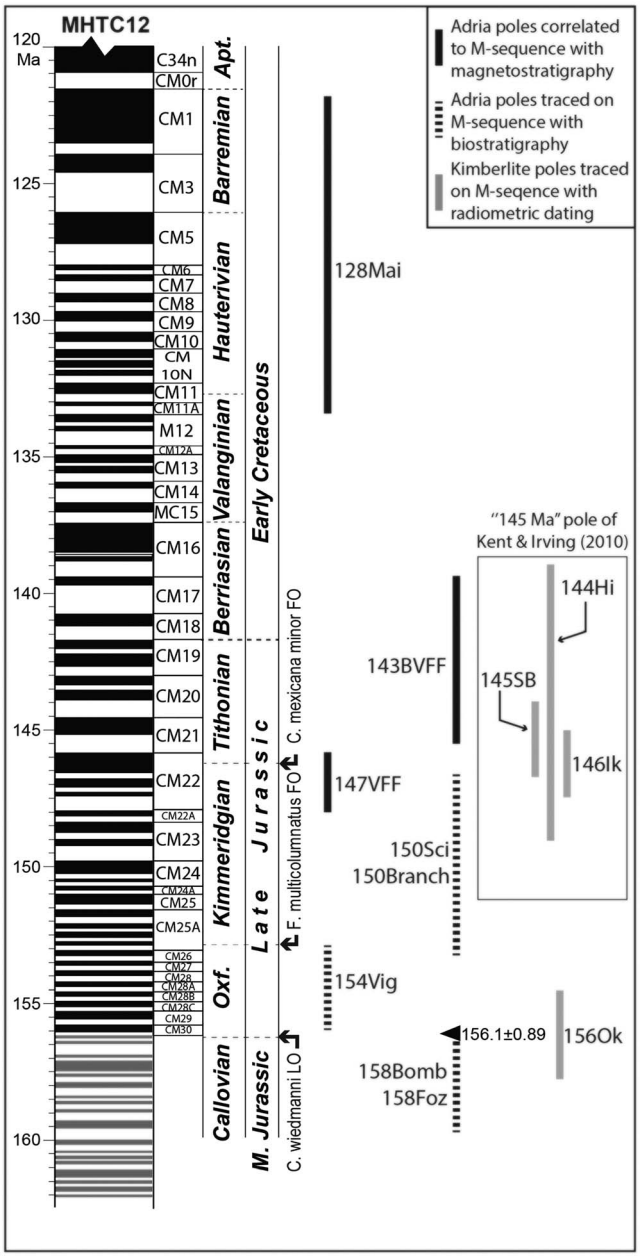


**Figure 5.** Chronology of Jurassic-Early Cretaceous poles from Adria (acronyms as in Table 1) derived from stratigraphic sections correlated to the M-sequence marine magnetic anomalies of Malinverno et al. (2012; MHTC12) by means of magnetostratigraphy (continuous solid lines) or correlated using key nannofossil events (dashed lines). These bioevents are the FO (=first occurrence) of *C. mexicana minor* and the FO of *F. multicolumnatus*, correlated to the MHTC12 sequence using magnetostratigraphy from the S'Adde section of Sardinia (Muttoni et al., 2018), and the LO (=last occurrence) of *C. wiedmanni*, estimated at ~156 Ma based on an Ar/Ar date (156.1 ± 0.89 Ma) on an ash layer at the top of the *Rosso Ammonitico Medio* at Kaberlaba (Pellenard et al., 2013), which is indicated. Also shown by gray bars are the age ranges of the 146.4 ± 1.4-Ma Ithaca kimberlite pole (146Ik; Van Fossen & Kent, 1993), the 144 ± 5-Ma Hinlopenstretet dikes pole (144Hi; Halvorsen, 1989), the 145.4 ± 1.4-Ma Swartruggens-Bumbeni kimberlites pole (145SB; Hargraves et al., 1997), and the 156.1 ± 1.6-Ma Ontario kimberlites pole (156Ok; Kent et al., 2015). See text for discussion and additional references.

the Dolomites) and the bordering Belluno Basin and eastern Lombardian Basin in the Southern Alps (Figures 2c and 2d), obtained from well-dated magnetobiostratigraphic sequences corrected for inclination shallowing or from radiometrically dated igneous rocks, show coherence with coeval data from Africa (Muttoni et al., 2013). Thus, these areas of northeastern Italy, as well as other foreland areas of the Alpine-Apennine orogeny around the Adriatic Sea, for example, Istria, Gargano-Apulia, and Iblei in southeastern Sicily (Figure 2c), are interpreted as parautochthonous with respect to the African craton (Channell et al., 2010; Muttoni et al., 2003; Muttoni et al., 2013).

The Trento Plateau, where most of the data considered in this study come from, is a sector of the Southern Alps where Alpine shortening was broadly oriented N-S and involved thick piles of Triassic platform carbonates overlying a 2-km-thick Permian volcanic unit resting above the Variscan crystalline basement, which together conferred rigidity to the thrust sheets and prevented large and systematic vertical axis rotations (Muttoni et al., 2013). Tectonic deformation involving various degrees of vertical axis rotations is more typical of the thin-skinned and largely basement-free Apennine thrust belt (Figure 2c) and thus magnetobiostratigraphic studies from the Apennines (Lowrie & Alvarez, 1977; Satolli & Turtù, 2016) were not considered here for reference poles because separate adjustments (rotations) of variable degrees would be required for incorporation into a global-composite APWP. In any case, we stress that these data from the allochthonous Apennines define altogether poles that are markedly African in aspect (Channell, 1996; Satolli et al., 2007), thus confirming the substantial tectonic coherence of parauthocthonous Adria and Africa and the confinement of systematic rotations to the Apenninic sector of Adria.

We consider key mean poles from the Trento Plateau and bordering Lombardian and Belluno basins from sedimentary units straddling the Middle Triassic, Middle and Late Jurassic, Early Cretaceous, and Paleogene (see descriptions below). Poles across the critical Jurassic interval were derived from various stratigraphic sections (Torre de' Busi, Vignola = Colme di Vignola, Branchetto = Passo del Branchetto, Bombatierle, Foza, Frisoni, Sciapala; Figure 2d) that have been previously studied for magnetostratigraphy and nannofossil biostratigraphy, and securely tied to the M-sequence of marine magnetic anomalies (Channell et al., 1995) as far back as CM22 (Channell et al., 2010). We express the chronology of these sections (and poles) relative to the updated (after Channell et al., 1995) M-sequence of Malinverno et al. (2012; MHTC12) down to CM30 (Figure 5). For sections (or portions of sections) older than CM22, the chronostratigraphy of the sections (and related poles) was estimated using three key biostratigraphic events: first occurrence (FO) of *Conusphaera mexicana minor*, FO of *Faviconus multicolumnatus*, and last occurrence (LO) of *Cyclagelosphaera wiedmanni*, which have proven particularly useful to subdivide the Oxfordian-Kimmeridgian interval in the Tethys realm, and two of which —*C. mexicana minor* FO and *F. multicolumnatus* FO—have been correlated to the M-sequence at CM22 and CM25A, respectively, using magnetostratigraphy from the expanded S'Adde section from Sardinia (Muttoni et al., 2018; Figure 5). The LO of *C. wiedmanni* is estimated at ~156 Ma and traced onto MHTC12 at CM30 (Figure 5) based on Ar/Ar dating (156.1 ± 0.89 Ma) of an ash level at the top of the *Rosso Ammonitico*

*Medio* unit at the Kaberlaba section (Pellenard et al., 2013) that was traced by means of lithostratigraphy to the nearby (1 km apart) Bombatierle section of this study, where the LO of *C. wiedmanni* is recorded also at the top of the Rosso Ammonitico Medio unit (Channell et al., 2010).

According to this chronostratigraphic framework for the Jurassic, and the available chronostratigraphy for the bracketing Triassic and Cretaceous-Paleogene, paleomagnetic poles from Adria sites considered in this study (Figure 2d) are as follows, older to younger (Table 1 and Figure 5):

•Pole 238Dol (Table 1, entry #8) is based on magnetostratigraphic data from radiometrically (U-Pb) constrained sections from the Trento Plateau: Belvedere (Brack & Muttoni, 2000), Froetschbach (Muttoni et al., 1997), Margon (Gialanella et al., 2001), and Stuores (Broglio Loriga et al., 1999), straddling altogether the Ladinian-Early Carnian (238 ± 3 Ma). Poles from these sections, which were previously corrected for inclination shallowing (Muttoni et al., 2013, Table 1, entries #21–24), yield a mean pole (Table 1, entry #8) that is virtually coincident with a pole from Middle Triassic sediments at Al-Azizia and Kaf Bates in Libya (Muttoni, et al., 2001) that was corrected for inclination shallowing by Muttoni et al. (2013, Table 1, entry #25).

•Poles 158Bomb and 158Foz (Table 1, items #9 and #10) are based on magnetostratigraphic data from the pre–*C. wiedmanni* LO interval of the Bombatierle and Foza sections, respectively (Channell et al., 2010). These poles are here checked for antipodality using the bootstrap reversal test (Tauxe, 2010; Tauxe et al., 2016) and corrected for inclination flattening ($f = 0.7$ and $f = 0.6$, respectively) with the $E/I$ method (supporting information S3, Figures S3 and S4, Table S5). Although a magnetostratigraphic correlation to the MHTC12 sequence is difficult to perform, these poles should be pre-CM30 in age (>156 Ma) based on the Ar/Ar age estimate of the *C. wiedmanni* LO (see above) and have thus been assigned a nominal age of ~158 Ma (Figure 5). They have been rotated from Northwest African to North American coordinates using a rotation pole interpolated between those for magnetic anomaly M25 (Roest et al., 1992) and the Blake Spur Magnetic Anomaly (Klitgord and Schouten, 1986).

•Pole 154Vig (Table 1, item #11) is based on magnetostratigraphic data from levels of the Colme di Vignola section older than the *F. multicolumnatus* FO and younger than the *C. wiedmanni* LO, not recorded in the section despite relatively dense sampling (Channell et al., 2010). This pole is here checked for antipodality and corrected for inclination flattening ($f = 0.8$; supporting information S3, Figure S5). As for poles described above, a magnetostratigraphic correlation of the interval defining pole 154Vig to the MHTC12 sequence was not possible to perform. In any case, this pole should broadly correspond to CM30–CM25 based on the correlation of *F. multicolumnatus* FO to CM25A and of *C. wiedmanni* LO (not recorded) to CM30 (see discussion above; Figure 5), and therefore, its age has been estimated to be on the order of 154 ± 2 Ma. It was rotated to North America at M25 time (Roest et al., 1992).

•Poles 150Branch and 150Sci (Table 1, items #12 and #13) are based on magnetostratigraphic data from the post–*F. multicolumnatus* FO and pre–*C. mexicana minor* FO interval of the Branchetto and Sciapala sections, respectively (Channell et al., 2010). Both sets of data are here corrected for inclination flattening ($f = 0.9$ and $f = 0.7$, respectively) and checked for antipodality, albeit the Branchetto data were found negative with the bootstrap reversal test (supporting information S3, Figures S6 and S7, respectively). These poles should broadly correspond to CM25–CM22 based on biostratigraphy (*F. multicolumnatus* FO in CM25A and *C. mexicana minor* FO in CM22; see above), and have thus been assigned an estimated age of 150 ± 3 Ma (Figure 5). They were rotated to North America at M25 time (Roest et al., 1992).

•Pole 147VFF (Table 1, item #14) is based on magnetostratigraphic data from the CM22 interval at Vignola, Foza, and Frisoni (Channell et al., 2010). These data have been previously checked for inclination flattening obtaining $f = 1$ for all intervals (Muttoni et al., 2013, Table 1, entries #44–46; note that at Vignola, $f$ was initially estimated at 0.9 by Channell et al. (2010) and averaged into an early Tithonian mean pole (Muttoni et al., 2013, Table 2) that is adopted here. This mean pole has been assigned a nominal age of 147 ± 1 Ma (Figure 5) and has been rotated to North America at M21 time (Roest et al., 1992).

Poles 154Vig, 150Branch, 150Sci, and 147VFF can be averaged into an overall mean pole termed 150Adria (Table 1, item #15).

•Pole 143BVFF (Table 1, item #16) is based on magnetostratigraphic data from the CM21–CM20 and CM19–CM17 intervals at Torre de' Busi, Vignola, Foza, and Frisoni (Channell et al., 2010). These data

were previously checked for inclination shallowing ($f$ comprised between 0.8 and 1.0; Muttoni et al., 2013, Table 1, entries #47–52) and averaged into a mid-Tithonian-Berriasian mean pole (Muttoni et al., 2013, Table 2) that is adopted here. This mean pole, broadly corresponding to CM21–CM17, has been assigned an age of 143 ± 3 Ma (Figure 5) and has been rotated to North America at M21 time (Roest et al., 1992).

•Pole 128Mai (Table 1, item #17) is based on magnetostratigraphic data from the Trento Plateau and Lombardian Basin: Capriolo (Channell et al., 1987), Cismon (Channell et al., 2000), Polaveno and San Giovanni (Channell & Erba, 1992), and Val del Mis (Channell et al., 1993), straddling the Maiolica Limestone of Hauterivian-Barremian (Early Cretaceous) age from CM11 to CM1 (128 ± 7 Ma). These entries, previously corrected for inclination shallowing (Muttoni et al., 2013, Table 1, entries #55–59), yield a mean pole (Table 1, item #17) that is consistent with coeval poles from the Etendeka Large Igneous Province of Namibia (Muttoni et al., 2013, Table 1, entries #60–61).

•Pole 50Sca (Table 1, item #18) is based on magnetostratigraphic data from the Belluno Basin and Trento Plateau: Cicogna (Dallanave et al., 2009), Alano di Piave (Agnini et al., 2011), and South Ardo (Dallanave et al., 2012), straddling the Scaglia Formation of Paleocene-Eocene age from C29 to C17. These poles, which show no statistical difference despite covering a large chronostratigraphic interval (50 ± 15 Ma), were previously corrected for inclination shallowing (Muttoni et al., 2013, Table 1, entries #68–70) and yield a mean pole (Table 1, item #18) that is consistent with poles from Africa (Muttoni et al., 2013, Table 1, entries #71–72).

In summary, bracketed between Middle Triassic pole 238Dol and Paleogene pole 50Sca, there is a total of eight Jurassic-Early Cretaceous poles from parauthocthonous Adria ranging in age from 158 to 128 Ma that have been correlated to the M-sequence by means of magnetostratigraphy or traced onto it by means of biostratigraphy (Figure 5). Some of these poles are comparable in age to monster shift propsoed by Kent and Irving (2010).

## 5. The Jurassic Monster Polar Shift

Poles from parauthochtonous Adria have been plotted relative to the completely independent APWP of Kent and Irving (2010) in common North American coordinates to assess the timing and tempo of the Jurassic monster polar shift (Figure 6).

Adria pole 238Dol at 238 ± 3 Ma lies close to the 230-Ma mean pole of Kent and Irving (2010), providing a first-order anchor point (see also Muttoni et al., 2013, for other anchor points) to validate the comparison of younger poles, especially those in the ensuing critical Jurassic time interval (Figure 6a). This agreement is further substantiated by data from the $E/I$ corrected Middle Triassic Al-Azizia and Kaf Bates pole from northern Libya (Muttoni et al., 2001), which upon rotation to North American coordinates, falls in the narrow space between pole 238Dol and the 230-Ma mean pole of Kent and Irving (2010).

The Early-Middle Jurassic (190–160 Ma) high-latitude stillstand (in North American coordinates; Figure 6a and Table 1, entry #1) is followed by the Jurassic monster shift to the 145-Ma mean cusp pole (Kent & Irving, 2010; Figure 6a and Table 1, entry #3) as defined by the Ithaca, Swartruggens-Bumbeni, and Hinlopenstretet igneous poles (Table 1, entries #4–#6), with the 156.1 ± 1.6-Ma Ontario kimberlites pole (156Ok) of Kent et al. (2015; Table 1, entry #2) bridging the gap between the 190- to 160-Ma stillstand and the 145-Ma cusp poles (Figure 6a).

Adria poles confirm and serve to refine the timing (see Figure 5 for poles chronology) of this overall APW pattern accurately and independently from the items originally defining the features. In particular, pole 158Foz falls at the edge of the Early-Middle Jurassic stillstand whereas the nearly coeval pole 158Bomb (both poles dated to around 158 Ma), falls close to the ~156 Ma Ontario kimberlites pole (156Ok). The Adria poles in (bio)stratigraphic superposition thus seem to delineate an onset of rapid polar motion in the 158- to 156-Ma time frame (Figure 6a).

The resolution of the polar motion is manifest by the extraordinary concordance of the just younger poles from Adria with the 145-Ma mean pole position (Kent & Irving, 2010), that is, the 154Vig pole (154 ± 2 Ma), the 150Sci pole (150 ± 3 Ma), the 150Branch pole (150 ± 3 Ma), and the 147VFF pole (147 ± 1 Ma; Figure 6a). The mean of these four Adria poles in North American coordinates (Table 1,

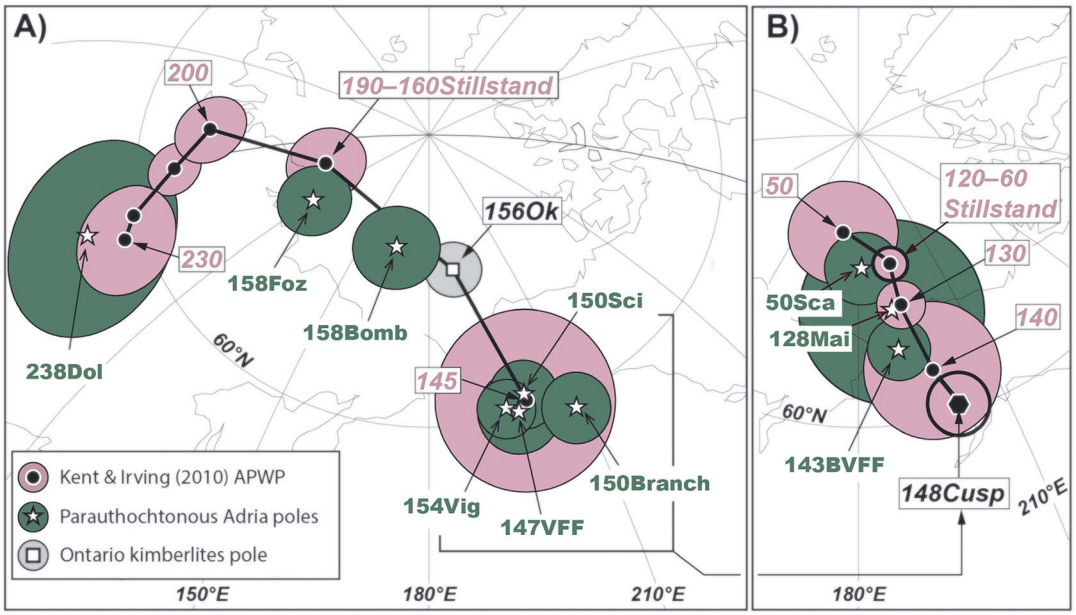


**Figure 6.** Sedimentary poles from Adria corrected for *I* error using the *E*/*I* method compared to the Kent and Irving (2010) reference APWP for (a) Late Triassic-Jurassic (230 to 145 Ma) that includes the Jurassic monster shift from 160 to 145 Ma and (b) Cretaceous-Paleogene (145 to 50 Ma). Poles in both panels are plotted in North American coordinates. Acronyms of Adria poles have a numerical prefix that refers to the central age of the pole (e.g., 238Dol has central age of 238 Ma; see Table 1 and text for further information). The 156-Ma Ontario kimberlites pole (156Ok; Kent et al., 2015) is also shown.

entry #15) is indistinguishable from the mean of the three igneous poles (146Ik, 145SB, and 144Hi) that originally defined the 145-Ma mean pole of Kent and Irving (2010; Table 1, entry #3). Together, the seven poles ranging in age from 144 to perhaps 154 Ma yield a well-grouped overall mean pole—termed 148Cusp—located at 60.8°N, 200.6°E (Table 1, entry #19). This mean pole is attributed a nominal age of 148 ± 3.5 Ma calculated as the mean of the dates for the seven constituent poles (± 2 standard deviations) and whose close agreement in pole space might even suggest a pause in polar motion of ~10-Myr duration.

The contribution of poles from parauthochtonous Adria extends across the Jurassic-Cretaceous boundary (Figure 6b). The 143BVFF pole at 143 ± 3 Ma (Table 1, entry #16) marks practically a rebound from the 148Cusp pole toward the 120- to 60-Ma Cretaceous stillstand (in North American coordinates; Table 1, entry #7). Pole 128Mai from Early Cretaceous (128 ± 7 Ma) magnetobiostratigraphic sections of the Maiolica Limestone (Table 1, entry #17) falls on the 130-Ma reference pole just to the south of the North American Cretaceous stillstand pole, whereas the 50Sca pole (50 ± 15 Ma) from Paleocene-Eocene sections of the Scaglia Formation (Table 1, entry #18) falls close to the 50-Ma reference pole just to the north of the North American Cretaceous stillstand pole (Figure 6b).

## 6. Discussion

We reconstructed the paleogeography of major continents from 190 to 60 Ma across the Jurassic monster shift using paleomagnetic poles discussed in this study coupled with reconstruction parameters from the literature, essentially corresponding to those summarized in Table 4 of Kent and Irving (2010; Figure 7).

From 190 to 160 Ma, North America, with Greenland and Eurasia attached, remained within uncertainties fixed relative to the spin axis (stillstand; Figures 7a and 7b). The ensuing Jurassic monster shift can be described geometrically as a ~30° rotation of the reconstructed continents in unison about a Euler pole centered on the equator in the Bight of Benin off western Africa (Kent et al., 2015; Figures 7b and 7c). This happens to be virtually the same Euler pole location used by Torsvik et al. (2012) to explain true polar wander (TPW). They argued that an Euler pole at about this location would have remained close to the center of masses of the African and Pacific Large Low Shear-wave Velocity Provinces (LLSVPs), which are

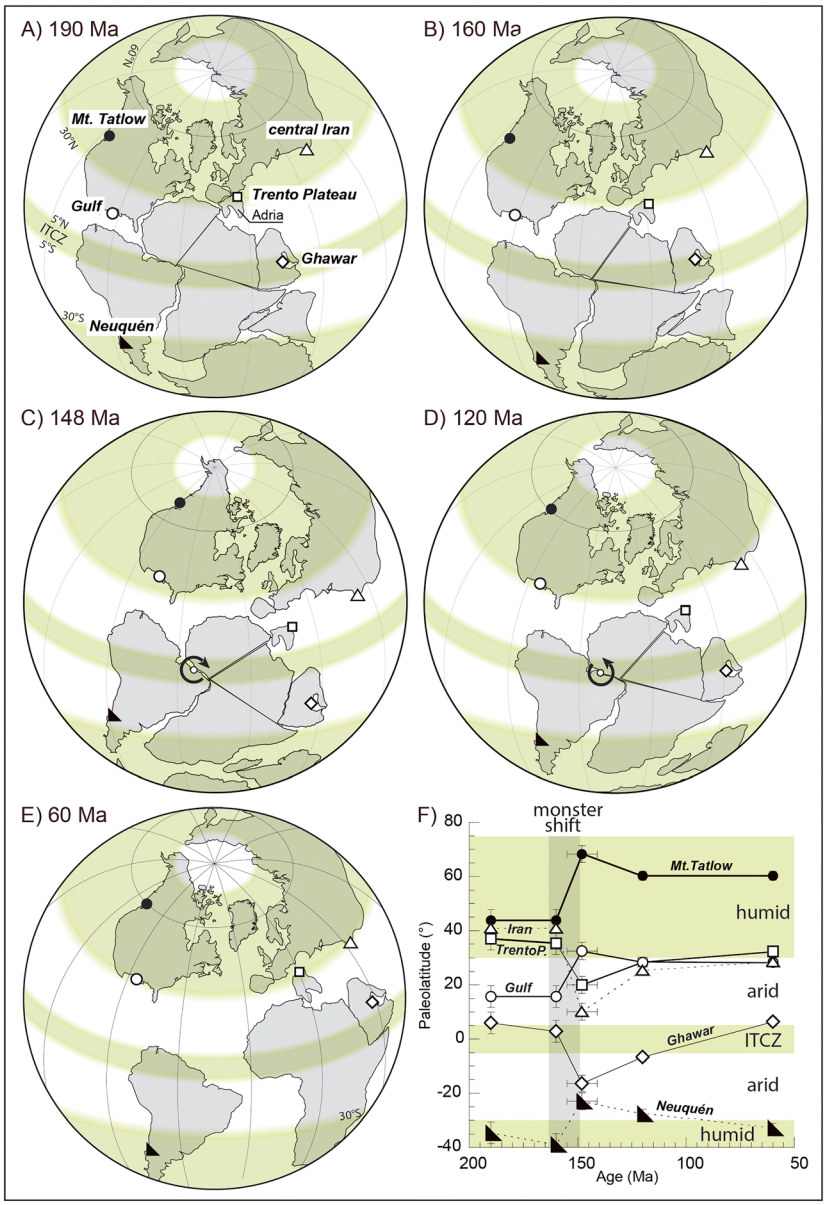


**Figure 7.** Paleocontinental reconstructions from 190- to 60-Ma bracketing the Late Jurassic monster polar shift. In panels (a) at 190 Ma and (b) at 160 Ma, North America has been reconstructed using the Early Jurassic 190- to 160-Ma still-stand pole, in panel (c) (148 Ma) using the Late Jurassic 148Cusp pole, and in panels (d) at 120 Ma and (e) at 60 Ma using the 120- to 60-Ma stillstand pole (Table 1). Europe has been rotated to North America using reconstruction Euler pivots in Srivastava and Tapscott (1986; panels a–c) and *Muller* et al. (1993) interpolated (panels d and e). Greenland has been rotated to North America using Srivastava and Tapscott (1986). Northwest Africa has been rotated to North America using Klitgord and Schouten (1986) at maximum fit (panel a), an interpolated Euler pivot between Klitgord and Schouten (1986) at Blake Spur and Roest et al. (1992) at M25 (panel B), Roest et al. (1992) at M25 (panel c), and Muller et al. (1993) interpolated at 120 and 60 Ma (panels d and e). South America has been rotated to northwest Africa using Royer et al. (1992; panels a–c), and to North America using Muller et al. (1993) interpolated (panels d and e). India, Antarctica, Arabia, and Australia have been rotated to northwest Africa using Besse and Courtillot (2002) interpolated (panels a–c) and to North America using Muller et al. (1993) interpolated (panels d and e). Rotation of continents during the Jurassic monster shift seems to have occurred about an Euler pivot centered on the equator in the Bight of Benin (circle with clockwise rotation symbol in panel c), followed by a slower counterclockwise rebound attained at 120 Ma (panel d). The variations of paleolatitude that selected sites (Mt. Tatlow in North America, Trento Plateau on Adria, and Ghawar in Arabia) experienced from 190 to 60 Ma and across the Jurassic monster shift are indicated in panel f (for sites location, see panel a). The green belts in all diagrams represent zonal climate belts where precipitation exceeds evaporation (mid latitude and equatorial humid belts) as opposed to areas with excess evaporation and/or little precipitation (tropical and polar arid belts). ITCZ is the intertropical convergence zone. See text for discussion.

associated with large-scale geoid highs and thus likely to constrain any whole-mantle rotations to the axis of minimum moment of inertia. Supporting evidence that the monster shift represents an episode of whole-mantle TPW rather than motion of the reconstructed continents relative to Earth's mantle, or APW, is the coherency of paleomagnetic results from practically the only available drill site recovering Late Jurassic sediments and igneous basement from the Pacific plate (Fu & Kent, 2018).

A gross estimate of the rate for the monster polar shift is 30° in 12 Myr (~160 Ma to 148Cusp), or about 2.5°/Myr. Taking into account only the best-dated (U-Pb perovskite) kimberlite poles (Kent et al., 2015) from Ontario (156.1 ± 1.6 Ma, with an associated A95 uncertainty of 2.8°), and from Ithaca (146.4 ± 1.4 Ma, with an A95 of 3.8°), the mean rate of polar motion would be 1.9°/Myr (min = 0.8°/Myr, max = 4.3°/Myr). These mean estimates are close to a theoretical limit for TPW of 2.4°/Myr as calculated by Tsai and Stevenson (2007). We stress that better age constraints are needed to pin down angular velocities more precisely within the Jurassic monster shift, for example, if the motion first accelerated and then decreased. A suggested geodynamic trigger for such an episode of TPW (Kent et al., 2015) is the break-off and sinking of a cold, dense subducting slab through the mantle at an optimal distance from the Euler pole (Greff-Lefftz & Besse, 2014), such as apparently occurred at about the right time in the America Cordillera (Sigloch & Mihalynuk, 2013).

After this large perturbation, a slower essentially return polar motion of about 10° in ~10 Myr occurred from the 148Cusp to pole 143BVFF at 143 Ma and continued up to the start of the Cretaceous stillstand (in North American coordinates; Figure 7d); this retromotion may reflect plate motion of North America but could also include an episode of TPW, a polar shift common to all tectonic plates, which may have been forced by the initiation of eastward subduction in the American Cordillera (Sigloch & Mihalynuk, 2013) and/or slab break-off during the latest Jurassic-earliest Cretaceous closure of the Mongol-Okhotsk Ocean (Van der Voo et al., 2015). Subsequent motions of the major continental plates through the Cretaceous stillstand (in North American coordinates) from about 120 to 60 Ma occurred essentially due to Atlantic and India Ocean openings (Figure 7e) with negligible contribution of TPW as essentially precluded by the stillstand.

Regardless of its ultimate geodynamic forcing, the Jurassic monster shift left an important albeit underestimated legacy in the evolution of sedimentary basins and climate-dependent sedimentary facies when viewed in the framework of Earth's dominantly zonal climate (Manabe & Bryan, 1985). For example, northern Adria (e.g., Trento Plateau, Figure 7a) experienced rapid southward motion of up to 20° from the mid-latitude temperate belt in the Early Jurassic to tropical paleolatitudes in the Late Jurassic (Figure 7f). Elaborating on Muttoni et al. (2005), we consider this motion as a main controlling agent on the style of deposition in pelagic settings on Adria (e.g., Lombardian Basin) whereby radiolarian oozes (Radiolarites) were deposited as Adria migrated to tropical (or even subequatorial) paleolatitudes, in general agreement with modern-day depositional settings controlled by zonal circulation patterns, for example, in subequatorial upwelling belts or regions of coastal upwelling related to the seaward deflection of western boundary currents. A similar plate-tectonic stratigraphic approach has been used by Mattei et al. (2014) to explain the first-order depositional history of central Iran (Figure 7a) whereby coal-bearing sedimentation stopped and carbonate platform productivity and evaporitic sedimentation ensued on the adjacent margin as Iran drifted from the humid temperate belt to arid tropical latitudes during the Jurassic monster shift (Figure 7f).

But perhaps the most startling implication of the monster shift is the role it seems to have played in the generation and preservation of major oil fields. According to Muttoni and Kent (2016), the Callovian-Oxfordian Tuwaiq Mountain and Hanifa formations, which represent the main source rocks of Jurassic oil in the Persian Gulf (e.g., Ghawar oil field, Figure 7a), were deposited when eastern Saudi Arabia resided near the intertropical convergence zone straddling the equator (Figures 7b and 7f), whereas the anhydrites of the overlying Tithonian Hith Fm., representing the main seal cap, were deposited as Saudi Arabia (Ghawar) rapidly drifted to the arid southern tropics as a consequence of the monster shift (Figures 7c and 7f). This tightly sequenced sediment package resulted in some of the world's largest oil fields, such as Ghawar. On the other side of Gondwana, the Neuquén Basin of Argentina (Figure 7a) resided at paleolatitudes higher than ~35°S within the presumed temperate humid belt of the Southern Hemisphere during most of the Mesozoic and Cenozoic (Figure 7f). A single northward incursion to ~30°S toward the austral arid belt occurred at 148 Ma and broadly coincided with the deposition of the Auquilco evaporites that

seal the underlying Los Molles marine shales, an important source rock of oil in the Neuquén Basin (Muttoni & Kent, 2016). And in North America, the Gulf of Mexico ("Gulf" in Figure 7a) resided at 10–15°N within the presumed boreal arid tropical belt during the Middle Jurassic when the Louann Salt was deposited. During the Late Jurassic polar shift, the Gulf drifted to ~30°N into a presumed more temperate belt, and the Late Jurassic Smackover and Bossier source rocks were deposited (Figure 7f; Muttoni & Kent, 2016). Other examples of abrupt sedimentary facies changes associated with the Late Jurassic monster polar shift can be expected to emerge.

The Jurassic monster shift also had important tectonic implications. For example, the Mt. Tatlow reference locality in southern British Columbia (Figure 7a) would have migrated rapidly from ~44°N at 160 Ma to ~68°N at 148 Ma to then migrate south to ~60°N by 120 Ma (Figure 7f). This change of motion of the western margin of North America from clockwise (monster shift) to counterclockwise (postshift rebound) caused a switch from sinistral to dextral convergence with the approaching Wrangellia and Stikinia exotic terranes, in line with geologic evidences as documented in Kent and Irving (2010).

## 7. Conclusions

We have elaborated on the character of the Jurassic global-composite APWP, which has long been a matter of debate (e.g., May & Butler, 1986, vs. Besse & Courtillot, 2002, vs. Kent & Irving, 2010, vs. Torsvik et al., 2012) and showed the following:

1. Poles from the Late Jurassic Morrison Fm. from the Colorado Plateau (e.g., Steiner & Helsley, 1975), which have often been used in reference APWPs since May and Butler (1986), are affected by a pervasive overprint of presumably Cretaceous age, precluding *E*/*I* analysis of *I* error and are therefore of limited value for APWP determination. The inclusion in reference APWPs of low-quality Jurassic paleomagnetic data from the Colorado Plateau as well as central Europe has tended to obscure what appears to be a real, pronounced feature referred to colloquially as the Jurassic monster polar shift.
2. Reliable Jurassic poles that have hardly been taken into consideration for construction of global-composite APWPs come from parauthocthonous Adria in the Southern Alps of Italy, which is a tectonic promontory of Africa and can thus be incorporated directly in plate reconstructions. Following Channell et al. (2010) and Muttoni et al. (2013), we obtained a revised set of seven Late Jurassic poles ranging in age from 143 to 158 Ma, bracketed by poles at 50, 128, and 238 Ma for control, from parauthocthonous Adria in the Southern Alps that are based on detailed sampling from strata with unambiguous time order that allowed their magnetobiostratigraphies to be correlated to the reference M-sequence time scale and the directions to be checked and corrected for *I* error.
3. These parauthocthonous Adria poles provide an excellent confirmation of the magnitude and timing of the so-called Jurassic monster shift between nominally 160 and 145 Ma, which is a unique feature of the global APWP revealed only when a strict selection of well-dated and inclination flattening-free poles are used (Kent & Irving, 2010; Kent et al., 2015; this study).
4. In North American coordinates, the Jurassic monster shift is a jump of ~30° arc distance from the 190- to 160-Ma stillstand pole at 79.5°N 104.8°E A95 = 4.0° to the 148 ± 3.5 Ma 148Cusp pole at 60.8°N 200.6°E A95 = 3.1°, the latter defined by the cluster of four Adria poles (northwest Africa) and the Ithaca (North America), Hinlopenstretet (Eurasia), and Swartsruggens-Bumbeni (southern Africa) igneous poles. The mean rate of polar motion calculated using the well-dated (U-Pb perovskite) Ontario (Kent et al., 2015) and Ithaca (Van Fossen & Kent, 1993) kimberlites poles from North America is 1.9°/Myr.
5. The Jurassic monster shift was common to the assembled continents, now including parauthocthonous Adria of northwest Africa, and most probably represents an episode of TPW, a rotation of the whole Earth about a pivot on the equator located, in this case, in the region off western Africa and that may have been triggered by an abrupt mass anomaly, such as the break-off and sinking into the mantle of a subducting slab. An episode of TPW in the Late Jurassic is compatible with the only available contemporaneous data from the Pacific oceanic realm (Fu & Kent, 2018).
6. The Jurassic monster shift controlled the first-order depositional architecture of several sedimentary basins worldwide through synchronous and rapid variations of paleolatitude of sign and magnitude that depend on the position relative to the equatorial Euler pivot. The geocentric axial dipole assumption at the basis of these paleolatitude estimates remains valid for TPW, as a mechanism to account for the Jurassic monster shift, insofar as the geodynamo in the fluid outer core will tend to align with the

rotation axis (due to the Coriolis effect) providing a stable reference frame for paleolatitude estimates even as the whole mantle-lithosphere rotates.

**Acknowledgments**
The data used in this paper can be found in the supporting information. We thank the Associate Editor, Mark Dekkers, Marco Maffione, and an anonymous reviewer for insightful comments on the submitted version of this manuscript. D. K. thanks the U.S. National Science Foundation, the Rutgers Board of Governors, and Lamont-Doherty Earth Observatory for support. LDEO contribution #8296.

## References

Agnini, C., Fornaciari, E., Giusberti, L., Grandesso, P., Lanci, L., Luciani, V., et al. (2011). Integrated biomagnetostratigraphy of the Alano section (NE Italy): A proposal for defining the middle-late Eocene boundary. *Geological Society of America Bulletin*, *123*(5-6), 841–872. https://doi.org/10.1130/B30158.1

Amidon, W. H., Roden-Tice, M., Anderson, A. J., McKeon, R. E., & Shuster, D. L. (2016). Late Cretaceous unroofing of the White Mountains, New Hampshire, USA: An episode of passive margin rejuvenation? *Geology*, *44*(6), 415–418. https://doi.org/10.1130/G37429.1

Aubourg, C., & Rochette, P. (1992). Mise en evidence d'une aimantation pre-tectonique dans les Terres Noires subalpines (Callovien-Oxfordien). *Comptes rendus de l'Academie des sciences Paris. Serie II*, *314*, 591–594.

Bazard, D. R., & Butler, R. F. (1994). Paleomagnetism of the Brushy Basin Member of the Morrison Formation: Implications for Jurassic apparent polar wander. *Journal of Geophysical Research*, *99*(B4), 6695–6710. https://doi.org/10.1029/93JB03208

Besse, J., & Courtillot, V. (1991). Revised and synthetic apparent polar wander paths of the African, Eurasian, North American and Indian Plates, and true polar wander since 200 Ma. *Journal of Geophysical Research*, *96*(B3), 4029–4050. https://doi.org/10.1029/90JB01916

Besse, J., & Courtillot, V. (2002). Apparent and true polar wander and the geometry of the geomagnetic field over the last 200 Myr. *Journal of Geophysical Research*, *107*(B11), 2300. https://doi.org/10.1029/2000JB000050

Brack, P., & Muttoni, G. (2000). High-resolution magnetostratigraphic and lithostratigraphic correlations in Middle Triassic pelagic carbonates from the Dolomites (northern Italy). *Palaeogeography, Palaeoclimatology, Palaeoecology*, *161*(3-4), 361–380. https://doi.org/10.1016/S0031-0182(00)00081-X

Broglio Loriga, C., et al. (1999). The Prati di Stuores/Stuores Wiesen section (Dolomites, Italy): A candidate global Stratotype section and point for the base of the Carnian stage. *Rivista Italiana di Paleontologia e Stratigrafia*, *105*, 37–78.

Bryan, P., & Gordon, R. G. (1986). Rotation of the Colorado Plateau: An analysis of paleomagnetic data. *Tectonics*, *5*(4), 661–667. https://doi.org/10.1029/TC005i004p00661

Bryan, P., & Gordon, R. G. (1990). Rotation of the Colorado Plateau: An updated analysis of paleomagnetic poles. *Geophysical Research Letters*, *17*(10), 1501–1504. https://doi.org/10.1029/GL017i010p01501

Bucker, C., Schult, A., Bloch, W., & Guerreiro, S. D. C. (1986). Rockmagnetism and paleomagnetism of an Early Cretaceous-Late Jurassic dike swarm in Rio Grande Do Norte, Brazil. *Journal of Geophysics-Zeitschrift Fur Geophysik*, *60*, 129–135.

Channell, J. E. T. (1996). Palaeomagnetism and palaeogeography of Adria. *Geological Society, London, Special Publications*, *105*(1), 119–132. https://doi.org/10.1144/GSL.SP.1996.105.01.11

Channell, J. E. T., Bralower, T. J., & Grandesso, P. (1987). Biostratigraphic correlation of Mesozoic polarity chrons CM1 to CM23 at Capriolo and Xausa (Southern Alps, Italy). *Earth and Planetary Science Letters*, *85*(1-3), 203–221. https://doi.org/10.1016/0012-821X(87)90032-X

Channell, J. E. T., Casellato, C. E., Muttoni, G., & Erba, E. (2010). Magnetostratigraphy, nannofossil stratigraphy and apparent polar wander for Adria-Africa in the Jurassic–Cretaceous boundary interval. *Palaegeography, Palaeoclimatology, Palaeoecology*, *293*(1-2), 51–75. https://doi.org/10.1016/j.palaeo.2010.04.030

Channell, J. E. T., & Erba, E. (1992). Early Cretaceous polarity chrons CM0 to CM11 recorded in northern Italian land sections near Brescia. *Earth and Planetary Science Letters*, *108*(4), 161–179. https://doi.org/10.1016/0012-821X(92)90020-V

Channell, J. E. T., Erba, E., & Lini, A. (1993). Magnetostratigraphic calibration of the Late Valanginian carbon isotope event in pelagic limestones from Northern Italy and Switzerland. *Earth and Planetary Science Letters*, *118*(1-4), 145–166. https://doi.org/10.1016/0012-821X(93)90165-6

Channell, J. E. T., Erba, E., Muttoni, G., & Tremolada, F. (2000). Early Cretaceous magnetic stratigraphy in the APTICORE drill core and adjacent outcrop at Cismon (Southern Alps, Italy), and correlation to the proposed Barremian-Aptian boundary stratotype. *Geological Society of America Bulletin*, *112*(9), 1430–1443. https://doi.org/10.1130/0016-7606(2000)112<1430:ECMSIT>2.0.CO;2

Channell, J. E. T., Erba, E., Nakanishi, M., & Tamaki, K. (1995). Late Jurassic-Early Cretaceous time scales and oceanic magnetic anomaly block models. In W. A. Berggren, D. V. Kent, M.-P. Aubry, & J. Hardenbol (Eds.), *Geochronology, time scales and global stratigraphic correlations* (pp. 51–63).

Channell, J. E. T., & Horvath, F. (1976). The African/Adriatic promontory as a palaeogeographical premise for Alpine orogeny and plate movements in the Carpatho-Balkan region. *Tectonophysics*, *35*(1-3), 71–101. https://doi.org/10.1016/0040-1951(76)90030-5

Courtillot, V., Besse, J., & Theveniaut, H. (1994). North American Jurassic apparent polar wander: The answer from other continents? *Physics of the Earth and Planetary Interiors*, *82*(2), 87–104. https://doi.org/10.1016/0031-9201(94)90082-5

Dallanave, E., Agnini, C., Muttoni, G., & Rio, D. (2009). Magneto-biostratigraphy of the Cicogna section (Italy): Implications for the late Paleocene-early Eocene time scale. *Earth and Planetary Science Letters*, *285*(1-2), 39–51. https://doi.org/10.1016/j.epsl.2009.05.033

Dallanave, E., Agnini, C., Muttoni, G., & Rio, D. (2012). Paleocene magneto-biostratigraphy and climate-controlled rock magnetism from the Belluno Basin, Tethys Ocean, Italy. *Palaeogeography, Palaeoclimatology, Palaeoecology*, *337-338*, 130–142. https://doi.org/10.1016/j.palaeo.2012.04.007

Fu, R. R., & Kent, D. V. (2018). Anomalous Late Jurassic motion of the Pacific Plate with implications for true polar wander. *Earth and Planetary Science Letters*, *490*, 20–30. https://doi.org/10.1016/j.epsl.2018.02.034

Gehring, A. U., Keller, P., & Heller, F. (1991). Paleomagnetism and tectonics of the Jura arcuate mountain belt in France and Switzerland. *Tectonophysics*, *186*(3–4), 269–278. https://doi.org/10.1016/0040-1951(91)90363-W

Gialanella, P. R., Heller, F., Mietto, P., Incoronato, A., De Zanche, V., Gianolla, P., & Roghi, G. (2001). Magnetostratigraphy and biostratigraphy of the Middle Triassic Margon section (Southern Alps, Italy). *Earth and Planetary Science Letters*, *187*(1-2), 17–25. https://doi.org/10.1016/S0012-821X(01)00275-8

Gordon, R. G., Cox, A., & O'Hare, S. (1984). Paleomagnetic Euler poles and the apparent polar wander and absolute motion of North America since the Carboniferous. *Tectonics*, *3*(5), 499–537. https://doi.org/10.1029/TC003i005p00499

Gose, W. A., & Kyle, R. J. (1993). Paleomagnetic dating of sulfide mineralization and cap-rock formation in Gulf Coast salt domes. *SEPM Special Publication*, *49*, 157–166.

Greff-Lefftz, M., & Besse, J. (2014). Sensitivity experiments on True Polar Wander. *Geochemistry, Geophysics, Geosystems*, *15*, 4599–4616. https://doi.org/10.1002/2014GC005504

Hagstrum, J. T. (1993). North American Jurassic APW: The current dilemma. *Eos, Transactions of the American Geophysical Union*, *74*, 65–69.
Hagstrum, J. T. (1994). Remagnetization of Jurassic volcanic rocks in the Santa Rita and Patagonia Mountains, Arizona: Implications for North American apparent polar wander. *Journal of Geophysical Research*, *99*(B8), 15103. https://doi.org/10.1029/94JB01056
Halvorsen, E. (1989). A paleomagnetic pole position of Late Jurassic/Early Cretaceous dolerites from Hinlopenstretet, Svalbard, and its tectonic implications. *Earth and Planetary Science Letters*, *94*(3-4), 398–408. https://doi.org/10.1016/0012-821X(89)90156-8
Hamilton, W. (1981). Plate-tectonic mechanism of Laramide deformation. *Contributions in Geology, University of Wyoming*, *19*, 87–92.
Hargraves, R. B., Rehacek, J., & Hooper, P. R. (1997). Palaeomagnetism of the Karoo igneous rocks in southern Africa. *South African Journal of Geology*, *100*, 195–212.
Heller, F. (1977). Palaeomagnetism of Upper Jurassic limestones from southern Germany. *Journal of Geophysics*, *42*, 475–488.
Heller, F. (1978). Rockmagnetic studies of Upper Jurassic limestones from southern Germany. *Journal of Geophysics*, *44*, 525–543.
Irving, E., & Irving, G. A. (1982). Apparent polar wander paths Carboniferous through Cenozoic and the assembly of Gondwana. *Geophysical Surveys*, *5*(2), 141–188. https://doi.org/10.1007/Bf01453983
Irving, E., & Wynne, P. J. (1990). Palaeomagnetic evidence bearing on the evolution of the Canadian Cordillera. *Philosophical Transactions of the Royal Society of London*, *331*(1620), 487–509. https://doi.org/10.1098/rsta.1990.0085
Johnson, R. J. E., Van der Voo, R., & Lowrie, W. (1984). Paleomagnetism and late diagenesis of Jurassic carbonates from the Jura Mountains, Switzerland and France. *Geological Society of America Bulletin*, *95*(4), 478–488. https://doi.org/10.1130/0016-7606(1984)95<478:PALDOJ>2.0.CO;2
Kądziałko-Hofmokl, M., Kruczyk, J., & Westphal, M. (1988). Paleomagnetism of Jurassic sediments from the western border of the Rheingraben, Alsace (France). *Journal of Geophysics*, *62*, 102–108.
Kądziałko-Hofmokl, M., & Kruczyk, J. (1987). Paleomagnetism of middle-late Jurassic sediments from Poland and implications for the polarity of the geomagnetic field. *Tectonophysics*, *139*(1–2), 53–66. https://doi.org/10.1016/0040-1951(87)90197-1
Kent, D. V., & Irving, E. (2010). Influence of inclination error in sedimentary rocks on the Triassic and Jurassic apparent polar wander path for North America and implications for Cordilleran tectonics. *Journal of Geophysical Research*, *115*, B10103. https://doi.org/10.11029/12009JB007205
Kent, D. V., Kjarsgaard, B. A., Gee, J. S., Muttoni, G., & Heaman, L. M. (2015). Tracking the Late Jurassic apparent (or true) polar shift in U-Pb-dated kimberlites from cratonic North America (Superior Province of Canada). *Geochemistry Geophysics Geosystems*, *16*, 983–994. https://doi.org/10.1002/2015GC005734
Kent, D. V., Olsen, P. E., Rasmussen, C., Lepre, C., Mundil, R., Irmis, R. B., et al. (2018). Empirical evidence for stability of the 405-kiloyear Jupiter-Venus eccentricity cycle over hundreds of millions of years. *Proceedings of the National Academy of Sciences*, *115*(24), 6153–6158. https://doi.org/10.1073/pnas.1800891115
Kent, D. V., & Witte, W. K. (1993). Slow apparent polar wander for North America in the Late Triassic and large Colorado Plateau rotation. *Tectonics*, *12*(1), 291–300. https://doi.org/10.1029/92TC01966
Klitgord, K. D., & Schouten, H. (1986). In B. E. Tucholke & P. R. Vogt (Eds.), *Plate kinematics of the central Atlantic* (pp. 351–378). Boulder, CO: Geological Society of America.
Kluth, C. F., Butler, R. F., & Harding, L. E. (1982). Paleomagnetism of Late Jurassic rock in the northern Canelo Hills, southeastern Arizona. *Journal of Geophysical Research*, *87*(B8), 7079–7086. https://doi.org/10.1029/JB087iB08p07079
Kowallis, B. J., Christiansen, E. H., Deino, A. L., Peterson, F., Turner, C. E., Kunk, M. J., & Obradovich, J. D. (1998). The age of the Morrison Formation. *Modern Geology*, *22*, 235–260.
Kruczyk, J., & Kądziałko-Hofmokl, M. (1988). Paleomagnetism of Oxfordian sediments from the Halokinetic structure in Kujawy, central Poland. In *2nd International Symposium on Jurassic Stratigraphy* (pp. 1139–1150). Lisbon, Portugal: National Institute of Scientific Research.
Lowrie, W., & Alvarez, W. (1977). Upper Cretaceous-Paleocene magnetic stratigraphy at Gubbio, Italy. III. Upper Cretaceous magnetic stratigraphy. *Geological Society of America Bulletin*, *88*(3), 374–377. https://doi.org/10.1130/0016-7606(1977)88<374:UCMSAG>2.0.CO;2
Malinverno, A., Hildebrandt, J., Tominaga, M., & Channell, J. E. T. (2012). M-sequence geomagnetic polarity time scale (MHTC12) that steadies global spreading rates and incorporates astrochronology constraints. *Journal of Geophysical Research*, *117*, PA4221. https://doi.org/10.1029/2012JB009260
Manabe, S., & Bryan, K. (1985). $CO_2$-induced change in a coupled ocean-atmosphere model and its paleoclimatic implications. *Journal of Geophysical Research*, *90*(C6), 11,689–11,707. https://doi.org/10.1029/JC090iC06p11689
Mattei, M., Muttoni, G., & Cifelli, F. (2014). A record of the Jurassic massive plate shift from the Garedu Formation of central Iran. *Geology*, *42*(6), 555–558. https://doi.org/10.1130/G35467.1
May, S. R., & Butler, R. F. (1986). North American Jurassic apparent polar wander: Implications for plate motion, paleogeography and Cordilleran tectonics. *Journal of Geophysical Research*, *91*(B11), 11,519–11,544. https://doi.org/10.1029/JB091iB11p11519
McWhinnie, S. T., Van der Pluijm, B. A., & Van der Voo, R. (1990). Remagentizations and thrusting in the Idaho-Wyoming overthrust belt. *Journal of Geophysical Research*, *95*(B4), 4551–4559. https://doi.org/10.1029/JB095iB04p04551
Muller, R. D., Royer, J. Y., & Lawver, L. A. (1993). Revised plate motions relative to the hotspots from combined Atlantic and Indian Ocean hotspot tracks. *Geology*, *21*(3), 275–278. https://doi.org/10.1130/0091-7613(1993)021<0275:RPMRTT>2.3.CO;2
Muttoni, G., Dallanave, E., & Channell, J. E. T. (2013). The drift history of Adria and Africa from 280 Ma to present, Jurassic true polar wander, and zonal climate control on Tethyan sedimentary facies. *Palaeogeography, Palaeoecology, Palaeoclimatology*, *386*, 415–435. https://doi.org/10.1016/j.palaeo.2013.06.011
Muttoni, G., Erba, E., Kent, D. V., & Bachtadse, V. (2005). Mesozoic Alpine facies deposition as a result of past latitudinal plate motion. *Nature*, *434*(7029), 59–63. https://doi.org/10.1038/nature03378
Muttoni, G., Garzanti, E., Alfonsi, L., Cirilli, S., Germani, D., & Lowrie, W. (2001). Motion of Africa and Adria since the Permian: Paleomagnetic and paleoclimatic constraints from northern Libya. *Earth and Planetary Science Letters*, *192*(2), 159–174. https://doi.org/10.1016/S0012-821X(01)00439-3
Muttoni, G., & Kent, D. V. (2016). A novel plate tectonic scenario for the genesis and sealing of some major mesozoic oil fields. *GSA Today*, *26*(12), 4–10.
Muttoni, G., Kent, D. V., Brack, P., Nicora, A., & Balini, M. (1997). Middle Triassic magnetostratigraphy and biostratigraphy from the Dolomites and Greece. *Earth and Planetary Science Letters*, *146*(1-2), 107–120. https://doi.org/10.1016/S0012-821X(96)00216-6
Muttoni, G., Kent, D. V., Garzanti, E., Brack, P., Abrahamsen, N., & Gaetani, M. (2003). Early Permian Pangea "B" to Late Permian Pangea "A". *Earth and Planetary Science Letters*, *215*(3-4), 379–394. https://doi.org/10.1016/S0012-821X(03)00452-7

Muttoni, G., Visconti, A., Channell, J. E. T., Casellato, C. E., Maron, M., & Jadoul, F. (2018). An expanded Tethyan Kimmeridgian magneto-biostratigraphy from the S'Adde section (Sardinia): Implications for the Jurassic timescale. *Palaeogeography, Palaeoclimatology, Palaeoecology*, *503*, 90–101. https://doi.org/10.1016/j.palaeo.2018.04.019

Nairn, A. E. M., Schmitt, T. J., & Smithwick, M. E. (1981). A palaeomagnetic study of the Upper Mesozoic succession in Northern Tunisia. *Geophysical Journal of the Royal Astronomical Society*, *65*(1), 1–18. https://doi.org/10.1111/j.1365-246X.1981.tb02697.x

Pellenard, P., Nomade, S., Martire, L., De Oliveira Ramalho, F., Monna, F., & Guillou, H. (2013). The first $^{40}Ar$–$^{39}Ar$ date from Oxfordian ammonite-calibrated volcanic layers (bentonites) as a tie-point for the Late Jurassic. *Geological Magazine*, *150*(06), 1136–1142. https://doi.org/10.1017/S0016756813000605

Peterson, F., & Turner, C. E. (1998). Stratigraphy of the Ralston Creek and Morrison Formations (Upper Jurassic) near Denver, Colorado. *Modern Geology*, *22*, 3–38.

Phillips, D. (1991). Argon isotope and halogen chemistry of phlogopite from South African kimberlites: A combined step-heating, laser probe, electron microprobe and TEM study. *Chemical Geology (Isotope Geoscience Section)*, *87*(2), 71–98. https://doi.org/10.1016/0168-9622(91)90043-V

Phillips, J. D., & Forsyth, D. (1972). Plate tectonics, paleomagnetism and the opening of the Atlantic. *Geological Society of America Bulletin*, *83*(6), 1579–1600. https://doi.org/10.1130/0016-7606(1972)83[1579:PTPATO]2.0.CO;2

Reeve, S. C. (1975). *Paleomagnetic studies of sedimentary rocks of Cambrian and Triassic age* (p. 426). Dallas: University of Texas at Dallas.

Roest, W. R., Danobeitia, J. J., Verhoef, J., & Collette, B. J. (1992). Magnetic anomalies in the Canary Basin and the Mesozoic evolution of the central North Atlantic. *Marine Geophysical Research*, *14*(1), 1–24. https://doi.org/10.1007/BF01674063

Royer, J.-Y., Müller, R. D., Gahagan, L. M., Lawver, L. A., Mayes, C. L., Nürnberg, D., & Sclater, J. G. (1992). A global isochron chart. *University of Texas Institute for Geophysics Technical Report*, *117*, 38.

Satolli, S., Besse, J., Speranza, F., & Calamita, F. (2007). The 125–150 Ma high-resolution Apparent Polar Wander Path for Adria from magnetostratigraphic sections in Umbria–Marche (Northern Apennines, Italy): Timing and duration of the global Jurassic–Cretaceous hairpin turn. *Earth and Planetary Science Letters*, *257*(1–2), 329–342. https://doi.org/10.1016/j.epsl.2007.03.009

Satolli, S., & Turtù, A. (2016). Early Cretaceous magnetostratigraphy of the Salto del Cieco section (Northern Apennines, Italy). *Newsletters on Stratigraphy*, *49*(2), 361–382. https://doi.org/10.1127/nos/2016/0076

Sigloch, K., & Mihalynuk, M. (2013). Intra-oceanic subduction shaped the assembly of Cordilleran North America. *Nature*, *496*(7443), 50–56. https://doi.org/10.1038/nature12019

Srivastava, S. P., & Tapscott, C. R. (1986). Plate kinematics of the North Atlantic. In B. E. Tucholke & P. R. Vogt (Eds.), *The geology of North America, The western North Atlantic region* (pp. 379–404). Boulder, CO: Geological Society of America.

Steiner, M. B. (1978). Magnetic polarity during the Middle Jurassic as recorded in the Summerville and Curtis Formations. *Earth and Planetary Science Letters*, *38*(2), 331–345. https://doi.org/10.1016/0012-821X(78)90107-3

Steiner, M. B. (1986). Rotation of the Colorado Plateau. *Tectonics*, *5*(4), 649–660. https://doi.org/10.1029/TC005i004p00649

Steiner, M. B. (1988). Paleomagnetism of the Late Pennsylvanian and Permian: A test of the rotation of the Colorado Plateau. *Journal of Geophysical Research*, *93*(B3), 2201–2215. https://doi.org/10.1029/JB093iB03p02201

Steiner, M. B., & Helsley, C. E. (1975). Reversal pattern and apparent polar wander for the Late Jurassic. *Geological Society of America Bulletin*, *86*(11), 1537–1543. https://doi.org/10.1130/0016-7606(1975)86<1537:RPAAPW>2.0.CO;2

Tauxe, L. (2010). *Essentials of paleomagnetism* (Vol. 512). Berkeley: University of California Press.

Tauxe, L., & Kent, D. V. (2004). A simplified statistical model for the geomagnetic field and the detection of shallow bias in paleomagnetic inclinations: Was the ancient magnetic field dipolar? In J. E. T. Channell, D. V. Kent, W. Lowrie, & J. Meert (Eds.), *Timescales of the paleomagnetic field, geophysical monograph 145* (pp. 101–116). Washington, DC: American Geophysical Union.

Tauxe, L., Shaar, R., Jonestrask, L., Swanson-Hysell, N. L., Minnett, R., Koppers, A. A. P., et al. (2016). PmagPy: Software package for paleomagnetic data analysis and a bridge to the Magnetics Information Consortium (MagIC) database. *Geochemistry, Geophysics, Geosystems*, *17*, 2450–2463. https://doi.org/10.1002/2016GC006307

Torsvik, T. H., Muller, R. D., Van der Voo, R., Steinberger, B., & Gaina, C. (2008). Global plate motion frames: Toward a unified model. *Reviews of Geophysics*, *46*, RG3004. https://doi.org/10.1029/2007RG000227

Torsvik, T. H., Van der Voo, R., Preeden, U., Mac Niocaill, C., Steinberger, B., Doubrovine, P. V., et al. (2012). Phanerozoic polar wander, palaeogeography and dynamics. *Earth-Science Reviews*, *114*(3-4), 325–368. https://doi.org/10.1016/j.earscirev.2012.06.007

Tsai, V. C., & Stevenson, D. J. (2007). Theoretical constraints on true polar wander. *Journal of Geophysical Research*, *112*, B05415. https://doi.org/10.01029/02005JB003923

Van der Voo, R. (1993). *Paleomagnetism of the Atlantic, Tethys and Iapetus Oceans* (p. 411). Cambridge: Cambridge University Press.

Van der Voo, R., Van Hinsbergen, D. J. J., Domeier, M., Spakman, W., & Torsvik, T. H. (2015). Latest Jurassic–earliest Cretaceous closure of the Mongol-Okhotsk Ocean: A paleomagnetic and seismological-tomographic analysis. *Geological Society of America Special Paper*, *513*(19), 589–606. https://doi.org/10.1130/2015.2513

Van Fossen, M. C., & Kent, D. V. (1990). High-latitude paleomagnetic poles from Middle Jurassic plutons and Moat Volcanics in New England and the controversy regarding Jurassic apparent polar wander for North America. *Journal of Geophysical Research*, *95*(B11), 17,503–517,516. https://doi.org/10.1029/JB095iB11p17503

Van Fossen, M. C., & Kent, D. V. (1992). Paleomagnetism of the Front Range Morisson Formation and an alternative model of late Jurassic apparent polar wander for North America. *Geology*, *20*(3), 223–226. https://doi.org/10.1130/0091-7613(1992)020<0223:POTFRC>2.3.CO;2

Van Fossen, M. C., & Kent, D. V. (1993). A palaeomagnetic study of 143 Ma kimberlite dikes in central New York state. *Geophysical Journal International*, *113*(1), 175–185. https://doi.org/10.1111/j.1365-246X.1993.tb02538.x

*Journal of Geophysical Research*

Supporting Information for

# Jurassic monster polar shift confirmed by sequential paleopoles from Adria, promontory of Africa

G. Muttoni[1], D. V. Kent[2]

[1] Dipartimento di Scienze della Terra 'Ardito Desio', Università degli Studi di Milano, via Mangiagalli 34, I-20133 Milan, Italy.

[2] Earth and Planetary Sciences, Rutgers University, Piscataway, NJ 08854, USA, and Lamont-Doherty Earth Observatory of Columbia University, Palisades, NY 10964, USA.

Corresponding author: Giovanni Muttoni (giovanni.muttoni1@unimi.it)

## Contents of this file

Supporting Information 1: Text S1, Figures S1 and S2.
Supporting Information 2: Tables S1, S2, S3, S4.
Supporting Information 3: Text S2, Figures S3, S4, S5, S6, S7, Tables S5, S6, S7, S8, S9.

## Introduction

Supporting Information 1 (Text S1 and Figures S1 and S2) refers to a critical analysis of poles in the 200–100 Ma interval used in *Torsvik et al.* (2008) and *Besse and Courtillot* (2002) to define their APWPs.

Supporting Information 2 reports the thermal demagnetization data of samples from the lower Morrison Fm. (Table S1) and the upper Morrison Fm. (Table S2), as well as the 'B' component directions (Table S3) and 'Ch' component directions (Table S4) extracted by means of least-square analysis.

Supporting Information 3 (Text S2, Figures S3 to S7, and Tables S5 to S9) refers to the magneto-biostratigraphic data and analyses used to define poles of this study: Bombatierle 158Bomb, Foza 158Foz, Colme di Vignola 154Vig, Sciapala 150Sci, and Passo del Branchetto 150Branch.

## Supporting Information 1

### Text S1. Poles in the 200–100 Ma interval used in *Torsvik et al.* (2008) and *Besse and Courtillot* (2002).

Beside meeting the usual minimum quality assessments (i.e., q≥3), the inventory of acceptable poles in *Torsvik et al.* (2008) (which is essentially the same as used in *Torsvik et al.*, 2012) were further critiqued by *Kent and Irving* (2010) according to dating issues but more critically by the general lack of *I*-error control on data from sedimentary units, which resulted in their preemptive exclusion from further consideration. Here we focus discussion on those poles especially in the interval of 170-140 Ma used by *Torsvik et al.* (2012) that seemed to have missed providing clear evidence of the 30° polar shift that we confirm to have occurred between 160 and 145 Ma.

Poles of *Torsvik et al.* (2012, their Table 1) are plotted for the broader 200–100 Ma interval as a frequency distribution histogram with vertical bars that represent numbers of observations within 5 Myr bins (**Fig. S1**). The interval from 160 to 140 Ma has relatively sparse data. The monster shift onset (bin at 160 Ma) is overwhelmingly represented by entries from Late Jurassic sediments from Europe. The Callovian–Oxfordian Blue Limestones from the Jura Mountains of France and Switzerland, which have apparently escaped pervasive remagnetization observed in other Late Jurassic tan-colored limestones in the region, yielded a pole (77.7°N, 148.4°E; *Johnson et al.*, 1984) that, when rotated to North American coordinates using the total closure Euler pole of (*Srivastava and Tapscott*, 1986), falls at 78.1°N, 143.3°E, not too far from the high latitude 156.1±1.6 Ma Ontario kimberlites pole (75.5°N, 189.5°E) of *Kent et al.* (2015) or the high latitude Front Range Morrison pole (83.7°N, 150.4°E) of *Van Fossen and Kent* (1992). The Blue Limestones pole could therefore be broadly compatible with these high latitude poles (as well as with additional high latitude poles from Adria such as 158Foz and 158Bomb discussed in the main text at the onset of the monster shift), albeit its position needs to be checked with a direct assessment of sedimentary *I*-error, at present lacking. Very similar

considerations can be applied to the Callovian–Oxfordian Terres Noires pole from France (*Aubourg and Rochette*, 1992, Global Paleomagnetic Database – GPDB – entry #3156), the pole from Callovian–Oxfordian Krakow-Czestochowa Upland limestones of Poland and the Bajocian–Oxfordian Subtatric Nappe sediments of Poland (*Kądziałko-Hofmokl and Kruczyk*, 1987, GPDB #1948), and the pole from Oxfordian sediments from the Pieniny Klippen Belt of Poland (*Kądziałko-Hofmokl et al.*, 1988, GPDB #616), which all lack *I*-error diagnosis and correction and may also have suffered postdepositional rotations and overprinting, especially in the Pieniny Klippen Belt, but nevertheless all fall above 70°N and between 120°E and 140°E upon rotation to North America, close to the Callovian–Oxfordian Blue Limestone and the other high latitude poles described above (Ontario, Front Range, Adria).

Data in the succeeding age bins are instead more problematic insofar as they are dominated in *Torsvik et al.* (2012) by the highly questionable (see main text) lower and upper Morrison poles of *Steiner and Helsley* (1975, GPDB #787) and *Bazard and Butler* (1994, GPDB #2870), corrected for an assumed flattening factor (f) of 0.6 and a Colorado Plateau rotation of 5.4° (whereas rotations of up to 13° have been proposed*; Kent and Witte,* 1993), as well as the Glance Conglomerate pole of the northern Canelo Hills (*Kluth*, 1982, GPDB #1256), in spite of the complicated structural evolution and evidence of post-emplacement metasomatism that these rocks suffered (*Hagstrum*, 1994). Another entry in the critical Late Jurassic interval is a vintage pole from Callovian–Berriasian limestones and marly limestones from northern Tunisia (*Nairn et al.*, 1981) that nominally straddles the entire monster shift time interval but which has no *I*-error diagnosis and correction and is in general difficult to evaluate with modern criteria. This Tunisia pole was not corrected for an assumed flattening factor of 0.6 as some other sedimentary poles, for example the Morrison poles (*Torsvik et al.* 2012, their Table 1), presumably because limestones are supposed to be free of inclination flattening compared to clastic facies like sandstones. However, this is not necessarily the case, as shown in this study of Adria carbonate rocks. Severe age uncertainties mar the use of the Rio Grande do Norte dykes pole

from Brazil (*Bucker et al.*, 1986, GPDB #1509) that reportedly span in age from 167 Ma to 125 Ma. *Torsvik et al.* (2012) do include in their compilation the Ithaca kimberlite pole of *Van Fossen and Kent* (1993; GPDB #2717) but both the Hinlopenstretet dikes pole from Svalbard (*Halvorsen*, 1989) and the Swartsruggens-Bumbeni kimberlite pole from southern Africa (*Hargraves et al.,* 1997) were inexplicably excluded and their omission alone virtually obviates the possibility of observing the Jurassic monster shift in the *Torsvik et al.* (2012) APWP.

The earlier but still widely used master APWP of *Besse and Courtillot* (2002) has even fewer entries in the Jurassic monster shift interval compared to *Torsvik et al.* (2012) (**Fig. S2**). The monster shift onset (bin at 160 Ma) is represented by basically the same entries as *Torsvik et al.* (2012) from inclination shallowing-uncorrected Callovian–Oxfordian sediments from Europe (Blue Limestones: *Johnson et al.,* 1984, GPDB #427; Terres Noire: *Aubourg and Rochette*, 1992, GPDP #8204; Krakow-Czestochowa Upland: *Kądziałko-Hofmokl and Kruczyk*, 1987, GPDB #1802; Pieniny Klippen Belt: *Kruczyk and Kądziałko-Hofmokl*, 1988, GPDB #3119). Note that the GPDP entry numbers in *Besse and Courtillot* 2002 are not the same as in *Torsvik et al*. (2012). These poles are augmented by data from Callovian ferrigenous oolitic beds from the Jura Mountains of France and Switzerland (*Gehring et al.*, 1991, GPDP #6501) that represent an extension and confirmation of previous results from the Blue Limestones from the same general area as Johnson et al. (1984). For all these European ~160 Ma poles that plot above 70°N, we refer to considerations made above for *Torsvik et al.* (2012); in short, these poles are broadly consistent with other high latitude poles of similar age such as the Ontario, Front Range, and 158 Ma Adria poles, but lack inclination flattening correction. The European database is completed by an entry from limestones from southern Germany (*Heller*, 1977, GPDP #2289) that the same author subsequently regarded as remagnetized (*Heller*, 1978).

Pole data in *Besse and Courtillot* (2002) of Late Jurassic age are provided by the Ithaca kimberlite pole from North America (*Van Fossen and Kent*, 1993, GPDB #6871) and the Hinlopenstretet dikes pole from Svalbard (*Halvorsen*,

1989, GPDB #6220) in conjunction with a magnetostratigraphy from the Winfield cap dome anhydrites of Louisiana that was tentatively correlated to the latest Jurassic–earliest Cretaceous CM22–CM16 sequence of marine magnetic anomalies (~145 Ma?) (*Gose and Kyle*, 1993, GPDB #7674) even though the pole (76.2°N, 120.5°E) would better conform to an older age of around 160 Ma as admitted also by the authors citing the high latitude Front Range Morrison pole of *Van Fossen and Kent* (1992). Aside from the age uncertainties, this entry comes from the (flat-lying) portion of a dome that rose 6 km through the sedimentary cover from the underlying Middle Jurassic Louann 'mother' salt and hence its 'cratonic' coherence is difficult to assess.

In conclusion, the critical Late Jurassic time interval (160–145 Ma) is relatively poorly represented by reliable poles in these compilations. Hence the importance of chronostratigraphically well constrained poles from parauthocthonous Adria (*Muttoni et al.*, 2013; this study).

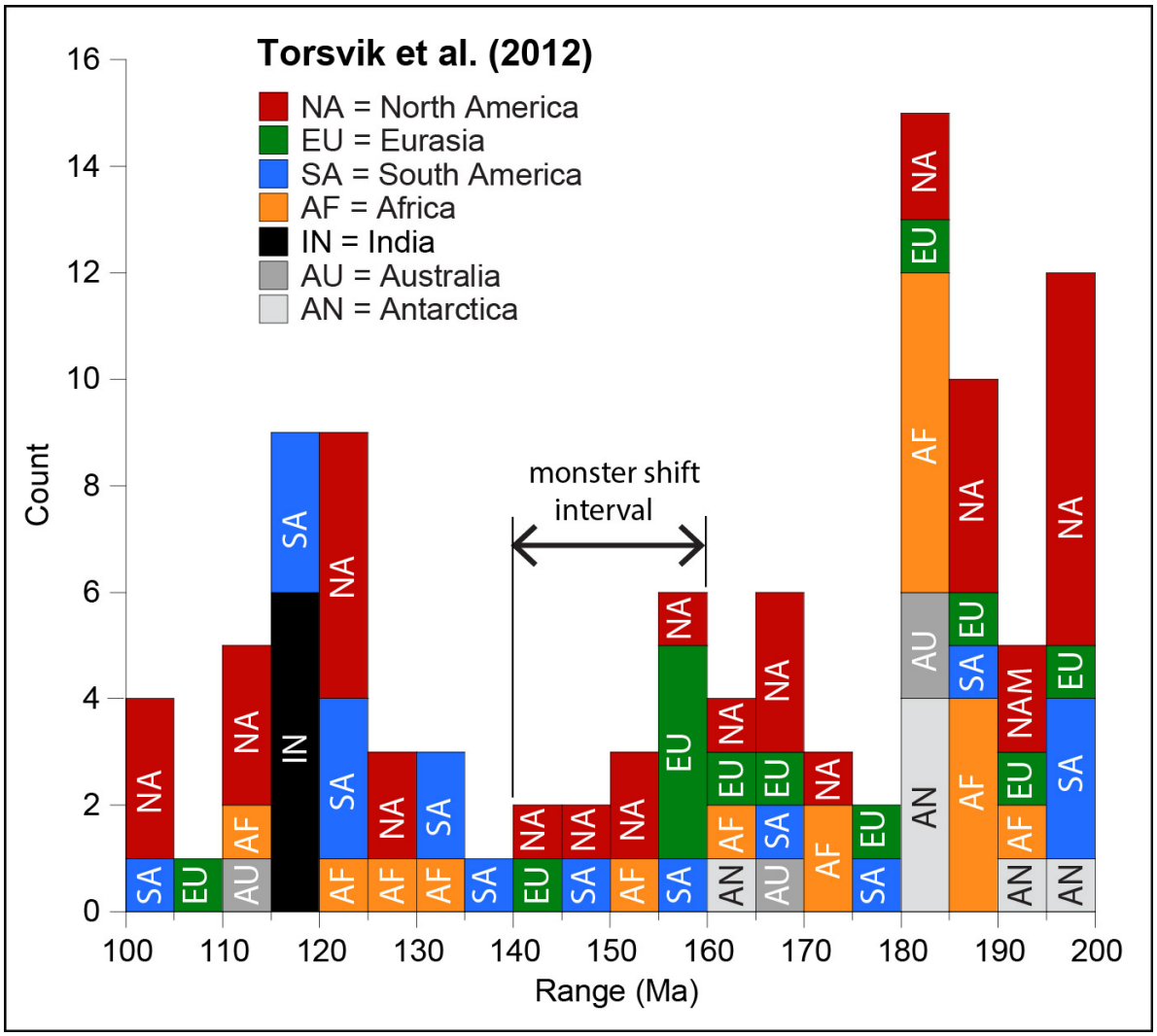


**Figure S1.** Poles of *Torsvik et al.* (2012) plotted for the 200–100 Ma interval as a frequency distribution histogram with vertical bars that represent numbers of observations within 5 Myr bins.

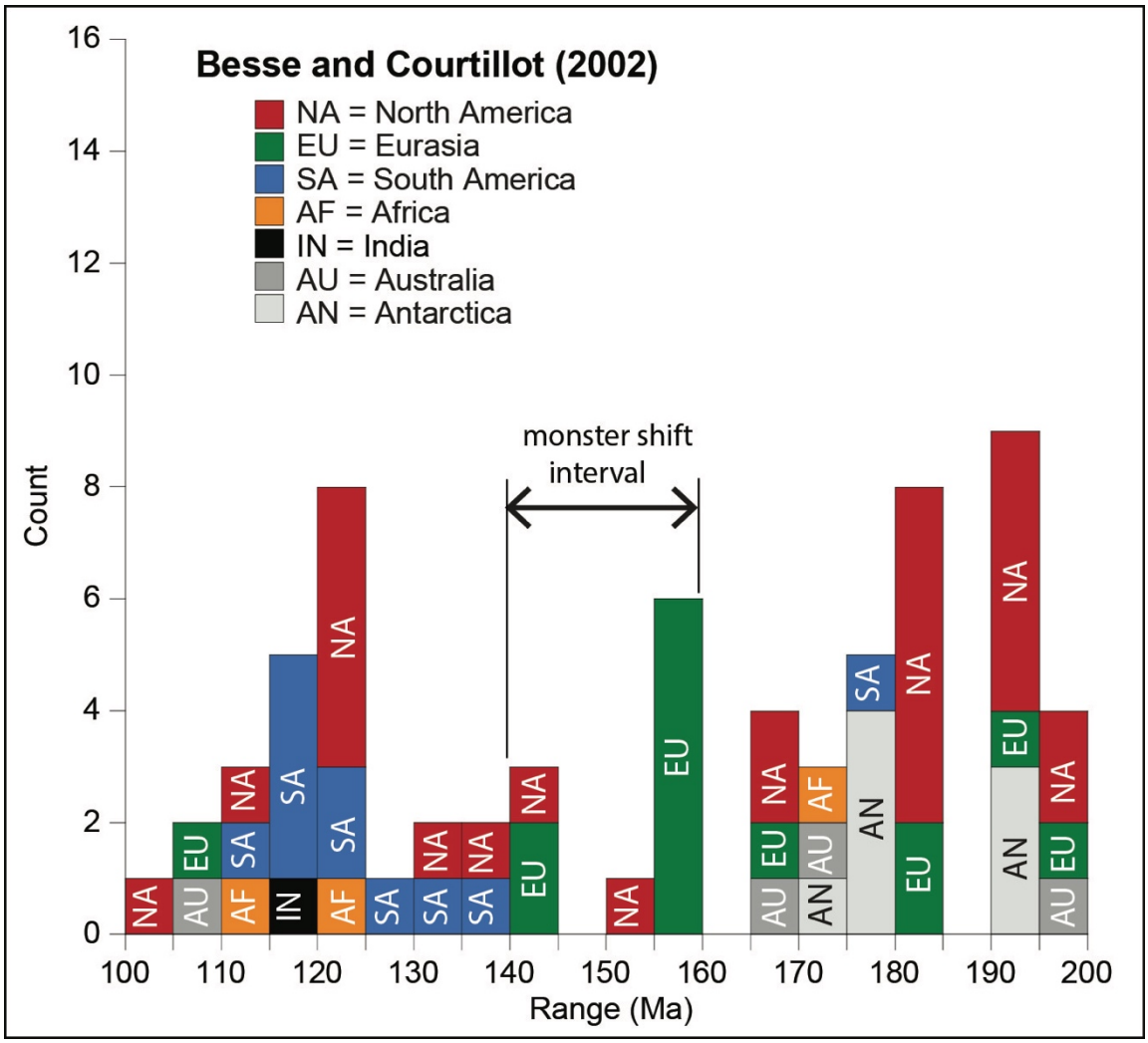


**Figure S2.** Poles of *Besse and Courtillot* (2002) plotted for the 200–100 Ma interval as a frequency distribution histogram with vertical bars that represent numbers of observations within 5 Myr bins.

## Supporting Information 2

Table S1. NRM thermal demagnetization data for samples from sites JMA-JML of the Lower Morrison Fm.

Lamont datafile format:
ID = sample identification (J=Jurassic, M=Morrison, A to L are sampling sites followed by drillcore sample number and specimen with 'a' at the bottom if more than one.
TREAT = demagnetization step (°C) where 0.0 = room temperature (NRM).
MC = machine code where Gh is 2G Model 760 cryogenic magnetometer in horizontal mode.
CD = circular standard deviation (°) of four successive full-vector measurements.
J = magnetization (10E-4 emu, equivalent to 10E-2 A/m for 10 cc volume).
CDECL, CINCL = declination and inclination in core coordinates.
GDECL, GINCL = declination and inclination in geographic (in-situ) coordinates.
BDECL, BINCL = declination and inclination in tilt-corrected coordinates.
SUSC = magnetic susceptibility (10E-6 cgs).

| ID | TREAT | MC | CD | J | CDECL | CINCL | GDECL | GINCL | BDECL | BINCL | SUSC |
|---|---|---|---|---|---|---|---|---|---|---|---|
| JMA01a | 0.0 | Gh | 0 | 0.10187 | 186.8 | 3.1 | 21.2 | 64.3 | 21.2 | 64.3 | 5.0 |
| JMA01a | 100.0 | Gh | 0 | 0.09785 | 182.1 | -0.6 | 9.8 | 61.3 | 9.8 | 61.3 | 2.5 |
| JMA01a | 200.0 | Gh | 0 | 0.08680 | 179.4 | -0.9 | 4.2 | 61.1 | 4.2 | 61.1 | 2.5 |
| JMA01a | 300.0 | Gh | 0 | 0.07849 | 178.7 | -2.5 | 2.8 | 59.5 | 2.8 | 59.5 | 3.0 |
| JMA01a | 400.0 | Gh | 0 | 0.07610 | 177.9 | -3.0 | 1.3 | 58.9 | 1.3 | 58.9 | 4.0 |
| JMA01a | 500.0 | Gh | 0 | 0.08033 | 181.0 | -12.1 | 7.0 | 49.9 | 7.0 | 49.9 | 4.0 |
| JMA01a | 550.0 | Gh | 0 | 0.05109 | 160.3 | -18.0 | 340.6 | 40.2 | 340.6 | 40.2 | 3.0 |
| JMA01a | 600.0 | Gh | 0 | 0.04262 | 170.2 | -7.3 | 348.8 | 53.5 | 348.8 | 53.5 | 3.0 |
| JMA01a | 625.0 | Gh | 0 | 0.03999 | 160.0 | 6.3 | 320.5 | 61.2 | 320.5 | 61.2 | 5.0 |
| JMA01a | 650.0 | Gh | 0 | 0.02674 | 157.2 | 35.4 | 248.6 | 69.3 | 248.6 | 69.3 | 9.0 |
| JMA01a | 660.0 | Gh | 0 | 0.01959 | 135.4 | 17.6 | 279.8 | 47.9 | 279.8 | 47.9 | 13.5 |
| JMA01a | 670.0 | Gh | 0 | 0.02854 | 195.4 | -68.8 | 10.9 | -7.5 | 10.9 | -7.5 | 22.0 |
| JMA01a | 680.0 | Gh | 0 | 0.02167 | 249.1 | -1.8 | 83.6 | 17.4 | 83.6 | 17.4 | 29.0 |
| JMA02a | 0.0 | Gh | 0 | 0.05023 | 3.8 | -23.8 | 358.1 | -76.7 | 358.1 | -76.7 | 4.0 |
| JMA02a | 100.0 | Gh | 0 | 0.05889 | 5.7 | -28.3 | 357.1 | -71.9 | 357.1 | -71.9 | 3.5 |
| JMA02a | 200.0 | Gh | 0 | 0.06724 | 5.8 | -25.1 | 352.9 | -74.9 | 352.9 | -74.9 | 4.0 |
| JMA02a | 300.0 | Gh | 0 | 0.07235 | 10.6 | -20.1 | 326.4 | -76.3 | 326.4 | -76.3 | 4.0 |
| JMA02a | 400.0 | Gh | 0 | 0.07037 | 13.3 | -18.8 | 316.2 | -75.0 | 316.2 | -75.0 | 3.0 |
| JMA02a | 500.0 | Gh | 0 | 0.06339 | 24.5 | -10.7 | 284.9 | -65.9 | 284.9 | -65.9 | 2.0 |
| JMA02a | 550.0 | Gh | 0 | 0.04528 | 14.3 | -36.3 | 338.2 | -61.6 | 338.2 | -61.6 | 3.5 |
| JMA02a | 600.0 | Gh | 2 | 0.04084 | 3.9 | -16.3 | 327.8 | -83.5 | 327.8 | -83.5 | 61.5 |
| JMA02a | 625.0 | Gh | 2 | 0.03755 | 354.7 | -28.2 | 18.4 | -72.1 | 18.4 | -72.1 | 62.0 |
| JMA02a | 650.0 | Gh | 9 | 0.00660 | 198.9 | 20.0 | 121.7 | 69.7 | 121.7 | 69.7 | 69.0 |
| JMA03a | 0.0 | Gh | 0 | 0.08232 | 134.5 | 1.0 | 291.3 | 42.7 | 291.3 | 42.7 | 3.0 |
| JMA03a | 100.0 | Gh | 0 | 0.08480 | 130.7 | 1.0 | 289.5 | 39.2 | 289.5 | 39.2 | 3.5 |
| JMA03a | 200.0 | Gh | 0 | 0.07700 | 125.2 | 2.5 | 285.5 | 34.4 | 285.5 | 34.4 | 3.5 |
| JMA03a | 300.0 | Gh | 0 | 0.08433 | 120.0 | 0.0 | 286.4 | 28.7 | 286.4 | 28.7 | 4.0 |
| JMA03a | 400.0 | Gh | 0 | 0.08553 | 115.8 | -0.4 | 285.4 | 24.6 | 285.4 | 24.6 | 3.0 |

| | | | | | | | | | | | |
|---|---|---|---|---|---|---|---|---|---|---|---|
| JMA03a | 500.0 | Gh | 0 | 0.06803 | 107.3 | 8.0 | 274.2 | 18.7 | 274.2 | 18.7 | 3.5 |
| JMA03a | 550.0 | Gh | 0 | 0.05415 | 74.1 | 6.9 | 266.1 | -13.2 | 266.1 | -13.2 | 3.0 |
| JMA03a | 600.0 | Gh | 0 | 0.05451 | 58.3 | 17.6 | 249.6 | -23.4 | 249.6 | -23.4 | 3.5 |
| JMA03a | 625.0 | Gh | 0 | 0.05504 | 56.8 | 3.0 | 263.9 | -30.7 | 263.9 | -30.7 | 4.0 |
| JMA03a | 650.0 | Gh | 0 | 0.05351 | 65.4 | 13.7 | 256.4 | -18.9 | 256.4 | -18.9 | 6.5 |
| JMA03a | 660.0 | Gh | 0 | 0.05312 | 63.7 | -4.6 | 274.5 | -26.5 | 274.5 | -26.5 | 8.5 |
| JMA03a | 670.0 | Gh | 0 | 0.04142 | 104.0 | -8.2 | 289.3 | 11.0 | 289.3 | 11.0 | 15.0 |
| JMA03a | 680.0 | Gh | 0 | 0.01221 | 61.5 | -46.4 | 322.3 | -31.1 | 322.3 | -31.1 | 21.5 |
| | | | | | | | | | | | |
| JMA04a | 0.0 | Gh | 0 | 0.04948 | 186.1 | 39.1 | 148.2 | 79.6 | 148.2 | 79.6 | 2.0 |
| JMA04a | 100.0 | Gh | 0 | 0.03587 | 177.4 | 36.9 | 192.1 | 82.8 | 192.1 | 82.8 | 2.0 |
| JMA04a | 200.0 | Gh | 0 | 0.03007 | 173.3 | 43.0 | 196.0 | 75.9 | 196.0 | 75.9 | 2.5 |
| JMA04a | 300.0 | Gh | 0 | 0.01993 | 197.4 | 33.0 | 101.3 | 74.9 | 101.3 | 74.9 | 3.5 |
| JMA04a | 400.0 | Gh | 0 | 0.01600 | 182.0 | 18.8 | 5.1 | 78.7 | 5.1 | 78.7 | 3.0 |
| JMA04a | 500.0 | Gh | 0 | 0.01564 | 254.1 | -10.4 | 68.3 | 8.2 | 68.3 | 8.2 | 3.0 |
| JMA04a | 550.0 | Gh | 0 | 0.02476 | 259.1 | -1.8 | 67.9 | 8.5 | 67.9 | 8.5 | 2.5 |
| JMA04a | 600.0 | Gh | 0 | 0.02880 | 257.3 | -8.4 | 61.3 | 6.6 | 61.3 | 6.6 | 2.0 |
| JMA04a | 625.0 | Gh | 0 | 0.03307 | 269.3 | -14.6 | 61.9 | -6.7 | 61.9 | -6.7 | 2.0 |
| JMA04a | 650.0 | Gh | 0 | 0.01560 | 242.8 | -6.6 | 54.8 | 19.6 | 54.8 | 19.6 | 4.0 |
| | | | | | | | | | | | |
| JMA05a | 0.0 | Gh | 0 | 0.06148 | 251.1 | -22.8 | 68.4 | 11.8 | 68.4 | 11.8 | 3.0 |
| JMA05a | 100.0 | Gh | 0 | 0.06003 | 254.9 | -29.8 | 62.8 | 6.2 | 62.8 | 6.2 | 4.0 |
| JMA05a | 200.0 | Gh | 0 | 0.06111 | 267.8 | -33.8 | 61.9 | -5.4 | 61.9 | -5.4 | 2.5 |
| JMA05a | 300.0 | Gh | 0 | 0.06513 | 287.8 | -28.9 | 69.2 | -21.7 | 69.2 | -21.7 | 3.0 |
| JMA05a | 400.0 | Gh | 0 | 0.06221 | 300.7 | -22.2 | 77.2 | -33.1 | 77.2 | -33.1 | 3.0 |
| JMA05a | 500.0 | Gh | 0 | 0.06867 | 301.6 | -21.2 | 78.4 | -33.9 | 78.4 | -33.9 | 3.5 |
| JMA05a | 550.0 | Gh | 0 | 0.06327 | 273.4 | -29.2 | 67.4 | -9.2 | 67.4 | -9.2 | 2.5 |
| JMA05a | 600.0 | Gh | 0 | 0.06493 | 288.4 | -21.4 | 77.3 | -21.6 | 77.3 | -21.6 | 2.0 |
| JMA05a | 625.0 | Gh | 0 | 0.05398 | 317.3 | -33.8 | 59.8 | -46.1 | 59.8 | -46.1 | 4.5 |
| JMA05a | 650.0 | Gh | 0 | 0.04472 | 303.9 | -14.8 | 86.3 | -35.6 | 86.3 | -35.6 | 6.5 |
| JMA05a | 660.0 | Gh | 0 | 0.03747 | 306.5 | -23.6 | 75.4 | -38.4 | 75.4 | -38.4 | 10.0 |
| JMA05a | 670.0 | Gh | 0 | 0.02576 | 297.7 | -51.5 | 43.7 | -27.3 | 43.7 | -27.3 | 15.0 |
| JMA05a | 680.0 | Gh | 0 | 0.01699 | 352.9 | 27.6 | 175.9 | -48.8 | 175.9 | -48.8 | 20.0 |
| | | | | | | | | | | | |
| JMA06a | 0.0 | Gh | 0 | 0.06236 | 219.8 | 8.0 | 91.4 | 50.6 | 91.4 | 50.6 | 1.0 |
| JMA06a | 100.0 | Gh | 0 | 0.05080 | 212.0 | 8.5 | 90.1 | 58.3 | 90.1 | 58.3 | 3.0 |
| JMA06a | 200.0 | Gh | 0 | 0.04147 | 219.1 | 9.1 | 93.0 | 51.5 | 93.0 | 51.5 | 2.0 |
| JMA06a | 300.0 | Gh | 0 | 0.02840 | 209.7 | 19.5 | 111.9 | 60.5 | 111.9 | 60.5 | 3.0 |
| JMA06a | 400.0 | Gh | 0 | 0.01789 | 197.3 | 40.4 | 158.3 | 57.8 | 158.3 | 57.8 | 3.0 |
| JMA06a | 500.0 | Gh | 0 | 0.02228 | 201.0 | 67.5 | 174.0 | 32.8 | 174.0 | 32.8 | 2.0 |
| JMA06a | 550.0 | Gh | 0 | 0.03656 | 257.9 | 58.2 | 140.5 | 16.5 | 140.5 | 16.5 | 3.0 |
| JMA06a | 600.0 | Gh | 0 | 0.04606 | 240.5 | 52.6 | 136.5 | 27.2 | 136.5 | 27.2 | 2.0 |
| JMA06a | 625.0 | Gh | 0 | 0.05070 | 256.4 | 44.5 | 126.2 | 18.1 | 126.2 | 18.1 | 3.0 |
| JMA06a | 650.0 | Gh | 0 | 0.03247 | 256.3 | 59.6 | 142.1 | 17.3 | 142.1 | 17.3 | 3.0 |
| | | | | | | | | | | | |
| JMA07a | 0.0 | Gh | 0 | 0.02431 | 1.4 | 59.9 | 212.1 | -17.1 | 212.1 | -17.1 | 3.0 |
| JMA07a | 100.0 | Gh | 0 | 0.02129 | 4.1 | 45.0 | 214.8 | -31.9 | 214.8 | -31.9 | 4.0 |
| JMA07a | 200.0 | Gh | 0 | 0.02832 | 356.5 | 31.6 | 207.2 | -45.3 | 207.2 | -45.3 | 3.5 |
| JMA07a | 300.0 | Gh | 0 | 0.02920 | 339.5 | 37.8 | 191.5 | -35.7 | 191.5 | -35.7 | 2.5 |
| JMA07a | 400.0 | Gh | 0 | 0.01985 | 356.9 | 33.2 | 207.8 | -43.7 | 207.8 | -43.7 | 3.0 |
| JMA07a | 500.0 | Gh | 0 | 0.02927 | 345.5 | 43.5 | 199.0 | -32.0 | 199.0 | -32.0 | 3.0 |
| JMA07a | 550.0 | Gh | 0 | 0.03453 | 339.4 | 28.9 | 186.2 | -43.6 | 186.2 | -43.6 | 3.0 |
| JMA07a | 600.0 | Gh | 0 | 0.04546 | 334.8 | 35.8 | 186.2 | -35.7 | 186.2 | -35.7 | 3.0 |

| | | | | | | | | | | | |
|---|---|---|---|---|---|---|---|---|---|---|---|
| JMA07a | 625.0 | Gh | 0 | 0.04887 | 334.8 | 37.1 | 187.0 | -34.6 | 187.0 | -34.6 | 3.0 |
| JMA07a | 650.0 | Gh | 0 | 0.04130 | 352.4 | 42.2 | 204.6 | -34.3 | 204.6 | -34.3 | 4.5 |
| JMA07a | 660.0 | Gh | 0 | 0.04239 | 336.0 | 44.0 | 191.9 | -29.0 | 191.9 | -29.0 | 6.0 |
| JMA07a | 670.0 | Gh | 0 | 0.03057 | 307.2 | 23.4 | 156.4 | -26.9 | 156.4 | -26.9 | 9.0 |
| JMA07a | 680.0 | Gh | 0 | 0.02638 | 298.7 | 11.1 | 140.2 | -24.6 | 140.2 | -24.6 | 13.0 |
| | | | | | | | | | | | |
| JMA08a | 0.0 | Gh | 0 | 0.02419 | 245.7 | -65.8 | 55.4 | -4.2 | 55.4 | -4.2 | 2.0 |
| JMA08a | 100.0 | Gh | 0 | 0.02796 | 286.4 | -84.8 | 38.6 | -16.4 | 38.6 | -16.4 | 2.0 |
| JMA08a | 200.0 | Gh | 0 | 0.03049 | 355.5 | -66.1 | 35.7 | -38.8 | 35.7 | -38.8 | 3.5 |
| JMA08a | 300.0 | Gh | 0 | 0.04679 | 344.7 | -56.1 | 45.9 | -47.3 | 45.9 | -47.3 | 3.0 |
| JMA08a | 400.0 | Gh | 0 | 0.06056 | 329.6 | -45.3 | 67.3 | -50.4 | 67.3 | -50.4 | 2.5 |
| JMA08a | 500.0 | Gh | 0 | 0.05200 | 342.8 | -35.6 | 67.1 | -64.3 | 67.1 | -64.3 | 2.0 |
| JMA08a | 550.0 | Gh | 0 | 0.04801 | 359.3 | -37.6 | 24.3 | -67.4 | 24.3 | -67.4 | 3.0 |
| JMA08a | 600.0 | Gh | 0 | 0.05457 | 6.7 | -31.6 | 3.8 | -72.3 | 3.8 | -72.3 | 1.5 |
| JMA08a | 625.0 | Gh | 0 | 0.05297 | 353.2 | -36.8 | 37.3 | -67.4 | 37.3 | -67.4 | 3.0 |
| JMA08a | 650.0 | Gh | 0 | 0.06149 | 342.1 | -33.0 | 61.9 | -65.8 | 61.9 | -65.8 | 3.0 |
| | | | | | | | | | | | |
| JMA09a | 0.0 | Gh | 0 | 0.11967 | 336.9 | -33.5 | 71.5 | -61.4 | 71.5 | -61.4 | 4.0 |
| JMA09a | 100.0 | Gh | 0 | 0.12703 | 343.4 | -34.5 | 61.7 | -64.6 | 61.7 | -64.6 | 3.0 |
| JMA09a | 200.0 | Gh | 0 | 0.13349 | 340.2 | -34.1 | 66.7 | -63.1 | 66.7 | -63.1 | 3.5 |
| JMA09a | 300.0 | Gh | 0 | 0.14185 | 337.0 | -35.9 | 67.6 | -59.9 | 67.6 | -59.9 | 4.5 |
| JMA09a | 400.0 | Gh | 0 | 0.14831 | 339.6 | -38.6 | 60.9 | -59.5 | 60.9 | -59.5 | 3.0 |
| JMA09a | 500.0 | Gh | 0 | 0.15919 | 342.8 | -32.5 | 65.9 | -65.8 | 65.9 | -65.8 | 3.0 |
| JMA09a | 550.0 | Gh | 0 | 0.15055 | 342.7 | -25.3 | 80.9 | -70.2 | 80.9 | -70.2 | 2.0 |
| JMA09a | 600.0 | Gh | 0 | 0.14419 | 337.0 | -21.3 | 96.8 | -66.9 | 96.8 | -66.9 | 2.5 |
| JMA09a | 625.0 | Gh | 0 | 0.12873 | 336.8 | -18.3 | 104.4 | -67.3 | 104.4 | -67.3 | 3.0 |
| JMA09a | 650.0 | Gh | 0 | 0.12116 | 333.3 | -30.2 | 80.6 | -60.6 | 80.6 | -60.6 | 3.0 |
| JMA09a | 660.0 | Gh | 0 | 0.10622 | 343.5 | -28.0 | 73.3 | -69.2 | 73.3 | -69.2 | 3.5 |
| JMA09a | 670.0 | Gh | 0 | 0.09495 | 342.4 | -38.9 | 57.2 | -60.7 | 57.2 | -60.7 | 7.0 |
| JMA09a | 680.0 | Gh | 0 | 0.08803 | 343.1 | -13.1 | 119.4 | -73.6 | 119.4 | -73.6 | 10.5 |
| | | | | | | | | | | | |
| JMA10a | 0.0 | Gh | 0 | 0.12700 | 279.6 | 4.4 | 120.5 | -7.9 | 120.5 | -7.9 | 2.0 |
| JMA10a | 100.0 | Gh | 0 | 0.12293 | 280.0 | 2.1 | 118.4 | -8.9 | 118.4 | -8.9 | 3.0 |
| JMA10a | 200.0 | Gh | 0 | 0.13115 | 284.2 | -1.7 | 116.0 | -14.1 | 116.0 | -14.1 | 3.0 |
| JMA10a | 300.0 | Gh | 0 | 0.13447 | 290.5 | -3.9 | 115.7 | -20.7 | 115.7 | -20.7 | 3.0 |
| JMA10a | 400.0 | Gh | 0 | 0.14274 | 294.1 | -9.6 | 110.7 | -25.7 | 110.7 | -25.7 | 2.5 |
| JMA10a | 500.0 | Gh | 0 | 0.14433 | 299.0 | -15.5 | 105.4 | -31.6 | 105.4 | -31.6 | 3.0 |
| JMA10a | 550.0 | Gh | 0 | 0.12683 | 304.3 | -15.4 | 96.2 | -36.7 | 96.2 | -36.7 | 2.0 |
| JMA10a | 600.0 | Gh | 0 | 0.13296 | 304.0 | -18.6 | 92.3 | -36.9 | 92.3 | -36.9 | 2.0 |
| JMA10a | 625.0 | Gh | 0 | 0.10793 | 312.8 | -9.8 | 105.5 | -43.6 | 105.5 | -43.6 | 2.5 |
| JMA10a | 650.0 | Gh | 0 | 0.10676 | 310.3 | -7.6 | 107.6 | -40.6 | 107.6 | -40.6 | 3.0 |
| | | | | | | | | | | | |
| JMA11a | 0.0 | Gh | 0 | 0.06464 | 181.8 | -11.8 | 22.9 | 60.1 | 22.9 | 60.1 | 2.0 |
| JMA11a | 100.0 | Gh | 0 | 0.06338 | 173.4 | -15.6 | 8.0 | 55.8 | 8.0 | 55.8 | 2.5 |
| JMA11a | 200.0 | Gh | 0 | 0.04974 | 170.4 | -22.0 | 5.8 | 48.9 | 5.8 | 48.9 | 3.0 |
| JMA11a | 300.0 | Gh | 0 | 0.03744 | 183.9 | -29.9 | 23.9 | 42.0 | 23.9 | 42.0 | 3.5 |
| JMA11a | 400.0 | Gh | 0 | 0.03352 | 190.7 | -49.0 | 27.0 | 22.3 | 27.0 | 22.3 | 3.0 |
| JMA11a | 500.0 | Gh | 0 | 0.03254 | 220.9 | -55.0 | 41.7 | 9.1 | 41.7 | 9.1 | 2.5 |
| JMA11a | 550.0 | Gh | 0 | 0.01912 | 266.0 | -34.8 | 75.0 | -7.0 | 75.0 | -7.0 | 1.5 |
| JMA11a | 600.0 | Gh | 0 | 0.02177 | 260.0 | -12.1 | 94.8 | 5.5 | 94.8 | 5.5 | 3.0 |
| JMA11a | 625.0 | Gh | 0 | 0.02019 | 275.6 | -33.3 | 78.5 | -14.3 | 78.5 | -14.3 | 3.0 |
| JMA11a | 650.0 | Gh | 0 | 0.01829 | 255.8 | -21.1 | 84.9 | 6.2 | 84.9 | 6.2 | 4.0 |
| JMA11a | 660.0 | Gh | 0 | 0.02085 | 238.6 | 2.2 | 101.1 | 30.5 | 101.1 | 30.5 | 5.0 |

| | | | | | | | | | | | |
|---|---|---|---|---|---|---|---|---|---|---|---|
| JMA11a | 670.0 | Gh | 0 | 0.01627 | 335.0 | 18.6 | 164.3 | -45.9 | 164.3 | -45.9 | 9.0 |
| JMA11a | 680.0 | Gh | 0 | 0.00719 | 269.6 | -42.3 | 68.4 | -11.7 | 68.4 | -11.7 | 12.5 |
| JMA12a | 0.0 | Gh | 0 | 0.07068 | 178.9 | 5.3 | 355.3 | 85.2 | 355.3 | 85.2 | 2.0 |
| JMA12a | 100.0 | Gh | 0 | 0.06776 | 175.5 | 0.9 | 341.9 | 79.9 | 341.9 | 79.9 | 3.0 |
| JMA12a | 200.0 | Gh | 0 | 0.06026 | 174.9 | 3.0 | 332.2 | 81.4 | 332.2 | 81.4 | 2.5 |
| JMA12a | 300.0 | Gh | 0 | 0.05054 | 173.7 | -1.5 | 339.5 | 76.9 | 339.5 | 76.9 | 2.0 |
| JMA12a | 400.0 | Gh | 0 | 0.05609 | 164.6 | -15.0 | 336.8 | 60.7 | 336.8 | 60.7 | 3.0 |
| JMA12a | 500.0 | Gh | 0 | 0.03532 | 168.2 | -9.2 | 336.6 | 67.5 | 336.6 | 67.5 | 2.0 |
| JMA12a | 550.0 | Gh | 0 | 0.02909 | 173.7 | -8.6 | 339.2 | 70.4 | 339.2 | 70.4 | 2.0 |
| JMA12a | 600.0 | Gh | 0 | 0.02701 | 196.4 | 14.2 | 104.3 | 73.4 | 104.3 | 73.4 | 2.5 |
| JMA12a | 625.0 | Gh | 0 | 0.01876 | 196.8 | -9.6 | 38.9 | 64.3 | 38.9 | 64.3 | 2.5 |
| JMA12a | 650.0 | Gh | 0 | 0.02534 | 176.4 | -11.2 | 348.3 | 68.4 | 348.3 | 68.4 | 4.0 |
| JMA13a | 0.0 | Gh | 0 | 0.05281 | 156.1 | 25.4 | 243.3 | 63.8 | 243.3 | 63.8 | 2.0 |
| JMA13a | 100.0 | Gh | 0 | 0.05093 | 144.6 | 20.1 | 259.4 | 55.1 | 259.4 | 55.1 | 3.5 |
| JMA13a | 200.0 | Gh | 0 | 0.04533 | 136.9 | 24.0 | 254.9 | 47.5 | 254.9 | 47.5 | 2.0 |
| JMA13a | 300.0 | Gh | 0 | 0.04473 | 132.7 | 30.1 | 247.3 | 42.7 | 247.3 | 42.7 | 4.0 |
| JMA13a | 400.0 | Gh | 0 | 0.04534 | 126.5 | 21.3 | 259.6 | 38.1 | 259.6 | 38.1 | 3.0 |
| JMA13a | 500.0 | Gh | 0 | 0.04573 | 136.7 | 30.5 | 245.6 | 45.9 | 245.6 | 45.9 | 2.5 |
| JMA13a | 550.0 | Gh | 0 | 0.04081 | 133.4 | 46.3 | 226.9 | 37.9 | 226.9 | 37.9 | 3.0 |
| JMA13a | 600.0 | Gh | 0 | 0.03984 | 132.6 | 49.8 | 223.3 | 35.9 | 223.3 | 35.9 | 2.0 |
| JMA13a | 625.0 | Gh | 0 | 0.03851 | 118.3 | 51.0 | 225.8 | 27.0 | 225.8 | 27.0 | 3.0 |
| JMA13a | 650.0 | Gh | 0 | 0.03948 | 134.4 | 40.5 | 233.4 | 41.0 | 233.4 | 41.0 | 4.0 |
| JMA13a | 660.0 | Gh | 0 | 0.03660 | 152.3 | 37.3 | 227.1 | 54.6 | 227.1 | 54.6 | 3.5 |
| JMA13a | 670.0 | Gh | 0 | 0.02986 | 141.8 | 54.1 | 214.9 | 38.2 | 214.9 | 38.2 | 5.0 |
| JMA13a | 680.0 | Gh | 0 | 0.03677 | 134.5 | 64.4 | 208.0 | 28.9 | 208.0 | 28.9 | 9.0 |
| JMA14a | 0.0 | Gh | 0 | 0.06116 | 175.0 | -16.7 | 358.2 | 61.9 | 358.2 | 61.9 | 2.0 |
| JMA14a | 100.0 | Gh | 0 | 0.05956 | 169.4 | -22.9 | 351.4 | 54.5 | 351.4 | 54.5 | 2.5 |
| JMA14a | 200.0 | Gh | 0 | 0.05251 | 162.9 | -21.6 | 341.2 | 53.3 | 341.2 | 53.3 | 2.5 |
| JMA14a | 300.0 | Gh | 0 | 0.03836 | 164.5 | -23.4 | 344.7 | 52.4 | 344.7 | 52.4 | 2.0 |
| JMA14a | 400.0 | Gh | 0 | 0.03751 | 183.8 | -20.0 | 15.3 | 58.8 | 15.3 | 58.8 | 2.5 |
| JMA14a | 500.0 | Gh | 0 | 0.02543 | 202.8 | -12.1 | 53.5 | 57.7 | 53.5 | 57.7 | 2.0 |
| JMA14a | 550.0 | Gh | 0 | 0.02953 | 180.7 | -20.6 | 359.3 | 58.4 | 359.3 | 58.4 | -47.0 |
| JMA14a | 600.0 | Gh | 0 | 0.02260 | 130.7 | -11.7 | 291.4 | 36.0 | 291.4 | 36.0 | 3.0 |
| JMA14a | 625.0 | Gh | 0 | 0.02605 | 170.2 | -10.0 | 332.8 | 66.8 | 332.8 | 66.8 | 3.0 |
| JMA14a | 650.0 | Gh | 0 | 0.02514 | 169.3 | -7.7 | 328.0 | 68.5 | 328.0 | 68.5 | 4.0 |
| JMA15a | 0.0 | Gh | 0 | 0.08947 | 198.5 | -4.0 | 69.2 | 68.5 | 69.2 | 68.5 | 2.0 |
| JMA15a | 100.0 | Gh | 0 | 0.08562 | 194.9 | -8.8 | 52.9 | 68.3 | 52.9 | 68.3 | 3.0 |
| JMA15a | 200.0 | Gh | 0 | 0.07894 | 195.0 | -8.6 | 53.4 | 68.4 | 53.4 | 68.4 | 4.0 |
| JMA15a | 300.0 | Gh | 0 | 0.07245 | 202.1 | -12.7 | 57.6 | 60.5 | 57.6 | 60.5 | 3.0 |
| JMA15a | 400.0 | Gh | 0 | 0.06378 | 224.2 | -7.0 | 82.7 | 43.7 | 82.7 | 43.7 | 2.5 |
| JMA15a | 500.0 | Gh | 0 | 0.06350 | 229.1 | 1.3 | 95.1 | 40.7 | 95.1 | 40.7 | 3.0 |
| JMA15a | 550.0 | Gh | 0 | 0.04704 | 228.0 | 8.3 | 104.3 | 42.4 | 104.3 | 42.4 | 2.0 |
| JMA15a | 600.0 | Gh | 0 | 0.04785 | 220.2 | 2.1 | 94.4 | 49.7 | 94.4 | 49.7 | 3.0 |
| JMA15a | 625.0 | Gh | 0 | 0.04387 | 228.8 | 10.5 | 107.2 | 41.7 | 107.2 | 41.7 | 2.5 |
| JMA15a | 650.0 | Gh | 0 | 0.03987 | 215.3 | 3.2 | 95.0 | 54.7 | 95.0 | 54.7 | 4.0 |
| JMA15a | 660.0 | Gh | 0 | 0.03732 | 224.0 | -1.4 | 90.3 | 45.3 | 90.3 | 45.3 | 5.0 |
| JMA15a | 670.0 | Gh | 0 | 0.03301 | 231.1 | 17.6 | 116.4 | 39.1 | 116.4 | 39.1 | 5.5 |
| JMA15a | 680.0 | Gh | 0 | 0.02895 | 249.5 | 3.1 | 100.1 | 20.7 | 100.1 | 20.7 | 8.5 |

| | | | | | | | | | | | |
|---|---|---|---|---|---|---|---|---|---|---|---|
| JMA16a | 0.0 | Gh | 0 | 0.10819 | 200.2 | -2.5 | 37.4 | 62.8 | 37.4 | 62.8 | 3.0 |
| JMA16a | 100.0 | Gh | 0 | 0.09929 | 198.5 | -5.4 | 30.4 | 61.8 | 30.4 | 61.8 | 2.5 |
| JMA16a | 200.0 | Gh | 0 | 0.08755 | 197.2 | -5.6 | 28.0 | 62.5 | 28.0 | 62.5 | 3.0 |
| JMA16a | 300.0 | Gh | 0 | 0.08019 | 197.8 | -6.1 | 28.3 | 61.7 | 28.3 | 61.7 | 2.5 |
| JMA16a | 400.0 | Gh | 0 | 0.06460 | 199.5 | -3.9 | 34.1 | 62.3 | 34.1 | 62.3 | 2.0 |
| JMA16a | 500.0 | Gh | 0 | 0.06160 | 203.4 | -3.9 | 39.7 | 59.5 | 39.7 | 59.5 | 3.0 |
| JMA16a | 550.0 | Gh | 0 | 0.03166 | 200.8 | 5.2 | 42.5 | 66.9 | 42.5 | 66.9 | 2.0 |
| JMA16a | 600.0 | Gh | 0 | 0.02881 | 200.3 | -5.8 | 22.3 | 60.4 | 22.3 | 60.4 | 2.0 |
| JMA16a | 625.0 | Gh | 0 | 0.02468 | 190.3 | -0.4 | 10.7 | 70.7 | 10.7 | 70.7 | 3.0 |
| JMA16a | 650.0 | Gh | 0 | 0.02950 | 204.0 | 1.9 | 39.6 | 62.4 | 39.6 | 62.4 | 4.0 |
| | | | | | | | | | | | |
| JMA17a | 0.0 | Gh | 0 | 0.05842 | 185.9 | 5.0 | 56.3 | 82.3 | 56.3 | 82.3 | 2.0 |
| JMA17a | 100.0 | Gh | 0 | 0.05475 | 181.9 | -0.1 | 17.1 | 79.7 | 17.1 | 79.7 | 3.0 |
| JMA17a | 200.0 | Gh | 0 | 0.04703 | 178.3 | -1.4 | 357.9 | 78.5 | 357.9 | 78.5 | 4.0 |
| JMA17a | 300.0 | Gh | 0 | 0.04139 | 181.2 | 0.4 | 13.6 | 80.3 | 13.6 | 80.3 | 2.0 |
| JMA17a | 400.0 | Gh | 0 | 0.03331 | 183.2 | -2.0 | 21.4 | 77.6 | 21.4 | 77.6 | 3.0 |
| JMA17a | 500.0 | Gh | 0 | 0.02877 | 189.7 | -3.5 | 42.4 | 73.4 | 42.4 | 73.4 | 3.5 |
| JMA17a | 550.0 | Gh | 0 | 0.01584 | 177.7 | -16.3 | 1.5 | 63.6 | 1.5 | 63.6 | 3.5 |
| JMA17a | 600.0 | Gh | 0 | 0.01627 | 165.9 | -14.3 | 336.1 | 62.0 | 336.1 | 62.0 | 3.0 |
| JMA17a | 625.0 | Gh | 0 | 0.01786 | 162.3 | -37.9 | 348.3 | 39.3 | 348.3 | 39.3 | 4.0 |
| JMA17a | 650.0 | Gh | 0 | 0.00574 | 150.5 | -30.4 | 332.3 | 40.7 | 332.3 | 40.7 | 4.0 |
| JMA17a | 660.0 | Gh | 0 | 0.00540 | 7.0 | -56.8 | 1.2 | -42.9 | 1.2 | -42.9 | 5.5 |
| JMA17a | 670.0 | Gh | 0 | 0.01101 | 259.9 | -59.4 | 36.5 | -3.5 | 36.5 | -3.5 | 7.0 |
| JMA17a | 680.0 | Gh | 1 | 0.00603 | 236.7 | 25.4 | 120.5 | 34.3 | 120.5 | 34.3 | 9.0 |
| | | | | | | | | | | | |
| JMA18a | 0.0 | Gh | 0 | 0.07648 | 177.4 | -29.3 | 358.9 | 49.6 | 358.9 | 49.6 | 2.0 |
| JMA18a | 100.0 | Gh | 0 | 0.07798 | 173.3 | -32.0 | 354.1 | 46.5 | 354.1 | 46.5 | 3.0 |
| JMA18a | 200.0 | Gh | 0 | 0.06939 | 172.0 | -35.5 | 353.5 | 42.9 | 353.5 | 42.9 | 3.0 |
| JMA18a | 300.0 | Gh | 0 | 0.06802 | 174.6 | -37.7 | 356.7 | 41.0 | 356.7 | 41.0 | 3.0 |
| JMA18a | 400.0 | Gh | 0 | 0.07021 | 173.9 | -37.5 | 356.0 | 41.2 | 356.0 | 41.2 | 3.0 |
| JMA18a | 500.0 | Gh | 0 | 0.07253 | 179.6 | -38.0 | 2.0 | 41.0 | 2.0 | 41.0 | 2.5 |
| JMA18a | 550.0 | Gh | 0 | 0.03102 | 181.8 | -49.0 | 353.3 | 29.9 | 353.3 | 29.9 | 3.0 |
| JMA18a | 600.0 | Gh | 0 | 0.02717 | 165.7 | -37.3 | 337.2 | 39.9 | 337.2 | 39.9 | 0.5 |
| JMA18a | 625.0 | Gh | 0 | 0.02721 | 149.4 | -18.9 | 306.5 | 47.5 | 306.5 | 47.5 | 3.0 |
| JMA18a | 650.0 | Gh | 0 | 0.02528 | 168.5 | -44.0 | 342.0 | 34.1 | 342.0 | 34.1 | 3.0 |
| | | | | | | | | | | | |
| JMA19a | 0.0 | Gh | 0 | 0.06024 | 296.3 | -38.8 | 79.0 | -29.7 | 79.0 | -29.7 | 4.0 |
| JMA19a | 100.0 | Gh | 0 | 0.06658 | 308.5 | -43.3 | 71.7 | -38.0 | 71.7 | -38.0 | 3.0 |
| JMA19a | 200.0 | Gh | 0 | 0.07285 | 318.5 | -37.7 | 75.6 | -46.9 | 75.6 | -46.9 | 3.0 |
| JMA19a | 300.0 | Gh | 0 | 0.08101 | 327.0 | -34.3 | 76.3 | -54.6 | 76.3 | -54.6 | 3.0 |
| JMA19a | 400.0 | Gh | 0 | 0.08360 | 328.7 | -31.1 | 80.6 | -57.2 | 80.6 | -57.2 | 3.5 |
| JMA19a | 500.0 | Gh | 0 | 0.08956 | 326.7 | -28.6 | 86.0 | -56.4 | 86.0 | -56.4 | 3.0 |
| JMA19a | 550.0 | Gh | 0 | 0.08887 | 333.9 | -33.7 | 72.4 | -59.9 | 72.4 | -59.9 | 2.5 |
| JMA19a | 600.0 | Gh | 0 | 0.09035 | 336.5 | -33.7 | 69.8 | -61.7 | 69.8 | -61.7 | 2.0 |
| JMA19a | 625.0 | Gh | 0 | 0.06648 | 331.7 | -36.1 | 70.2 | -57.1 | 70.2 | -57.1 | 2.5 |
| JMA19a | 650.0 | Gh | 0 | 0.06731 | 343.6 | -42.0 | 49.9 | -59.5 | 49.9 | -59.5 | 3.0 |
| JMA19a | 660.0 | Gh | 0 | 0.01120 | 305.8 | 15.9 | 143.1 | -28.2 | 143.1 | -28.2 | 12.0 |
| JMA19a | 670.0 | Gh | 0 | 0.02011 | 144.7 | -57.8 | 7.1 | 11.6 | 7.1 | 11.6 | 12.5 |
| JMA19a | 680.0 | Gh | 0 | 0.00991 | 49.2 | -8.9 | 294.1 | -41.6 | 294.1 | -41.6 | 17.5 |
| | | | | | | | | | | | |
| JMA20a | 0.0 | Gh | 0 | 0.03518 | 205.8 | -36.0 | 66.3 | 36.2 | 66.3 | 36.2 | 3.0 |
| JMA20a | 100.0 | Gh | 0 | 0.03292 | 205.1 | -53.3 | 56.2 | 21.3 | 56.2 | 21.3 | 3.0 |
| JMA20a | 200.0 | Gh | 0 | 0.02865 | 252.3 | -64.6 | 64.6 | -3.5 | 64.6 | -3.5 | 4.0 |

| | | | | | | | | | | | |
|---|---|---|---|---|---|---|---|---|---|---|---|
| JMA20a | 300.0 | Gh | 0 | 0.03228 | 303.0 | -63.3 | 65.0 | -25.2 | 65.0 | -25.2 | 4.0 |
| JMA20a | 400.0 | Gh | 0 | 0.03393 | 323.4 | -59.5 | 62.2 | -35.3 | 62.2 | -35.3 | 3.5 |
| JMA20a | 500.0 | Gh | 0 | 0.04468 | 334.0 | -42.5 | 72.1 | -52.1 | 72.1 | -52.1 | 5.0 |
| JMA20a | 550.0 | Gh | 0 | 0.04521 | 322.6 | -7.3 | 123.7 | -52.8 | 123.7 | -52.8 | 3.0 |
| JMA20a | 600.0 | Gh | 0 | 0.03807 | 315.1 | -20.8 | 102.3 | -46.1 | 102.3 | -46.1 | 3.0 |
| JMA20a | 625.0 | Gh | 0 | 0.04095 | 307.5 | -8.7 | 118.3 | -38.3 | 118.3 | -38.3 | 3.5 |
| JMA20a | 650.0 | Gh | 0 | 0.04560 | 319.8 | 9.0 | 145.9 | -44.8 | 145.9 | -44.8 | 5.5 |
| | | | | | | | | | | | |
| JMA21a | 0.0 | Gh | 0 | 0.07649 | 156.3 | 5.8 | 295.4 | 66.4 | 295.4 | 66.4 | 2.0 |
| JMA21a | 100.0 | Gh | 0 | 0.06792 | 151.4 | 0.2 | 307.1 | 61.0 | 307.1 | 61.0 | 3.0 |
| JMA21a | 200.0 | Gh | 0 | 0.05794 | 140.0 | -0.7 | 305.4 | 49.6 | 305.4 | 49.6 | 3.0 |
| JMA21a | 300.0 | Gh | 0 | 0.05756 | 132.9 | -9.4 | 315.4 | 40.9 | 315.4 | 40.9 | 2.5 |
| JMA21a | 400.0 | Gh | 0 | 0.06190 | 126.0 | -3.2 | 305.9 | 35.4 | 305.9 | 35.4 | 3.5 |
| JMA21a | 500.0 | Gh | 0 | 0.05693 | 112.0 | -3.8 | 304.5 | 21.5 | 304.5 | 21.5 | 2.5 |
| JMA21a | 550.0 | Gh | 0 | 0.02464 | 113.8 | -17.9 | 319.7 | 20.8 | 319.7 | 20.8 | 2.5 |
| JMA21a | 600.0 | Gh | 0 | 0.02813 | 86.4 | -11.6 | 309.7 | -4.6 | 309.7 | -4.6 | 2.5 |
| JMA21a | 625.0 | Gh | 0 | 0.02370 | 59.0 | -21.0 | 319.9 | -30.7 | 319.9 | -30.7 | 3.0 |
| JMA21a | 650.0 | Gh | 0 | 0.01969 | 66.7 | 48.6 | 246.7 | -11.3 | 246.7 | -11.3 | 3.0 |
| JMA21a | 660.0 | Gh | 0 | 0.01402 | 96.2 | 22.0 | 276.9 | 7.6 | 276.9 | 7.6 | 4.0 |
| JMA21a | 670.0 | Gh | 0 | 0.01356 | 199.1 | -41.6 | 47.1 | 40.3 | 47.1 | 40.3 | 13.0 |
| JMA21a | 680.0 | Gh | 0 | 0.01245 | 160.7 | -60.8 | 18.4 | 22.5 | 18.4 | 22.5 | 13.0 |
| | | | | | | | | | | | |
| JMA22a | 0.0 | Gh | 0 | 0.09687 | 203.8 | 7.1 | 49.0 | 62.6 | 49.0 | 62.6 | 1.0 |
| JMA22a | 100.0 | Gh | 0 | 0.08523 | 200.7 | 1.1 | 35.1 | 61.0 | 35.1 | 61.0 | 3.0 |
| JMA22a | 200.0 | Gh | 0 | 0.06869 | 196.6 | -0.3 | 26.5 | 62.4 | 26.5 | 62.4 | 4.0 |
| JMA22a | 300.0 | Gh | 0 | 0.06327 | 195.8 | -9.9 | 15.9 | 54.5 | 15.9 | 54.5 | 2.5 |
| JMA22a | 400.0 | Gh | 0 | 0.06748 | 199.6 | -5.0 | 26.1 | 56.9 | 26.1 | 56.9 | 3.5 |
| JMA22a | 500.0 | Gh | 0 | 0.04617 | 192.8 | -8.3 | 12.2 | 57.2 | 12.2 | 57.2 | 2.0 |
| JMA22a | 550.0 | Gh | 0 | 0.02168 | 226.7 | -24.7 | 24.8 | 24.9 | 24.8 | 24.9 | 2.0 |
| JMA22a | 600.0 | Gh | 0 | 0.02852 | 212.5 | -22.3 | 15.6 | 35.6 | 15.6 | 35.6 | 2.5 |
| JMA22a | 625.0 | Gh | 0 | 0.01500 | 194.6 | -14.0 | 1.1 | 51.3 | 1.1 | 51.3 | 3.5 |
| JMA22a | 650.0 | Gh | 0 | 0.00510 | 230.1 | -11.6 | 38.7 | 30.5 | 38.7 | 30.5 | 4.0 |
| | | | | | | | | | | | |
| JMA23a | 0.0 | Gh | 0 | 0.07693 | 158.5 | -10.8 | 312.4 | 54.2 | 312.4 | 54.2 | 4.0 |
| JMA23a | 100.0 | Gh | 0 | 0.07136 | 149.6 | -17.7 | 308.8 | 43.4 | 308.8 | 43.4 | 3.0 |
| JMA23a | 200.0 | Gh | 0 | 0.06228 | 135.9 | -20.1 | 299.7 | 32.4 | 299.7 | 32.4 | 3.0 |
| JMA23a | 300.0 | Gh | 0 | 0.05535 | 115.2 | -20.8 | 289.0 | 15.6 | 289.0 | 15.6 | 3.0 |
| JMA23a | 400.0 | Gh | 0 | 0.04672 | 107.3 | -11.0 | 276.6 | 12.6 | 276.6 | 12.6 | 4.0 |
| JMA23a | 500.0 | Gh | 0 | 0.04915 | 85.4 | -2.4 | 261.3 | -5.2 | 261.3 | -5.2 | 2.0 |
| JMA23a | 550.0 | Gh | 0 | 0.04214 | 56.4 | -4.3 | 253.6 | -33.2 | 253.6 | -33.2 | 2.5 |
| JMA23a | 600.0 | Gh | 0 | 0.04773 | 45.7 | -1.7 | 245.7 | -42.3 | 245.7 | -42.3 | 2.5 |
| JMA23a | 625.0 | Gh | 0 | 0.04220 | 43.9 | 7.3 | 233.9 | -39.9 | 233.9 | -39.9 | 3.5 |
| JMA23a | 650.0 | Gh | 0 | 0.03156 | 42.1 | 10.3 | 229.5 | -39.7 | 229.5 | -39.7 | 3.5 |
| JMA23a | 660.0 | Gh | 0 | 0.04709 | 52.3 | 15.6 | 230.5 | -28.5 | 230.5 | -28.5 | 4.0 |
| JMA23a | 670.0 | Gh | 0 | 0.03098 | 25.1 | 21.9 | 203.1 | -43.1 | 203.1 | -43.1 | 8.0 |
| JMA23a | 680.0 | Gh | 0 | 0.02750 | 359.5 | 8.0 | 169.3 | -64.0 | 169.3 | -64.0 | 9.0 |
| | | | | | | | | | | | |
| JMA24a | 0.0 | Gh | 0 | 0.10783 | 203.3 | 11.2 | 104.1 | 66.7 | 104.1 | 66.7 | 2.0 |
| JMA24a | 100.0 | Gh | 0 | 0.09569 | 205.2 | 6.1 | 94.5 | 63.1 | 94.5 | 63.1 | 3.0 |
| JMA24a | 200.0 | Gh | 0 | 0.08518 | 205.1 | 7.4 | 97.1 | 63.7 | 97.1 | 63.7 | 3.0 |
| JMA24a | 300.0 | Gh | 0 | 0.08349 | 206.3 | 2.7 | 89.3 | 60.5 | 89.3 | 60.5 | 3.5 |
| JMA24a | 400.0 | Gh | 0 | 0.05949 | 206.0 | -16.1 | 64.5 | 48.1 | 64.5 | 48.1 | 3.0 |
| JMA24a | 500.0 | Gh | 0 | 0.04126 | 224.1 | -16.0 | 80.6 | 35.4 | 80.6 | 35.4 | 3.0 |

| | | | | | | | | | | | |
|---|---|---|---|---|---|---|---|---|---|---|---|
| JMA24a | 550.0 | Gh | 0 | 0.03892 | 229.0 | -21.7 | 67.9 | 28.4 | 67.9 | 28.4 | 2.5 |
| JMA24a | 600.0 | Gh | 0 | 0.03584 | 247.8 | -21.0 | 77.7 | 13.4 | 77.7 | 13.4 | 2.0 |
| JMA24a | 625.0 | Gh | 0 | 0.03742 | 266.0 | -25.3 | 79.6 | -3.7 | 79.6 | -3.7 | 3.0 |
| JMA24a | 650.0 | Gh | 0 | 0.02932 | 276.9 | -41.0 | 66.2 | -16.2 | 66.2 | -16.2 | 5.5 |
| | | | | | | | | | | | |
| JMA25a | 0.0 | Gh | 0 | 0.12510 | 186.6 | -1.9 | 34.9 | 66.2 | 34.9 | 66.2 | 3.0 |
| JMA25a | 100.0 | Gh | 0 | 0.11465 | 185.2 | -7.3 | 29.2 | 61.2 | 29.2 | 61.2 | 2.0 |
| JMA25a | 200.0 | Gh | 0 | 0.10090 | 183.5 | -9.6 | 25.2 | 59.2 | 25.2 | 59.2 | 3.0 |
| JMA25a | 300.0 | Gh | 0 | 0.08023 | 188.0 | -11.6 | 32.7 | 56.5 | 32.7 | 56.5 | 4.0 |
| JMA25a | 400.0 | Gh | 0 | 0.06820 | 189.1 | -14.4 | 33.3 | 53.5 | 33.3 | 53.5 | 3.0 |
| JMA25a | 500.0 | Gh | 0 | 0.04144 | 188.0 | -1.4 | 38.5 | 66.3 | 38.5 | 66.3 | 2.5 |
| JMA25a | 550.0 | Gh | 0 | 0.02999 | 201.2 | 5.1 | 73.7 | 64.0 | 73.7 | 64.0 | 3.0 |
| JMA25a | 600.0 | Gh | 0 | 0.02508 | 186.7 | 1.0 | 37.4 | 68.9 | 37.4 | 68.9 | -2.0 |
| JMA25a | 625.0 | Gh | 0 | 0.02607 | 188.2 | -3.6 | 37.4 | 64.1 | 37.4 | 64.1 | 3.5 |
| JMA25a | 650.0 | Gh | 0 | 0.01489 | 186.4 | 22.0 | 119.1 | 83.9 | 119.1 | 83.9 | 4.0 |
| JMA25a | 660.0 | Gh | 0 | 0.01276 | 170.6 | 19.1 | 299.0 | 81.0 | 299.0 | 81.0 | 6.5 |
| JMA25a | 670.0 | Gh | 0 | 0.01181 | 60.3 | 59.0 | 225.1 | 3.9 | 225.1 | 3.9 | 8.5 |
| JMA25a | 680.0 | Gh | 0 | 0.00806 | 100.2 | 12.7 | 279.9 | 13.9 | 279.9 | 13.9 | 9.5 |
| | | | | | | | | | | | |
| JMA26a | 0.0 | Gh | 0 | 0.14483 | 187.3 | -5.6 | 11.3 | 62.5 | 11.3 | 62.5 | 3.0 |
| JMA26a | 100.0 | Gh | 0 | 0.13479 | 185.4 | -8.9 | 6.0 | 59.6 | 6.0 | 59.6 | 3.0 |
| JMA26a | 200.0 | Gh | 0 | 0.12246 | 184.7 | -9.1 | 4.6 | 59.5 | 4.6 | 59.5 | 2.5 |
| JMA26a | 300.0 | Gh | 0 | 0.11383 | 189.7 | -11.1 | 12.8 | 56.5 | 12.8 | 56.5 | 3.0 |
| JMA26a | 400.0 | Gh | 0 | 0.10323 | 186.2 | -11.5 | 6.6 | 56.9 | 6.6 | 56.9 | 3.0 |
| JMA26a | 500.0 | Gh | 0 | 0.08680 | 178.7 | -8.4 | 352.9 | 60.6 | 352.9 | 60.6 | 3.0 |
| JMA26a | 550.0 | Gh | 0 | 0.07119 | 179.1 | -6.4 | 343.2 | 62.6 | 343.2 | 62.6 | 3.0 |
| JMA26a | 600.0 | Gh | 0 | 0.08023 | 178.6 | -3.7 | 341.6 | 65.3 | 341.6 | 65.3 | 3.5 |
| JMA26a | 625.0 | Gh | 0 | 0.06668 | 178.6 | -3.3 | 341.7 | 65.6 | 341.7 | 65.6 | 4.0 |
| JMA26a | 650.0 | Gh | 0 | 0.05495 | 187.9 | -1.5 | 4.9 | 66.2 | 4.9 | 66.2 | 5.0 |
| | | | | | | | | | | | |
| JMA27a | 0.0 | Gh | 0 | 0.06456 | 195.8 | -7.0 | 57.2 | 66.1 | 57.2 | 66.1 | 2.0 |
| JMA27a | 100.0 | Gh | 0 | 0.06000 | 190.5 | -15.0 | 37.4 | 62.0 | 37.4 | 62.0 | 3.0 |
| JMA27a | 200.0 | Gh | 0 | 0.05088 | 193.7 | -18.1 | 40.5 | 57.9 | 40.5 | 57.9 | 3.5 |
| JMA27a | 300.0 | Gh | 0 | 0.04184 | 195.6 | -20.9 | 41.1 | 54.6 | 41.1 | 54.6 | 2.0 |
| JMA27a | 400.0 | Gh | 0 | 0.03088 | 174.2 | -27.1 | 7.1 | 51.5 | 7.1 | 51.5 | 2.5 |
| JMA27a | 500.0 | Gh | 0 | 0.01973 | 217.5 | -51.0 | 39.5 | 20.0 | 39.5 | 20.0 | 3.0 |
| JMA27a | 550.0 | Gh | 0 | 0.03026 | 223.2 | -32.1 | 57.6 | 30.3 | 57.6 | 30.3 | 2.0 |
| JMA27a | 600.0 | Gh | 0 | 0.02452 | 222.3 | -40.0 | 50.3 | 25.7 | 50.3 | 25.7 | 2.5 |
| JMA27a | 625.0 | Gh | 0 | 0.02428 | 212.1 | -57.9 | 32.5 | 16.3 | 32.5 | 16.3 | 2.0 |
| JMA27a | 650.0 | Gh | 0 | 0.03558 | 202.5 | -26.1 | 45.6 | 47.0 | 45.6 | 47.0 | 2.5 |
| JMA27a | 660.0 | Gh | 0 | 0.02525 | 218.4 | -56.4 | 36.3 | 15.5 | 36.3 | 15.5 | 4.5 |
| JMA27a | 670.0 | Gh | 0 | 0.01689 | 189.1 | -17.5 | 33.1 | 60.1 | 33.1 | 60.1 | 5.5 |
| JMA27a | 680.0 | Gh | 0 | 0.02305 | 232.8 | -36.7 | 58.7 | 21.2 | 58.7 | 21.2 | 6.0 |
| | | | | | | | | | | | |
| JMA28a | 0.0 | Gh | 0 | 0.05279 | 187.1 | 3.0 | 40.6 | 74.4 | 40.6 | 74.4 | 2.0 |
| JMA28a | 100.0 | Gh | 0 | 0.04385 | 177.4 | -5.0 | 6.5 | 67.9 | 6.5 | 67.9 | 3.0 |
| JMA28a | 200.0 | Gh | 0 | 0.03224 | 176.7 | -2.8 | 3.8 | 69.9 | 3.8 | 69.9 | 3.5 |
| JMA28a | 300.0 | Gh | 0 | 0.02006 | 161.1 | 3.3 | 317.8 | 66.9 | 317.8 | 66.9 | 2.5 |
| JMA28a | 400.0 | Gh | 0 | 0.00580 | 96.8 | 2.1 | 283.4 | 7.1 | 283.4 | 7.1 | 2.5 |
| JMA28a | 500.0 | Gh | 0 | 0.00701 | 116.6 | -23.8 | 315.1 | 15.9 | 315.1 | 15.9 | 2.5 |
| JMA28a | 550.0 | Gh | 0 | 0.00502 | 143.1 | -44.4 | 335.8 | 19.9 | 335.8 | 19.9 | 3.0 |
| JMA28a | 600.0 | Gh | 0 | 0.00369 | 172.3 | 29.4 | 211.4 | 75.8 | 211.4 | 75.8 | 2.0 |
| JMA28a | 625.0 | Gh | 0 | 0.00387 | 212.2 | 75.2 | 174.0 | 29.3 | 174.0 | 29.3 | 3.0 |

| | | | | | | | | | | | |
|---|---|---|---|---|---|---|---|---|---|---|---|
| JMA28a | 650.0 | Gh | 0 | 0.01300 | 29.3 | 33.7 | 211.7 | -32.1 | 211.7 | -32.1 | 4.0 |
| JMA29a | 0.0 | Gh | 0 | 0.10196 | 209.1 | 9.1 | 115.5 | 61.3 | 115.5 | 61.3 | 3.0 |
| JMA29a | 100.0 | Gh | 0 | 0.08851 | 209.5 | 6.0 | 109.4 | 60.3 | 109.4 | 60.3 | 2.5 |
| JMA29a | 200.0 | Gh | 0 | 0.07410 | 218.4 | 8.9 | 117.5 | 52.1 | 117.5 | 52.1 | 3.0 |
| JMA29a | 300.0 | Gh | 0 | 0.06103 | 219.3 | -3.7 | 98.9 | 47.9 | 98.9 | 47.9 | 3.5 |
| JMA29a | 400.0 | Gh | 0 | 0.04196 | 227.6 | -11.1 | 94.2 | 37.4 | 94.2 | 37.4 | 2.5 |
| JMA29a | 500.0 | Gh | 0 | 0.04558 | 251.4 | -11.9 | 102.4 | 15.2 | 102.4 | 15.2 | 2.5 |
| JMA29a | 550.0 | Gh | 0 | 0.05446 | 243.6 | -0.4 | 112.0 | 25.7 | 112.0 | 25.7 | 3.5 |
| JMA29a | 600.0 | Gh | 0 | 0.04951 | 244.1 | -9.2 | 102.9 | 22.8 | 102.9 | 22.8 | 3.5 |
| JMA29a | 625.0 | Gh | 0 | 0.04736 | 244.7 | -2.8 | 109.8 | 24.0 | 109.8 | 24.0 | 3.5 |
| JMA29a | 650.0 | Gh | 0 | 0.05747 | 237.0 | -0.9 | 109.6 | 32.0 | 109.6 | 32.0 | 4.5 |
| JMA29a | 660.0 | Gh | 0 | 0.04679 | 231.9 | 6.0 | 116.5 | 38.4 | 116.5 | 38.4 | 6.5 |
| JMA29a | 670.0 | Gh | 0 | 0.05402 | 238.5 | -3.1 | 107.7 | 30.0 | 107.7 | 30.0 | 7.5 |
| JMA29a | 680.0 | Gh | 0 | 0.03181 | 220.2 | 4.3 | 110.9 | 49.5 | 110.9 | 49.5 | 9.0 |
| JMA30a | 0.0 | Gh | 0 | 0.05033 | 192.3 | -57.3 | 27.5 | 21.0 | 27.5 | 21.0 | 3.0 |
| JMA30a | 100.0 | Gh | 0 | 0.05299 | 183.2 | -67.5 | 21.6 | 11.5 | 21.6 | 11.5 | 4.0 |
| JMA30a | 200.0 | Gh | 0 | 0.04832 | 177.6 | -81.2 | 20.0 | -2.2 | 20.0 | -2.2 | 3.0 |
| JMA30a | 300.0 | Gh | 0 | 0.04049 | 208.6 | -83.4 | 23.6 | -5.2 | 23.6 | -5.2 | 2.5 |
| JMA30a | 400.0 | Gh | 0 | 0.04554 | 325.5 | -76.6 | 28.5 | -21.9 | 28.5 | -21.9 | 3.5 |
| JMA30a | 500.0 | Gh | 0 | 0.05239 | 331.2 | -64.8 | 34.5 | -32.6 | 34.5 | -32.6 | 2.5 |
| JMA30a | 550.0 | Gh | 0 | 0.04457 | 318.5 | -53.6 | 39.1 | -36.2 | 39.1 | -36.2 | 3.0 |
| JMA30a | 600.0 | Gh | 0 | 0.03468 | 300.9 | -50.4 | 48.2 | -27.9 | 48.2 | -27.9 | 3.0 |
| JMA30a | 625.0 | Gh | 0 | 0.02653 | 301.2 | -59.2 | 39.0 | -25.1 | 39.0 | -25.1 | 2.0 |
| JMA30a | 650.0 | Gh | 0 | 0.03176 | 356.1 | -85.5 | 10.3 | -15.5 | 10.3 | -15.5 | 4.5 |
| JMA31a | 0.0 | Gh | 0 | 0.07182 | 219.2 | -12.1 | 63.0 | 38.0 | 63.0 | 38.0 | 2.0 |
| JMA31a | 100.0 | Gh | 0 | 0.06029 | 220.8 | -22.3 | 55.5 | 29.8 | 55.5 | 29.8 | 3.5 |
| JMA31a | 200.0 | Gh | 0 | 0.05052 | 225.6 | -27.0 | 55.3 | 23.4 | 55.3 | 23.4 | 3.0 |
| JMA31a | 300.0 | Gh | 0 | 0.04014 | 239.4 | -28.7 | 62.2 | 12.9 | 62.2 | 12.9 | 3.5 |
| JMA31a | 400.0 | Gh | 0 | 0.04989 | 260.0 | -24.8 | 74.8 | -1.1 | 74.8 | -1.1 | 3.5 |
| JMA31a | 500.0 | Gh | 0 | 0.04811 | 284.2 | -9.9 | 97.6 | -16.9 | 97.6 | -16.9 | 2.5 |
| JMA31a | 550.0 | Gh | 0 | 0.05755 | 283.6 | -2.0 | 104.9 | -13.3 | 104.9 | -13.3 | 3.0 |
| JMA31a | 600.0 | Gh | 0 | 0.05259 | 286.4 | -10.4 | 97.9 | -19.0 | 97.9 | -19.0 | 3.0 |
| JMA31a | 625.0 | Gh | 0 | 0.04288 | 300.3 | -10.6 | 103.1 | -31.9 | 103.1 | -31.9 | 4.0 |
| JMA31a | 650.0 | Gh | 0 | 0.04469 | 317.6 | -17.2 | 101.7 | -49.9 | 101.7 | -49.9 | 6.0 |
| JMA31a | 660.0 | Gh | 0 | 0.03930 | 312.2 | 20.1 | 140.3 | -26.5 | 140.3 | -26.5 | 8.5 |
| JMA31a | 670.0 | Gh | 0 | 0.02918 | 310.9 | -0.7 | 119.3 | -37.4 | 119.3 | -37.4 | 11.5 |
| JMA31a | 680.0 | Gh | 0 | 0.02529 | 356.0 | -22.0 | 116.1 | -86.1 | 116.1 | -86.1 | 16.5 |
| JMA32a | 0.0 | Gh | 0 | 0.06028 | 208.3 | 68.7 | 170.6 | 39.2 | 170.6 | 39.2 | 3.0 |
| JMA32a | 100.0 | Gh | 0 | 0.05011 | 204.5 | 77.3 | 177.2 | 32.4 | 177.2 | 32.4 | 3.5 |
| JMA32a | 200.0 | Gh | 0 | 0.04983 | 39.4 | 88.8 | 184.2 | 20.1 | 184.2 | 20.1 | 3.0 |
| JMA32a | 300.0 | Gh | 0 | 0.04442 | 31.2 | 82.4 | 187.5 | 14.5 | 187.5 | 14.5 | 3.5 |
| JMA32a | 400.0 | Gh | 0 | 0.04109 | 85.1 | 60.3 | 214.3 | 15.8 | 214.3 | 15.8 | 2.0 |
| JMA32a | 500.0 | Gh | 0 | 0.03658 | 81.3 | 71.7 | 202.4 | 17.2 | 202.4 | 17.2 | 2.5 |
| JMA32a | 550.0 | Gh | 0 | 0.02033 | 194.2 | 58.1 | 161.0 | 51.5 | 161.0 | 51.5 | 2.0 |
| JMA32a | 600.0 | Gh | 0 | 0.02108 | 238.8 | 65.0 | 147.8 | 32.0 | 147.8 | 32.0 | 3.0 |
| JMA32a | 625.0 | Gh | 0 | 0.02440 | 230.3 | 45.6 | 126.3 | 42.3 | 126.3 | 42.3 | 3.0 |
| JMA32a | 650.0 | Gh | 0 | 0.01914 | 197.1 | 56.9 | 157.9 | 51.9 | 157.9 | 51.9 | 3.5 |
| JMA33a | 0.0 | Gh | 0 | 0.07609 | 293.5 | -0.1 | 99.8 | -22.0 | 99.8 | -22.0 | 2.0 |

| | | | | | | | | | | | |
|---|---|---|---|---|---|---|---|---|---|---|---|
| JMA33a | 100.0 | Gh | 0 | 0.07718 | 304.0 | -5.1 | 98.8 | -33.6 | 98.8 | -33.6 | 4.0 |
| JMA33a | 200.0 | Gh | 0 | 0.08437 | 307.8 | -4.5 | 101.1 | -36.9 | 101.1 | -36.9 | 3.0 |
| JMA33a | 300.0 | Gh | 0 | 0.09165 | 306.7 | -2.7 | 102.7 | -35.2 | 102.7 | -35.2 | 4.0 |
| JMA33a | 400.0 | Gh | 0 | 0.08674 | 309.9 | -9.8 | 95.7 | -40.7 | 95.7 | -40.7 | 3.0 |
| JMA33a | 500.0 | Gh | 0 | 0.09332 | 306.7 | -10.8 | 93.2 | -38.0 | 93.2 | -38.0 | 4.0 |
| JMA33a | 550.0 | Gh | 0 | 0.09058 | 316.6 | -7.5 | 101.7 | -46.2 | 101.7 | -46.2 | 3.5 |
| JMA33a | 600.0 | Gh | 0 | 0.05918 | 312.7 | -26.5 | 73.5 | -46.3 | 73.5 | -46.3 | 3.0 |
| JMA33a | 625.0 | Gh | 0 | 0.04556 | 311.4 | -17.3 | 86.3 | -44.0 | 86.3 | -44.0 | 3.0 |
| JMA33a | 650.0 | Gh | 0 | 0.07294 | 317.9 | -4.7 | 106.2 | -46.3 | 106.2 | -46.3 | 4.0 |
| JMA33a | 660.0 | Gh | 0 | 0.05743 | 308.0 | -19.5 | 82.6 | -41.3 | 82.6 | -41.3 | 5.0 |
| JMA33a | 670.0 | Gh | 0 | 0.06828 | 309.7 | -18.9 | 83.7 | -42.7 | 83.7 | -42.7 | 8.0 |
| JMA33a | 680.0 | Gh | 0 | 0.03724 | 328.7 | 51.4 | 161.9 | -13.5 | 161.9 | -13.5 | 12.0 |
| | | | | | | | | | | | |
| JMA34a | 0.0 | Gh | 0 | 0.06048 | 13.8 | 35.2 | 202.7 | -3.9 | 202.7 | -3.9 | 4.0 |
| JMA34a | 100.0 | Gh | 0 | 0.06136 | 17.3 | 22.4 | 208.0 | -16.0 | 208.0 | -16.0 | 4.0 |
| JMA34a | 200.0 | Gh | 0 | 0.07522 | 15.6 | 11.5 | 208.6 | -27.0 | 208.6 | -27.0 | 4.0 |
| JMA34a | 300.0 | Gh | 0 | 0.09070 | 17.6 | 10.0 | 211.1 | -28.1 | 211.1 | -28.1 | 4.0 |
| JMA34a | 400.0 | Gh | 0 | 0.10670 | 21.0 | 11.5 | 214.4 | -25.8 | 214.4 | -25.8 | 5.0 |
| JMA34a | 500.0 | Gh | 0 | 0.11286 | 28.1 | 12.9 | 221.2 | -22.4 | 221.2 | -22.4 | 4.0 |
| JMA34a | 550.0 | Gh | 0 | 0.11238 | 45.4 | 3.0 | 232.2 | -24.2 | 232.2 | -24.2 | 3.5 |
| JMA34a | 600.0 | Gh | 0 | 0.08033 | 35.2 | -6.2 | 227.0 | -37.2 | 227.0 | -37.2 | 3.0 |
| JMA34a | 625.0 | Gh | 0 | 0.06845 | 62.2 | -24.2 | 266.6 | -36.0 | 266.6 | -36.0 | 5.0 |
| JMA34a | 650.0 | Gh | 0 | 0.05966 | 55.7 | -15.3 | 253.8 | -33.5 | 253.8 | -33.5 | 5.0 |
| | | | | | | | | | | | |
| JMA35a | 0.0 | Gh | 0 | 0.13112 | 16.9 | -7.9 | 291.9 | -73.2 | 291.9 | -73.2 | 3.0 |
| JMA35a | 100.0 | Gh | 0 | 0.13605 | 18.6 | -9.7 | 298.1 | -71.6 | 298.1 | -71.6 | 2.5 |
| JMA35a | 200.0 | Gh | 0 | 0.14536 | 15.4 | -7.8 | 291.1 | -74.7 | 291.1 | -74.7 | 3.5 |
| JMA35a | 300.0 | Gh | 0 | 0.15212 | 16.1 | -6.2 | 285.6 | -73.8 | 285.6 | -73.8 | 2.5 |
| JMA35a | 400.0 | Gh | 0 | 0.15981 | 13.3 | -6.7 | 285.5 | -76.6 | 285.5 | -76.6 | 3.0 |
| JMA35a | 500.0 | Gh | 0 | 0.14672 | 10.9 | -12.1 | 311.4 | -78.9 | 311.4 | -78.9 | 3.5 |
| JMA35a | 550.0 | Gh | 0 | 0.13190 | 2.4 | -4.3 | 231.4 | -84.8 | 231.4 | -84.8 | 2.0 |
| JMA35a | 600.0 | Gh | 0 | 0.11368 | 1.3 | -14.6 | 11.7 | -84.2 | 11.7 | -84.2 | 3.0 |
| JMA35a | 625.0 | Gh | 0 | 0.10276 | 357.0 | -17.0 | 44.0 | -81.5 | 44.0 | -81.5 | 3.5 |
| JMA35a | 650.0 | Gh | 0 | 0.09945 | 346.5 | -18.3 | 77.8 | -73.9 | 77.8 | -73.9 | 6.0 |
| JMA35a | 660.0 | Gh | 0 | 0.08401 | 352.1 | -32.1 | 40.9 | -65.8 | 40.9 | -65.8 | 9.0 |
| JMA35a | 670.0 | Gh | 0 | 0.09050 | 347.9 | -34.3 | 46.4 | -62.4 | 46.4 | -62.4 | 12.5 |
| JMA35a | 680.0 | Gh | 0 | 0.04526 | 35.0 | 4.3 | 275.0 | -52.7 | 275.0 | -52.7 | 18.0 |
| | | | | | | | | | | | |
| JMA36a | 0.0 | Gh | 0 | 0.02570 | 346.9 | -13.4 | 123.3 | -77.1 | 123.3 | -77.1 | 3.0 |
| JMA36a | 100.0 | Gh | 0 | 0.03356 | 358.2 | -19.5 | 49.2 | -86.1 | 49.2 | -86.1 | 3.0 |
| JMA36a | 200.0 | Gh | 0 | 0.04411 | 354.9 | -18.7 | 83.6 | -84.4 | 83.6 | -84.4 | 3.5 |
| JMA36a | 300.0 | Gh | 0 | 0.04918 | 5.9 | -22.5 | 343.7 | -81.4 | 343.7 | -81.4 | 3.0 |
| JMA36a | 400.0 | Gh | 0 | 0.06328 | 8.7 | -33.8 | 1.2 | -70.6 | 1.2 | -70.6 | 3.5 |
| JMA36a | 500.0 | Gh | 0 | 0.05907 | 30.4 | -30.2 | 325.9 | -58.8 | 325.9 | -58.8 | 2.5 |
| JMA36a | 550.0 | Gh | 0 | 0.04711 | 7.5 | -25.5 | 337.8 | -78.1 | 337.8 | -78.1 | 2.0 |
| JMA36a | 600.0 | Gh | 0 | 0.04129 | 1.0 | -33.4 | 10.1 | -72.6 | 10.1 | -72.6 | 3.0 |
| JMA36a | 625.0 | Gh | 0 | 0.02579 | 10.9 | -34.5 | 347.1 | -69.1 | 347.1 | -69.1 | 3.0 |
| JMA36a | 650.0 | Gh | 0 | 0.01603 | 17.0 | -0.7 | 242.4 | -67.3 | 242.4 | -67.3 | 4.0 |
| | | | | | | | | | | | |
| JMA37a | 0.0 | Gh | 0 | 0.16497 | 263.6 | -0.5 | 108.7 | 5.8 | 108.7 | 5.8 | 3.0 |
| JMA37a | 100.0 | Gh | 0 | 0.15881 | 267.2 | -2.1 | 108.5 | 1.9 | 108.5 | 1.9 | 3.0 |
| JMA37a | 200.0 | Gh | 0 | 0.15771 | 269.7 | -2.2 | 109.2 | -0.5 | 109.2 | -0.5 | 2.5 |
| JMA37a | 300.0 | Gh | 0 | 0.16183 | 276.9 | -5.9 | 108.2 | -8.5 | 108.2 | -8.5 | 3.0 |

| | | | | | | | | | | | |
|---|---|---|---|---|---|---|---|---|---|---|---|
| JMA37a | 400.0 | Gh | 0 | 0.15616 | 283.6 | -8.1 | 108.3 | -15.5 | 108.3 | -15.5 | 1.5 |
| JMA37a | 500.0 | Gh | 0 | 0.14735 | 283.8 | -9.9 | 106.6 | -16.3 | 106.6 | -16.3 | 2.5 |
| JMA37a | 550.0 | Gh | 0 | 0.13208 | 274.7 | -14.8 | 99.0 | -9.3 | 99.0 | -9.3 | 2.0 |
| JMA37a | 600.0 | Gh | 0 | 0.12113 | 277.3 | -20.0 | 94.7 | -13.3 | 94.7 | -13.3 | 3.0 |
| JMA37a | 625.0 | Gh | 0 | 0.11116 | 281.1 | -14.1 | 101.6 | -15.0 | 101.6 | -15.0 | 2.0 |
| JMA37a | 650.0 | Gh | 0 | 0.10299 | 290.4 | -21.0 | 96.9 | -25.4 | 96.9 | -25.4 | 4.0 |
| JMA37a | 660.0 | Gh | 0 | 0.10561 | 288.8 | -10.2 | 107.9 | -21.0 | 107.9 | -21.0 | 5.0 |
| JMA37a | 670.0 | Gh | 0 | 0.08207 | 291.8 | -6.1 | 113.1 | -22.6 | 113.1 | -22.6 | 8.0 |
| JMA37a | 680.0 | Gh | 0 | 0.03609 | 343.0 | -41.2 | 52.0 | -64.3 | 52.0 | -64.3 | 13.0 |
| JMA38a | 0.0 | Gh | 0 | 0.06756 | 252.5 | -28.0 | 77.3 | 6.2 | 77.3 | 6.2 | 2.0 |
| JMA38a | 100.0 | Gh | 0 | 0.06402 | 264.4 | -36.5 | 73.0 | -6.3 | 73.0 | -6.3 | 3.0 |
| JMA38a | 200.0 | Gh | 0 | 0.06997 | 270.1 | -31.5 | 79.2 | -9.4 | 79.2 | -9.4 | 2.5 |
| JMA38a | 300.0 | Gh | 0 | 0.06483 | 267.2 | -37.2 | 73.0 | -8.6 | 73.0 | -8.6 | 3.0 |
| JMA38a | 400.0 | Gh | 0 | 0.05255 | 278.7 | -21.2 | 91.3 | -14.2 | 91.3 | -14.2 | 3.0 |
| JMA38a | 500.0 | Gh | 0 | 0.05457 | 277.0 | -12.5 | 99.5 | -10.4 | 99.5 | -10.4 | 2.5 |
| JMA38a | 550.0 | Gh | 0 | 0.03013 | 320.3 | 17.2 | 138.8 | -37.4 | 138.8 | -37.4 | 3.0 |
| JMA38a | 600.0 | Gh | 0 | 0.03984 | 282.5 | 7.1 | 109.7 | -9.6 | 109.7 | -9.6 | 2.5 |
| JMA38a | 625.0 | Gh | 0 | 0.02355 | 270.5 | -3.2 | 96.2 | -1.5 | 96.2 | -1.5 | 3.5 |
| JMA38a | 650.0 | Gh | 0 | 0.01638 | 275.3 | 0.7 | 101.3 | -4.9 | 101.3 | -4.9 | 6.5 |
| JMA39a | 0.0 | Gh | 0 | 0.11162 | 291.9 | 44.0 | 155.5 | 2.1 | 155.5 | 2.1 | 4.0 |
| JMA39a | 100.0 | Gh | 0 | 0.11204 | 303.6 | 41.3 | 158.4 | -6.4 | 158.4 | -6.4 | 3.0 |
| JMA39a | 200.0 | Gh | 0 | 0.11871 | 306.1 | 41.9 | 160.1 | -7.4 | 160.1 | -7.4 | 2.5 |
| JMA39a | 300.0 | Gh | 0 | 0.14107 | 317.6 | 45.2 | 168.5 | -10.8 | 168.5 | -10.8 | 3.0 |
| JMA39a | 400.0 | Gh | 0 | 0.16597 | 328.4 | 45.8 | 175.2 | -14.5 | 175.2 | -14.5 | 2.5 |
| JMA39a | 500.0 | Gh | 0 | 0.16250 | 325.5 | 45.1 | 173.1 | -14.1 | 173.1 | -14.1 | 2.5 |
| JMA39a | 550.0 | Gh | 0 | 0.12663 | 324.7 | 31.8 | 164.6 | -24.8 | 164.6 | -24.8 | 2.0 |
| JMA39a | 600.0 | Gh | 0 | 0.11909 | 313.7 | 50.0 | 169.6 | -5.4 | 169.6 | -5.4 | 1.0 |
| JMA39a | 625.0 | Gh | 0 | 0.09059 | 318.0 | 53.9 | 174.1 | -4.1 | 174.1 | -4.1 | 2.5 |
| JMA39a | 650.0 | Gh | 0 | 0.07362 | 322.4 | 48.7 | 173.3 | -9.9 | 173.3 | -9.9 | 3.5 |
| JMA39a | 660.0 | Gh | 0 | 0.07878 | 320.8 | 55.2 | 176.2 | -4.0 | 176.2 | -4.0 | 4.0 |
| JMA39a | 670.0 | Gh | 0 | 0.06963 | 315.4 | 57.3 | 175.1 | -0.5 | 175.1 | -0.5 | 7.0 |
| JMA39a | 680.0 | Gh | 0 | 0.01579 | 316.3 | 44.1 | 167.1 | -11.0 | 167.1 | -11.0 | 9.5 |
| JMA40a | 0.0 | Gh | 0 | 0.21919 | 271.6 | -3.1 | 104.2 | -2.7 | 104.2 | -2.7 | 3.0 |
| JMA40a | 100.0 | Gh | 0 | 0.21592 | 275.0 | -4.3 | 104.5 | -6.3 | 104.5 | -6.3 | 4.0 |
| JMA40a | 200.0 | Gh | 0 | 0.23046 | 276.9 | -1.8 | 107.6 | -7.0 | 107.6 | -7.0 | 4.0 |
| JMA40a | 300.0 | Gh | 0 | 0.23393 | 287.2 | -3.3 | 110.4 | -17.0 | 110.4 | -17.0 | 4.0 |
| JMA40a | 400.0 | Gh | 0 | 0.24297 | 298.8 | -3.6 | 115.4 | -27.7 | 115.4 | -27.7 | 3.0 |
| JMA40a | 500.0 | Gh | 0 | 0.20619 | 300.6 | -8.7 | 110.9 | -31.4 | 110.9 | -31.4 | 4.0 |
| JMA40a | 550.0 | Gh | 0 | 0.18384 | 289.3 | 1.6 | 105.7 | -16.9 | 105.7 | -16.9 | 4.0 |
| JMA40a | 600.0 | Gh | 0 | 0.17269 | 290.4 | 5.1 | 109.4 | -16.3 | 109.4 | -16.3 | 3.5 |
| JMA40a | 625.0 | Gh | 0 | 0.14519 | 290.4 | 6.5 | 110.7 | -15.7 | 110.7 | -15.7 | 4.5 |
| JMA40a | 650.0 | Gh | 0 | 0.12844 | 295.3 | 19.2 | 124.5 | -13.6 | 124.5 | -13.6 | 5.5 |
| JMA41a | 0.0 | Gh | 0 | 0.05579 | 84.0 | -4.3 | 291.2 | -7.2 | 291.2 | -7.2 | 2.0 |
| JMA41a | 100.0 | Gh | 0 | 0.05925 | 76.9 | -9.9 | 293.9 | -15.7 | 293.9 | -15.7 | 1.5 |
| JMA41a | 200.0 | Gh | 0 | 0.06424 | 63.0 | -8.6 | 287.5 | -28.2 | 287.5 | -28.2 | 2.0 |
| JMA41a | 300.0 | Gh | 0 | 0.08129 | 52.8 | -6.8 | 281.1 | -36.9 | 281.1 | -36.9 | 3.0 |
| JMA41a | 400.0 | Gh | 0 | 0.08052 | 50.2 | -5.6 | 278.4 | -38.8 | 278.4 | -38.8 | 2.0 |
| JMA41a | 500.0 | Gh | 0 | 0.07493 | 77.9 | -2.5 | 287.1 | -12.2 | 287.1 | -12.2 | 1.5 |
| JMA41a | 550.0 | Gh | 0 | 0.05855 | 89.4 | -33.0 | 320.2 | -12.2 | 320.2 | -12.2 | 2.0 |

| | | | | | | | | | | | | |
|---|---|---|---|---|---|---|---|---|---|---|---|---|
| JMA41a | 600.0 | Gh | 0 | 0.04258 | 89.6 | -45.1 | 332.3 | -15.7 | 332.3 | -15.7 | 2.5 |
| JMA41a | 625.0 | Gh | 0 | 0.04375 | 78.1 | -39.3 | 324.3 | -22.6 | 324.3 | -22.6 | 2.5 |
| JMA41a | 650.0 | Gh | 0 | 0.03723 | 68.7 | -28.7 | 311.1 | -28.4 | 311.1 | -28.4 | 3.5 |
| JMA41a | 660.0 | Gh | 0 | 0.02999 | 64.6 | -2.8 | 282.2 | -24.5 | 282.2 | -24.5 | 2.5 |
| JMA41a | 670.0 | Gh | 0 | 0.03673 | 30.8 | -2.8 | 261.1 | -54.5 | 261.1 | -54.5 | 8.0 |
| JMA41a | 680.0 | Gh | 0 | 0.03043 | 51.8 | 1.4 | 271.4 | -34.3 | 271.4 | -34.3 | 10.0 |
| JMA42a | 0.0 | Gh | 0 | 0.10111 | 300.0 | 25.4 | 144.1 | -15.5 | 144.1 | -15.5 | 4.0 |
| JMA42a | 100.0 | Gh | 0 | 0.10096 | 308.0 | 20.9 | 144.6 | -24.1 | 144.6 | -24.1 | 3.5 |
| JMA42a | 200.0 | Gh | 0 | 0.11438 | 316.7 | 19.8 | 149.4 | -31.2 | 149.4 | -31.2 | 4.0 |
| JMA42a | 300.0 | Gh | 0 | 0.14301 | 330.3 | 15.2 | 157.1 | -43.5 | 157.1 | -43.5 | 3.0 |
| JMA42a | 400.0 | Gh | 0 | 0.14553 | 337.5 | 13.5 | 163.8 | -49.0 | 163.8 | -49.0 | 3.0 |
| JMA42a | 500.0 | Gh | 0 | 0.13815 | 331.0 | 24.2 | 165.0 | -36.7 | 165.0 | -36.7 | 3.0 |
| JMA42a | 550.0 | Gh | 0 | 0.13103 | 315.6 | 18.9 | 137.4 | -31.0 | 137.4 | -31.0 | 2.0 |
| JMA42a | 600.0 | Gh | 0 | 0.14080 | 319.0 | 14.2 | 135.7 | -36.5 | 135.7 | -36.5 | 2.5 |
| JMA42a | 625.0 | Gh | 0 | 0.11926 | 327.5 | 9.0 | 137.9 | -46.2 | 137.9 | -46.2 | 3.0 |
| JMA42a | 650.0 | Gh | 0 | 0.12487 | 330.7 | 33.2 | 160.1 | -29.0 | 160.1 | -29.0 | 3.0 |
| JMA43a | 0.0 | Gh | 0 | 0.11316 | 174.0 | 15.7 | 338.1 | 80.0 | 338.1 | 80.0 | 2.0 |
| JMA43a | 100.0 | Gh | 0 | 0.09960 | 169.7 | 13.6 | 328.5 | 75.8 | 328.5 | 75.8 | 3.5 |
| JMA43a | 200.0 | Gh | 0 | 0.09122 | 166.5 | 13.6 | 320.2 | 73.5 | 320.2 | 73.5 | 4.0 |
| JMA43a | 300.0 | Gh | 0 | 0.10146 | 166.4 | 3.7 | 338.4 | 65.8 | 338.4 | 65.8 | 4.0 |
| JMA43a | 400.0 | Gh | 0 | 0.10819 | 160.8 | 13.8 | 309.3 | 69.2 | 309.3 | 69.2 | 4.0 |
| JMA43a | 500.0 | Gh | 0 | 0.09373 | 157.4 | 11.3 | 310.0 | 65.1 | 310.0 | 65.1 | 3.0 |
| JMA43a | 550.0 | Gh | 0 | 0.08527 | 145.8 | 27.8 | 269.0 | 59.1 | 269.0 | 59.1 | 3.0 |
| JMA43a | 600.0 | Gh | 0 | 0.07692 | 154.1 | 35.4 | 250.4 | 64.9 | 250.4 | 64.9 | 3.0 |
| JMA43a | 625.0 | Gh | 0 | 0.04863 | 155.6 | 33.9 | 252.8 | 66.5 | 252.8 | 66.5 | 4.0 |
| JMA43a | 650.0 | Gh | 0 | 0.06818 | 188.8 | 26.8 | 124.9 | 81.6 | 124.9 | 81.6 | 4.0 |
| JMA43a | 660.0 | Gh | 0 | 0.04515 | 184.4 | 23.0 | 90.2 | 85.9 | 90.2 | 85.9 | 5.0 |
| JMA43a | 670.0 | Gh | 0 | 0.02544 | 165.4 | 40.2 | 226.9 | 69.7 | 226.9 | 69.7 | 9.0 |
| JMA43a | 680.0 | Gh | 0 | 0.02136 | 182.3 | 21.2 | 50.6 | 86.5 | 50.6 | 86.5 | 11.5 |
| JMA44a | 0.0 | Gh | 0 | 0.02096 | 66.2 | -2.0 | 275.8 | -23.0 | 275.8 | -23.0 | 2.0 |
| JMA44a | 100.0 | Gh | 0 | 0.02998 | 56.1 | -12.3 | 283.4 | -35.8 | 283.4 | -35.8 | 2.5 |
| JMA44a | 200.0 | Gh | 0 | 0.03827 | 36.2 | -10.9 | 273.3 | -54.0 | 273.3 | -54.0 | 2.0 |
| JMA44a | 300.0 | Gh | 0 | 0.03892 | 25.1 | 6.0 | 238.5 | -54.1 | 238.5 | -54.1 | 3.0 |
| JMA44a | 400.0 | Gh | 0 | 0.04359 | 28.0 | -9.3 | 264.9 | -60.9 | 264.9 | -60.9 | 3.0 |
| JMA44a | 500.0 | Gh | 0 | 0.05315 | 14.6 | -5.6 | 238.8 | -69.8 | 238.8 | -69.8 | 2.5 |
| JMA44a | 550.0 | Gh | 0 | 0.06182 | 9.3 | -20.7 | 278.2 | -81.2 | 278.2 | -81.2 | 2.5 |
| JMA44a | 600.0 | Gh | 0 | 0.05662 | 10.6 | -18.5 | 265.4 | -79.9 | 265.4 | -79.9 | 2.0 |
| JMA44a | 625.0 | Gh | 0 | 0.05457 | 0.3 | -13.9 | 184.3 | -83.8 | 184.3 | -83.8 | 2.0 |
| JMA44a | 650.0 | Gh | 0 | 0.06042 | 24.3 | -3.8 | 240.7 | -61.3 | 240.7 | -61.3 | 3.0 |
| JMA45a | 0.0 | Gh | 0 | 0.05426 | 140.6 | -71.7 | 4.8 | -6.5 | 4.8 | -6.5 | 2.0 |
| JMA45a | 100.0 | Gh | 0 | 0.06221 | 93.6 | -72.4 | 357.8 | -18.9 | 357.8 | -18.9 | 2.5 |
| JMA45a | 200.0 | Gh | 0 | 0.06422 | 55.1 | -70.0 | 357.2 | -31.3 | 357.2 | -31.3 | 3.5 |
| JMA45a | 300.0 | Gh | 0 | 0.07638 | 52.2 | -56.3 | 342.6 | -38.0 | 342.6 | -38.0 | 3.0 |
| JMA45a | 400.0 | Gh | 0 | 0.07820 | 77.2 | -36.3 | 318.3 | -22.3 | 318.3 | -22.3 | 2.5 |
| JMA45a | 500.0 | Gh | 0 | 0.08317 | 87.7 | -41.2 | 325.2 | -15.4 | 325.2 | -15.4 | 1.0 |
| JMA45a | 550.0 | Gh | 0 | 0.05496 | 68.9 | -60.0 | 344.3 | -28.6 | 344.3 | -28.6 | 3.5 |
| JMA45a | 600.0 | Gh | 0 | 0.05751 | 56.8 | -51.4 | 335.7 | -36.8 | 335.7 | -36.8 | 1.5 |
| JMA45a | 625.0 | Gh | 0 | 0.03923 | 22.7 | -50.2 | 350.3 | -55.7 | 350.3 | -55.7 | 4.5 |
| JMA45a | 650.0 | Gh | 0 | 0.03704 | 24.4 | -45.1 | 342.3 | -58.6 | 342.3 | -58.6 | 3.0 |

| | | | | | | | | | | | |
|---|---|---|---|---|---|---|---|---|---|---|---|
| JMA45a | 660.0 | Gh | 0 | 0.02260 | 45.8 | -25.8 | 302.1 | -47.9 | 302.1 | -47.9 | 12.0 |
| JMA45a | 670.0 | Gh | 0 | 0.02776 | 39.3 | -16.5 | 286.4 | -52.6 | 286.4 | -52.6 | 5.0 |
| JMA45a | 680.0 | Gh | 0 | 0.02773 | 18.6 | 11.3 | 227.6 | -52.9 | 227.6 | -52.9 | 6.0 |
| | | | | | | | | | | | |
| JMA46a | 0.0 | Gh | 0 | 0.11039 | 269.5 | 32.8 | 132.9 | 12.6 | 132.9 | 12.6 | 3.0 |
| JMA46a | 100.0 | Gh | 0 | 0.10006 | 277.3 | 32.0 | 134.6 | 6.2 | 134.6 | 6.2 | 3.0 |
| JMA46a | 200.0 | Gh | 0 | 0.09683 | 289.6 | 31.4 | 138.7 | -3.4 | 138.7 | -3.4 | 3.0 |
| JMA46a | 300.0 | Gh | 0 | 0.10579 | 296.3 | 30.5 | 141.0 | -8.8 | 141.0 | -8.8 | 4.5 |
| JMA46a | 400.0 | Gh | 0 | 0.12841 | 294.4 | 18.8 | 129.9 | -13.5 | 129.9 | -13.5 | 2.5 |
| JMA46a | 500.0 | Gh | 0 | 0.15645 | 297.5 | 21.7 | 134.1 | -14.6 | 134.1 | -14.6 | 3.5 |
| JMA46a | 550.0 | Gh | 0 | 0.14346 | 302.3 | 7.4 | 113.3 | -25.9 | 113.3 | -25.9 | 3.5 |
| JMA46a | 600.0 | Gh | 0 | 0.13573 | 303.2 | -0.7 | 105.7 | -30.5 | 105.7 | -30.5 | 3.0 |
| JMA46a | 625.0 | Gh | 0 | 0.11398 | 305.5 | 5.7 | 113.4 | -29.5 | 113.4 | -29.5 | 4.0 |
| JMA46a | 650.0 | Gh | 0 | 0.10597 | 298.1 | 2.9 | 106.7 | -24.4 | 106.7 | -24.4 | 4.0 |
| | | | | | | | | | | | |
| JMA47a | 0.0 | Gh | 0 | 0.16319 | 275.1 | -49.1 | 51.9 | -24.0 | 51.9 | -24.0 | 3.0 |
| JMA47a | 100.0 | Gh | 0 | 0.17011 | 283.3 | -52.5 | 49.4 | -29.7 | 49.4 | -29.7 | 3.5 |
| JMA47a | 200.0 | Gh | 0 | 0.16924 | 290.8 | -51.7 | 50.9 | -34.2 | 50.9 | -34.2 | 4.5 |
| JMA47a | 300.0 | Gh | 0 | 0.17535 | 297.4 | -56.6 | 44.7 | -38.0 | 44.7 | -38.0 | 4.0 |
| JMA47a | 400.0 | Gh | 0 | 0.17751 | 294.0 | -62.0 | 38.3 | -35.7 | 38.3 | -35.7 | 4.5 |
| JMA47a | 500.0 | Gh | 0 | 0.18201 | 294.3 | -56.8 | 44.6 | -36.3 | 44.6 | -36.3 | 4.0 |
| JMA47a | 550.0 | Gh | 0 | 0.13952 | 294.1 | -53.0 | 49.4 | -36.3 | 49.4 | -36.3 | 4.0 |
| JMA47a | 600.0 | Gh | 0 | 0.13911 | 294.2 | -47.5 | 56.2 | -36.2 | 56.2 | -36.2 | 4.0 |
| JMA47a | 625.0 | Gh | 0 | 0.10013 | 307.4 | -65.6 | 32.0 | -40.5 | 32.0 | -40.5 | 4.5 |
| JMA47a | 650.0 | Gh | 0 | 0.07215 | 315.7 | -72.3 | 22.5 | -39.8 | 22.5 | -39.8 | 4.5 |
| JMA47a | 660.0 | Gh | 0 | 0.06014 | 329.1 | -63.5 | 27.0 | -49.3 | 27.0 | -49.3 | 7.0 |
| JMA47a | 670.0 | Gh | 0 | 0.05045 | 299.1 | -53.6 | 48.4 | -39.3 | 48.4 | -39.3 | 10.0 |
| JMA47a | 680.0 | Gh | 0 | 0.05689 | 357.4 | -61.2 | 8.7 | -56.8 | 8.7 | -56.8 | 14.0 |
| | | | | | | | | | | | |
| JMA48a | 0.0 | Gh | 0 | 0.08424 | 203.7 | -2.2 | 51.0 | 55.1 | 51.0 | 55.1 | 2.0 |
| JMA48a | 100.0 | Gh | 0 | 0.07450 | 201.6 | -8.4 | 42.1 | 51.3 | 42.1 | 51.3 | 3.0 |
| JMA48a | 200.0 | Gh | 0 | 0.06172 | 200.9 | -8.1 | 41.4 | 52.0 | 41.4 | 52.0 | 3.0 |
| JMA48a | 300.0 | Gh | 0 | 0.05810 | 197.9 | -21.0 | 29.0 | 41.7 | 29.0 | 41.7 | 4.0 |
| JMA48a | 400.0 | Gh | 0 | 0.05407 | 200.6 | -34.1 | 25.8 | 28.7 | 25.8 | 28.7 | 4.0 |
| JMA48a | 500.0 | Gh | 0 | 0.05881 | 207.6 | -44.1 | 26.8 | 17.3 | 26.8 | 17.3 | 3.0 |
| JMA48a | 550.0 | Gh | 0 | 0.05384 | 223.7 | -24.3 | 40.4 | 25.8 | 40.4 | 25.8 | 3.0 |
| JMA48a | 600.0 | Gh | 0 | 0.04849 | 203.5 | 8.9 | 55.9 | 62.9 | 55.9 | 62.9 | 4.0 |
| JMA48a | 625.0 | Gh | 0 | 0.04984 | 201.1 | -19.5 | 23.1 | 41.9 | 23.1 | 41.9 | 3.5 |
| JMA48a | 650.0 | Gh | 0 | 0.02757 | 205.6 | -49.2 | 12.9 | 13.4 | 12.9 | 13.4 | 1.5 |
| | | | | | | | | | | | |
| JMA49a | 0.0 | Gh | 0 | 0.11244 | 282.4 | 6.9 | 113.4 | -9.0 | 113.4 | -9.0 | 3.0 |
| JMA49a | 100.0 | Gh | 0 | 0.10948 | 282.9 | 4.1 | 111.0 | -10.5 | 111.0 | -10.5 | 2.0 |
| JMA49a | 200.0 | Gh | 0 | 0.10911 | 287.1 | 2.5 | 111.1 | -15.0 | 111.1 | -15.0 | 2.0 |
| JMA49a | 300.0 | Gh | 0 | 0.11139 | 290.3 | 1.8 | 111.7 | -18.2 | 111.7 | -18.2 | 2.5 |
| JMA49a | 400.0 | Gh | 0 | 0.11251 | 293.6 | -0.6 | 110.7 | -22.2 | 110.7 | -22.2 | 2.0 |
| JMA49a | 500.0 | Gh | 0 | 0.10924 | 294.4 | -5.5 | 106.0 | -24.7 | 106.0 | -24.7 | 3.0 |
| JMA49a | 550.0 | Gh | 0 | 0.09041 | 299.9 | -14.7 | 98.1 | -32.7 | 98.1 | -32.7 | 2.0 |
| JMA49a | 600.0 | Gh | 0 | 0.07938 | 292.2 | -16.4 | 93.9 | -26.0 | 93.9 | -26.0 | 3.0 |
| JMA49a | 625.0 | Gh | 0 | 0.06274 | 303.1 | -24.1 | 87.5 | -37.8 | 87.5 | -37.8 | 3.5 |
| JMA49a | 650.0 | Gh | 0 | 0.06795 | 294.5 | -4.2 | 107.4 | -24.3 | 107.4 | -24.3 | 4.0 |
| JMA49a | 660.0 | Gh | 0 | 0.01010 | 124.4 | -37.8 | 330.7 | 11.4 | 330.7 | 11.4 | 8.0 |
| JMA49a | 670.0 | Gh | 0 | 0.01397 | 108.9 | 7.1 | 282.4 | 20.1 | 282.4 | 20.1 | 10.0 |
| JMA49a | 680.0 | Gh | 0 | 0.01993 | 45.9 | -1.1 | 264.5 | -41.1 | 264.5 | -41.1 | 14.5 |

| | | | | | | | | | | | |
|---|---|---|---|---|---|---|---|---|---|---|---|
| JMA50a | 0.0 | Gh | 0 | 0.09511 | 157.5 | 62.2 | 203.5 | 43.1 | 203.5 | 43.1 | 2.0 |
| JMA50a | 100.0 | Gh | 0 | 0.09022 | 150.8 | 61.0 | 208.0 | 42.3 | 208.0 | 42.3 | -9.9 |
| JMA50a | 200.0 | Gh | 0 | 0.08542 | 132.1 | 64.0 | 212.5 | 33.9 | 212.5 | 33.9 | 1.0 |
| JMA50a | 300.0 | Gh | 0 | 0.08179 | 124.9 | 67.1 | 211.0 | 29.8 | 211.0 | 29.8 | 3.0 |
| JMA50a | 400.0 | Gh | 0 | 0.09078 | 111.4 | 80.8 | 198.6 | 21.1 | 198.6 | 21.1 | 2.5 |
| JMA50a | 500.0 | Gh | 0 | 0.08748 | 34.6 | 84.1 | 192.9 | 13.1 | 192.9 | 13.1 | 3.0 |
| JMA50a | 550.0 | Gh | 0 | 0.07909 | 128.7 | 73.3 | 193.7 | 27.8 | 193.7 | 27.8 | 2.0 |
| JMA50a | 600.0 | Gh | 0 | 0.06859 | 94.5 | 63.6 | 206.8 | 18.1 | 206.8 | 18.1 | 2.5 |
| JMA50a | 625.0 | Gh | 0 | 0.06693 | 113.9 | 67.8 | 201.5 | 25.6 | 201.5 | 25.6 | 2.5 |
| JMA50a | 650.0 | Gh | 0 | 0.03986 | 110.4 | 83.6 | 185.4 | 20.1 | 185.4 | 20.1 | 3.5 |
| | | | | | | | | | | | |
| JMB01a | 0.0 | Gh | 0 | 0.13448 | 226.3 | -37.8 | 80.8 | 9.6 | 80.8 | 9.6 | 5.0 |
| JMB01a | 100.0 | Gh | 0 | 0.13586 | 230.9 | -40.4 | 81.8 | 5.3 | 81.8 | 5.3 | 5.5 |
| JMB01a | 200.0 | Gh | 0 | 0.13406 | 234.9 | -43.6 | 81.7 | 0.9 | 81.7 | 0.9 | 6.0 |
| JMB01a | 300.0 | Gh | 0 | 0.13477 | 241.6 | -46.9 | 82.5 | -4.8 | 82.5 | -4.8 | 4.5 |
| JMB01a | 400.0 | Gh | 0 | 0.13979 | 248.1 | -49.6 | 83.0 | -9.9 | 83.0 | -9.9 | 5.5 |
| JMB01a | 500.0 | Gh | 0 | 0.14059 | 249.4 | -50.2 | 83.0 | -10.9 | 83.0 | -10.9 | 6.0 |
| JMB01a | 550.0 | Gh | 0 | 0.16705 | 289.7 | -44.4 | 99.6 | -34.0 | 99.6 | -34.0 | 6.0 |
| JMB01a | 600.0 | Gh | 0 | 0.15353 | 283.2 | -44.7 | 98.0 | -29.5 | 98.0 | -29.5 | 14.5 |
| JMB01a | 625.0 | Gh | 0 | 0.14692 | 283.1 | -46.1 | 96.5 | -29.7 | 96.5 | -29.7 | 17.0 |
| JMB01a | 650.0 | Gh | 0 | 0.10382 | 287.6 | -40.5 | 103.7 | -31.6 | 103.7 | -31.6 | 28.5 |
| JMB01a | 660.0 | Gh | 0 | 0.10332 | 289.4 | -45.8 | 97.9 | -34.0 | 97.9 | -34.0 | 35.5 |
| JMB01a | 670.0 | Gh | 2 | 0.00982 | 149.0 | -79.8 | 39.8 | -21.1 | 39.8 | -21.1 | 76.5 |
| JMB01a | 680.0 | Gh | 1 | 0.00948 | 304.6 | 66.1 | 205.2 | 14.9 | 205.2 | 14.9 | 68.0 |
| | | | | | | | | | | | |
| JMB02a | 0.0 | Gh | 0 | 0.11295 | 250.2 | 1.4 | 116.8 | 19.1 | 116.8 | 19.1 | 5.0 |
| JMB02a | 100.0 | Gh | 0 | 0.10921 | 253.1 | 0.1 | 116.6 | 15.9 | 116.6 | 15.9 | 6.0 |
| JMB02a | 200.0 | Gh | 0 | 0.10586 | 258.7 | 0.4 | 118.9 | 10.7 | 118.9 | 10.7 | 5.0 |
| JMB02a | 300.0 | Gh | 0 | 0.10610 | 263.1 | 0.1 | 120.1 | 6.5 | 120.1 | 6.5 | 5.0 |
| JMB02a | 400.0 | Gh | 0 | 0.10715 | 273.0 | -1.2 | 122.3 | -3.2 | 122.3 | -3.2 | 5.5 |
| JMB02a | 500.0 | Gh | 0 | 0.10918 | 273.6 | -1.7 | 122.0 | -3.9 | 122.0 | -3.9 | 6.0 |
| JMB02a | 550.0 | Gh | 0 | 0.14134 | 302.2 | -0.0 | 124.1 | -30.1 | 124.1 | -30.1 | 5.0 |
| JMB02a | 600.0 | Gh | 0 | 0.13453 | 308.9 | -5.6 | 120.9 | -38.3 | 120.9 | -38.3 | 6.0 |
| JMB02a | 625.0 | Gh | 0 | 0.11449 | 310.0 | -5.1 | 122.1 | -39.2 | 122.1 | -39.2 | 9.0 |
| JMB02a | 650.0 | Gh | 0 | 0.11113 | 308.3 | -3.3 | 123.3 | -36.9 | 123.3 | -36.9 | 14.0 |
| | | | | | | | | | | | |
| JMB03a | 0.0 | Gh | 0 | 0.18356 | 206.8 | -3.8 | 84.9 | 58.5 | 84.9 | 58.5 | 6.5 |
| JMB03a | 100.0 | Gh | 0 | 0.17396 | 210.2 | -4.6 | 86.9 | 55.2 | 86.9 | 55.2 | 7.0 |
| JMB03a | 200.0 | Gh | 0 | 0.15552 | 212.6 | -3.6 | 90.4 | 53.6 | 90.4 | 53.6 | 6.0 |
| JMB03a | 300.0 | Gh | 0 | 0.14818 | 214.6 | -3.5 | 92.1 | 51.9 | 92.1 | 51.9 | 6.0 |
| JMB03a | 400.0 | Gh | 0 | 0.12789 | 222.6 | -7.7 | 91.7 | 42.9 | 91.7 | 42.9 | 6.0 |
| JMB03a | 500.0 | Gh | 0 | 0.11884 | 230.2 | -9.8 | 93.3 | 35.2 | 93.3 | 35.2 | 6.0 |
| JMB03a | 550.0 | Gh | 0 | 0.11768 | 275.7 | -2.1 | 114.7 | -6.0 | 114.7 | -6.0 | 6.0 |
| JMB03a | 600.0 | Gh | 0 | 0.10557 | 278.8 | -2.2 | 115.2 | -9.1 | 115.2 | -9.1 | 6.0 |
| JMB03a | 625.0 | Gh | 0 | 0.10063 | 276.0 | -0.9 | 115.8 | -6.1 | 115.8 | -6.1 | 6.5 |
| JMB03a | 650.0 | Gh | 0 | 0.10123 | 281.4 | -4.5 | 113.6 | -12.1 | 113.6 | -12.1 | 12.0 |
| JMB03a | 660.0 | Gh | 0 | 0.10199 | 280.4 | 2.5 | 120.3 | -9.5 | 120.3 | -9.5 | 17.5 |
| JMB03a | 670.0 | Gh | 0 | 0.05257 | 287.6 | -8.7 | 110.6 | -19.0 | 110.6 | -19.0 | 38.0 |
| JMB03a | 680.0 | Gh | 0 | 0.04494 | 296.3 | 1.8 | 123.7 | -25.1 | 123.7 | -25.1 | 39.0 |
| | | | | | | | | | | | |
| JMB04a | 0.0 | Gh | 0 | 0.11532 | 287.9 | -22.2 | 102.1 | -23.4 | 102.1 | -23.4 | 5.0 |
| JMB04a | 100.0 | Gh | 0 | 0.11822 | 291.0 | -23.9 | 100.9 | -26.5 | 100.9 | -26.5 | 6.0 |

| | | | | | | | | | | | |
|---|---|---|---|---|---|---|---|---|---|---|---|
| JMB04a | 200.0 | Gh | 0 | 0.12497 | 298.4 | -22.4 | 104.1 | -32.9 | 104.1 | -32.9 | 6.0 |
| JMB04a | 300.0 | Gh | 0 | 0.12988 | 304.9 | -21.2 | 106.8 | -38.7 | 106.8 | -38.7 | 6.0 |
| JMB04a | 400.0 | Gh | 0 | 0.14422 | 311.1 | -19.0 | 110.9 | -44.1 | 110.9 | -44.1 | 6.5 |
| JMB04a | 500.0 | Gh | 0 | 0.16335 | 313.7 | -16.2 | 115.5 | -45.9 | 115.5 | -45.9 | 6.0 |
| JMB04a | 550.0 | Gh | 0 | 0.17163 | 316.0 | -13.5 | 109.6 | -47.5 | 109.6 | -47.5 | 4.5 |
| JMB04a | 600.0 | Gh | 0 | 0.16448 | 318.0 | -12.0 | 112.7 | -49.0 | 112.7 | -49.0 | 5.0 |
| JMB04a | 625.0 | Gh | 0 | 0.15949 | 319.4 | -8.7 | 118.0 | -49.2 | 118.0 | -49.2 | 6.5 |
| JMB04a | 650.0 | Gh | 0 | 0.14646 | 320.4 | -4.5 | 124.6 | -48.5 | 124.6 | -48.5 | 11.0 |
| | | | | | | | | | | | |
| JMB05a | 0.0 | Gh | 0 | 0.21913 | 210.2 | -9.1 | 80.6 | 53.3 | 80.6 | 53.3 | 7.0 |
| JMB05a | 100.0 | Gh | 0 | 0.20632 | 215.3 | -10.9 | 82.6 | 48.1 | 82.6 | 48.1 | 6.0 |
| JMB05a | 200.0 | Gh | 0 | 0.18440 | 215.7 | -11.4 | 82.3 | 47.5 | 82.3 | 47.5 | 7.0 |
| JMB05a | 300.0 | Gh | 0 | 0.17960 | 222.1 | -11.2 | 87.0 | 42.2 | 87.0 | 42.2 | 7.0 |
| JMB05a | 400.0 | Gh | 0 | 0.16539 | 234.5 | -13.5 | 90.8 | 30.3 | 90.8 | 30.3 | 5.0 |
| JMB05a | 500.0 | Gh | 0 | 0.13912 | 249.6 | -11.3 | 98.5 | 17.1 | 98.5 | 17.1 | 6.0 |
| JMB05a | 550.0 | Gh | 0 | 0.11177 | 265.6 | -5.3 | 108.3 | 3.2 | 108.3 | 3.2 | 6.0 |
| JMB05a | 600.0 | Gh | 0 | 0.11890 | 272.1 | -2.6 | 112.3 | -2.6 | 112.3 | -2.6 | 5.0 |
| JMB05a | 625.0 | Gh | 0 | 0.11469 | 273.7 | -2.3 | 112.9 | -4.1 | 112.9 | -4.1 | 6.0 |
| JMB05a | 650.0 | Gh | 0 | 0.10911 | 284.1 | -1.8 | 115.6 | -14.2 | 115.6 | -14.2 | 7.0 |
| JMB05a | 660.0 | Gh | 0 | 0.11734 | 291.3 | 8.6 | 127.9 | -18.6 | 127.9 | -18.6 | 10.0 |
| JMB05a | 670.0 | Gh | 0 | 0.11337 | 294.3 | 4.4 | 124.4 | -22.6 | 124.4 | -22.6 | 23.0 |
| JMB05a | 680.0 | Gh | 0 | 0.11107 | 297.2 | 12.9 | 134.1 | -22.9 | 134.1 | -22.9 | 15.0 |
| | | | | | | | | | | | |
| JMB06a | 0.0 | Gh | 0 | 0.23981 | 277.2 | 10.2 | 126.3 | -3.6 | 126.3 | -3.6 | 6.0 |
| JMB06a | 100.0 | Gh | 0 | 0.24070 | 279.3 | 10.2 | 127.0 | -5.5 | 127.0 | -5.5 | 6.0 |
| JMB06a | 200.0 | Gh | 0 | 0.24784 | 284.5 | 10.3 | 128.9 | -10.3 | 128.9 | -10.3 | 6.0 |
| JMB06a | 300.0 | Gh | 0 | 0.25329 | 286.4 | 11.0 | 130.2 | -11.8 | 130.2 | -11.8 | 6.0 |
| JMB06a | 400.0 | Gh | 0 | 0.24959 | 291.4 | 12.9 | 133.9 | -15.6 | 133.9 | -15.6 | 5.0 |
| JMB06a | 500.0 | Gh | 0 | 0.24994 | 298.7 | 12.4 | 136.5 | -22.3 | 136.5 | -22.3 | 4.5 |
| JMB06a | 550.0 | Gh | 0 | 0.25033 | 300.4 | 7.5 | 122.1 | -25.9 | 122.1 | -25.9 | 5.0 |
| JMB06a | 600.0 | Gh | 0 | 0.22869 | 304.7 | 9.5 | 126.2 | -28.8 | 126.2 | -28.8 | 5.0 |
| JMB06a | 625.0 | Gh | 0 | 0.21649 | 306.4 | 10.4 | 128.0 | -30.0 | 128.0 | -30.0 | 6.0 |
| JMB06a | 650.0 | Gh | 0 | 0.21279 | 303.1 | 10.6 | 126.5 | -27.0 | 126.5 | -27.0 | 13.5 |
| | | | | | | | | | | | |
| JMB07a | 0.0 | Gh | 0 | 0.21548 | 227.4 | 28.6 | 104.2 | 47.8 | 104.2 | 47.8 | 6.0 |
| JMB07a | 100.0 | Gh | 0 | 0.19940 | 232.8 | 28.9 | 105.5 | 43.2 | 105.5 | 43.2 | 7.0 |
| JMB07a | 200.0 | Gh | 0 | 0.18490 | 235.9 | 33.8 | 112.5 | 41.1 | 112.5 | 41.1 | 6.5 |
| JMB07a | 300.0 | Gh | 0 | 0.18141 | 244.5 | 35.9 | 116.1 | 34.3 | 116.1 | 34.3 | 7.0 |
| JMB07a | 400.0 | Gh | 0 | 0.16820 | 256.5 | 38.6 | 121.1 | 25.4 | 121.1 | 25.4 | 6.0 |
| JMB07a | 500.0 | Gh | 0 | 0.15862 | 287.3 | 46.0 | 136.5 | 6.7 | 136.5 | 6.7 | 5.5 |
| JMB07a | 550.0 | Gh | 0 | 0.16280 | 288.8 | 49.7 | 140.2 | 7.6 | 140.2 | 7.6 | 6.0 |
| JMB07a | 600.0 | Gh | 0 | 0.15374 | 287.1 | 50.0 | 140.0 | 8.8 | 140.0 | 8.8 | 6.0 |
| JMB07a | 625.0 | Gh | 0 | 0.14361 | 292.7 | 50.5 | 142.2 | 5.9 | 142.2 | 5.9 | 6.0 |
| JMB07a | 650.0 | Gh | 0 | 0.13224 | 293.8 | 41.3 | 134.9 | 0.2 | 134.9 | 0.2 | 10.0 |
| JMB07a | 660.0 | Gh | 0 | 0.12512 | 305.7 | 45.9 | 143.9 | -3.7 | 143.9 | -3.7 | 16.5 |
| JMB07a | 670.0 | Gh | 0 | 0.11423 | 303.2 | 37.0 | 135.9 | -8.2 | 135.9 | -8.2 | 24.0 |
| JMB07a | 680.0 | Gh | 0 | 0.11521 | 305.7 | 39.1 | 138.9 | -8.3 | 138.9 | -8.3 | 28.0 |
| | | | | | | | | | | | |
| JMB09ai | 0.0 | Gh | 0 | 0.19787 | 199.2 | 12.1 | 42.7 | 66.0 | 42.7 | 66.0 | 7.0 |
| JMB09ai | 100.0 | Gh | 0 | 0.18191 | 199.5 | 11.5 | 42.2 | 65.4 | 42.2 | 65.4 | 7.0 |
| JMB09ai | 200.0 | Gh | 0 | 0.16018 | 196.9 | 13.3 | 40.8 | 68.5 | 40.8 | 68.5 | 6.0 |
| JMB09ai | 300.0 | Gh | 0 | 0.14518 | 199.5 | 15.1 | 48.9 | 67.8 | 48.9 | 67.8 | 7.0 |
| JMB09ai | 400.0 | Gh | 0 | 0.11542 | 205.8 | 27.4 | 85.0 | 67.2 | 85.0 | 67.2 | 5.5 |

| | | | | | | | | | | | |
|---|---|---|---|---|---|---|---|---|---|---|---|
| JMB09ai | 500.0 | Gh | 0 | 0.06788 | 233.3 | 46.4 | 131.5 | 42.8 | 131.5 | 42.8 | 5.5 |
| JMB09ai | 550.0 | Gh | 0 | 0.04832 | 262.8 | 33.0 | 107.8 | 20.3 | 107.8 | 20.3 | 6.0 |
| JMB09ai | 600.0 | Gh | 0 | 0.05272 | 283.4 | 27.8 | 111.0 | 2.2 | 111.0 | 2.2 | 7.0 |
| JMB09ai | 625.0 | Gh | 0 | 0.05178 | 279.5 | 37.2 | 117.6 | 9.6 | 117.6 | 9.6 | 8.0 |
| JMB09ai | 650.0 | Gh | 0 | 0.04043 | 289.4 | 35.5 | 120.2 | 1.9 | 120.2 | 1.9 | 12.5 |
| JMB09ai | 660.0 | Gh | 0 | 0.03412 | 303.9 | 32.2 | 125.0 | -9.6 | 125.0 | -9.6 | 22.0 |
| JMB09ai | 670.0 | Gh | 0 | 0.03985 | 301.1 | 10.0 | 105.3 | -21.6 | 105.3 | -21.6 | 33.0 |
| JMB09ai | 680.0 | Gh | 0 | 0.03002 | 341.1 | 31.0 | 152.0 | -28.4 | 152.0 | -28.4 | 39.0 |
| | | | | | | | | | | | |
| JMB09aii | 0.0 | Gh | 0 | 0.20584 | 196.0 | 4.0 | 196.0 | 4.0 | 196.0 | 4.0 | 6.0 |
| JMB09aii | 100.0 | Gh | 0 | 0.19553 | 197.3 | 2.3 | 197.3 | 2.3 | 197.3 | 2.3 | 6.5 |
| JMB09aii | 200.0 | Gh | 0 | 0.17362 | 195.8 | 2.2 | 195.8 | 2.2 | 195.8 | 2.2 | 5.5 |
| JMB09aii | 300.0 | Gh | 0 | 0.15697 | 198.5 | -0.6 | 198.5 | -0.6 | 198.5 | -0.6 | 6.0 |
| JMB09aii | 400.0 | Gh | 0 | 0.11066 | 199.4 | 0.4 | 199.4 | 0.4 | 199.4 | 0.4 | 5.5 |
| JMB09aii | 500.0 | Gh | 0 | 0.05756 | 212.9 | -4.3 | 40.0 | 44.8 | 40.0 | 44.8 | 6.0 |
| JMB09aii | 550.0 | Gh | 0 | 0.04488 | 230.0 | 2.1 | 62.8 | 36.7 | 62.8 | 36.7 | 6.5 |
| JMB09aii | 600.0 | Gh | 0 | 0.02420 | 228.7 | -12.4 | 47.6 | 29.6 | 47.6 | 29.6 | 5.5 |
| JMB09aii | 625.0 | Gh | 0 | 0.02920 | 237.4 | -22.3 | 44.6 | 17.0 | 44.6 | 17.0 | 9.0 |
| JMB09aii | 650.0 | Gh | 0 | 0.01456 | 270.5 | -14.8 | 66.7 | -6.6 | 66.7 | -6.6 | 15.0 |
| | | | | | | | | | | | |
| JMB10a | 0.0 | Gh | 0 | 0.16849 | 267.1 | 34.3 | 121.0 | 16.5 | 121.0 | 16.5 | 6.0 |
| JMB10a | 100.0 | Gh | 0 | 0.16348 | 271.9 | 34.5 | 122.7 | 12.9 | 122.7 | 12.9 | 6.0 |
| JMB10a | 200.0 | Gh | 0 | 0.15998 | 285.4 | 34.3 | 127.5 | 2.9 | 127.5 | 2.9 | 6.0 |
| JMB10a | 300.0 | Gh | 0 | 0.16717 | 295.1 | 33.9 | 131.5 | -4.1 | 131.5 | -4.1 | 5.0 |
| JMB10a | 400.0 | Gh | 0 | 0.18481 | 303.6 | 37.1 | 138.3 | -7.6 | 138.3 | -7.6 | 5.0 |
| JMB10a | 500.0 | Gh | 0 | 0.18892 | 311.6 | 36.2 | 142.1 | -12.9 | 142.1 | -12.9 | 6.0 |
| JMB10a | 550.0 | Gh | 0 | 0.18002 | 316.6 | 30.1 | 130.7 | -20.2 | 130.7 | -20.2 | 6.0 |
| JMB10a | 600.0 | Gh | 0 | 0.16673 | 318.9 | 27.5 | 130.6 | -23.5 | 130.6 | -23.5 | 8.0 |
| JMB10a | 625.0 | Gh | 0 | 0.15727 | 315.7 | 27.0 | 127.8 | -22.0 | 127.8 | -22.0 | 12.0 |
| JMB10a | 650.0 | Gh | 0 | 0.13414 | 318.6 | 27.8 | 130.5 | -23.1 | 130.5 | -23.1 | 20.5 |
| | | | | | | | | | | | |
| JMB11a | 0.0 | Gh | 0 | 0.23793 | 227.3 | 15.0 | 76.0 | 44.5 | 76.0 | 44.5 | 6.5 |
| JMB11a | 100.0 | Gh | 0 | 0.22249 | 228.8 | 15.6 | 77.6 | 43.4 | 77.6 | 43.4 | 6.5 |
| JMB11a | 200.0 | Gh | 0 | 0.20231 | 233.3 | 18.0 | 82.7 | 40.3 | 82.7 | 40.3 | 6.0 |
| JMB11a | 300.0 | Gh | 0 | 0.18935 | 239.3 | 17.8 | 85.0 | 34.9 | 85.0 | 34.9 | 6.5 |
| JMB11a | 400.0 | Gh | 0 | 0.16183 | 249.2 | 24.2 | 95.8 | 28.3 | 95.8 | 28.3 | 6.5 |
| JMB11a | 500.0 | Gh | 0 | 0.14275 | 268.7 | 27.2 | 105.5 | 13.0 | 105.5 | 13.0 | 6.0 |
| JMB11a | 550.0 | Gh | 0 | 0.14645 | 274.0 | 32.5 | 112.4 | 11.1 | 112.4 | 11.1 | 9.0 |
| JMB11a | 600.0 | Gh | 0 | 0.14468 | 281.4 | 35.7 | 118.1 | 7.0 | 118.1 | 7.0 | 10.5 |
| JMB11a | 625.0 | Gh | 0 | 0.12170 | 276.7 | 39.4 | 119.7 | 12.0 | 119.7 | 12.0 | 18.0 |
| JMB11a | 650.0 | Gh | 0 | 0.11043 | 286.3 | 33.8 | 118.4 | 2.6 | 118.4 | 2.6 | 23.0 |
| JMB11a | 660.0 | Gh | 0 | 0.09242 | 299.5 | 33.9 | 124.8 | -6.3 | 124.8 | -6.3 | 39.0 |
| JMB11a | 670.0 | Gh | 0 | 0.08864 | 299.2 | 43.0 | 131.7 | -0.5 | 131.7 | -0.5 | 53.5 |
| JMB11a | 680.0 | Gh | 0 | 0.04817 | 291.6 | 30.9 | 118.4 | -2.8 | 118.4 | -2.8 | 62.0 |
| | | | | | | | | | | | |
| JMB12a | 0.0 | Gh | 0 | 0.16870 | 218.5 | 1.5 | 61.1 | 48.1 | 61.1 | 48.1 | 5.0 |
| JMB12a | 100.0 | Gh | 0 | 0.15888 | 222.9 | 3.1 | 66.1 | 44.9 | 66.1 | 44.9 | 1.0 |
| JMB12a | 200.0 | Gh | 0 | 0.14353 | 223.5 | 3.9 | 67.4 | 44.7 | 67.4 | 44.7 | 3.5 |
| JMB12a | 300.0 | Gh | 0 | 0.13740 | 231.1 | 6.0 | 73.9 | 38.5 | 73.9 | 38.5 | 4.5 |
| JMB12a | 400.0 | Gh | 0 | 0.12070 | 239.4 | 4.2 | 75.4 | 30.1 | 75.4 | 30.1 | 5.0 |
| JMB12a | 500.0 | Gh | 0 | 0.09483 | 256.3 | 5.5 | 83.0 | 14.7 | 83.0 | 14.7 | 5.0 |
| JMB12a | 550.0 | Gh | 0 | 0.08919 | 267.0 | 6.4 | 77.0 | 4.9 | 77.0 | 4.9 | 6.0 |
| JMB12a | 600.0 | Gh | 0 | 0.07529 | 268.2 | 7.6 | 78.5 | 4.3 | 78.5 | 4.3 | 7.0 |

| | | | | | | | | | | | |
|---|---|---|---|---|---|---|---|---|---|---|---|
| JMB12a | 625.0 | Gh | 0 | 0.06089 | 267.4 | 9.3 | 79.9 | 5.6 | 79.9 | 5.6 | 9.5 |
| JMB12a | 650.0 | Gh | 0 | 0.05686 | 263.3 | 13.4 | 82.5 | 10.7 | 82.5 | 10.7 | 17.0 |
| | | | | | | | | | | | |
| JMB13a | 0.0 | Gh | 0 | 0.25101 | 245.0 | 30.2 | 101.9 | 28.9 | 101.9 | 28.9 | 6.0 |
| JMB13a | 100.0 | Gh | 0 | 0.23908 | 249.3 | 32.0 | 104.1 | 25.3 | 104.1 | 25.3 | 7.0 |
| JMB13a | 200.0 | Gh | 0 | 0.23076 | 255.4 | 36.7 | 109.5 | 20.5 | 109.5 | 20.5 | 6.0 |
| JMB13a | 300.0 | Gh | 0 | 0.22899 | 262.7 | 38.7 | 112.2 | 14.9 | 112.2 | 14.9 | 7.0 |
| JMB13a | 400.0 | Gh | 0 | 0.22175 | 270.9 | 40.2 | 114.8 | 8.9 | 114.8 | 8.9 | 6.0 |
| JMB13a | 500.0 | Gh | 0 | 0.20978 | 289.3 | 40.5 | 119.3 | -4.3 | 119.3 | -4.3 | 5.0 |
| JMB13a | 550.0 | Gh | 0 | 0.20024 | 289.2 | 39.6 | 118.5 | -4.6 | 118.5 | -4.6 | 7.0 |
| JMB13a | 600.0 | Gh | 0 | 0.18682 | 287.6 | 38.6 | 117.1 | -3.8 | 117.1 | -3.8 | 8.0 |
| JMB13a | 625.0 | Gh | 0 | 0.18377 | 292.4 | 38.6 | 118.6 | -7.2 | 118.6 | -7.2 | 12.0 |
| JMB13a | 650.0 | Gh | 0 | 0.16556 | 299.0 | 39.0 | 121.5 | -11.6 | 121.5 | -11.6 | 21.0 |
| JMB13a | 660.0 | Gh | 0 | 0.14695 | 298.3 | 37.7 | 120.0 | -11.8 | 120.0 | -11.8 | 35.0 |
| JMB13a | 670.0 | Gh | 0 | 0.14308 | 306.6 | 38.5 | 124.4 | -16.8 | 124.4 | -16.8 | 53.0 |
| JMB13a | 680.0 | Gh | 0 | 0.05420 | 315.2 | 27.7 | 119.8 | -29.1 | 119.8 | -29.1 | 63.5 |
| | | | | | | | | | | | |
| JMB14a | 0.0 | Gh | 0 | 0.29092 | 170.8 | -10.8 | 6.4 | 68.2 | 6.4 | 68.2 | 7.0 |
| JMB14a | 100.0 | Gh | 0 | 0.27602 | 170.9 | -11.5 | 7.4 | 67.6 | 7.4 | 67.6 | 6.0 |
| JMB14a | 200.0 | Gh | 0 | 0.24879 | 167.1 | -11.8 | 359.5 | 65.6 | 359.5 | 65.6 | 6.0 |
| JMB14a | 300.0 | Gh | 0 | 0.22564 | 168.1 | -12.6 | 2.5 | 65.4 | 2.5 | 65.4 | 6.0 |
| JMB14a | 400.0 | Gh | 0 | 0.18851 | 169.0 | -11.9 | 3.6 | 66.4 | 3.6 | 66.4 | 6.5 |
| JMB14a | 500.0 | Gh | 0 | 0.10786 | 170.6 | -13.5 | 8.9 | 65.7 | 8.9 | 65.7 | 5.0 |
| JMB14a | 550.0 | Gh | 0 | 0.07275 | 166.2 | -6.1 | 338.1 | 69.6 | 338.1 | 69.6 | 7.0 |
| JMB14a | 600.0 | Gh | 0 | 0.05930 | 157.9 | -13.4 | 336.4 | 58.6 | 336.4 | 58.6 | 8.5 |
| JMB14a | 625.0 | Gh | 0 | 0.03351 | 152.1 | -11.4 | 326.8 | 55.6 | 326.8 | 55.6 | 12.5 |
| JMB14a | 650.0 | Gh | 0 | 0.02462 | 162.6 | -29.8 | 358.3 | 47.8 | 358.3 | 47.8 | 20.0 |
| | | | | | | | | | | | |
| JMB15a | 0.0 | Gh | 0 | 0.19017 | 213.0 | 22.9 | 68.4 | 57.0 | 68.4 | 57.0 | 5.5 |
| JMB15a | 100.0 | Gh | 0 | 0.17799 | 211.3 | 21.7 | 64.8 | 57.3 | 64.8 | 57.3 | 6.5 |
| JMB15a | 200.0 | Gh | 0 | 0.15809 | 213.3 | 21.6 | 67.0 | 55.9 | 67.0 | 55.9 | 6.0 |
| JMB15a | 300.0 | Gh | 0 | 0.14723 | 217.5 | 21.4 | 71.1 | 52.8 | 71.1 | 52.8 | 6.0 |
| JMB15a | 400.0 | Gh | 0 | 0.12573 | 220.8 | 22.4 | 75.5 | 51.1 | 75.5 | 51.1 | 5.5 |
| JMB15a | 500.0 | Gh | 0 | 0.09191 | 233.1 | 26.4 | 90.0 | 44.2 | 90.0 | 44.2 | 6.0 |
| JMB15a | 550.0 | Gh | 0 | 0.06350 | 248.5 | 25.1 | 98.3 | 31.9 | 98.3 | 31.9 | 6.0 |
| JMB15a | 600.0 | Gh | 0 | 0.06090 | 249.1 | 16.2 | 90.4 | 26.2 | 90.4 | 26.2 | 7.5 |
| JMB15a | 625.0 | Gh | 0 | 0.05732 | 251.6 | 20.1 | 95.6 | 26.7 | 95.6 | 26.7 | 11.5 |
| JMB15a | 650.0 | Gh | 0 | 0.03501 | 264.6 | 11.0 | 96.3 | 11.3 | 96.3 | 11.3 | 19.5 |
| JMB15a | 660.0 | Gh | 0 | 0.03560 | 279.8 | 14.3 | 108.5 | 2.1 | 108.5 | 2.1 | 32.0 |
| JMB15a | 670.0 | Gh | 0 | 0.02685 | 292.6 | 16.8 | 118.8 | -5.0 | 118.8 | -5.0 | 49.0 |
| JMB15a | 680.0 | Gh | 0 | 0.01080 | 265.9 | 28.7 | 111.6 | 21.3 | 111.6 | 21.3 | 55.0 |
| | | | | | | | | | | | |
| JMB16a | 0.0 | Gh | 0 | 0.20001 | 176.3 | 5.9 | 351.7 | 71.6 | 351.7 | 71.6 | 6.0 |
| JMB16a | 100.0 | Gh | 0 | 0.18803 | 176.2 | 4.8 | 352.0 | 70.5 | 352.0 | 70.5 | 6.5 |
| JMB16a | 200.0 | Gh | 0 | 0.16586 | 172.8 | 4.1 | 343.1 | 68.9 | 343.1 | 68.9 | 6.0 |
| JMB16a | 300.0 | Gh | 0 | 0.14914 | 172.2 | 4.7 | 340.9 | 69.3 | 340.9 | 69.3 | 7.0 |
| JMB16a | 400.0 | Gh | 0 | 0.12662 | 170.8 | 3.6 | 338.5 | 67.8 | 338.5 | 67.8 | 6.0 |
| JMB16a | 500.0 | Gh | 0 | 0.09432 | 169.1 | 8.4 | 327.7 | 71.2 | 327.7 | 71.2 | 6.0 |
| JMB16a | 550.0 | Gh | 0 | 0.04619 | 149.8 | 25.5 | 253.5 | 62.6 | 253.5 | 62.6 | 6.0 |
| JMB16a | 600.0 | Gh | 3 | 0.03868 | 130.0 | 16.2 | 262.7 | 42.7 | 262.7 | 42.7 | 149.0 |
| JMB16a | 625.0 | Gh | 2 | 0.04740 | 120.7 | 16.5 | 258.8 | 34.3 | 258.8 | 34.3 | 151.5 |
| JMB16a | 650.0 | Gh | 5 | 0.01859 | 164.7 | -22.7 | 334.2 | 40.9 | 334.2 | 40.9 | 183.0 |

| | | | | | | | | | | | |
|---|---|---|---|---|---|---|---|---|---|---|---|
| JMB17a | 0.0 | Gh | 0 | 0.28176 | 183.5 | -1.6 | 6.8 | 65.2 | 6.8 | 65.2 | 5.5 |
| JMB17a | 100.0 | Gh | 0 | 0.27093 | 186.7 | -3.0 | 13.4 | 63.2 | 13.4 | 63.2 | 6.0 |
| JMB17a | 200.0 | Gh | 0 | 0.24597 | 183.9 | -3.3 | 7.1 | 63.4 | 7.1 | 63.4 | 5.5 |
| JMB17a | 300.0 | Gh | 0 | 0.23226 | 185.2 | -0.5 | 11.3 | 66.0 | 11.3 | 66.0 | 6.0 |
| JMB17a | 400.0 | Gh | 0 | 0.22118 | 186.0 | -3.9 | 11.4 | 62.5 | 11.4 | 62.5 | 5.5 |
| JMB17a | 500.0 | Gh | 0 | 0.19706 | 187.8 | 0.2 | 17.9 | 66.0 | 17.9 | 66.0 | 6.0 |
| JMB17a | 550.0 | Gh | 0 | 0.08707 | 187.6 | -2.2 | 15.8 | 63.8 | 15.8 | 63.8 | 5.5 |
| JMB17a | 600.0 | Gh | 0 | 0.07940 | 185.6 | -7.4 | 9.3 | 59.1 | 9.3 | 59.1 | 7.5 |
| JMB17a | 625.0 | Gh | 0 | 0.06142 | 192.0 | 2.4 | 29.6 | 66.3 | 29.6 | 66.3 | 12.5 |
| JMB17a | 650.0 | Gh | 0 | 0.03544 | 198.3 | -0.5 | 38.0 | 60.5 | 38.0 | 60.5 | 22.5 |
| JMB17a | 660.0 | Gh | 0 | 0.02438 | 195.8 | 12.7 | 56.6 | 71.8 | 56.6 | 71.8 | 33.0 |
| JMB17a | 670.0 | Gh | 0 | 0.01006 | 200.8 | -7.7 | 34.4 | 53.1 | 34.4 | 53.1 | 52.5 |
| JMB17a | 680.0 | Gh | 0 | 0.01048 | 182.3 | 31.6 | 165.5 | 81.2 | 165.5 | 81.2 | 62.5 |
| | | | | | | | | | | | |
| JMB18a | 0.0 | Gh | 0 | 0.31217 | 190.0 | 3.4 | 28.1 | 65.4 | 28.1 | 65.4 | 7.0 |
| JMB18a | 100.0 | Gh | 0 | 0.30081 | 188.7 | 2.3 | 24.2 | 64.9 | 24.2 | 64.9 | 6.0 |
| JMB18a | 200.0 | Gh | 0 | 0.26498 | 189.2 | 1.6 | 24.8 | 64.0 | 24.8 | 64.0 | 6.0 |
| JMB18a | 300.0 | Gh | 0 | 0.24626 | 190.5 | -0.3 | 26.1 | 61.8 | 26.1 | 61.8 | 6.0 |
| JMB18a | 400.0 | Gh | 0 | 0.23681 | 190.0 | -1.4 | 24.3 | 60.9 | 24.3 | 60.9 | 6.0 |
| JMB18a | 500.0 | Gh | 0 | 0.21848 | 189.5 | -2.0 | 23.0 | 60.5 | 23.0 | 60.5 | 5.5 |
| JMB18a | 550.0 | Gh | 0 | 0.08703 | 193.9 | -6.4 | 17.5 | 55.0 | 17.5 | 55.0 | 5.5 |
| JMB18a | 600.0 | Gh | 0 | 0.06955 | 203.6 | -13.4 | 26.0 | 44.4 | 26.0 | 44.4 | 30.0 |
| JMB18a | 625.0 | Gh | 0 | 0.06668 | 210.1 | -8.2 | 37.6 | 45.0 | 37.6 | 45.0 | 32.0 |
| JMB18a | 650.0 | Gh | 1 | 0.03753 | 215.1 | -11.6 | 39.7 | 39.2 | 39.7 | 39.2 | 40.0 |
| | | | | | | | | | | | |
| JMB19a | 0.0 | Gh | 0 | 0.11666 | 176.7 | 4.3 | 1.2 | 69.1 | 1.2 | 69.1 | 4.5 |
| JMB19a | 100.0 | Gh | 0 | 0.11152 | 179.3 | 6.2 | 8.2 | 71.2 | 8.2 | 71.2 | 5.0 |
| JMB19a | 200.0 | Gh | 0 | 0.09743 | 172.7 | 5.6 | 349.4 | 69.4 | 349.4 | 69.4 | 3.5 |
| JMB19a | 300.0 | Gh | 0 | 0.08420 | 177.3 | 6.9 | 1.8 | 71.7 | 1.8 | 71.7 | 5.0 |
| JMB19a | 400.0 | Gh | 0 | 0.07780 | 178.4 | 5.6 | 5.6 | 70.5 | 5.6 | 70.5 | 5.0 |
| JMB19a | 500.0 | Gh | 0 | 0.07514 | 178.7 | 8.7 | 5.7 | 73.6 | 5.7 | 73.6 | 5.5 |
| JMB19a | 550.0 | Gh | 1 | 0.00736 | 286.6 | 54.3 | 155.6 | 11.1 | 155.6 | 11.1 | 8.0 |
| JMB19a | 600.0 | Gh | 1 | 0.01022 | 288.2 | 32.2 | 136.9 | -0.8 | 136.9 | -0.8 | 11.0 |
| JMB19a | 625.0 | Gh | 1 | 0.01340 | 313.4 | 54.3 | 165.3 | -1.2 | 165.3 | -1.2 | 13.0 |
| JMB19a | 650.0 | Gh | 1 | 0.00882 | 265.9 | 67.9 | 166.0 | 24.6 | 166.0 | 24.6 | 20.0 |
| JMB19a | 660.0 | Gh | 1 | 0.01535 | 294.1 | 26.2 | 134.5 | -8.4 | 134.5 | -8.4 | 27.5 |
| JMB19a | 670.0 | Gh | 1 | 0.01699 | 1.6 | 19.4 | 192.5 | -45.6 | 192.5 | -45.6 | 42.5 |
| JMB19a | 680.0 | Gh | 1 | 0.01621 | 305.4 | 26.5 | 140.9 | -16.4 | 140.9 | -16.4 | 50.0 |
| | | | | | | | | | | | |
| JMB20a | 0.0 | Gh | 0 | 0.36287 | 182.3 | -3.7 | 7.7 | 64.2 | 7.7 | 64.2 | 6.0 |
| JMB20a | 100.0 | Gh | 0 | 0.35094 | 180.4 | -4.7 | 3.3 | 63.3 | 3.3 | 63.3 | 7.5 |
| JMB20a | 200.0 | Gh | 0 | 0.32761 | 179.3 | -4.8 | 0.9 | 63.2 | 0.9 | 63.2 | 6.0 |
| JMB20a | 300.0 | Gh | 0 | 0.30827 | 178.6 | -5.5 | 359.4 | 62.5 | 359.4 | 62.5 | 7.0 |
| JMB20a | 400.0 | Gh | 0 | 0.28821 | 177.7 | -5.5 | 357.5 | 62.4 | 357.5 | 62.4 | 6.5 |
| JMB20a | 500.0 | Gh | 0 | 0.26745 | 177.0 | -4.4 | 355.7 | 63.4 | 355.7 | 63.4 | 7.0 |
| JMB20a | 550.0 | Gh | 0 | 0.11899 | 176.3 | 1.1 | 341.6 | 68.8 | 341.6 | 68.8 | 6.5 |
| JMB20a | 600.0 | Gh | 0 | 0.08559 | 174.3 | -1.0 | 337.6 | 66.3 | 337.6 | 66.3 | 9.0 |
| JMB20a | 625.0 | Gh | 0 | 0.07280 | 183.3 | 2.6 | 1.8 | 70.4 | 1.8 | 70.4 | 10.5 |
| JMB20a | 650.0 | Gh | 0 | 0.04824 | 171.2 | -2.8 | 331.7 | 63.8 | 331.7 | 63.8 | 16.0 |
| | | | | | | | | | | | |
| JMB21a | 0.0 | Gh | 0 | 0.17868 | 201.5 | -3.0 | 47.3 | 58.8 | 47.3 | 58.8 | 6.0 |
| JMB21a | 100.0 | Gh | 0 | 0.16161 | 202.7 | -3.8 | 48.0 | 57.4 | 48.0 | 57.4 | 7.0 |
| JMB21a | 200.0 | Gh | 0 | 0.13672 | 200.4 | -2.8 | 46.0 | 59.7 | 46.0 | 59.7 | 6.5 |

| | | | | | | | | | | | |
|---|---|---|---|---|---|---|---|---|---|---|---|
| JMB21a | 300.0 | Gh | 0 | 0.11989 | 205.4 | -1.8 | 54.1 | 56.9 | 54.1 | 56.9 | 6.5 |
| JMB21a | 400.0 | Gh | 0 | 0.10055 | 208.7 | -0.5 | 59.7 | 55.2 | 59.7 | 55.2 | 6.0 |
| JMB21a | 500.0 | Gh | 0 | 0.07430 | 216.4 | 2.1 | 70.3 | 50.2 | 70.3 | 50.2 | 6.5 |
| JMB21a | 550.0 | Gh | 0 | 0.04213 | 255.0 | 0.4 | 87.6 | 14.3 | 87.6 | 14.3 | 8.0 |
| JMB21a | 600.0 | Gh | 0 | 0.03106 | 271.3 | -5.5 | 87.7 | -3.1 | 87.7 | -3.1 | 8.5 |
| JMB21a | 625.0 | Gh | 0 | 0.03966 | 278.4 | -7.3 | 88.3 | -10.4 | 88.3 | -10.4 | 14.0 |
| JMB21a | 650.0 | Gh | 0 | 0.02879 | 296.3 | 0.2 | 102.2 | -24.5 | 102.2 | -24.5 | 23.0 |
| JMB21a | 660.0 | Gh | 0 | 0.03485 | 287.0 | -4.8 | 93.7 | -17.6 | 93.7 | -17.6 | 29.0 |
| JMB21a | 670.0 | Gh | 0 | 0.01828 | 347.3 | -20.7 | 86.7 | -78.1 | 86.7 | -78.1 | 49.0 |
| JMB21a | 680.0 | Gh | 0 | 0.01013 | 109.5 | 86.1 | 186.3 | 21.3 | 186.3 | 21.3 | 63.0 |
| | | | | | | | | | | | |
| JMB22a | 0.0 | Gh | 0 | 0.35085 | 168.5 | -1.5 | 334.4 | 64.0 | 334.4 | 64.0 | 7.5 |
| JMB22a | 100.0 | Gh | 0 | 0.33338 | 168.8 | -2.4 | 335.9 | 63.3 | 335.9 | 63.3 | 7.5 |
| JMB22a | 200.0 | Gh | 0 | 0.30453 | 167.7 | -2.1 | 333.4 | 63.1 | 333.4 | 63.1 | 6.5 |
| JMB22a | 300.0 | Gh | 0 | 0.27970 | 168.5 | -2.2 | 335.1 | 63.3 | 335.1 | 63.3 | 6.5 |
| JMB22a | 400.0 | Gh | 0 | 0.24461 | 169.5 | -2.0 | 336.9 | 63.9 | 336.9 | 63.9 | 6.0 |
| JMB22a | 500.0 | Gh | 0 | 0.17275 | 171.5 | -1.0 | 340.6 | 65.5 | 340.6 | 65.5 | 5.5 |
| JMB22a | 550.0 | Gh | 0 | 0.10693 | 175.0 | -0.5 | 338.1 | 67.0 | 338.1 | 67.0 | 7.0 |
| JMB22a | 600.0 | Gh | 0 | 0.07025 | 177.7 | 2.2 | 344.4 | 70.0 | 344.4 | 70.0 | 8.0 |
| JMB22a | 625.0 | Gh | 0 | 0.05284 | 175.5 | 8.4 | 332.7 | 75.7 | 332.7 | 75.7 | 10.0 |
| JMB22a | 650.0 | Gh | 0 | 0.04298 | 165.8 | 18.8 | 272.1 | 76.3 | 272.1 | 76.3 | 16.0 |
| | | | | | | | | | | | |
| JMB23a | 0.0 | Gh | 0 | 0.40522 | 183.2 | -4.8 | 11.9 | 68.0 | 11.9 | 68.0 | 7.0 |
| JMB23a | 100.0 | Gh | 0 | 0.38315 | 184.5 | -5.4 | 15.0 | 67.2 | 15.0 | 67.2 | 7.0 |
| JMB23a | 200.0 | Gh | 0 | 0.34887 | 180.6 | -4.8 | 5.0 | 68.2 | 5.0 | 68.2 | 8.5 |
| JMB23a | 300.0 | Gh | 0 | 0.32331 | 185.2 | -5.5 | 16.7 | 66.9 | 16.7 | 66.9 | 7.5 |
| JMB23a | 400.0 | Gh | 0 | 0.26865 | 184.4 | -5.5 | 14.7 | 67.1 | 14.7 | 67.1 | 7.0 |
| JMB23a | 500.0 | Gh | 0 | 0.17426 | 190.0 | -1.5 | 32.5 | 69.0 | 32.5 | 69.0 | 7.0 |
| JMB23a | 550.0 | Gh | 0 | 0.09400 | 191.7 | 6.4 | 52.1 | 74.4 | 52.1 | 74.4 | 8.5 |
| JMB23a | 600.0 | Gh | 0 | 0.07624 | 192.9 | 13.2 | 78.3 | 77.0 | 78.3 | 77.0 | 10.5 |
| JMB23a | 625.0 | Gh | 0 | 0.06016 | 198.6 | 21.1 | 109.4 | 71.9 | 109.4 | 71.9 | 16.0 |
| JMB23a | 650.0 | Gh | 0 | 0.04771 | 200.8 | 21.8 | 110.4 | 69.8 | 110.4 | 69.8 | 22.5 |
| JMB23a | 660.0 | Gh | 0 | 0.04936 | 208.6 | 19.1 | 102.3 | 62.8 | 102.3 | 62.8 | 28.5 |
| JMB23a | 670.0 | Gh | 0 | 0.02476 | 249.2 | 32.5 | 121.8 | 26.3 | 121.8 | 26.3 | 50.0 |
| JMB23a | 680.0 | Gh | 0 | 0.01136 | 209.5 | -50.1 | 22.8 | 18.0 | 22.8 | 18.0 | 63.0 |
| | | | | | | | | | | | |
| JMB24a | 0.0 | Gh | 0 | 0.11803 | 209.9 | 44.5 | 84.0 | 68.7 | 84.0 | 68.7 | 6.0 |
| JMB24a | 100.0 | Gh | 0 | 0.10321 | 215.6 | 45.1 | 90.9 | 65.7 | 90.9 | 65.7 | 6.0 |
| JMB24a | 200.0 | Gh | 0 | 0.08299 | 222.5 | 47.7 | 101.5 | 62.8 | 101.5 | 62.8 | 5.5 |
| JMB24a | 300.0 | Gh | 0 | 0.07242 | 230.7 | 45.6 | 103.4 | 56.9 | 103.4 | 56.9 | 6.5 |
| JMB24a | 400.0 | Gh | 0 | 0.05684 | 239.6 | 36.2 | 97.8 | 45.8 | 97.8 | 45.8 | 6.0 |
| JMB24a | 500.0 | Gh | 0 | 0.04742 | 268.2 | 26.4 | 110.7 | 21.9 | 110.7 | 21.9 | 5.0 |
| JMB24a | 550.0 | Gh | 0 | 0.03825 | 280.3 | 14.4 | 101.8 | 5.4 | 101.8 | 5.4 | 5.5 |
| JMB24a | 600.0 | Gh | 0 | 0.04675 | 285.0 | 18.6 | 108.0 | 6.2 | 108.0 | 6.2 | 8.0 |
| JMB24a | 625.0 | Gh | 0 | 0.03655 | 276.4 | 14.5 | 98.9 | 7.7 | 98.9 | 7.7 | 11.0 |
| JMB24a | 650.0 | Gh | 0 | 0.02402 | 278.9 | -7.9 | 87.3 | -11.7 | 87.3 | -11.7 | 16.5 |
| | | | | | | | | | | | |
| JMB25a | 0.0 | Gh | 0 | 0.15827 | 191.1 | 19.0 | 54.9 | 74.4 | 54.9 | 74.4 | 4.5 |
| JMB25a | 100.0 | Gh | 0 | 0.14293 | 191.1 | 18.4 | 53.6 | 73.9 | 53.6 | 73.9 | 4.5 |
| JMB25a | 200.0 | Gh | 0 | 0.12031 | 188.4 | 24.8 | 64.6 | 80.3 | 64.6 | 80.3 | 5.5 |
| JMB25a | 300.0 | Gh | 0 | 0.10420 | 189.6 | 22.1 | 58.6 | 77.6 | 58.6 | 77.6 | 6.0 |
| JMB25a | 400.0 | Gh | 0 | 0.07061 | 195.8 | 37.9 | 134.6 | 75.3 | 134.6 | 75.3 | 5.0 |
| JMB25a | 500.0 | Gh | 0 | 0.04269 | 246.2 | 42.4 | 134.5 | 37.1 | 134.5 | 37.1 | 5.0 |

| | | | | | | | | | | | |
|---|---|---|---|---|---|---|---|---|---|---|---|
| JMB25a | 550.0 | Gh | 0 | 0.04043 | 256.1 | 46.9 | 141.6 | 31.1 | 141.6 | 31.1 | 6.0 |
| JMB25a | 600.0 | Gh | 0 | 0.04926 | 274.0 | 37.1 | 136.8 | 15.2 | 136.8 | 15.2 | 8.0 |
| JMB25a | 625.0 | Gh | 0 | 0.05017 | 274.3 | 29.7 | 130.3 | 11.5 | 130.3 | 11.5 | 11.5 |
| JMB25a | 650.0 | Gh | 0 | 0.04386 | 281.1 | 31.2 | 134.6 | 7.2 | 134.6 | 7.2 | 16.0 |
| JMB25a | 660.0 | Gh | 0 | 0.04319 | 289.3 | 40.0 | 145.7 | 6.5 | 145.7 | 6.5 | 19.5 |
| JMB25a | 670.0 | Gh | 0 | 0.02836 | 299.2 | 8.7 | 126.1 | -19.6 | 126.1 | -19.6 | 33.0 |
| JMB25a | 680.0 | Gh | 0 | 0.01336 | 337.0 | 6.8 | 158.3 | -46.3 | 158.3 | -46.3 | 42.0 |
| | | | | | | | | | | | |
| JMB26a | 0.0 | Gh | 0 | 0.16137 | 197.7 | 8.2 | 50.9 | 65.5 | 50.9 | 65.5 | 6.0 |
| JMB26a | 100.0 | Gh | 0 | 0.14358 | 201.4 | 6.4 | 54.3 | 61.7 | 54.3 | 61.7 | 6.0 |
| JMB26a | 200.0 | Gh | 0 | 0.11750 | 204.2 | 7.7 | 60.2 | 60.6 | 60.2 | 60.6 | 6.0 |
| JMB26a | 300.0 | Gh | 0 | 0.09984 | 212.2 | 9.4 | 71.8 | 55.3 | 71.8 | 55.3 | 6.0 |
| JMB26a | 400.0 | Gh | 0 | 0.07175 | 222.3 | 7.0 | 76.8 | 45.5 | 76.8 | 45.5 | 6.0 |
| JMB26a | 500.0 | Gh | 0 | 0.04467 | 272.7 | 7.2 | 102.1 | 0.8 | 102.1 | 0.8 | 5.0 |
| JMB26a | 550.0 | Gh | 0 | 0.04094 | 277.1 | 10.8 | 96.8 | -1.5 | 96.8 | -1.5 | 6.5 |
| JMB26a | 600.0 | Gh | 0 | 0.04864 | 297.5 | 5.9 | 102.4 | -21.6 | 102.4 | -21.6 | 10.0 |
| JMB26a | 625.0 | Gh | 0 | 0.04862 | 283.0 | -3.6 | 86.5 | -13.2 | 86.5 | -13.2 | 13.0 |
| JMB26a | 650.0 | Gh | 0 | 0.04628 | 290.7 | -0.6 | 92.8 | -18.8 | 92.8 | -18.8 | 19.5 |
| | | | | | | | | | | | |
| JMB27a | 0.0 | Gh | 0 | 0.31063 | 191.0 | 2.5 | 29.4 | 66.0 | 29.4 | 66.0 | 7.0 |
| JMB27a | 100.0 | Gh | 0 | 0.29546 | 190.4 | 2.0 | 27.5 | 65.8 | 27.5 | 65.8 | 7.5 |
| JMB27a | 200.0 | Gh | 0 | 0.27097 | 188.7 | 2.1 | 23.7 | 66.5 | 23.7 | 66.5 | 7.5 |
| JMB27a | 300.0 | Gh | 0 | 0.24988 | 192.0 | 1.0 | 30.0 | 64.2 | 30.0 | 64.2 | 8.0 |
| JMB27a | 400.0 | Gh | 0 | 0.20898 | 194.0 | 2.1 | 35.2 | 64.3 | 35.2 | 64.3 | 7.5 |
| JMB27a | 500.0 | Gh | 0 | 0.12633 | 193.6 | 2.7 | 35.3 | 65.0 | 35.3 | 65.0 | 6.5 |
| JMB27a | 550.0 | Gh | 0 | 0.10079 | 192.6 | 6.2 | 37.6 | 68.5 | 37.6 | 68.5 | 6.5 |
| JMB27a | 600.0 | Gh | 0 | 0.09337 | 195.3 | 0.3 | 35.7 | 62.0 | 35.7 | 62.0 | 7.0 |
| JMB27a | 625.0 | Gh | 0 | 0.07528 | 195.8 | 1.7 | 38.2 | 62.9 | 38.2 | 62.9 | 9.0 |
| JMB27a | 650.0 | Gh | 0 | 0.06681 | 198.8 | 9.3 | 55.3 | 66.8 | 55.3 | 66.8 | 13.0 |
| JMB27a | 660.0 | Gh | 0 | 0.05131 | 212.8 | 7.5 | 69.2 | 54.5 | 69.2 | 54.5 | 16.0 |
| JMB27a | 670.0 | Gh | 0 | 0.02861 | 212.7 | 1.5 | 60.9 | 51.2 | 60.9 | 51.2 | 28.0 |
| JMB27a | 680.0 | Gh | 0 | 0.01223 | 196.7 | 39.7 | 143.5 | 68.9 | 143.5 | 68.9 | 37.0 |
| | | | | | | | | | | | |
| JMB28a | 0.0 | Gh | 0 | 0.19100 | 190.6 | 3.9 | 40.0 | 72.5 | 40.0 | 72.5 | 5.0 |
| JMB28a | 100.0 | Gh | 0 | 0.17762 | 195.5 | 3.0 | 49.5 | 68.7 | 49.5 | 68.7 | 5.5 |
| JMB28a | 200.0 | Gh | 0 | 0.15726 | 192.5 | 3.1 | 43.3 | 70.7 | 43.3 | 70.7 | 5.0 |
| JMB28a | 300.0 | Gh | 0 | 0.14524 | 194.6 | 2.7 | 47.2 | 69.0 | 47.2 | 69.0 | 6.0 |
| JMB28a | 400.0 | Gh | 0 | 0.11261 | 195.9 | 6.8 | 58.5 | 70.9 | 58.5 | 70.9 | 4.5 |
| JMB28a | 500.0 | Gh | 0 | 0.06907 | 205.3 | 21.5 | 105.0 | 65.9 | 105.0 | 65.9 | 4.5 |
| JMB28a | 550.0 | Gh | 0 | 0.05467 | 214.4 | 39.7 | 125.3 | 53.2 | 125.3 | 53.2 | 5.0 |
| JMB28a | 600.0 | Gh | 0 | 0.04839 | 202.8 | 31.0 | 118.4 | 65.6 | 118.4 | 65.6 | 8.0 |
| JMB28a | 625.0 | Gh | 0 | 0.03273 | 207.5 | 36.4 | 124.8 | 59.6 | 124.8 | 59.6 | 10.5 |
| JMB28a | 650.0 | Gh | 0 | 0.02835 | 214.3 | 29.8 | 109.2 | 56.7 | 109.2 | 56.7 | 17.0 |
| | | | | | | | | | | | |
| JMB29 | 0.0 | Gh | 0 | 0.19388 | 175.9 | 28.6 | 336.7 | 78.1 | 336.7 | 78.1 | 3.5 |
| JMB29 | 100.0 | Gh | 0 | 0.18226 | 183.1 | 26.6 | 6.2 | 76.4 | 6.2 | 76.4 | 5.0 |
| JMB29 | 200.0 | Gh | 0 | 0.16356 | 179.7 | 28.6 | 353.1 | 78.6 | 353.1 | 78.6 | 5.0 |
| JMB29 | 300.0 | Gh | 0 | 0.14612 | 181.4 | 28.6 | 0.6 | 78.5 | 0.6 | 78.5 | 4.5 |
| JMB29 | 400.0 | Gh | 0 | 0.10812 | 189.8 | 30.1 | 36.4 | 77.3 | 36.4 | 77.3 | 4.5 |
| JMB29 | 500.0 | Gh | 0 | 0.06470 | 200.7 | 36.4 | 78.7 | 73.4 | 78.7 | 73.4 | 4.0 |
| JMB29 | 550.0 | Gh | 0 | 0.05459 | 212.2 | 47.8 | 113.8 | 65.7 | 113.8 | 65.7 | 5.0 |
| JMB29 | 600.0 | Gh | 0 | 0.04309 | 217.8 | 43.1 | 103.3 | 61.8 | 103.3 | 61.8 | 4.5 |
| JMB29 | 625.0 | Gh | 0 | 0.02621 | 219.1 | 34.1 | 86.3 | 58.5 | 86.3 | 58.5 | 5.0 |

| | | | | | | | | | | | |
|---|---|---|---|---|---|---|---|---|---|---|---|
| JMB29 | 650.0 | Gh | 0 | 0.02991 | 236.1 | 27.5 | 87.2 | 42.5 | 87.2 | 42.5 | 5.0 |
| JMB29 | 660.0 | Gh | 0 | 0.01769 | 262.3 | 30.6 | 104.7 | 24.5 | 104.7 | 24.5 | 6.0 |
| JMB29 | 670.0 | Gh | 0 | 0.01433 | 251.6 | 33.4 | 102.1 | 33.7 | 102.1 | 33.7 | 10.0 |
| JMB29 | 680.0 | Gh | 0 | 0.01003 | 200.7 | 25.9 | 51.4 | 67.7 | 51.4 | 67.7 | 14.0 |
| | | | | | | | | | | | |
| JMB30 | 0.0 | Gh | 0 | 0.18898 | 205.1 | 36.3 | 43.2 | 62.0 | 43.2 | 62.0 | 5.5 |
| JMB30 | 100.0 | Gh | 0 | 0.17214 | 205.4 | 33.6 | 41.2 | 59.5 | 41.2 | 59.5 | 5.0 |
| JMB30 | 200.0 | Gh | 0 | 0.14552 | 206.6 | 33.0 | 42.4 | 58.5 | 42.4 | 58.5 | 5.5 |
| JMB30 | 300.0 | Gh | 0 | 0.12513 | 208.3 | 30.7 | 43.0 | 55.8 | 43.0 | 55.8 | 5.5 |
| JMB30 | 400.0 | Gh | 0 | 0.09931 | 216.4 | 24.8 | 49.1 | 47.4 | 49.1 | 47.4 | 6.0 |
| JMB30 | 500.0 | Gh | 0 | 0.05167 | 229.5 | 18.5 | 59.6 | 36.1 | 59.6 | 36.1 | 4.0 |
| JMB30 | 550.0 | Gh | 0 | 0.04453 | 245.4 | 4.2 | 56.7 | 16.1 | 56.7 | 16.1 | 4.5 |
| JMB30 | 600.0 | Gh | 0 | 0.04169 | 255.4 | -10.0 | 58.3 | -1.2 | 58.3 | -1.2 | 5.0 |
| JMB30 | 625.0 | Gh | 0 | 0.02995 | 258.2 | -14.4 | 58.6 | -6.4 | 58.6 | -6.4 | 6.0 |
| JMB30 | 650.0 | Gh | 0 | 0.03226 | 268.7 | -29.9 | 58.5 | -24.7 | 58.5 | -24.7 | 10.0 |
| | | | | | | | | | | | |
| JMB31a | 0.0 | Gh | 0 | 0.26322 | 159.7 | -3.5 | 355.0 | 65.1 | 355.0 | 65.1 | 6.0 |
| JMB31a | 100.0 | Gh | 0 | 0.25072 | 161.4 | -3.9 | 358.2 | 66.2 | 358.2 | 66.2 | 6.5 |
| JMB31a | 200.0 | Gh | 0 | 0.21985 | 158.7 | -4.3 | 355.1 | 63.9 | 355.1 | 63.9 | 7.0 |
| JMB31a | 300.0 | Gh | 0 | 0.19639 | 158.0 | -6.2 | 357.5 | 62.2 | 357.5 | 62.2 | 5.0 |
| JMB31a | 400.0 | Gh | 0 | 0.16154 | 157.7 | -8.3 | 0.5 | 60.6 | 0.5 | 60.6 | 6.0 |
| JMB31a | 500.0 | Gh | 0 | 0.09993 | 160.5 | -11.5 | 9.1 | 60.3 | 9.1 | 60.3 | 6.0 |
| JMB31a | 550.0 | Gh | 0 | 0.08192 | 156.9 | -10.1 | 2.2 | 58.8 | 2.2 | 58.8 | 5.0 |
| JMB31a | 600.0 | Gh | 0 | 0.05024 | 155.8 | -16.3 | 8.7 | 53.7 | 8.7 | 53.7 | 6.0 |
| JMB31a | 625.0 | Gh | 0 | 0.04091 | 153.4 | -23.7 | 13.8 | 46.6 | 13.8 | 46.6 | 8.0 |
| JMB31a | 650.0 | Gh | 0 | 0.02558 | 153.1 | -23.8 | 13.5 | 46.4 | 13.5 | 46.4 | 9.5 |
| JMB31a | 660.0 | Gh | 0 | 0.00910 | 201.8 | -77.9 | 54.9 | 0.3 | 54.9 | 0.3 | 22.0 |
| JMB31a | 670.0 | Gh | 0 | 0.00563 | 255.5 | -38.5 | 99.9 | 4.2 | 99.9 | 4.2 | 28.0 |
| JMB31a | 680.0 | Gh | 0 | 0.00450 | 93.6 | -5.0 | 326.0 | 2.6 | 326.0 | 2.6 | 35.5 |
| | | | | | | | | | | | |
| JMB32a | 0.0 | Gh | 0 | 0.33781 | 160.0 | 5.8 | 351.8 | 67.5 | 351.8 | 67.5 | 5.0 |
| JMB32a | 100.0 | Gh | 0 | 0.32455 | 159.4 | 5.6 | 351.5 | 66.8 | 351.5 | 66.8 | 6.0 |
| JMB32a | 200.0 | Gh | 0 | 0.28591 | 156.4 | 6.2 | 346.7 | 64.5 | 346.7 | 64.5 | 6.0 |
| JMB32a | 300.0 | Gh | 0 | 0.25477 | 158.5 | 4.7 | 352.2 | 65.6 | 352.2 | 65.6 | 5.0 |
| JMB32a | 400.0 | Gh | 0 | 0.20944 | 157.4 | 3.0 | 354.2 | 63.8 | 354.2 | 63.8 | 5.0 |
| JMB32a | 500.0 | Gh | 0 | 0.13018 | 156.1 | 1.1 | 355.9 | 61.6 | 355.9 | 61.6 | 5.0 |
| JMB32a | 550.0 | Gh | 0 | 0.07304 | 166.0 | 1.5 | 0.9 | 69.2 | 0.9 | 69.2 | 6.0 |
| JMB32a | 600.0 | Gh | 0 | 0.04288 | 161.0 | 4.2 | 346.3 | 67.4 | 346.3 | 67.4 | 7.0 |
| JMB32a | 625.0 | Gh | 0 | 0.02229 | 164.5 | -18.3 | 20.0 | 51.5 | 20.0 | 51.5 | 8.5 |
| JMB32a | 650.0 | Gh | 1 | 0.00257 | 259.4 | -14.2 | 117.3 | 5.7 | 117.3 | 5.7 | 17.5 |
| | | | | | | | | | | | |
| JMB33a | 0.0 | Gh | 0 | 0.29926 | 164.8 | 2.0 | 4.4 | 67.4 | 4.4 | 67.4 | 5.5 |
| JMB33a | 100.0 | Gh | 0 | 0.28802 | 165.7 | 1.6 | 6.9 | 67.7 | 6.9 | 67.7 | 6.0 |
| JMB33a | 200.0 | Gh | 0 | 0.25731 | 163.8 | 1.8 | 2.8 | 66.6 | 2.8 | 66.6 | 5.5 |
| JMB33a | 300.0 | Gh | 0 | 0.23232 | 165.8 | 1.8 | 6.8 | 67.9 | 6.8 | 67.9 | 5.0 |
| JMB33a | 400.0 | Gh | 0 | 0.19233 | 164.6 | 2.1 | 3.8 | 67.4 | 3.8 | 67.4 | 5.0 |
| JMB33a | 500.0 | Gh | 0 | 0.13911 | 166.9 | 2.6 | 7.9 | 69.2 | 7.9 | 69.2 | 5.0 |
| JMB33a | 550.0 | Gh | 0 | 0.07179 | 164.8 | -4.4 | 13.3 | 62.2 | 13.3 | 62.2 | 5.0 |
| JMB33a | 600.0 | Gh | 0 | 0.04900 | 167.5 | -1.9 | 15.7 | 65.8 | 15.7 | 65.8 | 5.5 |
| JMB33a | 625.0 | Gh | 0 | 0.02880 | 182.9 | -15.9 | 52.3 | 55.0 | 52.3 | 55.0 | 7.0 |
| JMB33a | 650.0 | Gh | 0 | 0.01590 | 197.3 | -24.2 | 69.5 | 43.6 | 69.5 | 43.6 | 9.0 |
| JMB33a | 660.0 | Gh | 0 | 0.00829 | 93.5 | -31.8 | 348.6 | -7.1 | 348.6 | -7.1 | 40.5 |
| JMB33a | 670.0 | Gh | 0 | 0.01273 | 293.5 | -73.8 | 63.7 | -24.7 | 63.7 | -24.7 | 42.0 |

| | | | | | | | | | | | |
|---|---|---|---|---|---|---|---|---|---|---|---|
| JMB33a | 680.0 | Gh | 0 | 0.00669 | 248.6 | 43.3 | 177.1 | 28.3 | 177.1 | 28.3 | 51.0 |
| | | | | | | | | | | | |
| JMB34 | 0.0 | Gh | 0 | 0.26913 | 162.6 | 6.2 | 4.3 | 68.2 | 4.3 | 68.2 | 6.0 |
| JMB34 | 100.0 | Gh | 0 | 0.26851 | 159.8 | 5.7 | 0.7 | 65.7 | 0.7 | 65.7 | 6.0 |
| JMB34 | 200.0 | Gh | 0 | 0.24518 | 158.5 | 6.0 | 358.3 | 64.9 | 358.3 | 64.9 | 6.0 |
| JMB34 | 300.0 | Gh | 0 | 0.23789 | 159.5 | 5.6 | 0.5 | 65.4 | 0.5 | 65.4 | 5.5 |
| JMB34 | 400.0 | Gh | 0 | 0.20797 | 159.5 | 4.7 | 2.2 | 64.9 | 2.2 | 64.9 | 6.0 |
| JMB34 | 500.0 | Gh | 0 | 0.19145 | 157.8 | 5.6 | 358.1 | 64.1 | 358.1 | 64.1 | 5.5 |
| JMB34 | 550.0 | Gh | 0 | 0.05601 | 166.1 | 5.8 | 1.4 | 70.4 | 1.4 | 70.4 | 5.0 |
| JMB34 | 600.0 | Gh | 0 | 0.04022 | 154.5 | 15.1 | 324.3 | 65.2 | 324.3 | 65.2 | 6.0 |
| JMB34 | 625.0 | Gh | 0 | 0.02394 | 158.9 | -10.1 | 10.5 | 53.4 | 10.5 | 53.4 | 8.0 |
| JMB34 | 650.0 | Gh | 0 | 0.01635 | 149.0 | -8.1 | 356.6 | 48.5 | 356.6 | 48.5 | 14.0 |
| | | | | | | | | | | | |
| JMB35a | 0.0 | Gh | 0 | 0.24071 | 157.0 | 7.8 | 353.5 | 63.7 | 353.5 | 63.7 | 5.0 |
| JMB35a | 100.0 | Gh | 0 | 0.24005 | 159.4 | 7.5 | 357.4 | 65.4 | 357.4 | 65.4 | 5.5 |
| JMB35a | 200.0 | Gh | 0 | 0.21122 | 155.1 | 7.7 | 351.4 | 62.1 | 351.4 | 62.1 | 6.5 |
| JMB35a | 300.0 | Gh | 0 | 0.19625 | 158.5 | 7.4 | 356.3 | 64.7 | 356.3 | 64.7 | 5.5 |
| JMB35a | 400.0 | Gh | 0 | 0.16399 | 158.1 | 8.1 | 354.4 | 64.8 | 354.4 | 64.8 | 6.0 |
| JMB35a | 500.0 | Gh | 0 | 0.14091 | 155.3 | 8.6 | 350.0 | 62.7 | 350.0 | 62.7 | 6.0 |
| JMB35a | 550.0 | Gh | 0 | 0.05166 | 147.2 | 8.5 | 342.4 | 55.7 | 342.4 | 55.7 | 4.0 |
| JMB35a | 600.0 | Gh | 1 | 0.02383 | 142.5 | 18.9 | 322.5 | 54.8 | 322.5 | 54.8 | 19.0 |
| JMB35a | 625.0 | Gh | 1 | 0.01931 | 142.1 | 21.4 | 318.1 | 54.9 | 318.1 | 54.9 | 21.5 |
| JMB35a | 650.0 | Gh | 7 | 0.00280 | 303.1 | -35.7 | 115.5 | -39.0 | 115.5 | -39.0 | 33.0 |
| JMB35a | 660.0 | Gh | 3 | 0.00491 | 4.2 | -24.6 | 359.4 | -85.3 | 359.4 | -85.3 | 38.5 |
| JMB35a | 670.0 | Gh | 3 | 0.00566 | 126.1 | -44.8 | 19.1 | 7.1 | 19.1 | 7.1 | 74.0 |
| JMB35a | 680.0 | Gh | 1 | 0.00561 | 263.7 | 27.6 | 168.4 | 15.3 | 168.4 | 15.3 | 33.5 |
| | | | | | | | | | | | |
| JMB36a | 0.0 | Gh | 0 | 0.15916 | 156.2 | 13.5 | 335.0 | 65.8 | 335.0 | 65.8 | 5.0 |
| JMB36a | 100.0 | Gh | 0 | 0.15324 | 157.1 | 13.2 | 336.6 | 66.5 | 336.6 | 66.5 | 5.5 |
| JMB36a | 200.0 | Gh | 0 | 0.12923 | 154.6 | 14.1 | 332.2 | 64.6 | 332.2 | 64.6 | 7.0 |
| JMB36a | 300.0 | Gh | 0 | 0.11594 | 155.9 | 14.5 | 332.4 | 66.0 | 332.4 | 66.0 | 5.5 |
| JMB36a | 400.0 | Gh | 0 | 0.09575 | 157.2 | 12.1 | 339.1 | 66.1 | 339.1 | 66.1 | 6.5 |
| JMB36a | 500.0 | Gh | 0 | 0.07345 | 151.6 | 16.8 | 324.4 | 62.7 | 324.4 | 62.7 | 5.0 |
| JMB36a | 550.0 | Gh | 0 | 0.03761 | 135.8 | 19.4 | 303.3 | 48.7 | 303.3 | 48.7 | 5.0 |
| JMB36a | 600.0 | Gh | 0 | 0.02849 | 143.9 | 25.1 | 295.5 | 56.9 | 295.5 | 56.9 | 6.0 |
| JMB36a | 625.0 | Gh | 0 | 0.02480 | 133.0 | 32.5 | 283.3 | 47.3 | 283.3 | 47.3 | 8.5 |
| JMB36a | 650.0 | Gh | 0 | 0.01471 | 94.3 | 56.5 | 254.0 | 20.6 | 254.0 | 20.6 | 15.0 |
| | | | | | | | | | | | |
| JMB37 | 0.0 | Gh | 0 | 0.04637 | 157.7 | 1.7 | 0.8 | 59.6 | 0.8 | 59.6 | 5.5 |
| JMB37 | 100.0 | Gh | 0 | 0.04091 | 153.3 | 0.4 | 356.7 | 55.6 | 356.7 | 55.6 | 5.0 |
| JMB37 | 200.0 | Gh | 0 | 0.03000 | 137.2 | -0.8 | 343.2 | 42.1 | 343.2 | 42.1 | 6.0 |
| JMB37 | 300.0 | Gh | 0 | 0.02902 | 130.3 | -8.0 | 346.0 | 32.4 | 346.0 | 32.4 | 6.0 |
| JMB37 | 400.0 | Gh | 0 | 0.02475 | 98.7 | -25.3 | 346.0 | -2.4 | 346.0 | -2.4 | 5.5 |
| JMB37 | 500.0 | Gh | 0 | 0.01798 | 65.5 | -26.2 | 337.2 | -31.0 | 337.2 | -31.0 | 5.0 |
| JMB37 | 550.0 | Gh | 0 | 0.01064 | 77.6 | -26.1 | 340.1 | -20.4 | 340.1 | -20.4 | 4.0 |
| JMB37 | 600.0 | Gh | 0 | 0.00931 | 97.8 | -48.2 | 7.0 | -12.1 | 7.0 | -12.1 | 5.0 |
| JMB37 | 625.0 | Gh | 0 | 0.00922 | 75.5 | -34.8 | 348.7 | -24.3 | 348.7 | -24.3 | 6.0 |
| JMB37 | 650.0 | Gh | 0 | 0.00728 | 86.7 | -32.6 | 349.0 | -14.8 | 349.0 | -14.8 | 12.0 |
| JMB37 | 660.0 | Gh | 0 | 0.01204 | 99.7 | -9.2 | 331.7 | 5.2 | 331.7 | 5.2 | 16.5 |
| JMB37 | 670.0 | Gh | 1 | 0.00427 | 300.1 | 32.2 | 181.3 | -10.5 | 181.3 | -10.5 | 37.5 |
| JMB37 | 680.0 | Gh | 1 | 0.00190 | 43.4 | -12.9 | 313.3 | -47.7 | 313.3 | -47.7 | 37.0 |
| | | | | | | | | | | | |
| JMB38a | 0.0 | Gh | 0 | 0.33246 | 158.5 | 9.1 | 355.0 | 66.5 | 355.0 | 66.5 | 6.5 |

| | | | | | | | | | | | |
|---|---|---|---|---|---|---|---|---|---|---|---|
| JMB38a | 100.0 | Gh | 0 | 0.32287 | 158.7 | 9.4 | 354.6 | 66.9 | 354.6 | 66.9 | 6.0 |
| JMB38a | 200.0 | Gh | 0 | 0.28449 | 158.2 | 8.6 | 355.7 | 66.0 | 355.7 | 66.0 | 5.5 |
| JMB38a | 300.0 | Gh | 0 | 0.26232 | 160.9 | 8.6 | 359.4 | 68.3 | 359.4 | 68.3 | 6.0 |
| JMB38a | 400.0 | Gh | 0 | 0.21201 | 159.8 | 9.2 | 356.5 | 67.7 | 356.5 | 67.7 | 6.0 |
| JMB38a | 500.0 | Gh | 0 | 0.14870 | 163.6 | 7.5 | 6.3 | 69.8 | 6.3 | 69.8 | 5.0 |
| JMB38a | 550.0 | Gh | 0 | 0.08166 | 163.8 | 12.8 | 342.3 | 72.9 | 342.3 | 72.9 | 5.5 |
| JMB38a | 600.0 | Gh | 0 | 0.05205 | 165.6 | 2.3 | 9.7 | 67.4 | 9.7 | 67.4 | 6.5 |
| JMB38a | 625.0 | Gh | 0 | 0.02922 | 163.7 | -3.3 | 13.7 | 61.7 | 13.7 | 61.7 | 9.5 |
| JMB38a | 650.0 | Gh | 0 | 0.01221 | 180.5 | -8.8 | 51.0 | 61.2 | 51.0 | 61.2 | 16.0 |
| | | | | | | | | | | | |
| JMB39a | 0.0 | Gh | 0 | 0.35981 | 161.1 | 1.6 | 10.8 | 65.2 | 10.8 | 65.2 | 5.0 |
| JMB39a | 100.0 | Gh | 0 | 0.34677 | 160.4 | 1.4 | 10.0 | 64.6 | 10.0 | 64.6 | 5.5 |
| JMB39a | 200.0 | Gh | 0 | 0.31815 | 157.2 | 0.9 | 6.3 | 61.8 | 6.3 | 61.8 | 5.5 |
| JMB39a | 300.0 | Gh | 0 | 0.29998 | 160.7 | -1.6 | 15.3 | 62.7 | 15.3 | 62.7 | 5.0 |
| JMB39a | 400.0 | Gh | 0 | 0.23906 | 159.9 | -3.4 | 16.7 | 60.8 | 16.7 | 60.8 | 5.5 |
| JMB39a | 500.0 | Gh | 0 | 0.14357 | 162.7 | -3.9 | 21.9 | 62.2 | 21.9 | 62.2 | 5.0 |
| JMB39a | 550.0 | Gh | 0 | 0.10024 | 158.9 | -12.0 | 25.2 | 53.5 | 25.2 | 53.5 | 4.5 |
| JMB39a | 600.0 | Gh | 0 | 0.07583 | 162.9 | -12.2 | 31.0 | 55.4 | 31.0 | 55.4 | 6.0 |
| JMB39a | 625.0 | Gh | 0 | 0.07055 | 164.8 | -9.8 | 31.8 | 58.4 | 31.8 | 58.4 | 6.0 |
| JMB39a | 650.0 | Gh | 0 | 0.03394 | 169.5 | -19.1 | 45.4 | 51.5 | 45.4 | 51.5 | 9.0 |
| JMB39a | 660.0 | Gh | 0 | 0.03068 | 179.6 | -19.4 | 60.8 | 52.6 | 60.8 | 52.6 | 17.5 |
| JMB39a | 670.0 | Gh | 0 | 0.02068 | 209.5 | -22.2 | 98.3 | 40.5 | 98.3 | 40.5 | 26.0 |
| JMB39a | 680.0 | Gh | 0 | 0.01661 | 179.7 | -34.2 | 61.1 | 37.8 | 61.1 | 37.8 | 29.0 |
| | | | | | | | | | | | |
| JMB40a | 0.0 | Gh | 0 | 0.16001 | 179.2 | 9.8 | 25.9 | 81.8 | 25.9 | 81.8 | 6.5 |
| JMB40a | 100.0 | Gh | 0 | 0.15382 | 182.0 | 7.3 | 42.0 | 79.1 | 42.0 | 79.1 | 7.0 |
| JMB40a | 200.0 | Gh | 0 | 0.14003 | 178.2 | 5.7 | 23.0 | 77.6 | 23.0 | 77.6 | 6.0 |
| JMB40a | 300.0 | Gh | 0 | 0.12398 | 185.6 | 7.4 | 59.3 | 78.1 | 59.3 | 78.1 | 6.5 |
| JMB40a | 400.0 | Gh | 0 | 0.09835 | 186.7 | 8.5 | 66.7 | 78.5 | 66.7 | 78.5 | 6.0 |
| JMB40a | 500.0 | Gh | 0 | 0.05551 | 204.1 | 16.8 | 122.2 | 67.0 | 122.2 | 67.0 | 6.0 |
| JMB40a | 550.0 | Gh | 0 | 0.04759 | 223.7 | 17.0 | 116.5 | 48.4 | 116.5 | 48.4 | 5.5 |
| JMB40a | 600.0 | Gh | 0 | 0.03371 | 227.4 | 20.5 | 122.3 | 45.3 | 122.3 | 45.3 | 7.0 |
| JMB40a | 625.0 | Gh | 0 | 0.02855 | 228.9 | 14.0 | 113.6 | 42.9 | 113.6 | 42.9 | 10.0 |
| JMB40a | 650.0 | Gh | 0 | 0.02939 | 245.5 | 24.2 | 129.2 | 29.1 | 129.2 | 29.1 | 14.5 |
| | | | | | | | | | | | |
| JMB41a | 0.0 | Gh | 0 | 0.18360 | 174.9 | 10.8 | 11.3 | 75.9 | 11.3 | 75.9 | 8.0 |
| JMB41a | 100.0 | Gh | 0 | 0.17411 | 173.4 | 8.8 | 8.8 | 73.5 | 8.8 | 73.5 | 7.0 |
| JMB41a | 200.0 | Gh | 0 | 0.15800 | 171.1 | 9.6 | 0.4 | 73.3 | 0.4 | 73.3 | 7.5 |
| JMB41a | 300.0 | Gh | 0 | 0.14470 | 175.5 | 7.6 | 16.9 | 73.0 | 16.9 | 73.0 | 8.0 |
| JMB41a | 400.0 | Gh | 0 | 0.11958 | 175.4 | 3.6 | 19.4 | 69.1 | 19.4 | 69.1 | 7.0 |
| JMB41a | 500.0 | Gh | 0 | 0.07225 | 178.3 | 5.5 | 27.0 | 71.4 | 27.0 | 71.4 | 6.5 |
| JMB41a | 550.0 | Gh | 0 | 0.05234 | 177.6 | 0.9 | 26.4 | 66.8 | 26.4 | 66.8 | 7.0 |
| JMB41a | 600.0 | Gh | 0 | 0.04919 | 172.5 | 4.7 | 10.8 | 69.4 | 10.8 | 69.4 | 7.5 |
| JMB41a | 625.0 | Gh | 0 | 0.04247 | 171.0 | -3.9 | 13.8 | 60.8 | 13.8 | 60.8 | 9.0 |
| JMB41a | 650.0 | Gh | 0 | 0.03675 | 170.6 | 7.6 | 2.0 | 71.3 | 2.0 | 71.3 | 11.0 |
| JMB41a | 660.0 | Gh | 0 | 0.02360 | 162.1 | 2.4 | 351.1 | 62.3 | 351.1 | 62.3 | 20.5 |
| JMB41a | 670.0 | Gh | 0 | 0.01684 | 186.8 | 15.6 | 70.7 | 79.4 | 70.7 | 79.4 | 26.0 |
| JMB41a | 680.0 | Gh | 0 | 0.01194 | 196.6 | 40.4 | 176.1 | 68.5 | 176.1 | 68.5 | 31.0 |
| | | | | | | | | | | | |
| JMB42a | 0.0 | Gh | 0 | 0.09544 | 282.9 | -15.3 | 111.9 | -15.6 | 111.9 | -15.6 | 8.0 |
| JMB42a | 100.0 | Gh | 0 | 0.09710 | 288.8 | -20.1 | 107.7 | -21.9 | 107.7 | -21.9 | 7.5 |
| JMB42a | 200.0 | Gh | 0 | 0.10500 | 300.8 | -16.5 | 113.0 | -32.8 | 113.0 | -32.8 | 7.5 |
| JMB42a | 300.0 | Gh | 0 | 0.12134 | 309.0 | -12.4 | 119.1 | -40.3 | 119.1 | -40.3 | 6.5 |

| | | | | | | | | | | | |
|---|---|---|---|---|---|---|---|---|---|---|---|
| JMB42a | 400.0 | Gh | 0 | 0.13723 | 316.4 | -8.1 | 126.4 | -46.9 | 126.4 | -46.9 | 7.0 |
| JMB42a | 500.0 | Gh | 0 | 0.16458 | 322.9 | -3.8 | 135.2 | -52.2 | 135.2 | -52.2 | 6.5 |
| JMB42a | 550.0 | Gh | 0 | 0.16961 | 325.4 | -6.5 | 121.4 | -55.3 | 121.4 | -55.3 | 6.0 |
| JMB42a | 600.0 | Gh | 0 | 0.16618 | 323.3 | -5.2 | 122.8 | -53.0 | 122.8 | -53.0 | 8.0 |
| JMB42a | 625.0 | Gh | 0 | 0.13834 | 324.7 | -6.7 | 120.8 | -54.7 | 120.8 | -54.7 | 9.0 |
| JMB42a | 650.0 | Gh | 0 | 0.12691 | 326.4 | -7.1 | 120.7 | -56.4 | 120.7 | -56.4 | 15.0 |
| | | | | | | | | | | | |
| JMB43a | 0.0 | Gh | 0 | 0.09765 | 221.6 | 6.2 | 106.3 | 46.6 | 106.3 | 46.6 | 7.5 |
| JMB43a | 100.0 | Gh | 0 | 0.09199 | 223.4 | 4.7 | 105.5 | 44.3 | 105.5 | 44.3 | 8.0 |
| JMB43a | 200.0 | Gh | 0 | 0.07992 | 232.1 | 4.9 | 110.9 | 36.6 | 110.9 | 36.6 | 8.0 |
| JMB43a | 300.0 | Gh | 0 | 0.07784 | 249.6 | 2.6 | 116.6 | 19.8 | 116.6 | 19.8 | 7.5 |
| JMB43a | 400.0 | Gh | 0 | 0.06004 | 275.4 | -1.9 | 122.8 | -5.7 | 122.8 | -5.7 | 7.5 |
| JMB43a | 500.0 | Gh | 0 | 0.07350 | 310.9 | 3.9 | 145.3 | -35.1 | 145.3 | -35.1 | 6.5 |
| JMB43a | 550.0 | Gh | 0 | 0.08992 | 318.6 | -0.6 | 145.6 | -44.0 | 145.6 | -44.0 | 5.0 |
| JMB43a | 600.0 | Gh | 0 | 0.09400 | 311.0 | 4.3 | 145.8 | -35.0 | 145.8 | -35.0 | 7.0 |
| JMB43a | 625.0 | Gh | 0 | 0.07772 | 307.7 | -3.7 | 135.2 | -36.0 | 135.2 | -36.0 | 6.5 |
| JMB43a | 650.0 | Gh | 0 | 0.06992 | 318.8 | -7.1 | 137.7 | -47.3 | 137.7 | -47.3 | 11.5 |
| JMB43a | 660.0 | Gh | 0 | 0.07493 | 299.6 | 41.1 | 171.2 | -4.9 | 171.2 | -4.9 | 18.5 |
| JMB43a | 670.0 | Gh | 0 | 0.04499 | 322.4 | 1.8 | 151.4 | -45.8 | 151.4 | -45.8 | 23.0 |
| JMB43a | 680.0 | Gh | 0 | 0.04186 | 334.2 | -7.2 | 150.8 | -60.6 | 150.8 | -60.6 | 28.5 |
| | | | | | | | | | | | |
| JMB44a | 0.0 | Gh | 0 | 0.13310 | 217.9 | -46.2 | 66.8 | 17.2 | 66.8 | 17.2 | 8.0 |
| JMB44a | 100.0 | Gh | 0 | 0.12897 | 226.1 | -52.6 | 66.7 | 8.9 | 66.7 | 8.9 | 7.0 |
| JMB44a | 200.0 | Gh | 0 | 0.12417 | 240.3 | -58.9 | 67.1 | -1.2 | 67.1 | -1.2 | 8.0 |
| JMB44a | 300.0 | Gh | 0 | 0.12484 | 257.5 | -62.0 | 68.2 | -10.1 | 68.2 | -10.1 | 8.5 |
| JMB44a | 400.0 | Gh | 0 | 0.12450 | 284.9 | -57.2 | 75.1 | -23.1 | 75.1 | -23.1 | 7.5 |
| JMB44a | 500.0 | Gh | 0 | 0.13691 | 309.9 | -48.4 | 81.7 | -39.5 | 81.7 | -39.5 | 6.0 |
| JMB44a | 550.0 | Gh | 0 | 0.14455 | 321.8 | -44.1 | 72.3 | -48.7 | 72.3 | -48.7 | 7.0 |
| JMB44a | 600.0 | Gh | 0 | 0.14014 | 321.0 | -45.8 | 70.5 | -47.5 | 70.5 | -47.5 | 6.5 |
| JMB44a | 625.0 | Gh | 0 | 0.12212 | 321.5 | -46.4 | 69.5 | -47.5 | 69.5 | -47.5 | 9.0 |
| JMB44a | 650.0 | Gh | 0 | 0.10919 | 327.1 | -46.4 | 66.3 | -50.8 | 66.3 | -50.8 | 13.0 |
| | | | | | | | | | | | |
| JMB45a | 0.0 | Gh | 0 | 0.22844 | 296.2 | -47.0 | 77.1 | -38.8 | 77.1 | -38.8 | 8.0 |
| JMB45a | 100.0 | Gh | 0 | 0.23175 | 302.3 | -47.8 | 76.3 | -42.9 | 76.3 | -42.9 | 8.5 |
| JMB45a | 200.0 | Gh | 0 | 0.24418 | 308.6 | -44.8 | 80.4 | -47.4 | 80.4 | -47.4 | 6.5 |
| JMB45a | 300.0 | Gh | 0 | 0.25365 | 313.0 | -42.4 | 83.8 | -50.7 | 83.8 | -50.7 | 7.5 |
| JMB45a | 400.0 | Gh | 0 | 0.26465 | 316.7 | -41.9 | 84.3 | -53.4 | 84.3 | -53.4 | 7.0 |
| JMB45a | 500.0 | Gh | 0 | 0.26871 | 319.2 | -37.6 | 91.6 | -55.6 | 91.6 | -55.6 | 6.0 |
| JMB45a | 550.0 | Gh | 0 | 0.27073 | 316.0 | -35.5 | 95.0 | -52.9 | 95.0 | -52.9 | 6.0 |
| JMB45a | 600.0 | Gh | 0 | 0.25131 | 318.9 | -36.3 | 93.9 | -55.3 | 93.9 | -55.3 | 7.0 |
| JMB45a | 625.0 | Gh | 0 | 0.22941 | 314.5 | -36.7 | 92.9 | -51.8 | 92.9 | -51.8 | 9.0 |
| JMB45a | 650.0 | Gh | 0 | 0.19636 | 318.2 | -33.1 | 99.4 | -54.5 | 99.4 | -54.5 | 15.0 |
| JMB45a | 660.0 | Gh | 0 | 0.17696 | 319.0 | -30.7 | 103.5 | -54.8 | 103.5 | -54.8 | 25.0 |
| JMB45a | 670.0 | Gh | 0 | 0.16934 | 313.4 | -29.8 | 103.6 | -49.9 | 103.6 | -49.9 | 32.0 |
| JMB45a | 680.0 | Gh | 0 | 0.12490 | 325.0 | -34.4 | 97.6 | -60.2 | 97.6 | -60.2 | 40.0 |
| | | | | | | | | | | | |
| JMB46a | 0.0 | Gh | 0 | 0.08637 | 266.9 | -35.5 | 70.0 | -15.7 | 70.0 | -15.7 | 7.5 |
| JMB46a | 100.0 | Gh | 0 | 0.08810 | 278.0 | -38.1 | 71.6 | -24.8 | 71.6 | -24.8 | 8.0 |
| JMB46a | 200.0 | Gh | 0 | 0.09393 | 296.8 | -39.3 | 75.4 | -39.2 | 75.4 | -39.2 | 7.5 |
| JMB46a | 300.0 | Gh | 0 | 0.10189 | 311.7 | -36.5 | 82.2 | -50.2 | 82.2 | -50.2 | 7.0 |
| JMB46a | 400.0 | Gh | 0 | 0.11123 | 315.5 | -33.7 | 87.4 | -52.9 | 87.4 | -52.9 | 6.5 |
| JMB46a | 500.0 | Gh | 0 | 0.13099 | 330.0 | -25.9 | 107.8 | -63.2 | 107.8 | -63.2 | 5.5 |
| JMB46a | 550.0 | Gh | 0 | 0.13743 | 334.6 | -28.3 | 94.9 | -67.7 | 94.9 | -67.7 | 6.0 |

| | | | | | | | | | | | |
|---|---|---|---|---|---|---|---|---|---|---|---|
| JMB46a | 600.0 | Gh | 0 | 0.13240 | 333.5 | -25.3 | 101.3 | -65.8 | 101.3 | -65.8 | 6.5 |
| JMB46a | 625.0 | Gh | 0 | 0.11392 | 337.7 | -20.2 | 117.1 | -66.8 | 117.1 | -66.8 | 9.0 |
| JMB46a | 650.0 | Gh | 0 | 0.09311 | 340.1 | -20.8 | 119.4 | -69.0 | 119.4 | -69.0 | 13.5 |
| | | | | | | | | | | | |
| JMB47a | 0.0 | Gh | 0 | 0.27363 | 314.5 | -25.3 | 84.3 | -45.9 | 84.3 | -45.9 | 8.0 |
| JMB47a | 100.0 | Gh | 0 | 0.28411 | 317.3 | -25.8 | 83.2 | -48.4 | 83.2 | -48.4 | 9.5 |
| JMB47a | 200.0 | Gh | 0 | 0.30293 | 319.5 | -23.9 | 85.7 | -50.6 | 85.7 | -50.6 | 9.0 |
| JMB47a | 300.0 | Gh | 0 | 0.32275 | 324.1 | -22.3 | 87.4 | -55.0 | 87.4 | -55.0 | 9.5 |
| JMB47a | 400.0 | Gh | 0 | 0.32815 | 324.5 | -20.1 | 91.2 | -55.6 | 91.2 | -55.6 | 8.5 |
| JMB47a | 500.0 | Gh | 0 | 0.35511 | 327.0 | -16.1 | 98.4 | -58.1 | 98.4 | -58.1 | 7.0 |
| JMB47a | 550.0 | Gh | 0 | 0.36249 | 329.7 | -14.4 | 101.9 | -60.6 | 101.9 | -60.6 | 7.5 |
| JMB47a | 600.0 | Gh | 0 | 0.35160 | 327.0 | -14.9 | 100.5 | -58.1 | 100.5 | -58.1 | 9.5 |
| JMB47a | 625.0 | Gh | 0 | 0.31121 | 328.3 | -16.2 | 98.1 | -59.3 | 98.1 | -59.3 | 12.0 |
| JMB47a | 650.0 | Gh | 0 | 0.27524 | 328.0 | -16.7 | 97.1 | -59.1 | 97.1 | -59.1 | 20.0 |
| JMB47a | 660.0 | Gh | 0 | 0.25828 | 332.1 | -16.4 | 97.6 | -63.0 | 97.6 | -63.0 | 33.0 |
| JMB47a | 670.0 | Gh | 0 | 0.23779 | 329.9 | -14.2 | 102.3 | -60.9 | 102.3 | -60.9 | 41.0 |
| JMB47a | 680.0 | Gh | 0 | 0.10864 | 339.0 | -17.6 | 93.6 | -69.5 | 93.6 | -69.5 | 51.0 |
| | | | | | | | | | | | |
| JMB48a | 0.0 | Gh | 0 | 0.36171 | 195.3 | 10.3 | 53.7 | 63.3 | 53.7 | 63.3 | 8.0 |
| JMB48a | 100.0 | Gh | 0 | 0.35137 | 196.3 | 9.2 | 54.4 | 61.8 | 54.4 | 61.8 | 7.0 |
| JMB48a | 200.0 | Gh | 0 | 0.33159 | 196.3 | 9.1 | 54.3 | 61.8 | 54.3 | 61.8 | 8.0 |
| JMB48a | 300.0 | Gh | 0 | 0.31714 | 199.0 | 8.4 | 58.2 | 59.8 | 58.2 | 59.8 | 8.0 |
| JMB48a | 400.0 | Gh | 0 | 0.31470 | 197.5 | 8.3 | 55.5 | 60.5 | 55.5 | 60.5 | 7.0 |
| JMB48a | 500.0 | Gh | 0 | 0.26831 | 203.4 | 8.1 | 64.7 | 57.0 | 64.7 | 57.0 | 7.5 |
| JMB48a | 550.0 | Gh | 0 | 0.18604 | 214.4 | 6.1 | 65.5 | 48.3 | 65.5 | 48.3 | 7.0 |
| JMB48a | 600.0 | Gh | 0 | 0.18363 | 216.2 | 6.5 | 67.8 | 47.2 | 67.8 | 47.2 | 8.0 |
| JMB48a | 625.0 | Gh | 0 | 0.13830 | 214.1 | 7.3 | 66.4 | 49.3 | 66.4 | 49.3 | 14.0 |
| JMB48a | 650.0 | Gh | 0 | 0.12789 | 211.2 | 7.9 | 64.0 | 51.8 | 64.0 | 51.8 | 17.5 |
| | | | | | | | | | | | |
| JMB49a | 0.0 | Gh | 0 | 0.22433 | 242.1 | 20.9 | 112.3 | 34.0 | 112.3 | 34.0 | 8.5 |
| JMB49a | 100.0 | Gh | 0 | 0.21259 | 245.6 | 19.7 | 112.7 | 30.6 | 112.7 | 30.6 | 8.0 |
| JMB49a | 200.0 | Gh | 0 | 0.20343 | 250.3 | 19.6 | 114.9 | 26.6 | 114.9 | 26.6 | 8.5 |
| JMB49a | 300.0 | Gh | 0 | 0.20111 | 256.6 | 18.0 | 116.3 | 20.5 | 116.3 | 20.5 | 9.0 |
| JMB49a | 400.0 | Gh | 0 | 0.20139 | 257.8 | 18.0 | 116.9 | 19.5 | 116.9 | 19.5 | 9.0 |
| JMB49a | 500.0 | Gh | 0 | 0.20642 | 265.0 | 16.5 | 119.1 | 12.8 | 119.1 | 12.8 | 7.5 |
| JMB49a | 550.0 | Gh | 0 | 0.18955 | 287.9 | 11.0 | 126.4 | -9.0 | 126.4 | -9.0 | 8.0 |
| JMB49a | 600.0 | Gh | 0 | 0.18210 | 286.9 | 12.9 | 127.4 | -7.1 | 127.4 | -7.1 | 10.0 |
| JMB49a | 625.0 | Gh | 0 | 0.14502 | 289.1 | 11.5 | 127.6 | -9.6 | 127.6 | -9.6 | 12.0 |
| JMB49a | 650.0 | Gh | 0 | 0.15240 | 294.5 | 10.9 | 130.2 | -14.2 | 130.2 | -14.2 | 21.5 |
| JMB49a | 660.0 | Gh | 0 | 0.13934 | 291.0 | 7.7 | 125.4 | -13.3 | 125.4 | -13.3 | 35.0 |
| JMB49a | 670.0 | Gh | 0 | 0.10984 | 300.3 | 10.0 | 133.2 | -19.2 | 133.2 | -19.2 | 47.5 |
| JMB49a | 680.0 | Gh | 0 | 0.04943 | 305.2 | 16.0 | 141.3 | -18.9 | 141.3 | -18.9 | 62.0 |
| | | | | | | | | | | | |
| JMB50a | 0.0 | Gh | 0 | 0.09551 | 212.4 | 40.9 | 137.3 | 62.2 | 137.3 | 62.2 | 8.5 |
| JMB50a | 100.0 | Gh | 0 | 0.08225 | 215.3 | 42.4 | 139.5 | 59.8 | 139.5 | 59.8 | 9.0 |
| JMB50a | 200.0 | Gh | 0 | 0.06505 | 231.4 | 50.0 | 149.3 | 47.6 | 149.3 | 47.6 | 9.0 |
| JMB50a | 300.0 | Gh | 0 | 0.05959 | 253.5 | 53.4 | 153.8 | 34.0 | 153.8 | 34.0 | 9.0 |
| JMB50a | 400.0 | Gh | 0 | 0.05686 | 266.2 | 52.0 | 154.2 | 26.2 | 154.2 | 26.2 | 8.5 |
| JMB50a | 500.0 | Gh | 0 | 0.05382 | 291.7 | 39.1 | 151.0 | 4.5 | 151.0 | 4.5 | 9.0 |
| JMB50a | 550.0 | Gh | 0 | 0.12793 | 332.1 | 10.3 | 149.6 | -40.8 | 149.6 | -40.8 | 11.0 |
| JMB50a | 600.0 | Gh | 0 | 0.11851 | 332.9 | 3.2 | 145.0 | -47.2 | 145.0 | -47.2 | 11.5 |
| JMB50a | 625.0 | Gh | 0 | 0.10955 | 329.6 | 13.7 | 149.2 | -36.6 | 149.2 | -36.6 | 22.5 |
| JMB50a | 650.0 | Gh | 0 | 0.10001 | 326.1 | 9.8 | 142.8 | -37.8 | 142.8 | -37.8 | 29.0 |

| | | | | | | | | | | | |
|---|---|---|---|---|---|---|---|---|---|---|---|
| JMC01a | 0.0 | Gh | 0 | 0.12069 | 172.9 | 4.8 | 49.1 | 63.9 | 49.1 | 63.9 | 5.5 |
| JMC01a | 100.0 | Gh | 0 | 0.10833 | 173.7 | -0.8 | 53.2 | 58.6 | 53.2 | 58.6 | 6.0 |
| JMC01a | 200.0 | Gh | 0 | 0.09124 | 177.2 | -6.6 | 60.7 | 53.3 | 60.7 | 53.3 | 6.5 |
| JMC01a | 300.0 | Gh | 0 | 0.07308 | 179.7 | -11.3 | 65.0 | 48.7 | 65.0 | 48.7 | 5.5 |
| JMC01a | 400.0 | Gh | 0 | 0.05974 | 197.0 | -20.4 | 85.5 | 37.0 | 85.5 | 37.0 | 5.5 |
| JMC01a | 500.0 | Gh | 0 | 0.04411 | 230.2 | -39.1 | 102.3 | 6.6 | 102.3 | 6.6 | 6.0 |
| JMC01a | 525.0 | Gh | 0 | 0.05943 | 233.4 | -24.6 | 114.5 | 15.1 | 114.5 | 15.1 | 4.5 |
| JMC01a | 550.0 | Gh | 0 | 0.06907 | 236.3 | -29.7 | 112.6 | 9.8 | 112.6 | 9.8 | 6.0 |
| JMC01a | 575.0 | Gh | 0 | 0.06345 | 239.6 | -37.7 | 108.5 | 2.3 | 108.5 | 2.3 | 4.5 |
| JMC01a | 600.0 | Gh | 0 | 0.05763 | 244.5 | -40.5 | 108.8 | -2.4 | 108.8 | -2.4 | 5.0 |
| JMC01a | 625.0 | Gh | 0 | 0.06250 | 248.4 | -29.8 | 119.2 | 1.6 | 119.2 | 1.6 | 8.0 |
| JMC01a | 650.0 | Gh | 0 | 0.05471 | 233.9 | -28.8 | 111.8 | 11.9 | 111.8 | 11.9 | 10.0 |
| JMC01a | 660.0 | Gh | 0 | 0.04530 | 245.5 | -24.2 | 122.2 | 7.0 | 122.2 | 7.0 | 14.0 |
| JMC01a | 670.0 | Gh | 0 | 0.04340 | 287.2 | -38.7 | 125.7 | -30.8 | 125.7 | -30.8 | 24.0 |
| JMC01a | 675.0 | Gh | 0 | 0.01553 | 309.9 | -39.0 | 129.0 | -48.3 | 129.0 | -48.3 | 34.5 |
| | | | | | | | | | | | |
| JMC02 | 0.0 | Gh | 0 | 0.19349 | 154.8 | 18.0 | 356.2 | 65.4 | 356.2 | 65.4 | 6.0 |
| JMC02 | 100.0 | Gh | 0 | 0.16033 | 153.8 | 16.9 | 357.6 | 64.0 | 357.6 | 64.0 | 4.5 |
| JMC02 | 200.0 | Gh | 0 | 0.15846 | 155.1 | 15.3 | 2.2 | 64.4 | 2.2 | 64.4 | 5.0 |
| JMC02 | 300.0 | Gh | 0 | 0.14628 | 152.4 | 17.2 | 355.8 | 62.9 | 355.8 | 62.9 | 4.0 |
| JMC02 | 400.0 | Gh | 0 | 0.12446 | 151.1 | 15.7 | 357.6 | 61.2 | 357.6 | 61.2 | 4.5 |
| JMC02 | 500.0 | Gh | 0 | 0.08116 | 149.5 | 13.7 | 359.8 | 58.9 | 359.8 | 58.9 | 4.0 |
| JMC02 | 525.0 | Gh | 0 | 0.07353 | 150.4 | 12.9 | 1.9 | 59.3 | 1.9 | 59.3 | 4.0 |
| JMC02 | 550.0 | Gh | 0 | 0.06874 | 149.5 | 14.4 | 358.5 | 59.2 | 358.5 | 59.2 | 4.5 |
| JMC02 | 575.0 | Gh | 0 | 0.06357 | 141.1 | 18.9 | 345.4 | 53.5 | 345.4 | 53.5 | 4.5 |
| JMC02 | 600.0 | Gh | 0 | 0.05177 | 144.6 | 16.7 | 351.0 | 55.9 | 351.0 | 55.9 | 4.0 |
| JMC02 | 625.0 | Gh | 0 | 0.04461 | 146.9 | 19.0 | 348.4 | 58.7 | 348.4 | 58.7 | 5.0 |
| JMC02 | 650.0 | Gh | 0 | 0.04085 | 133.6 | 16.3 | 345.5 | 45.9 | 345.5 | 45.9 | 9.0 |
| JMC02 | 660.0 | Gh | 0 | 0.02622 | 140.6 | 16.3 | 349.2 | 52.2 | 349.2 | 52.2 | 14.0 |
| JMC02 | 670.0 | Gh | 0 | 0.02095 | 115.4 | -9.2 | 2.7 | 18.1 | 2.7 | 18.1 | 24.5 |
| JMC02 | 675.0 | Gh | 0 | 0.01249 | 173.5 | -24.2 | 64.7 | 39.4 | 64.7 | 39.4 | 27.0 |
| | | | | | | | | | | | |
| JMC03a | 0.0 | Gh | 0 | 0.20955 | 161.9 | 8.0 | 27.0 | 64.4 | 27.0 | 64.4 | 6.5 |
| JMC03a | 100.0 | Gh | 0 | 0.18543 | 160.8 | 6.6 | 27.1 | 62.6 | 27.1 | 62.6 | 6.0 |
| JMC03a | 200.0 | Gh | 0 | 0.16352 | 162.4 | 4.5 | 32.6 | 61.9 | 32.6 | 61.9 | 7.0 |
| JMC03a | 300.0 | Gh | 0 | 0.14449 | 164.9 | 3.5 | 38.2 | 62.4 | 38.2 | 62.4 | 7.0 |
| JMC03a | 400.0 | Gh | 0 | 0.12342 | 172.4 | -3.5 | 57.7 | 58.6 | 57.7 | 58.6 | 7.0 |
| JMC03a | 500.0 | Gh | 0 | 0.08419 | 180.2 | -12.8 | 72.7 | 50.2 | 72.7 | 50.2 | 7.0 |
| JMC03a | 525.0 | Gh | 0 | 0.07766 | 184.9 | -20.0 | 78.7 | 42.8 | 78.7 | 42.8 | 5.5 |
| JMC03a | 550.0 | Gh | 0 | 0.06650 | 187.1 | -14.6 | 82.7 | 47.8 | 82.7 | 47.8 | 6.0 |
| JMC03a | 575.0 | Gh | 0 | 0.06800 | 183.2 | -21.1 | 76.4 | 41.8 | 76.4 | 41.8 | 5.5 |
| JMC03a | 600.0 | Gh | 0 | 0.06006 | 195.8 | -18.2 | 92.9 | 42.3 | 92.9 | 42.3 | 6.5 |
| JMC03a | 625.0 | Gh | 0 | 0.05392 | 190.3 | -22.0 | 84.9 | 40.0 | 84.9 | 40.0 | 8.0 |
| JMC03a | 650.0 | Gh | 0 | 0.04851 | 189.7 | -28.7 | 82.6 | 33.5 | 82.6 | 33.5 | 14.0 |
| JMC03a | 660.0 | Gh | 0 | 0.05027 | 211.3 | -43.3 | 95.3 | 14.0 | 95.3 | 14.0 | 23.0 |
| JMC03a | 670.0 | Gh | 0 | 0.02327 | 212.2 | -49.7 | 92.8 | 8.1 | 92.8 | 8.1 | 35.5 |
| JMC03a | 675.0 | Gh | 0 | 0.01864 | 251.5 | -51.8 | 109.0 | -10.5 | 109.0 | -10.5 | 49.0 |
| | | | | | | | | | | | |
| JMC04a | 0.0 | Gh | 0 | 0.11279 | 172.8 | 9.4 | 49.0 | 69.3 | 49.0 | 69.3 | 5.0 |
| JMC04a | 100.0 | Gh | 0 | 0.06921 | 181.6 | 1.9 | 72.9 | 62.9 | 72.9 | 62.9 | 6.5 |
| JMC04a | 200.0 | Gh | 0 | 0.06816 | 182.3 | 0.7 | 74.2 | 61.6 | 74.2 | 61.6 | 6.5 |
| JMC04a | 300.0 | Gh | 0 | 0.05375 | 189.3 | 3.0 | 89.9 | 62.5 | 89.9 | 62.5 | 6.5 |

| | | | | | | | | | | | |
|---|---|---|---|---|---|---|---|---|---|---|---|
| JMC04a | 400.0 | Gh | 0 | 0.04871 | 194.8 | -5.6 | 94.1 | 52.6 | 94.1 | 52.6 | 5.5 |
| JMC04a | 500.0 | Gh | 0 | 0.03034 | 219.6 | -18.2 | 113.4 | 29.3 | 113.4 | 29.3 | 4.0 |
| JMC04a | 525.0 | Gh | 0 | 0.03153 | 221.0 | -33.2 | 104.4 | 16.7 | 104.4 | 16.7 | 5.0 |
| JMC04a | 550.0 | Gh | 0 | 0.02341 | 226.9 | -45.4 | 100.3 | 4.3 | 100.3 | 4.3 | 5.0 |
| JMC04a | 575.0 | Gh | 0 | 0.02238 | 239.5 | -39.3 | 111.3 | 2.1 | 111.3 | 2.1 | 5.0 |
| JMC04a | 600.0 | Gh | 0 | 0.02225 | 232.7 | -9.1 | 130.8 | 26.5 | 130.8 | 26.5 | 6.0 |
| JMC04a | 625.0 | Gh | 0 | 0.01420 | 245.2 | -17.2 | 131.8 | 12.0 | 131.8 | 12.0 | 7.0 |
| JMC04a | 650.0 | Gh | 0 | 0.01400 | 278.4 | -22.5 | 143.0 | -17.7 | 143.0 | -17.7 | 10.0 |
| JMC04a | 660.0 | Gh | 0 | 0.02276 | 286.0 | 9.6 | 175.7 | -9.0 | 175.7 | -9.0 | 16.0 |
| JMC04a | 670.0 | Gh | 0 | 0.01255 | 319.3 | 45.5 | 222.0 | -6.8 | 222.0 | -6.8 | 25.0 |
| JMC04a | 675.0 | Gh | 0 | 0.00968 | 271.5 | -41.6 | 122.0 | -19.8 | 122.0 | -19.8 | 31.5 |
| | | | | | | | | | | | |
| JMC05a | 0.0 | Gh | 0 | 0.20863 | 155.6 | 4.7 | 8.0 | 61.8 | 8.0 | 61.8 | 8.0 |
| JMC05a | 100.0 | Gh | 0 | 0.18264 | 155.1 | 4.4 | 7.9 | 61.2 | 7.9 | 61.2 | 7.0 |
| JMC05a | 200.0 | Gh | 0 | 0.15757 | 155.7 | 2.5 | 11.7 | 60.5 | 11.7 | 60.5 | 7.5 |
| JMC05a | 300.0 | Gh | 0 | 0.13253 | 154.0 | 0.8 | 12.3 | 58.1 | 12.3 | 58.1 | 7.0 |
| JMC05a | 400.0 | Gh | 0 | 0.09422 | 155.4 | -3.7 | 20.2 | 56.2 | 20.2 | 56.2 | 6.5 |
| JMC05a | 500.0 | Gh | 0 | 0.04970 | 146.7 | -22.1 | 29.0 | 36.8 | 29.0 | 36.8 | 6.0 |
| JMC05a | 525.0 | Gh | 0 | 0.04353 | 149.5 | -26.1 | 34.5 | 35.2 | 34.5 | 35.2 | 8.0 |
| JMC05a | 550.0 | Gh | 0 | 0.04077 | 159.8 | -30.7 | 47.0 | 35.7 | 47.0 | 35.7 | 7.0 |
| JMC05a | 575.0 | Gh | 0 | 0.03321 | 146.4 | -42.6 | 42.7 | 20.2 | 42.7 | 20.2 | 7.0 |
| JMC05a | 600.0 | Gh | 0 | 0.03069 | 167.1 | -42.1 | 57.7 | 26.8 | 57.7 | 26.8 | 7.0 |
| JMC05a | 625.0 | Gh | 0 | 0.01887 | 157.0 | -76.6 | 63.2 | -7.6 | 63.2 | -7.6 | 9.5 |
| JMC05a | 650.0 | Gh | 0 | 0.03224 | 338.4 | -84.2 | 70.8 | -25.4 | 70.8 | -25.4 | 16.0 |
| JMC05a | 660.0 | Gh | 0 | 0.03139 | 10.4 | -62.6 | 61.4 | -46.8 | 61.4 | -46.8 | 28.0 |
| JMC05a | 670.0 | Gh | 0 | 0.03791 | 336.1 | -57.9 | 87.3 | -48.3 | 87.3 | -48.3 | 40.0 |
| JMC05a | 675.0 | Gh | 0 | 0.01687 | 10.8 | -46.1 | 52.1 | -62.4 | 52.1 | -62.4 | 54.0 |
| | | | | | | | | | | | |
| JMD01a | 0.0 | Gh | 0 | 0.10343 | 177.1 | -13.7 | 10.1 | 58.2 | 10.1 | 58.2 | 5.0 |
| JMD01a | 100.0 | Gh | 0 | 0.09703 | 178.9 | -18.1 | 13.6 | 53.9 | 13.6 | 53.9 | 4.5 |
| JMD01a | 200.0 | Gh | 0 | 0.08615 | 178.1 | -18.7 | 12.4 | 53.3 | 12.4 | 53.3 | 5.0 |
| JMD01a | 300.0 | Gh | 0 | 0.07155 | 172.1 | -18.1 | 2.8 | 53.1 | 2.8 | 53.1 | 6.0 |
| JMD01a | 400.0 | Gh | 0 | 0.05233 | 169.9 | -7.4 | 353.1 | 62.7 | 353.1 | 62.7 | 4.0 |
| JMD01a | 500.0 | Gh | 0 | 0.02585 | 176.0 | -8.9 | 6.7 | 62.8 | 6.7 | 62.8 | 5.0 |
| JMD01a | 525.0 | Gh | 0 | 0.02175 | 185.9 | -25.3 | 23.1 | 46.3 | 23.1 | 46.3 | 4.0 |
| JMD01a | 550.0 | Gh | 0 | 0.02135 | 163.4 | -16.6 | 349.2 | 51.7 | 349.2 | 51.7 | 4.0 |
| JMD01a | 575.0 | Gh | 0 | 0.02046 | 181.5 | -26.9 | 17.3 | 45.1 | 17.3 | 45.1 | 3.5 |
| JMD01a | 600.0 | Gh | 0 | 0.01295 | 190.1 | -16.3 | 32.2 | 54.3 | 32.2 | 54.3 | 4.5 |
| JMD01a | 625.0 | Gh | 0 | 0.01330 | 184.2 | -12.3 | 23.5 | 59.4 | 23.5 | 59.4 | 6.5 |
| JMD01a | 650.0 | Gh | 0 | 0.01028 | 208.6 | -18.7 | 54.3 | 43.8 | 54.3 | 43.8 | 11.0 |
| JMD01a | 660.0 | Gh | 0 | 0.00500 | 323.4 | -40.7 | 61.7 | -51.3 | 61.7 | -51.3 | 21.0 |
| JMD01a | 670.0 | Gh | 0 | 0.00627 | 27.0 | 37.1 | 219.9 | -29.3 | 219.9 | -29.3 | 29.0 |
| JMD01a | 675.0 | Gh | 0 | 0.00950 | 195.4 | 64.4 | 186.5 | 42.4 | 186.5 | 42.4 | 40.0 |
| | | | | | | | | | | | |
| JMD02a | 0.0 | Gh | 0 | 0.13498 | 202.2 | -35.3 | 37.4 | 30.8 | 37.4 | 30.8 | 4.0 |
| JMD02a | 100.0 | Gh | 0 | 0.11621 | 207.6 | -43.6 | 37.5 | 21.5 | 37.5 | 21.5 | 5.0 |
| JMD02a | 200.0 | Gh | 0 | 0.11614 | 207.3 | -44.1 | 37.1 | 21.2 | 37.1 | 21.2 | 5.0 |
| JMD02a | 300.0 | Gh | 0 | 0.10919 | 210.8 | -47.7 | 37.5 | 16.9 | 37.5 | 16.9 | 4.5 |
| JMD02a | 400.0 | Gh | 0 | 0.09252 | 215.2 | -51.6 | 37.9 | 12.1 | 37.9 | 12.1 | 4.5 |
| JMD02a | 500.0 | Gh | 0 | 0.07143 | 234.8 | -65.5 | 36.3 | -5.0 | 36.3 | -5.0 | 3.0 |
| JMD02a | 525.0 | Gh | 0 | 0.06967 | 231.0 | -62.2 | 37.7 | -1.5 | 37.7 | -1.5 | 3.5 |
| JMD02a | 550.0 | Gh | 0 | 0.06049 | 255.0 | -67.2 | 39.0 | -12.8 | 39.0 | -12.8 | 3.5 |
| JMD02a | 575.0 | Gh | 0 | 0.06082 | 242.0 | -68.2 | 35.8 | -8.8 | 35.8 | -8.8 | 4.0 |

| | | | | | | | | | | | |
|---|---|---|---|---|---|---|---|---|---|---|---|
| JMD02a | 600.0 | Gh | 0 | 0.05434 | 229.7 | -76.1 | 27.1 | -10.7 | 27.1 | -10.7 | 4.0 |
| JMD02a | 625.0 | Gh | 0 | 0.05036 | 263.2 | -63.8 | 43.4 | -14.9 | 43.4 | -14.9 | 3.5 |
| JMD02a | 650.0 | Gh | 0 | 0.05181 | 274.5 | -67.9 | 39.9 | -20.2 | 39.9 | -20.2 | 7.0 |
| JMD02a | 660.0 | Gh | 0 | 0.06137 | 279.7 | -73.5 | 34.0 | -21.9 | 34.0 | -21.9 | 12.0 |
| JMD02a | 670.0 | Gh | 0 | 0.03502 | 287.6 | -77.8 | 29.1 | -23.2 | 29.1 | -23.2 | 18.0 |
| JMD02a | 675.0 | Gh | 0 | 0.01525 | 4.9 | -34.9 | 1.2 | -74.5 | 1.2 | -74.5 | 23.0 |
| | | | | | | | | | | | |
| JMD03a | 0.0 | Gh | 0 | 0.23030 | 259.6 | -9.1 | 92.8 | 5.7 | 92.8 | 5.7 | 5.0 |
| JMD03a | 100.0 | Gh | 0 | 0.22573 | 263.4 | -10.5 | 93.1 | 1.7 | 93.1 | 1.7 | 6.0 |
| JMD03a | 200.0 | Gh | 0 | 0.22827 | 270.1 | -10.1 | 96.2 | -4.2 | 96.2 | -4.2 | 5.0 |
| JMD03a | 300.0 | Gh | 0 | 0.21668 | 271.4 | -8.0 | 98.6 | -4.5 | 98.6 | -4.5 | 6.0 |
| JMD03a | 400.0 | Gh | 0 | 0.23002 | 275.6 | -10.1 | 98.4 | -9.2 | 98.4 | -9.2 | 5.0 |
| JMD03a | 500.0 | Gh | 0 | 0.21546 | 281.3 | -11.2 | 99.5 | -14.7 | 99.5 | -14.7 | 4.5 |
| JMD03a | 525.0 | Gh | 0 | 0.22000 | 280.8 | -9.4 | 101.0 | -13.6 | 101.0 | -13.6 | 4.0 |
| JMD03a | 550.0 | Gh | 0 | 0.21521 | 280.5 | -11.9 | 98.5 | -14.3 | 98.5 | -14.3 | 4.0 |
| JMD03a | 575.0 | Gh | 0 | 0.21523 | 283.4 | -9.1 | 102.3 | -15.9 | 102.3 | -15.9 | 4.5 |
| JMD03a | 600.0 | Gh | 0 | 0.21584 | 284.9 | -11.1 | 101.0 | -18.0 | 101.0 | -18.0 | 4.5 |
| JMD03a | 625.0 | Gh | 0 | 0.19591 | 288.0 | -10.7 | 102.6 | -20.7 | 102.6 | -20.7 | 5.0 |
| JMD03a | 650.0 | Gh | 0 | 0.16370 | 287.8 | -13.7 | 99.5 | -21.6 | 99.5 | -21.6 | 7.0 |
| JMD03a | 660.0 | Gh | 0 | 0.13707 | 299.9 | -11.5 | 106.5 | -31.8 | 106.5 | -31.8 | 15.0 |
| JMD03a | 670.0 | Gh | 0 | 0.13899 | 291.8 | -8.9 | 105.9 | -23.5 | 105.9 | -23.5 | 20.0 |
| JMD03a | 675.0 | Gh | 0 | 0.10708 | 298.7 | -8.0 | 109.8 | -29.4 | 109.8 | -29.4 | 29.0 |
| | | | | | | | | | | | |
| JMD04a | 0.0 | Gh | 0 | 0.12642 | 223.9 | -26.7 | 60.8 | 23.2 | 60.8 | 23.2 | 6.0 |
| JMD04a | 100.0 | Gh | 0 | 0.11204 | 241.3 | -39.3 | 61.3 | 4.0 | 61.3 | 4.0 | 5.5 |
| JMD04a | 200.0 | Gh | 0 | 0.11170 | 243.5 | -39.1 | 62.5 | 2.7 | 62.5 | 2.7 | 6.0 |
| JMD04a | 300.0 | Gh | 0 | 0.10469 | 247.3 | -37.5 | 65.5 | 1.2 | 65.5 | 1.2 | 6.0 |
| JMD04a | 400.0 | Gh | 0 | 0.09618 | 261.1 | -41.3 | 67.3 | -10.0 | 67.3 | -10.0 | 5.5 |
| JMD04a | 500.0 | Gh | 0 | 0.10403 | 300.1 | -34.1 | 83.5 | -37.8 | 83.5 | -37.8 | 6.0 |
| JMD04a | 525.0 | Gh | 0 | 0.11628 | 297.9 | -33.8 | 83.6 | -36.0 | 83.6 | -36.0 | 4.5 |
| JMD04a | 550.0 | Gh | 0 | 0.11541 | 302.8 | -31.2 | 87.6 | -39.7 | 87.6 | -39.7 | 4.0 |
| JMD04a | 575.0 | Gh | 0 | 0.11665 | 302.6 | -31.0 | 87.8 | -39.5 | 87.8 | -39.5 | 6.0 |
| JMD04a | 600.0 | Gh | 0 | 0.11167 | 296.0 | -34.8 | 82.1 | -34.6 | 82.1 | -34.6 | 5.5 |
| JMD04a | 625.0 | Gh | 0 | 0.10137 | 299.2 | -43.1 | 72.1 | -37.7 | 72.1 | -37.7 | 14.0 |
| JMD04a | 650.0 | Gh | 0 | 0.09910 | 304.5 | -27.9 | 92.1 | -40.6 | 92.1 | -40.6 | 10.0 |
| JMD04a | 660.0 | Gh | 0 | 0.09132 | 311.3 | -27.0 | 94.7 | -46.5 | 94.7 | -46.5 | 15.5 |
| JMD04a | 670.0 | Gh | 0 | 0.08518 | 325.3 | -20.3 | 109.6 | -57.7 | 109.6 | -57.7 | 26.0 |
| JMD04a | 675.0 | Gh | 0 | 0.05898 | 302.8 | -19.8 | 101.8 | -37.2 | 101.8 | -37.2 | 34.0 |
| | | | | | | | | | | | |
| JMD05E | 0.0 | Gh | 0 | 0.02263 | 169.9 | 44.7 | 217.5 | 71.5 | 217.5 | 71.5 | 2.0 |
| JMD05E | 100.0 | Gh | 0 | 0.01949 | 176.2 | 47.3 | 202.1 | 70.5 | 202.1 | 70.5 | 1.5 |
| JMD05E | 200.0 | Gh | 0 | 0.01304 | 189.6 | 65.7 | 188.0 | 51.8 | 188.0 | 51.8 | 2.0 |
| JMD05E | 300.0 | Gh | 0 | 0.01133 | 180.5 | 48.0 | 193.4 | 70.0 | 193.4 | 70.0 | 2.0 |
| JMD05E | 400.0 | Gh | 0 | 0.01906 | 184.6 | 22.1 | 50.6 | 82.8 | 50.6 | 82.8 | 3.0 |
| JMD05E | 500.0 | Gh | 0 | 0.01654 | 181.1 | 60.6 | 193.4 | 57.4 | 193.4 | 57.4 | 2.0 |
| JMD05E | 525.0 | Gh | 0 | 0.01166 | 189.7 | 50.0 | 178.4 | 66.8 | 178.4 | 66.8 | 2.0 |
| JMD05E | 550.0 | Gh | 0 | 0.01014 | 220.5 | 31.6 | 120.4 | 54.9 | 120.4 | 54.9 | 1.5 |
| JMD05E | 575.0 | Gh | 0 | 0.01021 | 160.2 | 65.9 | 206.9 | 50.2 | 206.9 | 50.2 | 1.0 |
| JMD05E | 600.0 | Gh | 0 | 0.01110 | 217.6 | -11.7 | 62.1 | 36.1 | 62.1 | 36.1 | 1.0 |
| JMD05E | 625.0 | Gh | 0 | 0.01414 | 240.6 | -4.6 | 85.3 | 23.2 | 85.3 | 23.2 | 1.5 |
| JMD05E | 650.0 | Gh | 0 | 0.00778 | 222.7 | 17.7 | 99.1 | 49.5 | 99.1 | 49.5 | 1.5 |
| JMD05E | 660.0 | Gh | 0 | 0.00837 | 271.6 | 50.3 | 151.5 | 20.2 | 151.5 | 20.2 | 5.0 |
| JMD05E | 670.0 | Gh | 0 | 0.00226 | 320.7 | 17.4 | 149.7 | -30.8 | 149.7 | -30.8 | 2.5 |

| | | | | | | | | | | | |
|---|---|---|---|---|---|---|---|---|---|---|---|
| JMD05E | 675.0 | Gh | 0 | 0.01242 | 255.0 | -1.9 | 95.5 | 12.3 | 95.5 | 12.3 | 2.5 |
| | | | | | | | | | | | |
| JMD05a | 0.0 | Gh | 0 | 0.12127 | 266.3 | -5.1 | 98.2 | 0.9 | 98.2 | 0.9 | 6.5 |
| JMD05a | 100.0 | Gh | 0 | 0.11192 | 272.0 | -6.5 | 99.6 | -4.8 | 99.6 | -4.8 | 5.0 |
| JMD05a | 200.0 | Gh | 0 | 0.10823 | 282.5 | -6.0 | 104.9 | -13.8 | 104.9 | -13.8 | 6.0 |
| JMD05a | 300.0 | Gh | 0 | 0.11100 | 290.7 | -8.3 | 106.7 | -22.1 | 106.7 | -22.1 | 6.0 |
| JMD05a | 400.0 | Gh | 0 | 0.10454 | 298.4 | -8.8 | 110.0 | -29.1 | 110.0 | -29.1 | 5.0 |
| JMD05a | 500.0 | Gh | 0 | 0.12613 | 316.3 | -5.0 | 125.2 | -42.6 | 125.2 | -42.6 | 5.0 |
| JMD05a | 525.0 | Gh | 0 | 0.12911 | 318.0 | -5.2 | 126.3 | -44.1 | 126.3 | -44.1 | 4.5 |
| JMD05a | 550.0 | Gh | 0 | 0.13502 | 318.0 | -8.9 | 121.9 | -46.1 | 121.9 | -46.1 | 5.0 |
| JMD05a | 575.0 | Gh | 0 | 0.12966 | 321.7 | -3.8 | 131.0 | -46.3 | 131.0 | -46.3 | 5.0 |
| JMD05a | 600.0 | Gh | 0 | 0.12405 | 323.1 | 1.3 | 137.8 | -44.0 | 137.8 | -44.0 | 5.0 |
| JMD05a | 625.0 | Gh | 0 | 0.10903 | 325.1 | -6.7 | 130.6 | -50.7 | 130.6 | -50.7 | 7.0 |
| JMD05a | 650.0 | Gh | 0 | 0.09663 | 322.1 | -5.6 | 129.2 | -47.7 | 129.2 | -47.7 | 10.0 |
| JMD05a | 660.0 | Gh | 0 | 0.08860 | 322.6 | -6.7 | 128.3 | -48.7 | 128.3 | -48.7 | 19.5 |
| JMD05a | 670.0 | Gh | 0 | 0.09316 | 327.6 | -5.8 | 134.2 | -52.1 | 134.2 | -52.1 | 25.0 |
| JMD05a | 675.0 | Gh | 0 | 0.07833 | 327.3 | -3.2 | 137.0 | -50.2 | 137.0 | -50.2 | 34.5 |
| | | | | | | | | | | | |
| JMD06a | 0.0 | Gh | 0 | 0.17086 | 270.2 | 11.4 | 107.7 | 6.7 | 107.7 | 6.7 | 6.0 |
| JMD06a | 100.0 | Gh | 0 | 0.17053 | 284.5 | 4.5 | 110.8 | -8.8 | 110.8 | -8.8 | 7.0 |
| JMD06a | 200.0 | Gh | 0 | 0.17025 | 282.7 | 3.4 | 108.8 | -8.0 | 108.8 | -8.0 | 5.0 |
| JMD06a | 300.0 | Gh | 0 | 0.17384 | 288.4 | 3.7 | 112.7 | -12.3 | 112.7 | -12.3 | 6.0 |
| JMD06a | 400.0 | Gh | 0 | 0.17208 | 295.4 | 4.0 | 117.6 | -17.4 | 117.6 | -17.4 | 6.0 |
| JMD06a | 500.0 | Gh | 0 | 0.15314 | 299.5 | -1.2 | 116.2 | -23.9 | 116.2 | -23.9 | 5.0 |
| JMD06a | 525.0 | Gh | 0 | 0.16162 | 297.5 | -0.2 | 115.6 | -21.8 | 115.6 | -21.8 | 4.5 |
| JMD06a | 550.0 | Gh | 0 | 0.16124 | 299.2 | 0.9 | 117.7 | -22.3 | 117.7 | -22.3 | 5.5 |
| JMD06a | 575.0 | Gh | 0 | 0.14781 | 304.4 | -2.3 | 118.9 | -28.4 | 118.9 | -28.4 | 6.0 |
| JMD06a | 600.0 | Gh | 0 | 0.15252 | 300.5 | 0.2 | 118.1 | -23.8 | 118.1 | -23.8 | 5.0 |
| JMD06a | 625.0 | Gh | 0 | 0.14533 | 307.8 | -1.6 | 122.1 | -30.4 | 122.1 | -30.4 | 7.5 |
| JMD06a | 650.0 | Gh | 0 | 0.11853 | 308.1 | 0.7 | 124.2 | -29.0 | 124.2 | -29.0 | 14.0 |
| JMD06a | 660.0 | Gh | 0 | 0.12421 | 314.2 | 11.9 | 137.8 | -24.9 | 137.8 | -24.9 | 23.0 |
| JMD06a | 670.0 | Gh | 0 | 0.08931 | 311.6 | 7.0 | 132.0 | -26.9 | 132.0 | -26.9 | 35.5 |
| JMD06a | 675.0 | Gh | 0 | 0.04830 | 311.3 | 35.7 | 150.7 | -4.4 | 150.7 | -4.4 | 44.0 |
| | | | | | | | | | | | |
| JME01a | 0.0 | Gh | 0 | 0.34868 | 7.6 | 52.9 | 204.4 | -22.8 | 204.4 | -22.8 | 6.0 |
| JME01a | 100.0 | Gh | 0 | 0.35195 | 7.2 | 51.1 | 204.4 | -24.6 | 204.4 | -24.6 | 7.0 |
| JME01a | 200.0 | Gh | 0 | 0.36981 | 7.3 | 51.7 | 204.3 | -24.0 | 204.3 | -24.0 | 6.0 |
| JME01a | 300.0 | Gh | 0 | 0.40213 | 4.0 | 49.8 | 202.3 | -26.1 | 202.3 | -26.1 | 7.0 |
| JME01a | 400.0 | Gh | 0 | 0.41426 | 4.7 | 49.3 | 202.8 | -26.6 | 202.8 | -26.6 | 6.0 |
| JME01a | 500.0 | Gh | 0 | 0.39611 | 5.1 | 44.3 | 203.7 | -31.5 | 203.7 | -31.5 | 5.5 |
| JME01a | 525.0 | Gh | 0 | 0.38244 | 5.8 | 44.0 | 204.3 | -31.8 | 204.3 | -31.8 | 4.5 |
| JME01a | 550.0 | Gh | 0 | 0.39253 | 9.5 | 42.3 | 207.8 | -33.0 | 207.8 | -33.0 | 4.0 |
| JME01a | 575.0 | Gh | 0 | 0.36248 | 6.3 | 41.2 | 205.1 | -34.5 | 205.1 | -34.5 | 5.0 |
| JME01a | 600.0 | Gh | 0 | 0.36514 | 2.5 | 46.6 | 201.4 | -29.4 | 201.4 | -29.4 | 5.5 |
| JME01a | 625.0 | Gh | 0 | 0.29545 | 350.8 | 42.3 | 191.3 | -33.1 | 191.3 | -33.1 | 5.0 |
| JME01a | 650.0 | Gh | 0 | 0.27969 | 355.2 | 37.4 | 194.5 | -38.4 | 194.5 | -38.4 | 5.0 |
| JME01a | 660.0 | Gh | 0 | 0.27620 | 356.6 | 35.1 | 195.7 | -40.8 | 195.7 | -40.8 | 7.0 |
| JME01a | 670.0 | Gh | 0 | 0.27539 | 353.0 | 36.0 | 192.1 | -39.6 | 192.1 | -39.6 | 8.0 |
| JME01a | 675.0 | Gh | 0 | 0.23177 | 353.8 | 41.0 | 193.7 | -34.7 | 193.7 | -34.7 | 11.0 |
| | | | | | | | | | | | |
| JME02a | 0.0 | Gh | 0 | 0.08963 | 260.1 | 49.5 | 155.7 | 22.1 | 155.7 | 22.1 | 5.0 |
| JME02a | 100.0 | Gh | 0 | 0.10228 | 293.0 | 46.2 | 159.8 | 0.4 | 159.8 | 0.4 | 5.5 |
| JME02a | 200.0 | Gh | 0 | 0.10243 | 295.8 | 46.6 | 161.2 | -1.1 | 161.2 | -1.1 | 6.0 |

| | | | | | | | | | | | |
|---|---|---|---|---|---|---|---|---|---|---|---|
| JME02a | 300.0 | Gh | 0 | 0.11672 | 298.0 | 45.9 | 161.4 | -2.7 | 161.4 | -2.7 | 5.0 |
| JME02a | 400.0 | Gh | 0 | 0.12154 | 311.7 | 42.7 | 165.2 | -12.3 | 165.2 | -12.3 | 5.0 |
| JME02a | 500.0 | Gh | 0 | 0.13753 | 317.1 | 39.3 | 165.9 | -17.6 | 165.9 | -17.6 | 3.5 |
| JME02a | 525.0 | Gh | 0 | 0.13879 | 321.8 | 38.8 | 168.5 | -20.3 | 168.5 | -20.3 | 3.0 |
| JME02a | 550.0 | Gh | 0 | 0.13363 | 325.0 | 33.9 | 167.5 | -25.8 | 167.5 | -25.8 | 5.0 |
| JME02a | 575.0 | Gh | 0 | 0.13352 | 324.6 | 33.6 | 167.0 | -25.8 | 167.0 | -25.8 | 4.5 |
| JME02a | 600.0 | Gh | 0 | 0.12664 | 326.1 | 37.0 | 170.3 | -23.8 | 170.3 | -23.8 | 4.5 |
| JME02a | 625.0 | Gh | 0 | 0.10831 | 330.5 | 32.4 | 170.8 | -29.6 | 170.8 | -29.6 | 5.0 |
| JME02a | 650.0 | Gh | 0 | 0.09184 | 322.2 | 29.8 | 162.6 | -27.5 | 162.6 | -27.5 | 7.0 |
| JME02a | 660.0 | Gh | 0 | 0.07811 | 315.6 | 18.8 | 148.8 | -31.1 | 148.8 | -31.1 | 10.0 |
| JME02a | 670.0 | Gh | 0 | 0.06485 | 335.3 | 23.2 | 169.5 | -39.7 | 169.5 | -39.7 | 15.0 |
| JME02a | 675.0 | Gh | 0 | 0.03843 | 324.2 | -7.6 | 125.3 | -52.9 | 125.3 | -52.9 | 20.0 |
| | | | | | | | | | | | |
| JME03a | 0.0 | Gh | 0 | 0.08222 | 288.0 | -1.0 | 116.8 | -17.5 | 116.8 | -17.5 | 5.0 |
| JME03a | 100.0 | Gh | 0 | 0.08277 | 289.5 | -4.1 | 114.2 | -19.8 | 114.2 | -19.8 | 4.5 |
| JME03a | 200.0 | Gh | 0 | 0.08746 | 299.5 | -3.4 | 118.1 | -29.2 | 118.1 | -29.2 | 4.5 |
| JME03a | 300.0 | Gh | 0 | 0.09624 | 306.3 | -9.3 | 113.6 | -37.3 | 113.6 | -37.3 | 4.5 |
| JME03a | 400.0 | Gh | 0 | 0.11754 | 309.4 | -7.2 | 117.2 | -39.7 | 117.2 | -39.7 | 5.0 |
| JME03a | 500.0 | Gh | 0 | 0.10652 | 319.2 | 1.7 | 133.3 | -45.6 | 133.3 | -45.6 | 4.0 |
| JME03a | 525.0 | Gh | 0 | 0.11050 | 319.9 | 2.4 | 134.7 | -45.9 | 134.7 | -45.9 | 4.0 |
| JME03a | 550.0 | Gh | 0 | 0.10528 | 321.3 | 9.3 | 144.0 | -43.6 | 144.0 | -43.6 | 3.5 |
| JME03a | 575.0 | Gh | 0 | 0.10793 | 326.7 | 3.5 | 141.3 | -51.3 | 141.3 | -51.3 | 4.0 |
| JME03a | 600.0 | Gh | 0 | 0.10355 | 322.5 | 2.9 | 137.1 | -48.0 | 137.1 | -48.0 | 4.0 |
| JME03a | 625.0 | Gh | 0 | 0.10349 | 316.6 | 5.7 | 136.5 | -41.5 | 136.5 | -41.5 | 4.0 |
| JME03a | 650.0 | Gh | 0 | 0.10772 | 318.9 | 0.8 | 132.0 | -45.8 | 132.0 | -45.8 | 5.0 |
| JME03a | 660.0 | Gh | 0 | 0.08961 | 319.3 | -7.5 | 120.8 | -49.2 | 120.8 | -49.2 | 7.0 |
| JME03a | 670.0 | Gh | 0 | 0.08926 | 327.1 | -14.3 | 112.6 | -58.2 | 112.6 | -58.2 | 6.5 |
| JME03a | 675.0 | Gh | 0 | 0.08914 | 333.6 | -10.7 | 122.7 | -63.6 | 122.7 | -63.6 | 8.0 |
| | | | | | | | | | | | |
| JME04a | 0.0 | Gh | 0 | 0.05238 | 41.3 | 7.8 | 256.6 | -38.1 | 256.6 | -38.1 | 4.0 |
| JME04a | 100.0 | Gh | 0 | 0.07115 | 28.4 | 0.9 | 251.3 | -52.2 | 251.3 | -52.2 | 3.5 |
| JME04a | 200.0 | Gh | 0 | 0.07066 | 26.9 | 1.8 | 248.5 | -52.6 | 248.5 | -52.6 | 3.0 |
| JME04a | 300.0 | Gh | 0 | 0.07878 | 25.6 | 1.4 | 247.4 | -53.8 | 247.4 | -53.8 | 3.5 |
| JME04a | 400.0 | Gh | 0 | 0.09459 | 15.5 | 1.2 | 232.5 | -59.8 | 232.5 | -59.8 | 4.0 |
| JME04a | 500.0 | Gh | 0 | 0.09646 | 5.2 | -0.5 | 212.8 | -65.0 | 212.8 | -65.0 | 3.0 |
| JME04a | 525.0 | Gh | 0 | 0.10936 | 0.5 | 17.9 | 201.1 | -47.1 | 201.1 | -47.1 | 3.0 |
| JME04a | 550.0 | Gh | 0 | 0.10516 | 355.3 | 24.5 | 194.8 | -40.3 | 194.8 | -40.3 | 2.0 |
| JME04a | 575.0 | Gh | 0 | 0.09432 | 356.3 | 29.1 | 196.4 | -35.8 | 196.4 | -35.8 | 3.0 |
| JME04a | 600.0 | Gh | 0 | 0.08279 | 358.2 | 25.5 | 198.3 | -39.5 | 198.3 | -39.5 | 3.0 |
| JME04a | 625.0 | Gh | 0 | 0.07906 | 12.2 | 29.6 | 213.2 | -34.2 | 213.2 | -34.2 | 3.0 |
| JME04a | 650.0 | Gh | 0 | 0.07682 | 12.9 | 24.8 | 215.4 | -38.7 | 215.4 | -38.7 | 5.5 |
| JME04a | 660.0 | Gh | 0 | 0.07915 | 16.3 | 31.6 | 216.6 | -31.3 | 216.6 | -31.3 | 5.5 |
| JME04a | 670.0 | Gh | 0 | 0.04712 | 22.8 | 13.2 | 233.2 | -45.8 | 233.2 | -45.8 | 8.0 |
| JME04a | 675.0 | Gh | 0 | 0.03542 | 10.8 | 34.3 | 210.7 | -29.8 | 210.7 | -29.8 | 10.5 |
| | | | | | | | | | | | |
| JMF01a | 0.0 | Gh | 0 | 0.33052 | 176.5 | -16.6 | 10.9 | 52.2 | 10.9 | 52.2 | 8.0 |
| JMF01a | 100.0 | Gh | 0 | 0.31312 | 172.0 | -17.8 | 4.4 | 50.4 | 4.4 | 50.4 | 8.0 |
| JMF01a | 200.0 | Gh | 0 | 0.28356 | 170.6 | -18.9 | 2.8 | 49.1 | 2.8 | 49.1 | 9.0 |
| JMF01a | 300.0 | Gh | 0 | 0.26448 | 168.1 | -19.6 | 359.6 | 47.8 | 359.6 | 47.8 | 8.0 |
| JMF01a | 400.0 | Gh | 0 | 0.22609 | 168.9 | -21.2 | 1.3 | 46.4 | 1.3 | 46.4 | 7.5 |
| JMF01a | 500.0 | Gh | 0 | 0.16976 | 169.0 | -26.8 | 3.4 | 41.0 | 3.4 | 41.0 | 0.0 |
| JMF01a | 525.0 | Gh | 0 | 0.15383 | 170.9 | -28.6 | 6.0 | 39.6 | 6.0 | 39.6 | 7.0 |
| JMF01a | 550.0 | Gh | 0 | 0.14176 | 169.6 | -31.5 | 5.4 | 36.6 | 5.4 | 36.6 | 5.5 |

| | | | | | | | | | | | |
|---|---|---|---|---|---|---|---|---|---|---|---|
| JMF01a | 575.0 | Gh | 0 | 0.12648 | 170.5 | -31.9 | 6.4 | 36.3 | 6.4 | 36.3 | 7.0 |
| JMF01a | 600.0 | Gh | 0 | 0.11358 | 169.2 | -33.1 | 5.4 | 34.9 | 5.4 | 34.9 | 6.0 |
| JMF01a | 625.0 | Gh | 0 | 0.11400 | 164.3 | -31.1 | 359.8 | 35.8 | 359.8 | 35.8 | -9.9 |
| JMF01a | 650.0 | Gh | 0 | 0.09959 | 168.7 | -34.3 | 5.2 | 33.7 | 5.2 | 33.7 | 6.5 |
| JMF01a | 660.0 | Gh | 0 | 0.08256 | 169.6 | -35.0 | 6.2 | 33.1 | 6.2 | 33.1 | 10.0 |
| JMF01a | 670.0 | Gh | 0 | 0.07316 | 153.2 | -43.4 | 355.8 | 21.1 | 355.8 | 21.1 | 10.0 |
| JMF01a | 675.0 | Gh | 0 | 0.04973 | 159.1 | -44.1 | 0.3 | 22.1 | 0.3 | 22.1 | 13.5 |
| | | | | | | | | | | | |
| JMF02a | 0.0 | Gh | 0 | 0.05984 | 66.2 | 57.3 | 224.1 | 3.9 | 224.1 | 3.9 | 5.0 |
| JMF02a | 100.0 | Gh | 0 | 0.05978 | 36.0 | 37.1 | 225.4 | -24.4 | 225.4 | -24.4 | 5.0 |
| JMF02a | 200.0 | Gh | 0 | 0.05983 | 37.3 | 36.1 | 227.0 | -24.6 | 227.0 | -24.6 | 6.0 |
| JMF02a | 300.0 | Gh | 0 | 0.06986 | 25.4 | 28.2 | 222.6 | -36.8 | 222.6 | -36.8 | 6.5 |
| JMF02a | 400.0 | Gh | 0 | 0.07047 | 12.2 | 32.4 | 207.4 | -37.3 | 207.4 | -37.3 | 5.0 |
| JMF02a | 500.0 | Gh | 0 | 0.07623 | 5.1 | 30.8 | 200.1 | -40.0 | 200.1 | -40.0 | 5.0 |
| JMF02a | 525.0 | Gh | 0 | 0.07574 | 19.4 | 24.5 | 218.6 | -42.6 | 218.6 | -42.6 | 4.0 |
| JMF02a | 550.0 | Gh | 0 | 0.06867 | 2.8 | 15.7 | 199.1 | -55.2 | 199.1 | -55.2 | 4.0 |
| JMF02a | 575.0 | Gh | 0 | 0.08061 | 1.1 | 25.6 | 195.8 | -45.4 | 195.8 | -45.4 | 4.0 |
| JMF02a | 600.0 | Gh | 0 | 0.05258 | 3.5 | 17.9 | 199.9 | -52.9 | 199.9 | -52.9 | 4.0 |
| JMF02a | 625.0 | Gh | 0 | 0.05367 | 11.9 | 29.7 | 207.9 | -40.0 | 207.9 | -40.0 | 5.0 |
| JMF02a | 650.0 | Gh | 0 | 0.04324 | 350.4 | 26.4 | 182.5 | -43.7 | 182.5 | -43.7 | 5.5 |
| JMF02a | 660.0 | Gh | 0 | 0.03862 | 340.2 | 41.6 | 177.9 | -26.7 | 177.9 | -26.7 | 8.0 |
| JMF02a | 670.0 | Gh | 0 | 0.01491 | 308.0 | -33.6 | 75.9 | -41.7 | 75.9 | -41.7 | 11.0 |
| JMF02a | 675.0 | Gh | 0 | 0.02653 | 354.4 | 29.2 | 187.9 | -41.5 | 187.9 | -41.5 | 12.5 |
| | | | | | | | | | | | |
| JMF03a | 0.0 | Gh | 0 | 0.19186 | 159.7 | 22.9 | 344.0 | 63.8 | 344.0 | 63.8 | 7.0 |
| JMF03a | 100.0 | Gh | 0 | 0.18533 | 157.1 | 19.8 | 343.6 | 59.9 | 343.6 | 59.9 | 6.0 |
| JMF03a | 200.0 | Gh | 0 | 0.15966 | 156.9 | 18.6 | 344.6 | 58.8 | 344.6 | 58.8 | 6.5 |
| JMF03a | 300.0 | Gh | 0 | 0.13929 | 151.3 | 20.0 | 335.1 | 56.7 | 335.1 | 56.7 | 5.5 |
| JMF03a | 400.0 | Gh | 0 | 0.10925 | 151.0 | 27.1 | 325.0 | 61.7 | 325.0 | 61.7 | 6.0 |
| JMF03a | 500.0 | Gh | 0 | 0.07635 | 158.7 | 22.1 | 343.4 | 62.6 | 343.4 | 62.6 | 5.0 |
| JMF03a | 525.0 | Gh | 0 | 0.06176 | 156.1 | 16.0 | 346.0 | 56.2 | 346.0 | 56.2 | 6.0 |
| JMF03a | 550.0 | Gh | 0 | 0.06488 | 163.8 | 11.4 | 1.6 | 55.4 | 1.6 | 55.4 | 5.0 |
| JMF03a | 575.0 | Gh | 0 | 0.05052 | 145.2 | 13.7 | 334.2 | 48.2 | 334.2 | 48.2 | 4.5 |
| JMF03a | 600.0 | Gh | 0 | 0.04209 | 145.0 | -5.1 | 347.8 | 32.4 | 347.8 | 32.4 | 5.0 |
| JMF03a | 625.0 | Gh | 0 | 0.03751 | 145.4 | 0.2 | 344.9 | 37.2 | 344.9 | 37.2 | 5.0 |
| JMF03a | 650.0 | Gh | 0 | 0.04046 | 140.4 | 10.6 | 331.8 | 42.8 | 331.8 | 42.8 | 6.0 |
| JMF03a | 660.0 | Gh | 0 | 0.05462 | 140.9 | 24.0 | 318.3 | 52.7 | 318.3 | 52.7 | 7.5 |
| JMF03a | 670.0 | Gh | 0 | 0.04041 | 121.7 | 21.4 | 305.2 | 37.3 | 305.2 | 37.3 | 9.0 |
| JMF03a | 675.0 | Gh | 0 | 0.02535 | 167.3 | 53.5 | 244.6 | 76.6 | 244.6 | 76.6 | 11.0 |
| | | | | | | | | | | | |
| JMG01a | 0.0 | Gh | 0 | 0.29595 | 213.9 | 5.7 | 28.4 | 55.4 | 28.4 | 55.4 | 7.5 |
| JMG01a | 100.0 | Gh | 0 | 0.26899 | 216.1 | 5.4 | 29.1 | 53.3 | 29.1 | 53.3 | 6.5 |
| JMG01a | 200.0 | Gh | 0 | 0.24141 | 216.8 | 6.0 | 30.4 | 52.8 | 30.4 | 52.8 | 7.5 |
| JMG01a | 300.0 | Gh | 0 | 0.19917 | 215.2 | 4.9 | 27.8 | 54.0 | 27.8 | 54.0 | 8.0 |
| JMG01a | 400.0 | Gh | 0 | 0.16585 | 214.4 | 2.7 | 23.8 | 53.9 | 23.8 | 53.9 | 7.0 |
| JMG01a | 500.0 | Gh | 0 | 0.09485 | 229.1 | 2.8 | 31.2 | 40.1 | 31.2 | 40.1 | 7.0 |
| JMG01a | 525.0 | Gh | 0 | 0.08892 | 228.9 | 12.4 | 43.6 | 42.5 | 43.6 | 42.5 | 6.5 |
| JMG01a | 550.0 | Gh | 0 | 0.08857 | 236.0 | 9.9 | 42.0 | 35.2 | 42.0 | 35.2 | 7.0 |
| JMG01a | 575.0 | Gh | 0 | 0.08063 | 229.7 | 10.9 | 41.8 | 41.5 | 41.8 | 41.5 | 7.0 |
| JMG01a | 600.0 | Gh | 0 | 0.07752 | 233.9 | 11.6 | 43.6 | 37.6 | 43.6 | 37.6 | 6.0 |
| JMG01a | 625.0 | Gh | 0 | 0.06472 | 230.2 | 20.2 | 54.3 | 42.0 | 54.3 | 42.0 | 7.5 |
| JMG01a | 650.0 | Gh | 0 | 0.02169 | 286.1 | 28.8 | 72.5 | -6.3 | 72.5 | -6.3 | 18.0 |
| JMG01a | 660.0 | Gh | 0 | 0.02570 | 269.2 | 38.0 | 77.3 | 9.8 | 77.3 | 9.8 | 21.0 |

| | | | | | | | | | | | |
|---|---|---|---|---|---|---|---|---|---|---|---|
| JMG01a | 670.0 | Gh | 0 | 0.01130 | 352.9 | -14.2 | 46.1 | -83.1 | 46.1 | -83.1 | 32.0 |
| JMG01a | 675.0 | Gh | 0 | 0.01633 | 287.3 | 49.9 | 92.4 | 0.7 | 92.4 | 0.7 | 39.0 |
| | | | | | | | | | | | |
| JMG02a | 0.0 | Gh | 0 | 0.28834 | 217.3 | 1.8 | 20.9 | 50.3 | 20.9 | 50.3 | 8.0 |
| JMG02a | 100.0 | Gh | 0 | 0.23411 | 214.8 | 0.0 | 16.6 | 51.7 | 16.6 | 51.7 | 7.0 |
| JMG02a | 200.0 | Gh | 0 | 0.23208 | 212.7 | 0.2 | 15.2 | 53.7 | 15.2 | 53.7 | 8.0 |
| JMG02a | 300.0 | Gh | 0 | 0.21315 | 213.0 | -1.2 | 13.4 | 52.7 | 13.4 | 52.7 | 7.0 |
| JMG02a | 400.0 | Gh | 0 | 0.14477 | 218.1 | 7.5 | 29.8 | 51.7 | 29.8 | 51.7 | 8.0 |
| JMG02a | 500.0 | Gh | 0 | 0.08791 | 224.0 | 10.5 | 36.7 | 46.9 | 36.7 | 46.9 | 6.5 |
| JMG02a | 525.0 | Gh | 0 | 0.07346 | 227.2 | 14.6 | 43.3 | 44.6 | 43.3 | 44.6 | 6.5 |
| JMG02a | 550.0 | Gh | 0 | 0.05511 | 221.8 | 13.8 | 40.9 | 49.6 | 40.9 | 49.6 | 6.5 |
| JMG02a | 575.0 | Gh | 0 | 0.05699 | 235.5 | 14.9 | 45.6 | 36.8 | 45.6 | 36.8 | 6.0 |
| JMG02a | 600.0 | Gh | 0 | 0.04480 | 230.3 | 21.2 | 52.9 | 42.5 | 52.9 | 42.5 | 7.0 |
| JMG02a | 625.0 | Gh | 0 | 0.03430 | 237.1 | 28.3 | 62.4 | 36.6 | 62.4 | 36.6 | 9.0 |
| JMG02a | 650.0 | Gh | 0 | 0.03849 | 236.4 | 16.5 | 47.7 | 36.2 | 47.7 | 36.2 | 15.0 |
| JMG02a | 660.0 | Gh | 0 | 0.01717 | 250.0 | 27.5 | 62.3 | 25.2 | 62.3 | 25.2 | 24.0 |
| JMG02a | 670.0 | Gh | 0 | 0.02623 | 33.7 | 5.8 | 187.9 | -49.6 | 187.9 | -49.6 | 32.5 |
| JMG02a | 675.0 | Gh | 0 | 0.02174 | 4.4 | 37.4 | 133.7 | -35.4 | 133.7 | -35.4 | 40.5 |
| | | | | | | | | | | | |
| JMG03a | 0.0 | Gh | 0 | 0.29543 | 205.8 | -9.3 | 2.5 | 55.4 | 2.5 | 55.4 | 8.0 |
| JMG03a | 100.0 | Gh | 0 | 0.27217 | 201.3 | -10.1 | 355.8 | 57.9 | 355.8 | 57.9 | 8.0 |
| JMG03a | 200.0 | Gh | 0 | 0.24683 | 202.4 | -10.9 | 356.3 | 56.6 | 356.3 | 56.6 | 8.0 |
| JMG03a | 300.0 | Gh | 0 | 0.21878 | 199.5 | -12.3 | 350.6 | 57.4 | 350.6 | 57.4 | 8.5 |
| JMG03a | 400.0 | Gh | 0 | 0.16943 | 197.1 | -13.5 | 345.8 | 57.7 | 345.8 | 57.7 | 8.5 |
| JMG03a | 500.0 | Gh | 0 | 0.10746 | 196.9 | -28.9 | 334.2 | 44.1 | 334.2 | 44.1 | 7.0 |
| JMG03a | 525.0 | Gh | 0 | 0.09957 | 192.2 | -28.0 | 329.1 | 46.4 | 329.1 | 46.4 | 7.0 |
| JMG03a | 550.0 | Gh | 0 | 0.08537 | 185.8 | -24.0 | 321.9 | 51.6 | 321.9 | 51.6 | 6.0 |
| JMG03a | 575.0 | Gh | 0 | 0.07502 | 186.0 | -25.4 | 321.9 | 50.2 | 321.9 | 50.2 | 7.5 |
| JMG03a | 600.0 | Gh | 0 | 0.06554 | 190.1 | -30.1 | 325.8 | 44.8 | 325.8 | 44.8 | 6.5 |
| JMG03a | 625.0 | Gh | 0 | 0.04947 | 167.4 | -46.1 | 303.5 | 28.8 | 303.5 | 28.8 | 6.5 |
| JMG03a | 650.0 | Gh | 0 | 0.03439 | 72.5 | -84.3 | 307.8 | -15.6 | 307.8 | -15.6 | 11.0 |
| JMG03a | 660.0 | Gh | 0 | 0.03331 | 157.6 | -82.5 | 310.5 | -7.1 | 310.5 | -7.1 | 12.5 |
| JMG03a | 670.0 | Gh | 0 | 0.03579 | 27.1 | -59.9 | 296.1 | -40.0 | 296.1 | -40.0 | 18.0 |
| JMG03a | 675.0 | Gh | 0 | 0.01541 | 53.4 | -65.9 | 291.8 | -27.2 | 291.8 | -27.2 | 22.0 |
| | | | | | | | | | | | |
| JMH01a | 0.0 | Gh | 0 | 0.49859 | 108.6 | 48.7 | 309.7 | 37.7 | 309.7 | 37.7 | 7.0 |
| JMH01a | 100.0 | Gh | 0 | 0.48752 | 106.2 | 48.9 | 308.9 | 36.2 | 308.9 | 36.2 | 8.0 |
| JMH01a | 200.0 | Gh | 0 | 0.47592 | 104.4 | 49.0 | 308.4 | 35.1 | 308.4 | 35.1 | 6.5 |
| JMH01a | 300.0 | Gh | 0 | 0.46806 | 98.1 | 48.9 | 306.9 | 31.2 | 306.9 | 31.2 | 7.0 |
| JMH01a | 400.0 | Gh | 0 | 0.46309 | 95.8 | 48.1 | 307.1 | 29.5 | 307.1 | 29.5 | 6.0 |
| JMH01a | 500.0 | Gh | 0 | 0.42726 | 93.6 | 49.0 | 305.6 | 28.5 | 305.6 | 28.5 | 4.5 |
| JMH01a | 525.0 | Gh | 0 | 0.41928 | 93.9 | 49.2 | 305.4 | 28.7 | 305.4 | 28.7 | 6.0 |
| JMH01a | 550.0 | Gh | 0 | 0.40560 | 93.8 | 49.4 | 305.2 | 28.8 | 305.2 | 28.8 | 5.5 |
| JMH01a | 575.0 | Gh | 0 | 0.39576 | 95.4 | 50.5 | 304.5 | 30.1 | 304.5 | 30.1 | 5.5 |
| JMH01a | 600.0 | Gh | 0 | 0.38774 | 96.8 | 50.9 | 304.4 | 31.1 | 304.4 | 31.1 | 5.0 |
| JMH01a | 625.0 | Gh | 0 | 0.35309 | 92.9 | 50.4 | 303.9 | 28.6 | 303.9 | 28.6 | 5.5 |
| JMH01a | 650.0 | Gh | 0 | 0.30202 | 97.2 | 50.7 | 304.7 | 31.3 | 304.7 | 31.3 | 7.0 |
| JMH01a | 660.0 | Gh | 0 | 0.29957 | 96.2 | 49.5 | 305.8 | 30.2 | 305.8 | 30.2 | 8.5 |
| JMH01a | 670.0 | Gh | 0 | 0.26176 | 102.0 | 53.5 | 302.6 | 34.9 | 302.6 | 34.9 | 11.0 |
| JMH01a | 675.0 | Gh | 0 | 0.24628 | 103.9 | 53.1 | 303.4 | 35.9 | 303.4 | 35.9 | 12.5 |
| | | | | | | | | | | | |
| JMH02a | 0.0 | Gh | 0 | 0.29036 | 142.6 | 22.9 | 354.4 | 55.9 | 354.4 | 55.9 | 6.0 |
| JMH02a | 100.0 | Gh | 0 | 0.27351 | 135.7 | 19.6 | 355.5 | 48.7 | 355.5 | 48.7 | 5.5 |

| | | | | | | | | | | | |
|---|---|---|---|---|---|---|---|---|---|---|---|
| JMH02a | 200.0 | Gh | 0 | 0.27519 | 135.3 | 19.2 | 355.8 | 48.2 | 355.8 | 48.2 | 7.0 |
| JMH02a | 300.0 | Gh | 0 | 0.26821 | 137.0 | 19.6 | 356.2 | 49.9 | 356.2 | 49.9 | 7.0 |
| JMH02a | 400.0 | Gh | 0 | 0.25501 | 133.1 | 23.0 | 349.4 | 47.7 | 349.4 | 47.7 | 5.5 |
| JMH02a | 500.0 | Gh | 0 | 0.24331 | 133.4 | 20.4 | 353.1 | 47.1 | 353.1 | 47.1 | 5.0 |
| JMH02a | 525.0 | Gh | 0 | 0.23385 | 131.6 | 20.1 | 352.6 | 45.4 | 352.6 | 45.4 | 4.0 |
| JMH02a | 550.0 | Gh | 0 | 0.22787 | 128.7 | 19.6 | 351.7 | 42.7 | 351.7 | 42.7 | 5.0 |
| JMH02a | 575.0 | Gh | 0 | 0.22991 | 126.7 | 17.7 | 353.0 | 40.2 | 353.0 | 40.2 | 6.0 |
| JMH02a | 600.0 | Gh | 0 | 0.20812 | 126.0 | 16.1 | 354.5 | 38.9 | 354.5 | 38.9 | 7.0 |
| JMH02a | 625.0 | Gh | 0 | 0.18407 | 127.0 | 21.3 | 348.8 | 41.9 | 348.8 | 41.9 | 8.0 |
| JMH02a | 650.0 | Gh | 0 | 0.15770 | 122.0 | 24.8 | 342.3 | 38.8 | 342.3 | 38.8 | 15.0 |
| JMH02a | 660.0 | Gh | 0 | 0.14311 | 127.3 | 27.7 | 340.6 | 44.2 | 340.6 | 44.2 | 20.0 |
| JMH02a | 670.0 | Gh | 0 | 0.11593 | 116.1 | 24.9 | 339.9 | 33.8 | 339.9 | 33.8 | 22.5 |
| JMH02a | 675.0 | Gh | 0 | 0.10972 | 106.3 | 33.3 | 327.3 | 28.5 | 327.3 | 28.5 | 25.0 |
| | | | | | | | | | | | |
| JMH03a | 0.0 | Gh | 0 | 0.11107 | 165.5 | 35.8 | 44.0 | 68.4 | 44.0 | 68.4 | 7.0 |
| JMH03a | 100.0 | Gh | 0 | 0.09960 | 161.5 | 32.8 | 39.5 | 64.3 | 39.5 | 64.3 | 7.5 |
| JMH03a | 200.0 | Gh | 0 | 0.08497 | 160.2 | 31.5 | 38.5 | 62.6 | 38.5 | 62.6 | 7.0 |
| JMH03a | 300.0 | Gh | 0 | 0.07424 | 158.6 | 28.2 | 38.7 | 59.1 | 38.7 | 59.1 | 7.0 |
| JMH03a | 400.0 | Gh | 0 | 0.05901 | 166.0 | 30.7 | 49.4 | 63.7 | 49.4 | 63.7 | 7.5 |
| JMH03a | 500.0 | Gh | 0 | 0.04402 | 163.9 | 24.5 | 49.6 | 57.3 | 49.6 | 57.3 | 6.0 |
| JMH03a | 525.0 | Gh | 0 | 0.03391 | 172.0 | 23.7 | 63.4 | 58.1 | 63.4 | 58.1 | 6.0 |
| JMH03a | 550.0 | Gh | 0 | 0.03564 | 161.3 | 36.4 | 35.2 | 67.4 | 35.2 | 67.4 | 6.5 |
| JMH03a | 575.0 | Gh | 0 | 0.04292 | 164.4 | 34.1 | 43.5 | 66.4 | 43.5 | 66.4 | 6.0 |
| JMH03a | 600.0 | Gh | 0 | 0.03742 | 184.6 | 39.3 | 90.4 | 74.0 | 90.4 | 74.0 | 6.5 |
| JMH03a | 625.0 | Gh | 0 | 0.04278 | 177.0 | 35.6 | 70.1 | 70.5 | 70.1 | 70.5 | 7.5 |
| JMH03a | 650.0 | Gh | 0 | 0.04400 | 172.5 | 23.0 | 64.5 | 57.5 | 64.5 | 57.5 | 10.0 |
| JMH03a | 660.0 | Gh | 0 | 0.04092 | 175.1 | 33.4 | 66.4 | 68.1 | 66.4 | 68.1 | 12.5 |
| JMH03a | 670.0 | Gh | 0 | 0.02781 | 172.6 | 34.3 | 60.4 | 68.7 | 60.4 | 68.7 | 18.0 |
| JMH03a | 675.0 | Gh | 0 | 0.02993 | 182.0 | 12.1 | 80.3 | 47.1 | 80.3 | 47.1 | 23.5 |
| | | | | | | | | | | | |
| JMI01a | 0.0 | Gh | 0 | 0.07986 | 148.6 | 5.3 | 304.4 | 54.0 | 304.4 | 54.0 | 2.5 |
| JMI01a | 100.0 | Gh | 0 | 0.08057 | 146.4 | 5.3 | 302.2 | 52.3 | 302.2 | 52.3 | 2.0 |
| JMI01a | 200.0 | Gh | 0 | 0.07575 | 142.9 | 6.6 | 297.5 | 50.1 | 297.5 | 50.1 | 2.5 |
| JMI01a | 300.0 | Gh | 0 | 0.07049 | 139.3 | 7.5 | 293.5 | 47.4 | 293.5 | 47.4 | 2.5 |
| JMI01a | 400.0 | Gh | 0 | 0.06178 | 141.2 | 7.8 | 294.5 | 49.2 | 294.5 | 49.2 | 2.0 |
| JMI01a | 500.0 | Gh | 0 | 0.06731 | 138.4 | 0.2 | 301.6 | 42.8 | 301.6 | 42.8 | 1.0 |
| JMI01a | 525.0 | Gh | 0 | 0.06381 | 133.6 | 3.3 | 294.7 | 40.4 | 294.7 | 40.4 | 2.0 |
| JMI01a | 550.0 | Gh | 0 | 0.05676 | 140.1 | -8.2 | 311.7 | 38.9 | 311.7 | 38.9 | 2.5 |
| JMI01a | 575.0 | Gh | 0 | 0.05875 | 146.1 | -5.3 | 314.3 | 45.2 | 314.3 | 45.2 | 2.5 |
| JMI01a | 600.0 | Gh | 0 | 0.06420 | 145.2 | -0.2 | 307.9 | 48.0 | 307.9 | 48.0 | 3.0 |
| JMI01a | 625.0 | Gh | 0 | 0.04179 | 158.2 | 1.3 | 321.4 | 58.3 | 321.4 | 58.3 | 2.0 |
| JMI01a | 650.0 | Gh | 0 | 0.03312 | 147.5 | -8.9 | 319.2 | 43.6 | 319.2 | 43.6 | 3.0 |
| JMI01a | 660.0 | Gh | 0 | 0.04025 | 140.7 | 2.4 | 300.9 | 45.9 | 300.9 | 45.9 | 3.5 |
| JMI01a | 670.0 | Gh | 0 | 0.03626 | 141.1 | 6.5 | 296.2 | 48.5 | 296.2 | 48.5 | 5.5 |
| JMI01a | 675.0 | Gh | 0 | 0.03447 | 150.5 | 21.8 | 277.0 | 62.8 | 277.0 | 62.8 | 6.0 |
| | | | | | | | | | | | |
| JMI02a | 0.0 | Gh | 0 | 0.06982 | 116.4 | -24.1 | 310.1 | 10.7 | 310.1 | 10.7 | 2.5 |
| JMI02a | 100.0 | Gh | 0 | 0.08549 | 103.3 | -22.7 | 302.5 | 1.2 | 302.5 | 1.2 | 1.5 |
| JMI02a | 200.0 | Gh | 0 | 0.08541 | 102.9 | -22.1 | 301.8 | 1.2 | 301.8 | 1.2 | 1.5 |
| JMI02a | 300.0 | Gh | 0 | 0.10095 | 95.7 | -25.2 | 301.5 | -6.1 | 301.5 | -6.1 | 2.5 |
| JMI02a | 400.0 | Gh | 0 | 0.11886 | 102.4 | -24.8 | 303.9 | -0.5 | 303.9 | -0.5 | 1.0 |
| JMI02a | 500.0 | Gh | 0 | 0.11322 | 104.5 | -27.5 | 307.2 | -0.2 | 307.2 | -0.2 | 2.0 |
| JMI02a | 525.0 | Gh | 0 | 0.08453 | 115.9 | -31.7 | 316.1 | 6.0 | 316.1 | 6.0 | 1.5 |

| | | | | | | | | | | | |
|---|---|---|---|---|---|---|---|---|---|---|---|
| JMI02a | 550.0 | Gh | 0 | 0.08565 | 119.9 | -22.9 | 311.0 | 14.0 | 311.0 | 14.0 | 2.0 |
| JMI02a | 575.0 | Gh | 0 | 0.08981 | 117.8 | -25.8 | 312.2 | 10.8 | 312.2 | 10.8 | 3.0 |
| JMI02a | 600.0 | Gh | 0 | 0.08771 | 116.6 | -25.6 | 311.4 | 10.0 | 311.4 | 10.0 | 3.0 |
| JMI02a | 625.0 | Gh | 0 | 0.05945 | 110.5 | -28.0 | 310.4 | 4.1 | 310.4 | 4.1 | 4.5 |
| JMI02a | 650.0 | Gh | 0 | 0.06621 | 107.7 | -17.7 | 300.2 | 7.3 | 300.2 | 7.3 | 5.0 |
| JMI02a | 660.0 | Gh | 0 | 0.05731 | 111.6 | -14.8 | 299.6 | 12.0 | 299.6 | 12.0 | 9.0 |
| JMI02a | 670.0 | Gh | 0 | 0.05783 | 116.8 | -24.5 | 310.6 | 10.8 | 310.6 | 10.8 | 10.0 |
| JMI02a | 675.0 | Gh | 0 | 0.05934 | 111.1 | -23.6 | 306.9 | 6.9 | 306.9 | 6.9 | 9.0 |
| | | | | | | | | | | | |
| JMI03a | 0.0 | Gh | 0 | 0.08592 | 176.0 | 38.1 | 201.0 | 76.5 | 201.0 | 76.5 | 3.0 |
| JMI03a | 100.0 | Gh | 0 | 0.08157 | 171.1 | 40.8 | 210.4 | 72.5 | 210.4 | 72.5 | 1.5 |
| JMI03a | 200.0 | Gh | 0 | 0.07886 | 169.6 | 46.2 | 206.2 | 67.2 | 206.2 | 67.2 | 1.5 |
| JMI03a | 300.0 | Gh | 0 | 0.07082 | 172.9 | 43.4 | 203.2 | 70.7 | 203.2 | 70.7 | 2.0 |
| JMI03a | 400.0 | Gh | 0 | 0.07900 | 164.2 | 50.7 | 208.6 | 61.6 | 208.6 | 61.6 | 1.5 |
| JMI03a | 500.0 | Gh | 0 | 0.05192 | 170.4 | 44.1 | 207.3 | 69.4 | 207.3 | 69.4 | 1.0 |
| JMI03a | 525.0 | Gh | 0 | 0.04814 | 181.0 | 35.5 | 182.9 | 79.5 | 182.9 | 79.5 | 1.0 |
| JMI03a | 550.0 | Gh | 0 | 0.04543 | 171.8 | 45.5 | 203.2 | 68.5 | 203.2 | 68.5 | 1.0 |
| JMI03a | 575.0 | Gh | 0 | 0.03088 | 163.9 | 46.8 | 213.8 | 64.7 | 213.8 | 64.7 | 2.0 |
| JMI03a | 600.0 | Gh | 0 | 0.03992 | 116.8 | 43.7 | 240.3 | 36.0 | 240.3 | 36.0 | 1.0 |
| JMI03a | 625.0 | Gh | 0 | 0.02600 | 139.5 | 22.8 | 272.2 | 53.0 | 272.2 | 53.0 | 2.5 |
| JMI03a | 650.0 | Gh | 0 | 0.02513 | 109.4 | 16.9 | 269.3 | 24.3 | 269.3 | 24.3 | 2.5 |
| JMI03a | 660.0 | Gh | 0 | 0.01144 | 126.0 | 27.5 | 262.0 | 41.9 | 262.0 | 41.9 | 2.5 |
| JMI03a | 670.0 | Gh | 0 | 0.00587 | 53.5 | -5.4 | 265.8 | -35.2 | 265.8 | -35.2 | 5.0 |
| JMI03a | 675.0 | Gh | 0 | 0.01109 | 51.7 | -40.4 | 310.4 | -44.6 | 310.4 | -44.6 | 6.5 |
| | | | | | | | | | | | |
| JMI04a | 0.0 | Gh | 0 | 0.02490 | 74.7 | 54.3 | 225.9 | 6.8 | 225.9 | 6.8 | 1.0 |
| JMI04a | 100.0 | Gh | 0 | 0.02242 | 74.0 | 36.7 | 241.8 | -0.8 | 241.8 | -0.8 | 0.5 |
| JMI04a | 200.0 | Gh | 0 | 0.02346 | 75.3 | 35.8 | 243.1 | -0.2 | 243.1 | -0.2 | 1.0 |
| JMI04a | 300.0 | Gh | 0 | 0.01936 | 72.8 | 31.8 | 245.9 | -3.8 | 245.9 | -3.8 | 1.5 |
| JMI04a | 400.0 | Gh | 0 | 0.01584 | 55.9 | 48.0 | 225.3 | -6.5 | 225.3 | -6.5 | 1.0 |
| JMI04a | 500.0 | Gh | 0 | 0.01932 | 20.0 | 55.4 | 202.9 | -13.7 | 202.9 | -13.7 | 1.0 |
| JMI04a | 525.0 | Gh | 0 | 0.01516 | 79.4 | 21.4 | 257.8 | -2.5 | 257.8 | -2.5 | 1.0 |
| JMI04a | 550.0 | Gh | 0 | 0.01121 | 54.3 | 15.3 | 252.5 | -26.5 | 252.5 | -26.5 | 1.0 |
| JMI04a | 575.0 | Gh | 0 | 0.01926 | 35.7 | 30.1 | 227.1 | -30.1 | 227.1 | -30.1 | 1.5 |
| JMI04a | 600.0 | Gh | 0 | 0.01640 | 20.8 | 29.6 | 214.3 | -37.4 | 214.3 | -37.4 | 3.0 |
| JMI04a | 625.0 | Gh | 0 | 0.01252 | 44.9 | 7.8 | 254.4 | -38.3 | 254.4 | -38.3 | 3.0 |
| JMI04a | 650.0 | Gh | 0 | 0.01027 | 28.3 | 21.9 | 226.8 | -40.6 | 226.8 | -40.6 | 3.5 |
| JMI04a | 660.0 | Gh | 0 | 0.01119 | 134.9 | 11.3 | 284.7 | 45.9 | 284.7 | 45.9 | 6.0 |
| JMI04a | 670.0 | Gh | 0 | 0.01595 | 103.8 | -4.4 | 290.2 | 11.5 | 290.2 | 11.5 | 5.0 |
| JMI04a | 675.0 | Gh | 0 | 0.00894 | 63.4 | 33.5 | 240.6 | -10.0 | 240.6 | -10.0 | 4.5 |
| | | | | | | | | | | | |
| JMI05a | 0.0 | Gh | 0 | 0.15060 | 171.6 | 8.3 | 324.1 | 78.1 | 324.1 | 78.1 | 1.0 |
| JMI05a | 100.0 | Gh | 0 | 0.14636 | 170.0 | 7.9 | 320.2 | 76.7 | 320.2 | 76.7 | 1.5 |
| JMI05a | 200.0 | Gh | 0 | 0.14203 | 167.2 | 6.4 | 317.2 | 73.6 | 317.2 | 73.6 | 2.5 |
| JMI05a | 300.0 | Gh | 0 | 0.14082 | 160.7 | 9.1 | 298.8 | 69.6 | 298.8 | 69.6 | 2.0 |
| JMI05a | 400.0 | Gh | 0 | 0.15017 | 164.1 | 12.1 | 293.9 | 73.9 | 293.9 | 73.9 | 1.0 |
| JMI05a | 500.0 | Gh | 0 | 0.13426 | 157.3 | 9.8 | 293.6 | 66.8 | 293.6 | 66.8 | 1.5 |
| JMI05a | 525.0 | Gh | 0 | 0.11631 | 155.3 | 3.2 | 305.3 | 62.1 | 305.3 | 62.1 | 2.0 |
| JMI05a | 550.0 | Gh | 0 | 0.09945 | 150.3 | -0.1 | 305.7 | 56.1 | 305.7 | 56.1 | 1.5 |
| JMI05a | 575.0 | Gh | 0 | 0.10640 | 144.7 | 1.2 | 299.1 | 51.9 | 299.1 | 51.9 | 1.5 |
| JMI05a | 600.0 | Gh | 0 | 0.09800 | 154.4 | 4.6 | 301.8 | 62.0 | 301.8 | 62.0 | 1.0 |
| JMI05a | 625.0 | Gh | 0 | 0.10735 | 149.6 | 12.7 | 282.5 | 60.3 | 282.5 | 60.3 | 2.0 |
| JMI05a | 650.0 | Gh | 0 | 0.10365 | 147.8 | 21.0 | 265.7 | 59.3 | 265.7 | 59.3 | 3.0 |

| | | | | | | | | | | | |
|---|---|---|---|---|---|---|---|---|---|---|---|
| JMI05a | 660.0 | Gh | 0 | 0.09792 | 149.2 | 29.7 | 248.5 | 59.1 | 248.5 | 59.1 | 4.0 |
| JMI05a | 670.0 | Gh | 0 | 0.10106 | 151.6 | 24.5 | 257.8 | 62.5 | 257.8 | 62.5 | 5.0 |
| JMI05a | 675.0 | Gh | 0 | 0.09748 | 147.1 | 12.9 | 281.2 | 58.0 | 281.2 | 58.0 | 7.0 |
| | | | | | | | | | | | |
| JMJ01a | 0.0 | Gh | 0 | 0.34306 | 194.4 | 5.6 | 7.6 | 70.6 | 7.6 | 70.6 | 2.5 |
| JMJ01a | 100.0 | Gh | 0 | 0.33423 | 191.6 | 4.9 | 359.6 | 71.9 | 359.6 | 71.9 | 3.0 |
| JMJ01a | 200.0 | Gh | 0 | 0.32330 | 191.8 | 3.7 | 357.9 | 70.8 | 357.9 | 70.8 | 2.5 |
| JMJ01a | 300.0 | Gh | 0 | 0.33512 | 186.8 | 2.1 | 341.7 | 71.8 | 341.7 | 71.8 | 3.0 |
| JMJ01a | 400.0 | Gh | 0 | 0.31839 | 187.0 | -1.0 | 339.1 | 68.9 | 339.1 | 68.9 | 3.0 |
| JMJ01a | 500.0 | Gh | 0 | 0.26811 | 188.3 | -0.8 | 342.7 | 68.6 | 342.7 | 68.6 | 3.0 |
| JMJ01a | 525.0 | Gh | 0 | 0.22153 | 187.5 | -2.0 | 339.5 | 67.7 | 339.5 | 67.7 | 2.5 |
| JMJ01a | 550.0 | Gh | 0 | 0.19083 | 187.8 | -3.3 | 339.2 | 66.4 | 339.2 | 66.4 | 2.0 |
| JMJ01a | 575.0 | Gh | 0 | 0.17485 | 187.5 | -2.3 | 339.3 | 67.5 | 339.3 | 67.5 | 2.0 |
| JMJ01a | 600.0 | Gh | 0 | 0.16099 | 190.5 | -4.1 | 344.6 | 64.7 | 344.6 | 64.7 | 3.0 |
| JMJ01a | 625.0 | Gh | 0 | 0.15330 | 187.2 | -3.9 | 337.3 | 66.0 | 337.3 | 66.0 | 3.5 |
| JMJ01a | 650.0 | Gh | 0 | 0.12689 | 182.4 | -8.0 | 324.6 | 62.9 | 324.6 | 62.9 | 3.5 |
| JMJ01a | 660.0 | Gh | 0 | 0.11904 | 181.9 | -9.4 | 323.3 | 61.5 | 323.3 | 61.5 | 6.0 |
| JMJ01a | 670.0 | Gh | 0 | 0.09161 | 171.4 | -10.3 | 302.6 | 59.5 | 302.6 | 59.5 | 7.5 |
| JMJ01a | 675.0 | Gh | 0 | 0.07593 | 160.6 | -12.4 | 286.6 | 53.2 | 286.6 | 53.2 | 8.5 |
| | | | | | | | | | | | |
| JMJ02a | 0.0 | Gh | 0 | 0.19039 | 190.6 | -7.1 | 341.9 | 62.8 | 341.9 | 62.8 | 2.0 |
| JMJ02a | 100.0 | Gh | 0 | 0.17277 | 186.4 | -6.1 | 333.7 | 65.1 | 333.7 | 65.1 | 3.5 |
| JMJ02a | 200.0 | Gh | 0 | 0.17087 | 185.7 | -8.0 | 331.1 | 63.4 | 331.1 | 63.4 | 2.0 |
| JMJ02a | 300.0 | Gh | 0 | 0.16321 | 183.6 | -11.3 | 325.6 | 60.5 | 325.6 | 60.5 | 2.5 |
| JMJ02a | 400.0 | Gh | 0 | 0.15259 | 176.1 | -19.8 | 312.4 | 52.0 | 312.4 | 52.0 | 2.5 |
| JMJ02a | 500.0 | Gh | 0 | 0.09820 | 173.1 | -19.4 | 307.8 | 52.0 | 307.8 | 52.0 | 2.0 |
| JMJ02a | 525.0 | Gh | 0 | 0.09322 | 176.5 | -17.6 | 312.7 | 54.2 | 312.7 | 54.2 | 3.0 |
| JMJ02a | 550.0 | Gh | 0 | 0.10389 | 176.2 | -22.9 | 313.1 | 48.9 | 313.1 | 48.9 | 2.5 |
| JMJ02a | 575.0 | Gh | 0 | 0.09509 | 177.5 | -27.1 | 315.3 | 44.8 | 315.3 | 44.8 | 2.0 |
| JMJ02a | 600.0 | Gh | 0 | 0.10730 | 180.0 | -34.4 | 318.4 | 37.6 | 318.4 | 37.6 | 4.0 |
| JMJ02a | 625.0 | Gh | 0 | 0.11314 | 174.7 | -42.5 | 313.9 | 29.3 | 313.9 | 29.3 | 4.0 |
| JMJ02a | 650.0 | Gh | 0 | 0.09668 | 179.8 | -38.3 | 318.2 | 33.7 | 318.2 | 33.7 | 5.5 |
| JMJ02a | 660.0 | Gh | 0 | 0.09317 | 178.7 | -38.5 | 317.2 | 33.5 | 317.2 | 33.5 | 7.0 |
| JMJ02a | 670.0 | Gh | 0 | 0.08010 | 170.7 | -56.4 | 313.1 | 15.2 | 313.1 | 15.2 | 9.0 |
| JMJ02a | 675.0 | Gh | 0 | 0.07781 | 204.4 | -60.3 | 330.4 | 9.2 | 330.4 | 9.2 | 7.0 |
| | | | | | | | | | | | |
| JMJ03a | 0.0 | Gh | 0 | 0.20156 | 205.8 | 3.9 | 23.9 | 61.5 | 23.9 | 61.5 | 2.0 |
| JMJ03a | 100.0 | Gh | 0 | 0.19579 | 205.0 | 3.8 | 22.9 | 62.2 | 22.9 | 62.2 | 4.0 |
| JMJ03a | 200.0 | Gh | 0 | 0.19133 | 205.2 | 3.2 | 22.0 | 61.7 | 22.0 | 61.7 | 3.0 |
| JMJ03a | 300.0 | Gh | 0 | 0.21093 | 212.3 | 4.6 | 30.7 | 56.0 | 30.7 | 56.0 | 3.5 |
| JMJ03a | 400.0 | Gh | 0 | 0.19743 | 215.1 | 7.4 | 37.1 | 54.4 | 37.1 | 54.4 | 3.0 |
| JMJ03a | 500.0 | Gh | 0 | 0.14823 | 211.8 | 6.7 | 33.9 | 57.3 | 33.9 | 57.3 | 2.0 |
| JMJ03a | 525.0 | Gh | 0 | 0.12518 | 199.3 | 2.0 | 12.1 | 65.8 | 12.1 | 65.8 | -47.5 |
| JMJ03a | 550.0 | Gh | 0 | 0.09664 | 190.8 | -12.2 | 339.2 | 58.9 | 339.2 | 58.9 | 3.0 |
| JMJ03a | 575.0 | Gh | 0 | 0.10269 | 180.3 | -14.6 | 319.0 | 58.4 | 319.0 | 58.4 | 3.0 |
| JMJ03a | 600.0 | Gh | 0 | 0.10807 | 190.5 | -8.0 | 341.8 | 62.9 | 341.8 | 62.9 | 3.0 |
| JMJ03a | 625.0 | Gh | 0 | 0.08801 | 203.4 | -0.7 | 13.2 | 60.9 | 13.2 | 60.9 | 3.0 |
| JMJ03a | 650.0 | Gh | 0 | 0.08287 | 228.3 | -1.7 | 31.8 | 38.8 | 31.8 | 38.8 | 4.5 |
| JMJ03a | 660.0 | Gh | 0 | 0.08151 | 229.4 | -11.7 | 21.3 | 33.4 | 21.3 | 33.4 | 6.0 |
| JMJ03a | 670.0 | Gh | 0 | 0.07078 | 226.5 | -6.9 | 24.8 | 38.2 | 24.8 | 38.2 | 8.0 |
| JMJ03a | 675.0 | Gh | 0 | 0.07181 | 232.9 | 6.8 | 43.9 | 37.4 | 43.9 | 37.4 | 10.0 |
| | | | | | | | | | | | |
| JMJ04a | 0.0 | Gh | 0 | 0.12458 | 169.0 | 25.4 | 178.9 | 74.6 | 178.9 | 74.6 | 2.0 |

| | | | | | | | | | | | |
|---|---|---|---|---|---|---|---|---|---|---|---|
| JMJ04a | 100.0 | Gh | 0 | 0.12255 | 162.9 | 28.7 | 182.8 | 68.4 | 182.8 | 68.4 | 3.0 |
| JMJ04a | 200.0 | Gh | 0 | 0.12336 | 160.3 | 29.3 | 185.2 | 66.2 | 185.2 | 66.2 | 3.0 |
| JMJ04a | 300.0 | Gh | 0 | 0.13202 | 159.2 | 33.3 | 179.2 | 63.0 | 179.2 | 63.0 | 2.0 |
| JMJ04a | 400.0 | Gh | 0 | 0.12523 | 143.8 | 47.0 | 173.3 | 45.3 | 173.3 | 45.3 | 3.0 |
| JMJ04a | 500.0 | Gh | 0 | 0.10721 | 132.4 | 46.7 | 178.8 | 38.7 | 178.8 | 38.7 | 2.5 |
| JMJ04a | 525.0 | Gh | 0 | 0.08921 | 130.1 | 38.4 | 189.7 | 39.8 | 189.7 | 39.8 | 2.0 |
| JMJ04a | 550.0 | Gh | 0 | 0.08250 | 137.4 | 43.2 | 181.1 | 43.3 | 181.1 | 43.3 | 3.0 |
| JMJ04a | 575.0 | Gh | 0 | 0.08896 | 134.2 | 41.0 | 185.1 | 42.0 | 185.1 | 42.0 | 3.0 |
| JMJ04a | 600.0 | Gh | 0 | 0.07278 | 142.9 | 53.0 | 167.3 | 41.2 | 167.3 | 41.2 | 3.0 |
| JMJ04a | 625.0 | Gh | 0 | 0.07182 | 156.6 | 49.0 | 162.3 | 50.1 | 162.3 | 50.1 | 4.0 |
| JMJ04a | 650.0 | Gh | 0 | 0.05829 | 187.8 | 41.1 | 125.8 | 62.1 | 125.8 | 62.1 | 5.0 |
| JMJ04a | 660.0 | Gh | 0 | 0.04871 | 165.3 | 23.0 | 193.4 | 73.4 | 193.4 | 73.4 | 8.5 |
| JMJ04a | 670.0 | Gh | 0 | 0.03923 | 140.4 | 37.1 | 187.7 | 47.9 | 187.7 | 47.9 | 11.0 |
| JMJ04a | 675.0 | Gh | 0 | 0.01210 | 141.1 | 14.3 | 223.0 | 52.3 | 223.0 | 52.3 | 10.0 |
| | | | | | | | | | | | |
| JMJ05 | 0.0 | Gh | 0 | 0.13832 | 162.9 | 27.1 | 185.4 | 68.7 | 185.4 | 68.7 | 2.0 |
| JMJ05 | 100.0 | Gh | 0 | 0.13369 | 156.5 | 27.9 | 191.6 | 63.5 | 191.6 | 63.5 | 2.5 |
| JMJ05 | 200.0 | Gh | 0 | 0.13742 | 149.7 | 29.4 | 194.3 | 57.5 | 194.3 | 57.5 | 2.5 |
| JMJ05 | 300.0 | Gh | 0 | 0.15920 | 146.2 | 34.2 | 188.9 | 52.8 | 188.9 | 52.8 | 2.5 |
| JMJ05 | 400.0 | Gh | 0 | 0.17428 | 138.6 | 35.5 | 190.9 | 46.5 | 190.9 | 46.5 | 2.0 |
| JMJ05 | 500.0 | Gh | 0 | 0.15749 | 129.9 | 36.4 | 192.6 | 39.5 | 192.6 | 39.5 | 3.0 |
| JMJ05 | 525.0 | Gh | 0 | 0.12558 | 125.5 | 27.9 | 204.1 | 37.3 | 204.1 | 37.3 | 3.0 |
| JMJ05 | 550.0 | Gh | 0 | 0.09270 | 127.3 | 18.0 | 216.6 | 39.1 | 216.6 | 39.1 | 2.5 |
| JMJ05 | 575.0 | Gh | 0 | 0.08499 | 116.0 | 22.1 | 211.1 | 28.7 | 211.1 | 28.7 | 2.5 |
| JMJ05 | 600.0 | Gh | 0 | 0.08698 | 118.3 | 20.5 | 213.1 | 30.8 | 213.1 | 30.8 | 2.5 |
| JMJ05 | 625.0 | Gh | 0 | 0.06672 | 111.0 | 29.4 | 202.8 | 24.5 | 202.8 | 24.5 | 3.0 |
| JMJ05 | 650.0 | Gh | 0 | 0.05154 | 129.3 | 35.5 | 193.9 | 39.3 | 193.9 | 39.3 | 4.5 |
| JMJ05 | 660.0 | Gh | 0 | 0.04604 | 123.3 | 41.3 | 188.2 | 33.4 | 188.2 | 33.4 | 7.0 |
| JMJ05 | 670.0 | Gh | 0 | 0.05958 | 124.6 | 43.4 | 185.4 | 33.8 | 185.4 | 33.8 | 8.0 |
| JMJ05 | 675.0 | Gh | 0 | 0.03456 | 133.3 | 27.6 | 203.4 | 44.1 | 203.4 | 44.1 | 1.5 |
| | | | | | | | | | | | |
| JML02a | 0.0 | Gh | 0 | 0.21800 | 208.2 | 12.2 | 89.7 | 58.9 | 89.7 | 58.9 | 4.5 |
| JML02a | 100.0 | Gh | 0 | 0.20626 | 212.8 | 8.2 | 88.9 | 52.8 | 88.9 | 52.8 | 6.0 |
| JML02a | 200.0 | Gh | 0 | 0.20719 | 214.1 | 8.4 | 90.5 | 51.9 | 90.5 | 51.9 | 4.0 |
| JML02a | 300.0 | Gh | 0 | 0.20956 | 215.3 | 6.2 | 88.9 | 49.6 | 88.9 | 49.6 | 4.5 |
| JML02a | 400.0 | Gh | 0 | 0.20583 | 220.9 | 6.6 | 94.3 | 45.4 | 94.3 | 45.4 | 4.5 |
| JML02a | 500.0 | Gh | 0 | 0.15627 | 225.5 | 9.4 | 101.1 | 43.2 | 101.1 | 43.2 | 3.0 |
| JML02a | 525.0 | Gh | 0 | 0.13283 | 224.8 | 10.8 | 102.3 | 44.5 | 102.3 | 44.5 | 3.5 |
| JML02a | 550.0 | Gh | 0 | 0.11640 | 230.9 | 9.2 | 104.5 | 38.5 | 104.5 | 38.5 | 4.0 |
| JML02a | 575.0 | Gh | 0 | 0.11942 | 231.2 | 12.0 | 107.8 | 39.6 | 107.8 | 39.6 | 4.5 |
| JML02a | 600.0 | Gh | 0 | 0.10109 | 230.4 | 6.0 | 100.7 | 37.2 | 100.7 | 37.2 | 5.0 |
| JML02a | 625.0 | Gh | 0 | 0.09573 | 236.6 | 4.4 | 103.0 | 31.1 | 103.0 | 31.1 | 5.5 |
| JML02a | 650.0 | Gh | 0 | 0.07742 | 238.8 | 5.9 | 105.8 | 30.0 | 105.8 | 30.0 | 11.0 |
| JML02a | 660.0 | Gh | 0 | 0.07056 | 239.9 | 14.8 | 115.6 | 33.2 | 115.6 | 33.2 | 15.0 |
| JML02a | 670.0 | Gh | 0 | 0.05198 | 254.5 | 12.6 | 120.3 | 19.5 | 120.3 | 19.5 | 17.5 |
| JML02a | 675.0 | Gh | 0 | 0.03703 | 240.1 | 8.0 | 108.6 | 29.9 | 108.6 | 29.9 | 13.5 |
| | | | | | | | | | | | |
| JML03a | 0.0 | Gh | 0 | 0.15687 | 186.6 | 3.0 | 33.7 | 57.4 | 33.7 | 57.4 | 4.0 |
| JML03a | 100.0 | Gh | 0 | 0.14901 | 186.7 | 1.0 | 33.3 | 55.4 | 33.3 | 55.4 | 4.5 |
| JML03a | 200.0 | Gh | 0 | 0.13784 | 183.0 | -7.6 | 25.8 | 47.3 | 25.8 | 47.3 | 4.0 |
| JML03a | 300.0 | Gh | 0 | 0.12819 | 185.1 | -14.6 | 27.9 | 40.2 | 27.9 | 40.2 | 4.0 |
| JML03a | 400.0 | Gh | 0 | 0.11401 | 194.6 | -29.2 | 35.4 | 24.3 | 35.4 | 24.3 | 5.0 |
| JML03a | 500.0 | Gh | 0 | 0.06527 | 216.3 | -40.1 | 48.6 | 7.8 | 48.6 | 7.8 | 2.5 |

| | | | | | | | | | | | |
|---|---|---|---|---|---|---|---|---|---|---|---|
| JML03a | 525.0 | Gh | 0 | 0.04972 | 218.5 | -24.8 | 58.4 | 20.0 | 58.4 | 20.0 | 3.0 |
| JML03a | 550.0 | Gh | 0 | 0.05357 | 220.3 | -35.7 | 53.6 | 9.9 | 53.6 | 9.9 | 4.0 |
| JML03a | 575.0 | Gh | 0 | 0.05792 | 217.9 | -42.4 | 48.5 | 5.2 | 48.5 | 5.2 | 3.0 |
| JML03a | 600.0 | Gh | 0 | 0.05278 | 218.2 | -37.5 | 51.2 | 9.3 | 51.2 | 9.3 | 4.5 |
| JML03a | 625.0 | Gh | 0 | 0.04944 | 239.3 | -57.5 | 50.0 | -15.0 | 50.0 | -15.0 | 5.0 |
| JML03a | 650.0 | Gh | 0 | 0.03155 | 263.1 | -54.0 | 61.1 | -24.0 | 61.1 | -24.0 | 6.5 |
| JML03a | 660.0 | Gh | 0 | 0.04043 | 281.7 | -57.2 | 61.7 | -34.9 | 61.7 | -34.9 | 8.0 |
| JML03a | 670.0 | Gh | 0 | 0.02899 | 275.8 | -21.4 | 96.6 | -16.6 | 96.6 | -16.6 | 10.5 |
| JML03a | 675.0 | Gh | 0 | 0.02215 | 310.5 | -70.8 | 42.4 | -45.8 | 42.4 | -45.8 | 12.5 |
| | | | | | | | | | | | |
| JML04a | 0.0 | Gh | 0 | 0.27402 | 156.6 | 19.6 | 319.2 | 64.7 | 319.2 | 64.7 | 4.5 |
| JML04a | 100.0 | Gh | 0 | 0.26180 | 151.1 | 15.7 | 318.4 | 58.2 | 318.4 | 58.2 | 4.0 |
| JML04a | 200.0 | Gh | 0 | 0.25799 | 150.8 | 15.7 | 318.0 | 58.0 | 318.0 | 58.0 | 5.0 |
| JML04a | 300.0 | Gh | 0 | 0.25430 | 150.8 | 14.0 | 320.4 | 56.9 | 320.4 | 56.9 | 4.0 |
| JML04a | 400.0 | Gh | 0 | 0.23254 | 146.1 | 10.3 | 319.7 | 51.0 | 319.7 | 51.0 | 4.0 |
| JML04a | 500.0 | Gh | 0 | 0.17019 | 138.5 | 12.3 | 310.2 | 46.5 | 310.2 | 46.5 | 4.0 |
| JML04a | 525.0 | Gh | 0 | 0.13320 | 137.9 | 17.4 | 303.4 | 49.0 | 303.4 | 49.0 | 3.0 |
| JML04a | 550.0 | Gh | 0 | 0.11743 | 136.9 | 18.5 | 301.2 | 48.7 | 301.2 | 48.7 | 2.5 |
| JML04a | 575.0 | Gh | 0 | 0.11306 | 139.4 | 15.4 | 307.2 | 49.1 | 307.2 | 49.1 | 5.0 |
| JML04a | 600.0 | Gh | 0 | 0.10790 | 138.9 | 13.2 | 309.4 | 47.4 | 309.4 | 47.4 | 3.5 |
| JML04a | 625.0 | Gh | 0 | 0.10289 | 155.5 | 5.6 | 336.3 | 53.6 | 336.3 | 53.6 | 4.5 |
| JML04a | 650.0 | Gh | 0 | 0.07140 | 145.1 | -3.5 | 332.1 | 40.1 | 332.1 | 40.1 | 7.0 |
| JML04a | 660.0 | Gh | 0 | 0.06710 | 131.1 | -9.9 | 324.6 | 26.2 | 324.6 | 26.2 | 11.0 |
| JML04a | 670.0 | Gh | 0 | 0.06399 | 146.7 | -43.0 | 356.5 | 7.2 | 356.5 | 7.2 | 12.0 |
| JML04a | 675.0 | Gh | 0 | 0.03016 | 66.8 | -48.9 | 328.9 | -39.5 | 328.9 | -39.5 | 11.5 |
| | | | | | | | | | | | |
| JML05a | 0.0 | Gh | 0 | 0.27632 | 176.9 | 13.2 | 10.5 | 70.0 | 10.5 | 70.0 | 4.0 |
| JML05a | 100.0 | Gh | 0 | 0.26916 | 176.0 | 12.9 | 8.2 | 69.6 | 8.2 | 69.6 | 4.5 |
| JML05a | 200.0 | Gh | 0 | 0.26032 | 175.6 | 13.7 | 6.6 | 70.3 | 6.6 | 70.3 | 4.5 |
| JML05a | 300.0 | Gh | 0 | 0.26346 | 173.8 | 14.9 | 0.7 | 71.0 | 0.7 | 71.0 | 4.0 |
| JML05a | 400.0 | Gh | 0 | 0.25544 | 173.3 | 14.4 | 359.7 | 70.4 | 359.7 | 70.4 | 3.5 |
| JML05a | 500.0 | Gh | 0 | 0.18228 | 172.6 | 10.6 | 0.8 | 66.6 | 0.8 | 66.6 | 3.0 |
| JML05a | 525.0 | Gh | 0 | 0.15966 | 171.1 | 9.0 | 358.5 | 64.6 | 358.5 | 64.6 | 3.5 |
| JML05a | 550.0 | Gh | 0 | 0.13571 | 166.6 | 9.1 | 349.0 | 63.1 | 349.0 | 63.1 | 4.0 |
| JML05a | 575.0 | Gh | 0 | 0.13730 | 166.7 | 6.8 | 351.3 | 61.0 | 351.3 | 61.0 | 4.0 |
| JML05a | 600.0 | Gh | 0 | 0.13172 | 164.2 | 4.1 | 349.0 | 57.5 | 349.0 | 57.5 | 3.0 |
| JML05a | 625.0 | Gh | 0 | 0.11450 | 174.1 | 3.0 | 7.7 | 59.5 | 7.7 | 59.5 | 4.5 |
| JML05a | 650.0 | Gh | 0 | 0.10485 | 182.9 | -5.8 | 24.0 | 51.1 | 24.0 | 51.1 | 5.0 |
| JML05a | 660.0 | Gh | 0 | 0.08279 | 175.0 | -6.4 | 11.6 | 50.3 | 11.6 | 50.3 | 7.0 |
| JML05a | 670.0 | Gh | 0 | 0.06304 | 184.9 | -15.1 | 25.7 | 41.7 | 25.7 | 41.7 | 8.0 |
| JML05a | 675.0 | Gh | 0 | 0.04774 | 175.0 | -16.5 | 13.1 | 40.3 | 13.1 | 40.3 | 9.5 |
| | | | | | | | | | | | |
| JML06a | 0.0 | Gh | 0 | 0.18698 | 164.0 | 12.5 | 334.7 | 67.1 | 334.7 | 67.1 | 3.5 |
| JML06a | 100.0 | Gh | 0 | 0.16532 | 160.8 | 12.3 | 329.1 | 64.9 | 329.1 | 64.9 | 3.5 |
| JML06a | 200.0 | Gh | 0 | 0.16670 | 160.8 | 12.0 | 329.6 | 64.7 | 329.6 | 64.7 | 4.0 |
| JML06a | 300.0 | Gh | 0 | 0.16029 | 160.5 | 15.7 | 322.7 | 67.1 | 322.7 | 67.1 | 3.0 |
| JML06a | 400.0 | Gh | 0 | 0.14712 | 151.5 | 19.6 | 303.8 | 62.2 | 303.8 | 62.2 | 5.0 |
| JML06a | 500.0 | Gh | 0 | 0.08939 | 147.2 | 13.6 | 309.7 | 55.6 | 309.7 | 55.6 | 3.0 |
| JML06a | 525.0 | Gh | 0 | 0.08744 | 146.2 | 4.4 | 320.5 | 49.1 | 320.5 | 49.1 | 3.0 |
| JML06a | 550.0 | Gh | 0 | 0.08009 | 146.4 | -7.7 | 332.4 | 40.4 | 332.4 | 40.4 | 4.0 |
| JML06a | 575.0 | Gh | 0 | 0.07151 | 142.3 | -10.7 | 330.8 | 35.5 | 330.8 | 35.5 | 4.5 |
| JML06a | 600.0 | Gh | 0 | 0.04552 | 145.9 | -22.3 | 342.3 | 28.3 | 342.3 | 28.3 | 3.5 |
| JML06a | 625.0 | Gh | 0 | 0.06130 | 143.5 | 5.5 | 316.6 | 47.8 | 316.6 | 47.8 | 5.0 |

| | | | | | | | | | | | |
|---|---|---|---|---|---|---|---|---|---|---|---|
| JML06a | 650.0 | Gh | 0 | 0.05136 | 143.7 | 36.0 | 267.5 | 59.2 | 267.5 | 59.2 | 6.0 |
| JML06a | 660.0 | Gh | 0 | 0.04948 | 129.5 | 23.1 | 284.6 | 44.7 | 284.6 | 44.7 | 10.0 |
| JML06a | 670.0 | Gh | 0 | 0.04330 | 85.9 | 22.3 | 267.0 | 7.6 | 267.0 | 7.6 | 10.0 |
| JML06a | 675.0 | Gh | 0 | 0.02537 | 295.2 | 68.6 | 177.9 | 19.3 | 177.9 | 19.3 | 8.0 |
| | | | | | | | | | | | |
| JML07a | 0.0 | Gh | 0 | 0.22693 | 159.8 | 14.5 | 322.8 | 65.8 | 322.8 | 65.8 | 3.5 |
| JML07a | 100.0 | Gh | 0 | 0.22296 | 159.1 | 14.4 | 321.9 | 65.2 | 321.9 | 65.2 | 4.0 |
| JML07a | 200.0 | Gh | 0 | 0.21675 | 157.7 | 14.3 | 319.9 | 64.1 | 319.9 | 64.1 | 4.5 |
| JML07a | 300.0 | Gh | 0 | 0.22080 | 153.2 | 13.9 | 314.6 | 60.5 | 314.6 | 60.5 | 4.0 |
| JML07a | 400.0 | Gh | 0 | 0.20461 | 145.5 | 16.0 | 303.5 | 55.5 | 303.5 | 55.5 | 4.5 |
| JML07a | 500.0 | Gh | 0 | 0.16245 | 136.5 | 13.1 | 300.6 | 46.5 | 300.6 | 46.5 | 3.0 |
| JML07a | 525.0 | Gh | 0 | 0.13770 | 138.8 | 10.6 | 305.4 | 47.1 | 305.4 | 47.1 | 3.5 |
| JML07a | 550.0 | Gh | 0 | 0.12519 | 144.2 | 4.2 | 317.7 | 47.5 | 317.7 | 47.5 | 3.0 |
| JML07a | 575.0 | Gh | 0 | 0.12402 | 144.0 | 7.5 | 313.7 | 49.5 | 313.7 | 49.5 | 3.0 |
| JML07a | 600.0 | Gh | 0 | 0.11661 | 141.6 | 6.7 | 312.4 | 47.1 | 312.4 | 47.1 | 2.5 |
| JML07a | 625.0 | Gh | 0 | 0.09687 | 134.9 | 11.2 | 301.8 | 44.2 | 301.8 | 44.2 | 3.0 |
| JML07a | 650.0 | Gh | 0 | 0.08127 | 125.5 | 20.9 | 284.6 | 40.4 | 284.6 | 40.4 | 4.0 |
| JML07a | 660.0 | Gh | 0 | 0.07930 | 128.3 | 21.3 | 285.4 | 43.0 | 285.4 | 43.0 | 6.0 |
| JML07a | 670.0 | Gh | 0 | 0.07034 | 127.8 | 30.6 | 272.8 | 45.3 | 272.8 | 45.3 | 7.5 |
| JML07a | 675.0 | Gh | 0 | 0.06356 | 111.1 | 30.3 | 268.1 | 31.4 | 268.1 | 31.4 | 9.0 |
| | | | | | | | | | | | |
| JML08a | 0.0 | Gh | 0 | 0.14924 | 171.4 | -7.2 | 3.5 | 44.1 | 3.5 | 44.1 | 4.0 |
| JML08a | 100.0 | Gh | 0 | 0.13300 | 170.3 | -16.6 | 4.1 | 34.6 | 4.1 | 34.6 | 4.0 |
| JML08a | 200.0 | Gh | 0 | 0.13314 | 170.6 | -17.2 | 4.5 | 34.1 | 4.5 | 34.1 | 4.5 |
| JML08a | 300.0 | Gh | 0 | 0.12882 | 168.7 | -20.7 | 3.1 | 30.3 | 3.1 | 30.3 | 4.0 |
| JML08a | 400.0 | Gh | 0 | 0.11995 | 168.3 | -39.4 | 6.2 | 11.9 | 6.2 | 11.9 | 3.5 |
| JML08a | 500.0 | Gh | 0 | 0.09672 | 165.2 | -58.5 | 7.7 | -7.3 | 7.7 | -7.3 | 4.5 |
| JML08a | 525.0 | Gh | 0 | 0.08689 | 150.0 | -54.7 | 358.5 | -6.2 | 358.5 | -6.2 | 3.0 |
| JML08a | 550.0 | Gh | 0 | 0.06837 | 137.7 | -55.7 | 352.7 | -10.4 | 352.7 | -10.4 | 2.5 |
| JML08a | 575.0 | Gh | 0 | 0.06561 | 131.2 | -59.6 | 352.1 | -15.6 | 352.1 | -15.6 | 3.5 |
| JML08a | 600.0 | Gh | 0 | 0.03917 | 136.9 | -69.5 | 0.4 | -22.0 | 0.4 | -22.0 | 4.0 |
| JML08a | 625.0 | Gh | 0 | 0.03555 | 215.2 | -56.3 | 34.3 | -8.9 | 34.3 | -8.9 | 3.5 |
| JML08a | 650.0 | Gh | 0 | 0.02062 | 6.8 | -52.8 | 359.9 | -74.5 | 359.9 | -74.5 | 6.5 |
| JML08a | 660.0 | Gh | 0 | 0.04026 | 304.9 | -55.9 | 60.7 | -49.7 | 60.7 | -49.7 | 9.5 |
| JML08a | 670.0 | Gh | 0 | 0.02766 | 278.5 | -45.0 | 70.2 | -31.2 | 70.2 | -31.2 | 9.0 |
| JML08a | 675.0 | Gh | 0 | 0.02263 | 322.4 | -54.4 | 60.3 | -59.8 | 60.3 | -59.8 | 7.0 |
| | | | | | | | | | | | |
| JML09a | 0.0 | Gh | 0 | 0.27245 | 179.7 | 11.6 | 16.8 | 60.6 | 16.8 | 60.6 | 4.0 |
| JML09a | 100.0 | Gh | 0 | 0.26627 | 178.8 | 11.0 | 15.0 | 60.0 | 15.0 | 60.0 | 4.5 |
| JML09a | 200.0 | Gh | 0 | 0.24938 | 176.3 | 9.7 | 10.4 | 58.5 | 10.4 | 58.5 | 4.5 |
| JML09a | 300.0 | Gh | 0 | 0.23487 | 174.7 | 7.5 | 7.9 | 56.2 | 7.9 | 56.2 | 3.0 |
| JML09a | 400.0 | Gh | 0 | 0.20169 | 173.0 | 3.3 | 6.1 | 51.8 | 6.1 | 51.8 | 4.5 |
| JML09a | 500.0 | Gh | 0 | 0.14603 | 169.5 | -1.9 | 2.2 | 46.0 | 2.2 | 46.0 | 4.0 |
| JML09a | 525.0 | Gh | 0 | 0.13942 | 168.2 | 1.4 | 359.2 | 49.0 | 359.2 | 49.0 | 3.0 |
| JML09a | 550.0 | Gh | 0 | 0.12500 | 165.0 | 7.3 | 351.7 | 53.8 | 351.7 | 53.8 | 3.0 |
| JML09a | 575.0 | Gh | 0 | 0.11430 | 165.2 | 7.6 | 351.8 | 54.1 | 351.8 | 54.1 | 4.0 |
| JML09a | 600.0 | Gh | 0 | 0.10777 | 164.5 | 8.8 | 350.0 | 55.0 | 350.0 | 55.0 | 3.0 |
| JML09a | 625.0 | Gh | 0 | 0.09743 | 171.4 | 13.7 | 359.6 | 61.7 | 359.6 | 61.7 | 3.0 |
| JML09a | 650.0 | Gh | 0 | 0.09714 | 166.0 | 8.6 | 352.6 | 55.3 | 352.6 | 55.3 | 4.5 |
| JML09a | 660.0 | Gh | 0 | 0.09084 | 164.5 | 10.7 | 348.8 | 56.8 | 348.8 | 56.8 | 5.0 |
| JML09a | 670.0 | Gh | 0 | 0.07946 | 160.6 | 6.8 | 345.3 | 51.7 | 345.3 | 51.7 | 6.0 |
| JML09a | 675.0 | Gh | 0 | 0.07429 | 155.5 | 9.3 | 336.2 | 51.6 | 336.2 | 51.6 | 7.0 |

| | | | | | | | | | | | |
|---|---|---|---|---|---|---|---|---|---|---|---|
| JML10a | 0.0 | Gh | 0 | 0.23932 | 178.6 | 9.5 | 12.7 | 59.5 | 12.7 | 59.5 | 4.0 |
| JML10a | 100.0 | Gh | 0 | 0.21815 | 176.0 | 5.7 | 8.4 | 55.5 | 8.4 | 55.5 | 4.0 |
| JML10a | 200.0 | Gh | 0 | 0.21672 | 178.7 | 5.5 | 13.1 | 55.5 | 13.1 | 55.5 | 4.0 |
| JML10a | 300.0 | Gh | 0 | 0.20888 | 177.4 | 4.9 | 10.9 | 54.8 | 10.9 | 54.8 | 4.5 |
| JML10a | 400.0 | Gh | 0 | 0.18270 | 174.2 | -0.9 | 6.6 | 48.8 | 6.6 | 48.8 | 3.5 |
| JML10a | 500.0 | Gh | 0 | 0.14682 | 172.7 | -4.6 | 5.1 | 44.9 | 5.1 | 44.9 | 4.0 |
| JML10a | 525.0 | Gh | 0 | 0.12030 | 170.6 | -1.8 | 1.5 | 47.3 | 1.5 | 47.3 | 2.5 |
| JML10a | 550.0 | Gh | 0 | 0.11247 | 172.4 | -6.8 | 5.1 | 42.7 | 5.1 | 42.7 | 2.5 |
| JML10a | 575.0 | Gh | 0 | 0.10563 | 176.4 | -7.0 | 10.5 | 42.9 | 10.5 | 42.9 | 5.0 |
| JML10a | 600.0 | Gh | 0 | 0.08578 | 173.9 | -7.8 | 7.3 | 41.9 | 7.3 | 41.9 | 3.5 |
| JML10a | 625.0 | Gh | 0 | 0.07915 | 177.8 | -17.7 | 12.9 | 32.3 | 12.9 | 32.3 | 4.0 |
| JML10a | 650.0 | Gh | 0 | 0.07341 | 174.7 | -25.9 | 10.2 | 23.9 | 10.2 | 23.9 | 6.0 |
| JML10a | 660.0 | Gh | 0 | 0.05730 | 169.8 | -40.7 | 7.6 | 8.8 | 7.6 | 8.8 | 9.0 |
| JML10a | 670.0 | Gh | 0 | 0.02430 | 156.0 | -10.7 | 346.3 | 34.6 | 346.3 | 34.6 | 9.5 |
| JML10a | 675.0 | Gh | 0 | 0.03092 | 142.0 | 58.6 | 234.8 | 59.7 | 234.8 | 59.7 | 9.0 |
| | | | | | | | | | | | |
| JML11a | 0.0 | Gh | 0 | 0.20307 | 151.8 | 5.1 | 331.6 | 49.0 | 331.6 | 49.0 | 4.5 |
| JML11a | 100.0 | Gh | 0 | 0.19732 | 150.5 | 4.8 | 330.2 | 48.0 | 330.2 | 48.0 | 4.0 |
| JML11a | 200.0 | Gh | 0 | 0.19154 | 149.2 | 3.6 | 329.7 | 46.3 | 329.7 | 46.3 | 4.0 |
| JML11a | 300.0 | Gh | 0 | 0.17209 | 136.9 | 0.9 | 319.4 | 36.3 | 319.4 | 36.3 | 4.0 |
| JML11a | 400.0 | Gh | 0 | 0.15433 | 123.9 | -2.0 | 311.1 | 25.1 | 311.1 | 25.1 | 4.0 |
| JML11a | 500.0 | Gh | 0 | 0.13427 | 109.7 | -11.8 | 308.8 | 8.1 | 308.8 | 8.1 | 4.0 |
| JML11a | 525.0 | Gh | 0 | 0.11914 | 116.5 | -16.1 | 316.5 | 10.1 | 316.5 | 10.1 | 3.0 |
| JML11a | 550.0 | Gh | 0 | 0.13127 | 121.5 | -14.1 | 318.5 | 15.0 | 318.5 | 15.0 | 3.5 |
| JML11a | 575.0 | Gh | 0 | 0.12852 | 128.8 | -14.8 | 324.4 | 19.3 | 324.4 | 19.3 | 4.0 |
| JML11a | 600.0 | Gh | 0 | 0.12409 | 128.8 | -15.3 | 324.8 | 18.9 | 324.8 | 18.9 | 3.0 |
| JML11a | 625.0 | Gh | 0 | 0.09288 | 133.6 | -14.9 | 328.3 | 22.2 | 328.3 | 22.2 | 3.5 |
| JML11a | 650.0 | Gh | 0 | 0.08489 | 137.7 | -15.3 | 332.0 | 24.3 | 332.0 | 24.3 | 3.5 |
| JML11a | 660.0 | Gh | 0 | 0.06039 | 143.6 | -10.6 | 334.3 | 31.4 | 334.3 | 31.4 | 5.0 |
| JML11a | 670.0 | Gh | 0 | 0.06993 | 142.1 | -21.9 | 339.7 | 21.1 | 339.7 | 21.1 | 6.5 |
| JML11a | 675.0 | Gh | 0 | 0.05713 | 130.0 | -11.6 | 323.1 | 22.4 | 323.1 | 22.4 | 7.5 |
| | | | | | | | | | | | |
| JML12a | 0.0 | Gh | 0 | 0.24496 | 178.3 | 17.0 | 11.2 | 67.0 | 11.2 | 67.0 | 4.0 |
| JML12a | 100.0 | Gh | 0 | 0.23036 | 176.2 | 13.9 | 7.1 | 63.7 | 7.1 | 63.7 | 4.0 |
| JML12a | 200.0 | Gh | 0 | 0.23003 | 176.4 | 13.6 | 7.6 | 63.4 | 7.6 | 63.4 | 4.5 |
| JML12a | 300.0 | Gh | 0 | 0.23205 | 177.5 | 12.5 | 10.1 | 62.4 | 10.1 | 62.4 | 3.0 |
| JML12a | 400.0 | Gh | 0 | 0.22101 | 172.4 | 12.1 | 359.8 | 61.3 | 359.8 | 61.3 | 3.5 |
| JML12a | 500.0 | Gh | 0 | 0.15282 | 172.2 | 3.9 | 2.3 | 53.2 | 2.3 | 53.2 | 3.5 |
| JML12a | 525.0 | Gh | 0 | 0.11917 | 174.9 | 5.2 | 6.5 | 54.9 | 6.5 | 54.9 | 4.0 |
| JML12a | 550.0 | Gh | 0 | 0.11816 | 175.6 | 14.5 | 5.6 | 64.2 | 5.6 | 64.2 | 3.0 |
| JML12a | 575.0 | Gh | 0 | 0.10324 | 169.3 | 9.4 | 355.2 | 58.0 | 355.2 | 58.0 | 4.0 |
| JML12a | 600.0 | Gh | 0 | 0.09541 | 164.6 | 3.8 | 350.4 | 51.2 | 350.4 | 51.2 | 4.0 |
| JML12a | 625.0 | Gh | 0 | 0.08951 | 164.7 | -6.7 | 355.0 | 41.2 | 355.0 | 41.2 | 4.0 |
| JML12a | 650.0 | Gh | 0 | 0.05357 | 165.0 | -4.4 | 354.6 | 43.5 | 354.6 | 43.5 | 6.0 |
| JML12a | 660.0 | Gh | 0 | 0.04765 | 184.7 | -17.3 | 20.7 | 32.5 | 20.7 | 32.5 | 10.0 |
| JML12a | 670.0 | Gh | 0 | 0.04079 | 202.4 | -8.7 | 43.6 | 37.1 | 43.6 | 37.1 | 8.5 |
| JML12a | 675.0 | Gh | 0 | 0.04223 | 186.2 | -26.1 | 21.5 | 23.6 | 21.5 | 23.6 | 9.5 |
| | | | | | | | | | | | |
| JML13a | 0.0 | Gh | 0 | 0.23533 | 190.2 | 10.9 | 91.6 | 70.4 | 91.6 | 70.4 | 5.0 |
| JML13a | 100.0 | Gh | 0 | 0.22609 | 190.0 | 10.4 | 90.4 | 70.1 | 90.4 | 70.1 | 3.5 |
| JML13a | 200.0 | Gh | 0 | 0.21108 | 188.5 | 10.4 | 86.5 | 70.7 | 86.5 | 70.7 | 4.0 |
| JML13a | 300.0 | Gh | 0 | 0.18346 | 185.9 | 9.0 | 77.8 | 70.2 | 77.8 | 70.2 | 3.5 |
| JML13a | 400.0 | Gh | 0 | 0.11882 | 187.0 | 4.9 | 77.7 | 66.0 | 77.7 | 66.0 | 4.0 |

| | | | | | | | | | | | |
|---|---|---|---|---|---|---|---|---|---|---|---|
| JML13a | 500.0 | Gh | 0 | 0.08580 | 190.3 | 0.9 | 82.2 | 61.2 | 82.2 | 61.2 | 4.0 |
| JML13a | 525.0 | Gh | 0 | 0.09898 | 188.4 | 8.2 | 83.8 | 68.7 | 83.8 | 68.7 | 3.0 |
| JML13a | 550.0 | Gh | 0 | 0.10142 | 183.4 | 11.2 | 71.8 | 72.9 | 71.8 | 72.9 | 4.0 |
| JML13a | 575.0 | Gh | 0 | 0.10294 | 187.0 | 10.4 | 82.3 | 71.2 | 82.3 | 71.2 | 2.5 |
| JML13a | 600.0 | Gh | 0 | 0.09350 | 190.9 | 7.3 | 88.9 | 66.9 | 88.9 | 66.9 | 3.0 |
| JML13a | 625.0 | Gh | 0 | 0.06439 | 219.1 | 0.3 | 120.7 | 43.4 | 120.7 | 43.4 | 4.0 |
| JML13a | 650.0 | Gh | 0 | 0.05419 | 217.0 | -3.8 | 114.6 | 42.3 | 114.6 | 42.3 | 4.0 |
| JML13a | 660.0 | Gh | 0 | 0.03583 | 234.5 | -4.0 | 128.1 | 28.6 | 128.1 | 28.6 | 5.0 |
| JML13a | 670.0 | Gh | 0 | 0.03828 | 211.0 | -8.4 | 104.4 | 42.9 | 104.4 | 42.9 | 5.0 |
| JML13a | 675.0 | Gh | 0 | 0.04961 | 262.4 | -11.6 | 136.6 | 1.1 | 136.6 | 1.1 | 5.5 |
| | | | | | | | | | | | |
| JML14a | 0.0 | Gh | 0 | 0.19734 | 183.7 | 14.8 | 75.7 | 76.4 | 75.7 | 76.4 | 4.5 |
| JML14a | 100.0 | Gh | 0 | 0.17127 | 187.2 | 8.4 | 80.9 | 69.3 | 80.9 | 69.3 | 4.0 |
| JML14a | 200.0 | Gh | 0 | 0.17173 | 187.6 | 7.7 | 81.3 | 68.5 | 81.3 | 68.5 | 4.0 |
| JML14a | 300.0 | Gh | 0 | 0.15161 | 189.2 | 4.4 | 82.4 | 64.8 | 82.4 | 64.8 | 5.0 |
| JML14a | 400.0 | Gh | 0 | 0.12637 | 191.6 | 1.9 | 85.4 | 61.6 | 85.4 | 61.6 | 3.0 |
| JML14a | 500.0 | Gh | 0 | 0.09995 | 204.0 | -4.6 | 99.5 | 50.0 | 99.5 | 50.0 | 4.5 |
| JML14a | 525.0 | Gh | 0 | 0.08224 | 205.7 | -9.5 | 97.6 | 45.0 | 97.6 | 45.0 | 3.0 |
| JML14a | 550.0 | Gh | 0 | 0.08583 | 209.2 | -2.0 | 108.3 | 48.9 | 108.3 | 48.9 | 4.0 |
| JML14a | 575.0 | Gh | 0 | 0.08422 | 217.8 | 1.8 | 121.2 | 45.4 | 121.2 | 45.4 | 3.0 |
| JML14a | 600.0 | Gh | 0 | 0.09384 | 212.5 | -2.2 | 111.7 | 46.6 | 111.7 | 46.6 | 3.5 |
| JML14a | 625.0 | Gh | 0 | 0.06211 | 208.5 | 6.8 | 117.6 | 55.7 | 117.6 | 55.7 | 4.5 |
| JML14a | 650.0 | Gh | 0 | 0.07428 | 185.8 | 15.7 | 85.2 | 76.6 | 85.2 | 76.6 | 6.5 |
| JML14a | 660.0 | Gh | 0 | 0.06798 | 197.4 | 8.2 | 103.4 | 64.3 | 103.4 | 64.3 | 7.5 |
| JML14a | 670.0 | Gh | 0 | 0.06714 | 183.9 | 10.8 | 73.2 | 72.4 | 73.2 | 72.4 | 5.5 |
| JML14a | 675.0 | Gh | 0 | 0.06392 | 166.7 | -1.9 | 35.1 | 57.5 | 35.1 | 57.5 | 5.0 |
| | | | | | | | | | | | |
| JML15a | 0.0 | Gh | 0 | 0.19291 | 149.5 | 10.9 | 352.9 | 57.9 | 352.9 | 57.9 | 4.0 |
| JML15a | 100.0 | Gh | 0 | 0.18145 | 143.5 | 10.4 | 348.7 | 52.5 | 348.7 | 52.5 | 4.0 |
| JML15a | 200.0 | Gh | 0 | 0.16724 | 143.3 | 7.0 | 353.2 | 50.6 | 353.2 | 50.6 | 4.5 |
| JML15a | 300.0 | Gh | 0 | 0.16180 | 138.9 | 4.8 | 352.6 | 45.7 | 352.6 | 45.7 | 4.0 |
| JML15a | 400.0 | Gh | 0 | 0.13291 | 139.4 | 0.3 | 358.3 | 43.7 | 358.3 | 43.7 | 4.0 |
| JML15a | 500.0 | Gh | 0 | 0.10994 | 124.2 | -7.8 | 356.0 | 26.6 | 356.0 | 26.6 | 3.5 |
| JML15a | 525.0 | Gh | 0 | 0.11870 | 114.2 | -5.2 | 348.1 | 19.4 | 348.1 | 19.4 | 4.0 |
| JML15a | 550.0 | Gh | 0 | 0.11687 | 115.7 | -4.3 | 348.0 | 21.1 | 348.0 | 21.1 | 3.0 |
| JML15a | 575.0 | Gh | 0 | 0.11130 | 114.9 | -0.9 | 344.4 | 22.0 | 344.4 | 22.0 | 3.0 |
| JML15a | 600.0 | Gh | 0 | 0.09845 | 113.4 | -0.2 | 343.0 | 21.0 | 343.0 | 21.0 | 1.5 |
| JML15a | 625.0 | Gh | 0 | 0.06093 | 108.0 | -9.6 | 349.0 | 11.9 | 349.0 | 11.9 | 4.0 |
| JML15a | 650.0 | Gh | 0 | 0.03940 | 110.3 | -24.8 | 3.5 | 6.2 | 3.5 | 6.2 | 4.5 |
| JML15a | 660.0 | Gh | 0 | 0.02229 | 87.4 | -46.5 | 15.5 | -19.6 | 15.5 | -19.6 | 4.5 |
| JML15a | 670.0 | Gh | 0 | 0.02269 | 91.5 | -62.8 | 33.0 | -21.4 | 33.0 | -21.4 | 4.5 |
| JML15a | 675.0 | Gh | 0 | 0.02453 | 6.2 | 35.0 | 248.2 | -29.7 | 248.2 | -29.7 | 5.5 |
| | | | | | | | | | | | |
| JML16a | 0.0 | Gh | 0 | 0.21331 | 154.6 | 12.9 | 353.7 | 63.9 | 353.7 | 63.9 | 4.0 |
| JML16a | 100.0 | Gh | 0 | 0.19136 | 153.9 | 7.8 | 2.5 | 60.7 | 2.5 | 60.7 | 4.5 |
| JML16a | 200.0 | Gh | 0 | 0.18989 | 154.6 | 7.7 | 3.4 | 61.2 | 3.4 | 61.2 | 4.5 |
| JML16a | 300.0 | Gh | 0 | 0.18630 | 152.1 | 5.3 | 4.5 | 57.8 | 4.5 | 57.8 | 3.5 |
| JML16a | 400.0 | Gh | 0 | 0.17450 | 155.5 | -1.2 | 17.5 | 56.0 | 17.5 | 56.0 | 4.5 |
| JML16a | 500.0 | Gh | 0 | 0.13246 | 159.2 | 2.6 | 17.7 | 61.3 | 17.7 | 61.3 | 3.5 |
| JML16a | 525.0 | Gh | 0 | 0.12030 | 154.6 | 9.7 | 359.9 | 62.3 | 359.9 | 62.3 | 3.0 |
| JML16a | 550.0 | Gh | 0 | 0.10645 | 150.2 | 14.6 | 346.7 | 60.6 | 346.7 | 60.6 | 3.0 |
| JML16a | 575.0 | Gh | 0 | 0.10429 | 140.3 | 13.2 | 343.0 | 51.1 | 343.0 | 51.1 | 2.5 |
| JML16a | 600.0 | Gh | 0 | 0.09525 | 138.5 | 15.3 | 338.9 | 50.2 | 338.9 | 50.2 | 3.0 |

```
JML16a     625.0  Gh  0 0.09235 139.7  16.6  337.5  51.7  337.5  51.7   5.5
JML16a     650.0  Gh  0 0.07722 143.6  18.3  336.4  55.7  336.4  55.7   6.0
JML16a     660.0  Gh  0 0.05584 165.0  13.5    6.5  72.9    6.5  72.9   6.5
JML16a     670.0  Gh  0 0.07185 153.1  19.7  337.8  64.8  337.8  64.8   4.5
JML16a     675.0  Gh  0 0.06694 158.2  19.5  341.1  69.4  341.1  69.4   4.0

JML17a       0.0  Gh  0 0.10777 148.1  11.5  351.2  57.3  351.2  57.3   3.5
JML17a     100.0  Gh  0 0.10032 144.3  10.4  350.0  53.4  350.0  53.4   5.0
JML17a     200.0  Gh  0 0.09577 138.1  11.7  344.0  48.4  344.0  48.4   3.5
JML17a     300.0  Gh  0 0.08454 140.3  13.7  342.4  51.2  342.4  51.2   4.5
JML17a     400.0  Gh  0 0.08080 154.6   9.4    1.1  61.7    1.1  61.7   2.0
JML17a     500.0  Gh  0 0.06542 158.2   9.8    5.0  64.8    5.0  64.8   4.0
JML17a     525.0  Gh  0 0.03668 130.4   6.7  346.0  39.5  346.0  39.5   4.0
JML17a     550.0  Gh  0 0.04468 136.3  -1.0  358.6  40.8  358.6  40.8   3.0
JML17a     575.0  Gh  0 0.03286 152.7  -8.8   22.0  47.7   22.0  47.7   3.0
JML17a     600.0  Gh  0 0.03618 142.3  -0.2    2.4  46.2    2.4  46.2   3.0
JML17a     625.0  Gh  0 0.05010 200.1  34.4  189.7  69.7  189.7  69.7   4.0
JML17a     650.0  Gh  0 0.05143 213.1  23.6  160.5  59.8  160.5  59.8   4.0
JML17a     660.0  Gh  0 0.01400 201.2 -28.1   87.0  34.0   87.0  34.0   6.5
JML17a     670.0  Gh  0 0.02599 215.9  42.4  195.1  55.2  195.1  55.2   4.5
JML17a     675.0  Gh  0 0.01409 239.1   4.7  145.5  30.1  145.5  30.1   5.5

JML18a       0.0  Gh  0 0.12198 150.9  10.8  350.9  60.3  350.9  60.3   4.0
JML18a     100.0  Gh  0 0.10393 147.5   7.8  353.4  56.0  353.4  56.0   4.0
JML18a     200.0  Gh  0 0.10426 148.5   8.1  353.7  57.0  353.7  57.0   4.0
JML18a     300.0  Gh  0 0.09670 150.8   9.5  353.2  59.6  353.2  59.6   5.0
JML18a     400.0  Gh  0 0.09439 145.9   7.2  353.1  54.3  353.1  54.3   4.5
JML18a     500.0  Gh  0 0.06922 131.1   4.7  347.3  39.9  347.3  39.9   2.5
JML18a     525.0  Gh  0 0.05314 125.4  14.0  333.6  37.7  333.6  37.7   3.0
JML18a     550.0  Gh  0 0.04894 131.9  14.5  335.2  43.9  335.2  43.9   4.0
JML18a     575.0  Gh  0 0.04717 130.9  20.3  327.1  44.2  327.1  44.2   4.0
JML18a     600.0  Gh  0 0.04678 143.9   4.8  355.1  51.4  355.1  51.4   5.5
JML18a     625.0  Gh  0 0.04624 163.2  32.5  294.4  71.1  294.4  71.1   6.5
JML18a     650.0  Gh  0 0.04305 164.6  49.5  265.0  59.0  265.0  59.0   7.5
JML18a     660.0  Gh  0 0.04575 193.3  42.8  221.4  65.5  221.4  65.5   9.0
JML18a     670.0  Gh  0 0.02313 197.9  -4.2  102.3  59.3  102.3  59.3   6.5
JML18a     675.0  Gh  0 0.03543 191.7 -13.5   84.8  53.6   84.8  53.6   5.5
!_____________________________END OF FILE_________________________________________
```

Table S2. NRM thermal demagnetization data for samples from sites JBA-JBR of the Upper Morrison Fm.

Lamont datafile format:
ID = sample identification (J=Jurassic, M=Morrison, A to L are sampling sites followed by drillcore sample number and specimen with 'a' at the bottom if more than one.
TREAT = demagnetization step (°C) where 0.0 = room temperature (NRM).
MC = machine code where Gh is 2G Model 760 cryogenic magnetometer in horizontal mode.
CD = circular standard deviation (°) of four successive full-vector measurements.
J = magnetization (10E-4 emu, equivalent to 10E-2 A/m for 10 cc volume).
CDECL, CINCL = declination and inclination in core coordinates.
GDECL, GINCL = declination and inclination in geographic (in-situ) coordinates.
BDECL, BINCL = declination and inclination in tilt-corrected coordinates.
SUSC = magnetic susceptibility (10E-6 cgs).

| ID | TREAT | MC | CD | J | CDECL | CINCL | GDECL | GINCL | BDECL | BINCL | SUSC |
|---|---|---|---|---|---|---|---|---|---|---|---|
| JBA01 | 0.0 | Gh | 0 | 0.05978 | 155.5 | 19.1 | 316.7 | 65.9 | 316.7 | 65.9 | 7.5 |
| JBA01 | 100.0 | Gh | 0 | 0.05233 | 149.3 | 20.8 | 308.0 | 61.2 | 308.0 | 61.2 | 7.0 |
| JBA01 | 200.0 | Gh | 0 | 0.04735 | 143.8 | 19.2 | 307.3 | 55.8 | 307.3 | 55.8 | 7.0 |
| JBA01 | 300.0 | Gh | 0 | 0.04011 | 140.2 | 15.6 | 310.5 | 51.2 | 310.5 | 51.2 | 6.5 |
| JBA01 | 400.0 | Gh | 0 | 0.04215 | 137.1 | 6.3 | 320.3 | 44.0 | 320.3 | 44.0 | 7.5 |
| JBA01 | 500.0 | Gh | 0 | 0.02314 | 130.4 | -6.2 | 328.1 | 31.2 | 328.1 | 31.2 | 11.0 |
| JBA01 | 525.0 | Gh | 0 | 0.02773 | 113.8 | 13.8 | 298.7 | 27.3 | 298.7 | 27.3 | 10.0 |
| JBA01 | 550.0 | Gh | 0 | 0.01857 | 88.2 | 5.2 | 295.0 | 0.9 | 295.0 | 0.9 | 25.0 |
| JBA01 | 575.0 | Gh | 2 | 0.01650 | 106.7 | 7.4 | 301.6 | 18.2 | 301.6 | 18.2 | 22.0 |
| JBA01 | 600.0 | Gh | 2 | 0.01604 | 101.7 | 5.4 | 301.1 | 12.9 | 301.1 | 12.9 | 67.5 |
| JBA01 | 625.0 | Gh | 3 | 0.06220 | 143.0 | 13.3 | 315.8 | 52.6 | 315.8 | 52.6 | 291.0 |
| JBA01 | 650.0 | Gh | 2 | 0.18518 | 168.3 | 23.8 | 319.5 | 78.7 | 319.5 | 78.7 | 892.0 |
| JBA01 | 660.0 | Gh | 8 | 0.07588 | 173.9 | 9.9 | 11.6 | 71.0 | 11.6 | 71.0 | 980.0 |
| JBA01 | 670.0 | Gh | 7 | 0.08679 | 152.1 | 5.9 | 335.1 | 55.5 | 335.1 | 55.5 | 1003 |
| JBA01 | 675.0 | Gh | 13 | 0.07385 | 168.9 | 8.2 | 0.4 | 67.6 | 0.4 | 67.6 | 997.5 |
| JBA02 | 0.0 | Gh | 0 | 0.12901 | 160.2 | 0.5 | 345.9 | 61.1 | 345.9 | 61.1 | 8.0 |
| JBA02 | 100.0 | Gh | 0 | 0.10264 | 156.7 | -4.7 | 347.1 | 54.9 | 347.1 | 54.9 | 9.0 |
| JBA02 | 200.0 | Gh | 0 | 0.10133 | 156.7 | -4.8 | 347.2 | 54.8 | 347.2 | 54.8 | 8.0 |
| JBA02 | 300.0 | Gh | 0 | 0.09194 | 155.4 | -7.0 | 347.9 | 52.3 | 347.9 | 52.3 | 8.0 |
| JBA02 | 400.0 | Gh | 0 | 0.07024 | 162.0 | -1.3 | 351.1 | 60.8 | 351.1 | 60.8 | 10.0 |
| JBA02 | 500.0 | Gh | 0 | 0.05436 | 167.1 | -6.7 | 5.2 | 58.6 | 5.2 | 58.6 | 9.0 |
| JBA02 | 525.0 | Gh | 0 | 0.04842 | 168.9 | -5.4 | 7.5 | 60.5 | 7.5 | 60.5 | 10.0 |
| JBA02 | 550.0 | Gh | 0 | 0.03677 | 159.1 | 0.1 | 344.7 | 60.1 | 344.7 | 60.1 | 11.0 |
| JBA02 | 575.0 | Gh | 0 | 0.03463 | 161.1 | -5.4 | 354.2 | 56.9 | 354.2 | 56.9 | 13.5 |
| JBA02 | 600.0 | Gh | 0 | 0.03449 | 151.2 | -7.0 | 342.9 | 49.5 | 342.9 | 49.5 | 71.5 |
| JBA02 | 625.0 | Gh | 3 | 0.04758 | 159.6 | 9.2 | 330.4 | 66.6 | 330.4 | 66.6 | 232.5 |
| JBA02 | 650.0 | Gh | 4 | 0.05493 | 51.0 | -15.6 | 302.1 | -41.5 | 302.1 | -41.5 | 890.0 |
| JBA02 | 660.0 | Gh | 3 | 0.13231 | 157.2 | 10.3 | 324.9 | 65.2 | 324.9 | 65.2 | 1110 |
| JBA02 | 670.0 | Gh | 3 | 0.13890 | 168.7 | 5.2 | 355.7 | 70.0 | 355.7 | 70.0 | 1118 |
| JBA02 | 675.0 | Gh | 6 | 0.12440 | 149.8 | 14.1 | 310.6 | 60.3 | 310.6 | 60.3 | 1127 |

| | | | | | | | | | | | |
|---|---|---|---|---|---|---|---|---|---|---|---|
| JBA03a | 0.0 | Gh | 0 | 0.13353 | 175.7 | 0.9 | 18.5 | 70.4 | 18.5 | 70.4 | 7.0 |
| JBA03a | 100.0 | Gh | 0 | 0.11710 | 178.3 | -2.1 | 26.9 | 67.8 | 26.9 | 67.8 | 6.5 |
| JBA03a | 200.0 | Gh | 0 | 0.10554 | 176.6 | -3.5 | 22.9 | 66.3 | 22.9 | 66.3 | 7.0 |
| JBA03a | 300.0 | Gh | 0 | 0.10380 | 172.5 | -4.0 | 13.5 | 64.9 | 13.5 | 64.9 | 7.0 |
| JBA03a | 400.0 | Gh | 0 | 0.07541 | 178.0 | -2.5 | 26.2 | 67.4 | 26.2 | 67.4 | 8.0 |
| JBA03a | 500.0 | Gh | 0 | 0.06317 | 173.6 | -3.3 | 15.6 | 65.9 | 15.6 | 65.9 | 5.5 |
| JBA03a | 525.0 | Gh | 0 | 0.06520 | 167.4 | -8.6 | 6.8 | 58.8 | 6.8 | 58.8 | 6.5 |
| JBA03a | 550.0 | Gh | 0 | 0.05193 | 180.1 | 7.0 | 31.8 | 77.0 | 31.8 | 77.0 | 6.0 |
| JBA03a | 575.0 | Gh | 0 | 0.05612 | 167.2 | 4.9 | 350.2 | 70.4 | 350.2 | 70.4 | 6.0 |
| JBA03a | 600.0 | Gh | 0 | 0.03955 | 179.5 | 7.5 | 29.1 | 77.5 | 29.1 | 77.5 | 26.0 |
| JBA03a | 625.0 | Gh | 1 | 0.04246 | 177.5 | 4.3 | 22.3 | 74.1 | 22.3 | 74.1 | 51.0 |
| JBA03a | 650.0 | Gh | 2 | 0.04827 | 173.0 | 8.1 | 0.8 | 76.3 | 0.8 | 76.3 | 191.5 |
| JBA03a | 660.0 | Gh | 2 | 0.04072 | 175.7 | 10.0 | 8.3 | 79.2 | 8.3 | 79.2 | 245.0 |
| JBA03a | 670.0 | Gh | 4 | 0.02184 | 167.3 | -8.2 | 6.3 | 59.2 | 6.3 | 59.2 | 257.0 |
| JBA03a | 675.0 | Gh | 6 | 0.03238 | 185.9 | 3.7 | 51.6 | 72.7 | 51.6 | 72.7 | 262.0 |
| | | | | | | | | | | | |
| JBB01 | 0.0 | Gh | 0 | 0.12172 | 155.0 | -2.7 | 335.2 | 57.2 | 335.2 | 57.2 | 10.5 |
| JBB01 | 100.0 | Gh | 0 | 0.11434 | 152.3 | -0.9 | 329.5 | 56.3 | 329.5 | 56.3 | 10.0 |
| JBB01 | 200.0 | Gh | 0 | 0.10608 | 152.1 | -1.1 | 329.6 | 56.0 | 329.6 | 56.0 | 10.5 |
| JBB01 | 300.0 | Gh | 0 | 0.10520 | 145.4 | 0.6 | 320.8 | 51.4 | 320.8 | 51.4 | 11.0 |
| JBB01 | 400.0 | Gh | 0 | 0.09843 | 144.1 | 1.1 | 319.1 | 50.5 | 319.1 | 50.5 | 10.0 |
| JBB01 | 500.0 | Gh | 0 | 0.08224 | 144.7 | 0.7 | 320.1 | 50.9 | 320.1 | 50.9 | 8.0 |
| JBB01 | 525.0 | Gh | 0 | 0.07908 | 150.0 | -3.1 | 330.1 | 53.1 | 330.1 | 53.1 | 9.5 |
| JBB01 | 550.0 | Gh | 0 | 0.07460 | 147.0 | -1.5 | 325.1 | 51.6 | 325.1 | 51.6 | 9.5 |
| JBB01 | 575.0 | Gh | 0 | 0.07110 | 150.6 | -0.1 | 326.6 | 55.4 | 326.6 | 55.4 | 11.0 |
| JBB01 | 600.0 | Gh | 0 | 0.06520 | 152.4 | -4.3 | 334.2 | 54.2 | 334.2 | 54.2 | 19.0 |
| JBB01 | 625.0 | Gh | 0 | 0.06827 | 152.4 | -4.9 | 335.0 | 53.8 | 335.0 | 53.8 | 43.0 |
| JBB01 | 650.0 | Gh | 1 | 0.07762 | 153.7 | -4.0 | 335.3 | 55.4 | 335.3 | 55.4 | 151.5 |
| JBB01 | 660.0 | Gh | 2 | 0.10561 | 160.9 | -8.6 | 350.4 | 56.6 | 350.4 | 56.6 | 275.0 |
| JBB01 | 670.0 | Gh | 5 | 0.06932 | 154.5 | -25.5 | 356.4 | 39.1 | 356.4 | 39.1 | 371.0 |
| JBB01 | 675.0 | Gh | 4 | 0.14415 | 164.1 | -9.9 | 356.6 | 57.1 | 356.6 | 57.1 | 505.5 |
| | | | | | | | | | | | |
| JBB03a | 0.0 | Gh | 0 | 0.02610 | 165.8 | 17.0 | 338.0 | 72.3 | 338.0 | 72.3 | 4.5 |
| JBB03a | 100.0 | Gh | 0 | 0.02098 | 169.2 | 18.7 | 342.3 | 75.7 | 342.3 | 75.7 | 6.0 |
| JBB03a | 200.0 | Gh | 0 | 0.01592 | 168.3 | 21.9 | 329.7 | 77.3 | 329.7 | 77.3 | 6.0 |
| JBB03a | 300.0 | Gh | 0 | 0.01339 | 162.8 | 20.8 | 322.3 | 72.4 | 322.3 | 72.4 | 5.0 |
| JBB03a | 400.0 | Gh | 0 | 0.01029 | 164.1 | 28.5 | 296.6 | 76.1 | 296.6 | 76.1 | 5.0 |
| JBB03a | 500.0 | Gh | 0 | 0.01059 | 176.7 | 29.2 | 293.6 | 87.1 | 293.6 | 87.1 | 4.5 |
| JBB03a | 525.0 | Gh | 0 | 0.00913 | 179.5 | 33.7 | 213.5 | 85.3 | 213.5 | 85.3 | 5.0 |
| JBB03a | 550.0 | Gh | 0 | 0.00606 | 168.5 | 36.1 | 259.2 | 78.0 | 259.2 | 78.0 | 4.5 |
| JBB03a | 575.0 | Gh | 0 | 0.00694 | 168.0 | 39.4 | 248.8 | 75.7 | 248.8 | 75.7 | 5.0 |
| JBB03a | 600.0 | Gh | 1 | 0.00594 | 158.8 | 28.0 | 296.3 | 71.4 | 296.3 | 71.4 | 12.5 |
| JBB03a | 625.0 | Gh | 1 | 0.00743 | 176.7 | 40.1 | 221.2 | 78.6 | 221.2 | 78.6 | 21.5 |
| JBB03a | 650.0 | Gh | 5 | 0.01231 | 178.3 | 16.9 | 20.7 | 77.8 | 20.7 | 77.8 | 63.0 |
| JBB03a | 660.0 | Gh | 5 | 0.01841 | 159.8 | -0.5 | 351.7 | 54.7 | 351.7 | 54.7 | 114.0 |
| JBB03a | 670.0 | Gh | 7 | 0.01974 | 187.3 | 10.2 | 49.8 | 70.0 | 49.8 | 70.0 | 153.5 |
| JBB03a | 675.0 | Gh | 10 | 0.02819 | 181.2 | -4.6 | 30.6 | 56.4 | 30.6 | 56.4 | 227.0 |
| | | | | | | | | | | | |
| JBC01a | 0.0 | Gh | 0 | 0.15536 | 165.2 | -2.0 | 343.5 | 66.0 | 343.5 | 66.0 | 9.5 |
| JBC01a | 100.0 | Gh | 0 | 0.13159 | 164.0 | -1.8 | 340.9 | 65.5 | 340.9 | 65.5 | 9.5 |
| JBC01a | 200.0 | Gh | 0 | 0.10920 | 164.7 | -3.4 | 344.5 | 64.6 | 344.5 | 64.6 | 10.0 |
| JBC01a | 300.0 | Gh | 0 | 0.09180 | 163.6 | -3.8 | 343.0 | 63.6 | 343.0 | 63.6 | 10.0 |
| JBC01a | 400.0 | Gh | 0 | 0.06781 | 162.2 | -2.2 | 338.3 | 64.0 | 338.3 | 64.0 | 9.0 |

| | | | | | | | | | | | |
|---|---|---|---|---|---|---|---|---|---|---|---|
| JBC01a | 500.0 | Gh | 0 | 0.03490 | 161.1 | -4.9 | 340.3 | 61.2 | 340.3 | 61.2 | 9.0 |
| JBC01a | 525.0 | Gh | 0 | 0.03006 | 160.9 | -5.0 | 340.1 | 61.0 | 340.1 | 61.0 | 11.0 |
| JBC01a | 550.0 | Gh | 0 | 0.02538 | 156.6 | -2.6 | 330.5 | 59.7 | 330.5 | 59.7 | 11.0 |
| JBC01a | 575.0 | Gh | 0 | 0.02236 | 160.1 | -2.1 | 334.7 | 62.6 | 334.7 | 62.6 | 13.5 |
| JBC01a | 600.0 | Gh | 1 | 0.01703 | 154.8 | -5.6 | 332.5 | 56.4 | 332.5 | 56.4 | 26.0 |
| JBC01a | 625.0 | Gh | 1 | 0.01377 | 128.5 | -21.9 | 328.3 | 26.3 | 328.3 | 26.3 | 44.5 |
| JBC01a | 650.0 | Gh | 6 | 0.01534 | 116.6 | 34.1 | 262.4 | 31.2 | 262.4 | 31.2 | 146.0 |
| JBC01a | 660.0 | Gh | 7 | 0.02791 | 85.2 | -19.5 | 309.9 | -10.0 | 309.9 | -10.0 | 240.0 |
| JBC01a | 670.0 | Gh | 6 | 0.03065 | 76.7 | 65.0 | 227.1 | 9.9 | 227.1 | 9.9 | 359.5 |
| JBC01a | 675.0 | Gh | 4 | 0.12159 | 194.8 | -8.2 | 53.7 | 60.9 | 53.7 | 60.9 | 514.0 |
| | | | | | | | | | | | |
| JBC03 | 0.0 | Gh | 0 | 0.11961 | 181.7 | -2.8 | 27.3 | 73.1 | 27.3 | 73.1 | 8.0 |
| JBC03 | 100.0 | Gh | 0 | 0.11016 | 179.5 | -1.3 | 19.5 | 74.7 | 19.5 | 74.7 | 7.0 |
| JBC03 | 200.0 | Gh | 0 | 0.10040 | 180.2 | -0.6 | 22.2 | 75.4 | 22.2 | 75.4 | 7.5 |
| JBC03 | 300.0 | Gh | 0 | 0.09235 | 180.3 | -0.6 | 22.6 | 75.4 | 22.6 | 75.4 | 6.5 |
| JBC03 | 400.0 | Gh | 0 | 0.08125 | 178.8 | -0.4 | 16.6 | 75.6 | 16.6 | 75.6 | 7.0 |
| JBC03 | 500.0 | Gh | 0 | 0.05819 | 180.0 | -0.1 | 21.4 | 75.9 | 21.4 | 75.9 | 6.5 |
| JBC03 | 525.0 | Gh | 0 | 0.05438 | 180.1 | 0.8 | 21.8 | 76.8 | 21.8 | 76.8 | 7.0 |
| JBC03 | 550.0 | Gh | 0 | 0.04848 | 182.4 | 3.2 | 34.0 | 78.9 | 34.0 | 78.9 | 9.0 |
| JBC03 | 575.0 | Gh | 0 | 0.04599 | 181.1 | 1.7 | 26.5 | 77.7 | 26.5 | 77.7 | 12.0 |
| JBC03 | 600.0 | Gh | 1 | 0.03871 | 176.8 | 10.2 | 341.6 | 85.1 | 341.6 | 85.1 | 32.5 |
| JBC03 | 625.0 | Gh | 2 | 0.03717 | 158.0 | -2.4 | 326.7 | 62.7 | 326.7 | 62.7 | 90.5 |
| JBC03 | 650.0 | Gh | 2 | 0.09621 | 199.0 | 35.3 | 166.0 | 62.7 | 166.0 | 62.7 | 383.5 |
| JBC03 | 660.0 | Gh | 5 | 0.16641 | 159.8 | -9.1 | 339.3 | 59.4 | 339.3 | 59.4 | 729.0 |
| JBC03 | 670.0 | Gh | 14 | 0.06875 | 155.7 | 17.9 | 278.7 | 66.3 | 278.7 | 66.3 | 965.5 |
| JBC03 | 675.0 | Gh | 6 | 0.17376 | 177.4 | -8.4 | 14.7 | 67.5 | 14.7 | 67.5 | 1083 |
| | | | | | | | | | | | |
| JBD01 | 0.0 | Gh | 0 | 0.30264 | 170.6 | -6.6 | 11.4 | 66.5 | 11.4 | 66.5 | 13.0 |
| JBD01 | 100.0 | Gh | 0 | 0.27430 | 168.7 | -6.5 | 7.1 | 65.8 | 7.1 | 65.8 | 12.5 |
| JBD01 | 200.0 | Gh | 0 | 0.24426 | 169.1 | -7.4 | 8.9 | 65.1 | 8.9 | 65.1 | 12.0 |
| JBD01 | 300.0 | Gh | 0 | 0.21938 | 166.2 | -7.1 | 2.7 | 64.0 | 2.7 | 64.0 | 13.0 |
| JBD01 | 400.0 | Gh | 0 | 0.17336 | 166.2 | -8.3 | 4.1 | 63.0 | 4.1 | 63.0 | 12.5 |
| JBD01 | 500.0 | Gh | 0 | 0.10755 | 166.3 | -6.8 | 2.5 | 64.3 | 2.5 | 64.3 | 12.5 |
| JBD01 | 525.0 | Gh | 0 | 0.09617 | 166.5 | -7.2 | 3.4 | 64.1 | 3.4 | 64.1 | 13.0 |
| JBD01 | 550.0 | Gh | 0 | 0.08546 | 165.8 | -8.8 | 3.9 | 62.3 | 3.9 | 62.3 | 15.0 |
| JBD01 | 575.0 | Gh | 0 | 0.07891 | 165.2 | -6.1 | 359.5 | 64.3 | 359.5 | 64.3 | 20.0 |
| JBD01 | 600.0 | Gh | 0 | 0.06678 | 162.6 | -5.6 | 354.2 | 63.1 | 354.2 | 63.1 | 37.5 |
| JBD01 | 625.0 | Gh | 1 | 0.05072 | 157.4 | -13.1 | 355.8 | 54.1 | 355.8 | 54.1 | 65.0 |
| JBD01 | 650.0 | Gh | 2 | 0.05393 | 160.8 | 4.0 | 333.7 | 68.1 | 333.7 | 68.1 | 211.0 |
| JBD01 | 660.0 | Gh | 2 | 0.07009 | 177.1 | -7.8 | 28.0 | 67.0 | 28.0 | 67.0 | 333.5 |
| JBD01 | 670.0 | Gh | 5 | 0.06570 | 175.4 | 4.9 | 10.8 | 78.9 | 10.8 | 78.9 | 431.0 |
| JBD01 | 675.0 | Gh | 5 | 0.09218 | 170.5 | -18.0 | 19.2 | 55.7 | 19.2 | 55.7 | 492.5 |
| | | | | | | | | | | | |
| JBD03a | 0.0 | Gh | 0 | 0.31834 | 167.4 | 13.8 | 356.3 | 64.2 | 356.3 | 64.2 | 12.0 |
| JBD03a | 100.0 | Gh | 0 | 0.29441 | 166.1 | 14.3 | 353.1 | 64.1 | 353.1 | 64.1 | 12.5 |
| JBD03a | 200.0 | Gh | 0 | 0.27013 | 165.3 | 13.8 | 352.1 | 63.3 | 352.1 | 63.3 | 11.0 |
| JBD03a | 300.0 | Gh | 0 | 0.24483 | 163.0 | 14.1 | 347.5 | 62.5 | 347.5 | 62.5 | 12.0 |
| JBD03a | 400.0 | Gh | 0 | 0.19092 | 161.4 | 13.7 | 345.1 | 61.4 | 345.1 | 61.4 | 11.5 |
| JBD03a | 500.0 | Gh | 0 | 0.10826 | 158.3 | 13.5 | 340.2 | 59.5 | 340.2 | 59.5 | 12.5 |
| JBD03a | 525.0 | Gh | 0 | 0.09646 | 159.9 | 14.1 | 342.1 | 60.9 | 342.1 | 60.9 | 14.0 |
| JBD03a | 550.0 | Gh | 0 | 0.08308 | 160.3 | 14.7 | 342.0 | 61.6 | 342.0 | 61.6 | 15.5 |
| JBD03a | 575.0 | Gh | 0 | 0.07393 | 157.4 | 12.6 | 339.9 | 58.3 | 339.9 | 58.3 | 21.5 |
| JBD03a | 600.0 | Gh | 0 | 0.06254 | 152.2 | 18.3 | 325.3 | 59.3 | 325.3 | 59.3 | 45.5 |

| | | | | | | | | | | | |
|---|---|---|---|---|---|---|---|---|---|---|---|
| JBD03a | 625.0 | Gh | 2 | 0.06563 | 152.7 | 1.9 | 343.3 | 46.8 | 343.3 | 46.8 | 107.0 |
| JBD03a | 650.0 | Gh | 3 | 0.07313 | 164.7 | 20.1 | 342.9 | 68.5 | 342.9 | 68.5 | 289.0 |
| JBD03a | 660.0 | Gh | 3 | 0.06861 | 207.4 | -19.7 | 54.7 | 27.7 | 54.7 | 27.7 | 466.0 |
| JBD03a | 670.0 | Gh | 8 | 0.06657 | 111.8 | 19.8 | 291.5 | 28.9 | 291.5 | 28.9 | 604.5 |
| JBD03a | 675.0 | Gh | 6 | 0.12228 | 91.9 | -33.0 | 323.7 | -17.8 | 323.7 | -17.8 | 706.0 |
| | | | | | | | | | | | |
| JBE01a | 0.0 | Gh | 0 | 0.17553 | 174.4 | 20.0 | 23.1 | 66.5 | 23.1 | 66.5 | 10.0 |
| JBE01a | 100.0 | Gh | 0 | 0.14358 | 175.8 | 17.0 | 27.3 | 63.8 | 27.3 | 63.8 | 8.5 |
| JBE01a | 200.0 | Gh | 0 | 0.10971 | 176.5 | 15.3 | 29.2 | 62.1 | 29.2 | 62.1 | 8.5 |
| JBE01a | 300.0 | Gh | 0 | 0.08126 | 177.1 | 15.7 | 30.3 | 62.6 | 30.3 | 62.6 | 8.0 |
| JBE01a | 400.0 | Gh | 0 | 0.04285 | 184.9 | 7.6 | 44.8 | 54.3 | 44.8 | 54.3 | 7.5 |
| JBE01a | 500.0 | Gh | 0 | 0.01272 | 183.8 | -37.0 | 39.5 | 9.9 | 39.5 | 9.9 | 8.5 |
| JBE01a | 525.0 | Gh | 0 | 0.01198 | 210.9 | -26.1 | 65.0 | 15.3 | 65.0 | 15.3 | 7.0 |
| JBE01a | 550.0 | Gh | 0 | 0.00841 | 219.9 | -40.9 | 65.4 | -1.3 | 65.4 | -1.3 | 8.5 |
| JBE01a | 575.0 | Gh | 1 | 0.00544 | 209.7 | -22.2 | 65.5 | 19.3 | 65.5 | 19.3 | 10.0 |
| JBE01a | 600.0 | Gh | 0 | 0.01088 | 276.9 | -51.9 | 85.8 | -36.2 | 85.8 | -36.2 | 12.0 |
| JBE01a | 625.0 | Gh | 0 | 0.01407 | 327.1 | -57.6 | 79.5 | -64.8 | 79.5 | -64.8 | 12.0 |
| JBE01a | 650.0 | Gh | 1 | 0.01381 | 334.2 | -40.6 | 124.7 | -70.7 | 124.7 | -70.7 | 12.5 |
| JBE01a | 660.0 | Gh | 0 | 0.01785 | 318.0 | -43.4 | 111.0 | -59.7 | 111.0 | -59.7 | 14.0 |
| JBE01a | 670.0 | Gh | 1 | 0.00918 | 341.7 | -18.3 | 178.7 | -60.9 | 178.7 | -60.9 | 14.5 |
| JBE01a | 675.0 | Gh | 1 | 0.00892 | 329.4 | -38.7 | 126.5 | -66.6 | 126.5 | -66.6 | 14.0 |
| | | | | | | | | | | | |
| JBF01a | 0.0 | Gh | 0 | 0.19385 | 210.3 | 6.1 | 106.2 | 54.9 | 106.2 | 54.9 | 7.5 |
| JBF01a | 100.0 | Gh | 0 | 0.17463 | 217.9 | 3.4 | 109.9 | 47.2 | 109.9 | 47.2 | 8.0 |
| JBF01a | 200.0 | Gh | 0 | 0.15980 | 227.8 | 0.6 | 114.4 | 37.5 | 114.4 | 37.5 | 8.5 |
| JBF01a | 300.0 | Gh | 0 | 0.14648 | 239.9 | -2.4 | 118.8 | 25.6 | 118.8 | 25.6 | 8.0 |
| JBF01a | 400.0 | Gh | 0 | 0.12812 | 258.2 | 0.0 | 130.2 | 10.6 | 130.2 | 10.6 | 7.0 |
| JBF01a | 500.0 | Gh | 0 | 0.10947 | 269.3 | 2.4 | 137.3 | 1.7 | 137.3 | 1.7 | 7.0 |
| JBF01a | 525.0 | Gh | 0 | 0.10575 | 268.7 | -3.7 | 131.5 | -0.5 | 131.5 | -0.5 | 7.0 |
| JBF01a | 550.0 | Gh | 0 | 0.10277 | 272.3 | -3.4 | 133.3 | -3.6 | 133.3 | -3.6 | 8.0 |
| JBF01a | 575.0 | Gh | 0 | 0.10266 | 274.5 | -2.1 | 135.5 | -5.0 | 135.5 | -5.0 | 8.5 |
| JBF01a | 600.0 | Gh | 0 | 0.10209 | 279.0 | -4.2 | 135.5 | -9.9 | 135.5 | -9.9 | 8.0 |
| JBF01a | 625.0 | Gh | 0 | 0.10422 | 286.7 | -4.4 | 138.8 | -16.9 | 138.8 | -16.9 | 8.0 |
| JBF01a | 650.0 | Gh | 0 | 0.10675 | 293.0 | -5.5 | 140.7 | -23.1 | 140.7 | -23.1 | 9.0 |
| JBF01a | 660.0 | Gh | 0 | 0.10084 | 295.4 | -5.0 | 142.3 | -25.0 | 142.3 | -25.0 | 8.5 |
| JBF01a | 670.0 | Gh | 0 | 0.08560 | 295.2 | -7.3 | 139.9 | -25.8 | 139.9 | -25.8 | 10.0 |
| JBF01a | 675.0 | Gh | 0 | 0.05324 | 299.9 | -10.0 | 139.4 | -31.2 | 139.4 | -31.2 | 10.5 |
| | | | | | | | | | | | |
| JBF03a | 0.0 | Gh | 0 | 0.17515 | 200.3 | 4.5 | 89.3 | 58.1 | 89.3 | 58.1 | 7.0 |
| JBF03a | 100.0 | Gh | 0 | 0.15438 | 203.2 | 3.4 | 92.4 | 55.5 | 92.4 | 55.5 | 8.5 |
| JBF03a | 200.0 | Gh | 0 | 0.13134 | 206.2 | 2.2 | 95.1 | 52.7 | 95.1 | 52.7 | 8.5 |
| JBF03a | 300.0 | Gh | 0 | 0.10404 | 214.6 | -0.8 | 101.7 | 44.9 | 101.7 | 44.9 | 9.0 |
| JBF03a | 400.0 | Gh | 0 | 0.07242 | 232.4 | -6.2 | 111.7 | 28.1 | 111.7 | 28.1 | 7.5 |
| JBF03a | 500.0 | Gh | 0 | 0.04879 | 262.7 | -11.9 | 124.5 | 0.3 | 124.5 | 0.3 | 7.0 |
| JBF03a | 525.0 | Gh | 0 | 0.04674 | 272.8 | -20.5 | 121.7 | -12.4 | 121.7 | -12.4 | 8.0 |
| JBF03a | 550.0 | Gh | 0 | 0.04458 | 290.7 | -20.4 | 129.6 | -27.5 | 129.6 | -27.5 | 8.0 |
| JBF03a | 575.0 | Gh | 0 | 0.04742 | 292.9 | -22.0 | 128.8 | -30.0 | 128.8 | -30.0 | 10.0 |
| JBF03a | 600.0 | Gh | 0 | 0.05086 | 303.0 | -17.9 | 137.9 | -37.1 | 137.9 | -37.1 | 12.0 |
| JBF03a | 625.0 | Gh | 0 | 0.05567 | 323.9 | -20.0 | 147.0 | -56.0 | 147.0 | -56.0 | 19.0 |
| JBF03a | 650.0 | Gh | 0 | 0.06118 | 327.7 | -15.7 | 156.9 | -57.1 | 156.9 | -57.1 | 23.0 |
| JBF03a | 660.0 | Gh | 0 | 0.05705 | 331.6 | -17.5 | 157.7 | -61.3 | 157.7 | -61.3 | 24.0 |
| JBF03a | 670.0 | Gh | 0 | 0.04731 | 333.0 | -11.9 | 168.5 | -59.1 | 168.5 | -59.1 | 26.0 |
| JBF03a | 675.0 | Gh | 0 | 0.03363 | 330.9 | -13.7 | 163.3 | -58.6 | 163.3 | -58.6 | 27.0 |

| | | | | | | | | | | | |
|---|---|---|---|---|---|---|---|---|---|---|---|
| JBG01a | 0.0 | Gh | 0 | 0.43556 | 165.1 | -1.1 | 8.3 | 62.7 | 8.3 | 62.7 | 14.5 |
| JBG01a | 100.0 | Gh | 0 | 0.38510 | 163.9 | -2.1 | 7.3 | 61.2 | 7.3 | 61.2 | 15.0 |
| JBG01a | 200.0 | Gh | 0 | 0.30264 | 164.2 | -2.2 | 7.9 | 61.3 | 7.9 | 61.3 | 15.0 |
| JBG01a | 300.0 | Gh | 0 | 0.24781 | 163.2 | -3.4 | 7.5 | 59.7 | 7.5 | 59.7 | 16.0 |
| JBG01a | 400.0 | Gh | 0 | 0.19175 | 161.9 | -5.8 | 7.8 | 57.0 | 7.8 | 57.0 | 14.0 |
| JBG01a | 500.0 | Gh | 0 | 0.12261 | 169.1 | -3.4 | 18.3 | 62.5 | 18.3 | 62.5 | 13.0 |
| JBG01a | 525.0 | Gh | 0 | 0.10495 | 163.0 | -7.3 | 10.9 | 56.3 | 10.9 | 56.3 | 13.0 |
| JBG01a | 550.0 | Gh | 0 | 0.08237 | 165.6 | -10.1 | 17.2 | 54.9 | 17.2 | 54.9 | 13.0 |
| JBG01a | 575.0 | Gh | 0 | 0.07498 | 170.0 | -11.7 | 25.2 | 54.9 | 25.2 | 54.9 | 13.0 |
| JBG01a | 600.0 | Gh | 0 | 0.05654 | 169.7 | -8.8 | 23.2 | 57.6 | 23.2 | 57.6 | 11.0 |
| JBG01a | 625.0 | Gh | 0 | 0.04042 | 179.1 | -15.9 | 41.0 | 52.1 | 41.0 | 52.1 | 11.0 |
| JBG01a | 650.0 | Gh | 0 | 0.02256 | 197.6 | -20.3 | 65.8 | 44.3 | 65.8 | 44.3 | 11.0 |
| JBG01a | 660.0 | Gh | 0 | 0.01484 | 237.7 | -30.3 | 91.1 | 13.8 | 91.1 | 13.8 | 12.5 |
| JBG01a | 670.0 | Gh | 0 | 0.01069 | 285.8 | -53.7 | 82.1 | -26.8 | 82.1 | -26.8 | 12.0 |
| JBG01a | 675.0 | Gh | 0 | 0.01106 | 284.6 | -25.3 | 112.8 | -21.8 | 112.8 | -21.8 | 12.0 |
| | | | | | | | | | | | |
| JBG03a | 0.0 | Gh | 0 | 0.33382 | 158.7 | -3.9 | 1.6 | 59.7 | 1.6 | 59.7 | 11.5 |
| JBG03a | 100.0 | Gh | 0 | 0.28835 | 156.2 | -4.1 | 358.4 | 57.8 | 358.4 | 57.8 | 10.5 |
| JBG03a | 200.0 | Gh | 0 | 0.25353 | 158.1 | -5.2 | 2.4 | 58.3 | 2.4 | 58.3 | 19.0 |
| JBG03a | 300.0 | Gh | 0 | 0.20541 | 156.3 | -6.6 | 1.8 | 56.1 | 1.8 | 56.1 | 9.5 |
| JBG03a | 400.0 | Gh | 0 | 0.14830 | 156.1 | -10.0 | 5.4 | 53.4 | 5.4 | 53.4 | 10.0 |
| JBG03a | 500.0 | Gh | 0 | 0.08888 | 156.3 | -10.3 | 6.0 | 53.3 | 6.0 | 53.3 | 11.0 |
| JBG03a | 525.0 | Gh | 0 | 0.07169 | 154.8 | -9.2 | 2.9 | 53.1 | 2.9 | 53.1 | 10.0 |
| JBG03a | 550.0 | Gh | 0 | 0.06174 | 153.2 | -9.7 | 1.6 | 51.7 | 1.6 | 51.7 | 13.0 |
| JBG03a | 575.0 | Gh | 0 | 0.05066 | 159.0 | -4.7 | 3.1 | 59.3 | 3.1 | 59.3 | 15.5 |
| JBG03a | 600.0 | Gh | 0 | 0.04332 | 153.8 | -9.5 | 2.1 | 52.2 | 2.1 | 52.2 | 16.5 |
| JBG03a | 625.0 | Gh | 0 | 0.02297 | 154.1 | -23.1 | 14.8 | 41.7 | 14.8 | 41.7 | 25.0 |
| JBG03a | 650.0 | Gh | 1 | 0.01321 | 145.7 | -20.4 | 4.6 | 39.0 | 4.6 | 39.0 | 31.0 |
| JBG03a | 660.0 | Gh | 2 | 0.00730 | 25.2 | -67.4 | 35.4 | -38.0 | 35.4 | -38.0 | 34.5 |
| JBG03a | 670.0 | Gh | 3 | 0.00797 | 144.8 | -21.4 | 4.7 | 37.6 | 4.7 | 37.6 | 37.0 |
| JBG03a | 675.0 | Gh | 6 | 0.00426 | 64.1 | -29.0 | 341.0 | -30.9 | 341.0 | -30.9 | 36.5 |
| | | | | | | | | | | | |
| JBH01a | 0.0 | Gh | 0 | 0.22026 | 180.6 | -3.9 | 50.0 | 68.1 | 50.0 | 68.1 | 10.5 |
| JBH01a | 100.0 | Gh | 0 | 0.19031 | 179.4 | -5.4 | 46.9 | 66.6 | 46.9 | 66.6 | 10.0 |
| JBH01a | 200.0 | Gh | 0 | 0.16401 | 179.3 | -7.8 | 46.8 | 64.2 | 46.8 | 64.2 | 11.0 |
| JBH01a | 300.0 | Gh | 0 | 0.13576 | 180.8 | -11.7 | 50.0 | 60.3 | 50.0 | 60.3 | 10.5 |
| JBH01a | 400.0 | Gh | 0 | 0.08568 | 185.4 | -12.7 | 58.6 | 58.8 | 58.6 | 58.8 | 8.0 |
| JBH01a | 500.0 | Gh | 0 | 0.05365 | 201.8 | -10.6 | 87.0 | 54.2 | 87.0 | 54.2 | 8.0 |
| JBH01a | 525.0 | Gh | 0 | 0.05101 | 207.0 | -17.4 | 86.8 | 45.7 | 86.8 | 45.7 | 8.0 |
| JBH01a | 550.0 | Gh | 0 | 0.04470 | 227.2 | -18.8 | 102.4 | 30.8 | 102.4 | 30.8 | 7.0 |
| JBH01a | 575.0 | Gh | 0 | 0.03912 | 221.6 | -20.8 | 96.7 | 33.7 | 96.7 | 33.7 | 8.0 |
| JBH01a | 600.0 | Gh | 0 | 0.03200 | 240.4 | -26.0 | 103.1 | 16.7 | 103.1 | 16.7 | 9.0 |
| JBH01a | 625.0 | Gh | 0 | 0.03248 | 265.3 | -33.0 | 105.6 | -5.9 | 105.6 | -5.9 | 9.5 |
| JBH01a | 650.0 | Gh | 0 | 0.03731 | 286.3 | -25.6 | 117.4 | -22.0 | 117.4 | -22.0 | 8.0 |
| JBH01a | 660.0 | Gh | 0 | 0.04332 | 303.6 | -20.7 | 125.7 | -37.0 | 125.7 | -37.0 | -9.9 |
| JBH01a | 670.0 | Gh | 0 | 0.04349 | 301.4 | -23.3 | 122.2 | -35.3 | 122.2 | -35.3 | 9.0 |
| JBH01a | 675.0 | Gh | 0 | 0.04766 | 305.8 | -20.7 | 126.0 | -39.0 | 126.0 | -39.0 | 16.5 |
| | | | | | | | | | | | |
| JBH03a | 0.0 | Gh | 0 | 0.38193 | 162.5 | 5.4 | 2.9 | 65.6 | 2.9 | 65.6 | 9.0 |
| JBH03a | 100.0 | Gh | 0 | 0.34225 | 161.9 | 5.2 | 2.2 | 65.1 | 2.2 | 65.1 | 9.0 |
| JBH03a | 200.0 | Gh | 0 | 0.29947 | 161.9 | 4.3 | 3.6 | 64.4 | 3.6 | 64.4 | 10.0 |
| JBH03a | 300.0 | Gh | 0 | 0.25066 | 160.3 | 4.3 | 0.9 | 63.3 | 0.9 | 63.3 | 8.5 |

| | | | | | | | | | | | |
|---|---|---|---|---|---|---|---|---|---|---|---|
| JBH03a | 400.0 | Gh | 0 | 0.17678 | 161.6 | 3.1 | 4.9 | 63.3 | 4.9 | 63.3 | 4.0 |
| JBH03a | 500.0 | Gh | 0 | 0.11275 | 161.5 | -0.8 | 9.8 | 60.2 | 9.8 | 60.2 | 8.5 |
| JBH03a | 525.0 | Gh | 0 | 0.09684 | 162.5 | -2.8 | 13.6 | 59.1 | 13.6 | 59.1 | 8.0 |
| JBH03a | 550.0 | Gh | 0 | 0.08454 | 162.7 | -4.1 | 15.3 | 58.1 | 15.3 | 58.1 | 9.0 |
| JBH03a | 575.0 | Gh | 0 | 0.06841 | 160.0 | -7.2 | 14.1 | 54.0 | 14.1 | 54.0 | 10.5 |
| JBH03a | 600.0 | Gh | 0 | 0.06215 | 162.9 | -9.3 | 20.1 | 53.6 | 20.1 | 53.6 | 12.5 |
| JBH03a | 625.0 | Gh | 0 | 0.04168 | 168.3 | -12.6 | 30.4 | 52.6 | 30.4 | 52.6 | 29.0 |
| JBH03a | 650.0 | Gh | 0 | 0.02499 | 177.1 | -5.6 | 43.4 | 61.3 | 43.4 | 61.3 | 32.0 |
| JBH03a | 660.0 | Gh | 0 | 0.01505 | 203.9 | -32.1 | 72.8 | 30.4 | 72.8 | 30.4 | 34.0 |
| JBH03a | 670.0 | Gh | 1 | 0.00877 | 246.5 | -54.6 | 81.7 | -6.1 | 81.7 | -6.1 | 33.0 |
| JBH03a | 675.0 | Gh | 1 | 0.00865 | 262.9 | -73.4 | 67.0 | -20.0 | 67.0 | -20.0 | 34.0 |
| | | | | | | | | | | | |
| JBI01 | 0.0 | Gh | 0 | 0.27768 | 193.6 | -5.7 | 54.6 | 59.3 | 54.6 | 59.3 | 8.0 |
| JBI01 | 100.0 | Gh | 0 | 0.22327 | 194.5 | -10.7 | 52.4 | 54.3 | 52.4 | 54.3 | 8.0 |
| JBI01 | 200.0 | Gh | 0 | 0.18478 | 197.8 | -11.9 | 56.4 | 51.9 | 56.4 | 51.9 | 8.5 |
| JBI01 | 300.0 | Gh | 0 | 0.15450 | 202.3 | -13.2 | 61.3 | 48.6 | 61.3 | 48.6 | 9.0 |
| JBI01 | 400.0 | Gh | 0 | 0.11024 | 216.9 | -13.6 | 76.3 | 39.2 | 76.3 | 39.2 | 9.0 |
| JBI01 | 500.0 | Gh | 0 | 0.08002 | 239.9 | -10.2 | 95.1 | 23.0 | 95.1 | 23.0 | 7.0 |
| JBI01 | 525.0 | Gh | 0 | 0.07059 | 245.4 | -7.7 | 100.2 | 19.4 | 100.2 | 19.4 | 7.5 |
| JBI01 | 550.0 | Gh | 0 | 0.06736 | 253.7 | -6.5 | 105.0 | 12.5 | 105.0 | 12.5 | 6.0 |
| JBI01 | 575.0 | Gh | 0 | 0.06680 | 263.0 | -6.2 | 109.0 | 4.1 | 109.0 | 4.1 | 6.0 |
| JBI01 | 600.0 | Gh | 0 | 0.06556 | 273.9 | -5.5 | 113.7 | -5.7 | 113.7 | -5.7 | 8.0 |
| JBI01 | 625.0 | Gh | 0 | 0.06811 | 289.1 | -1.4 | 123.4 | -18.2 | 123.4 | -18.2 | 8.0 |
| JBI01 | 650.0 | Gh | 0 | 0.07129 | 297.5 | -0.9 | 127.5 | -25.7 | 127.5 | -25.7 | 8.5 |
| JBI01 | 660.0 | Gh | 0 | 0.06810 | 306.4 | 2.2 | 135.2 | -32.4 | 135.2 | -32.4 | 9.0 |
| JBI01 | 670.0 | Gh | 0 | 0.06390 | 301.2 | 2.3 | 132.5 | -27.7 | 132.5 | -27.7 | 10.0 |
| JBI01 | 675.0 | Gh | 0 | 0.04546 | 308.4 | 4.9 | 139.1 | -32.8 | 139.1 | -32.8 | 9.5 |
| | | | | | | | | | | | |
| JBI03 | 0.0 | Gh | 0 | 0.11429 | 215.9 | 8.4 | 96.0 | 52.3 | 96.0 | 52.3 | 6.0 |
| JBI03 | 100.0 | Gh | 0 | 0.09195 | 230.7 | 6.8 | 103.5 | 38.5 | 103.5 | 38.5 | 5.5 |
| JBI03 | 200.0 | Gh | 0 | 0.08667 | 248.0 | 7.1 | 112.0 | 22.9 | 112.0 | 22.9 | 5.0 |
| JBI03 | 300.0 | Gh | 0 | 0.08725 | 256.8 | 8.8 | 117.3 | 15.6 | 117.3 | 15.6 | 5.5 |
| JBI03 | 400.0 | Gh | 0 | 0.09382 | 269.3 | 10.0 | 123.3 | 4.7 | 123.3 | 4.7 | 5.0 |
| JBI03 | 500.0 | Gh | 0 | 0.09107 | 274.4 | 11.4 | 126.6 | 0.7 | 126.6 | 0.7 | 4.5 |
| JBI03 | 525.0 | Gh | 0 | 0.08776 | 280.7 | 10.7 | 128.6 | -5.2 | 128.6 | -5.2 | 5.0 |
| JBI03 | 550.0 | Gh | 0 | 0.08643 | 278.2 | 11.1 | 127.9 | -2.8 | 127.9 | -2.8 | 4.5 |
| JBI03 | 575.0 | Gh | 0 | 0.08638 | 283.9 | 8.2 | 127.7 | -9.2 | 127.7 | -9.2 | 6.5 |
| JBI03 | 600.0 | Gh | 0 | 0.08498 | 287.7 | 10.5 | 131.5 | -11.5 | 131.5 | -11.5 | 7.5 |
| JBI03 | 625.0 | Gh | 0 | 0.08379 | 292.3 | 8.6 | 131.9 | -16.4 | 131.9 | -16.4 | 11.5 |
| JBI03 | 650.0 | Gh | 0 | 0.07998 | 290.6 | 7.5 | 130.1 | -15.4 | 130.1 | -15.4 | 14.0 |
| JBI03 | 660.0 | Gh | 0 | 0.06478 | 294.3 | 8.8 | 133.1 | -18.0 | 133.1 | -18.0 | 15.0 |
| JBI03 | 670.0 | Gh | 0 | 0.05252 | 287.4 | 14.6 | 135.0 | -9.3 | 135.0 | -9.3 | 17.5 |
| JBI03 | 675.0 | Gh | 1 | 0.01939 | 293.9 | 23.1 | 145.6 | -10.4 | 145.6 | -10.4 | 18.0 |
| | | | | | | | | | | | |
| JBJ01a | 0.0 | Gh | 0 | 0.17404 | 151.9 | 20.3 | 337.1 | 55.5 | 337.1 | 55.5 | 8.0 |
| JBJ01a | 100.0 | Gh | 0 | 0.17314 | 151.3 | 19.8 | 336.8 | 54.8 | 336.8 | 54.8 | 7.5 |
| JBJ01a | 200.0 | Gh | 0 | 0.16465 | 150.4 | 18.7 | 336.7 | 53.4 | 336.7 | 53.4 | 8.5 |
| JBJ01a | 300.0 | Gh | 0 | 0.15938 | 147.4 | 18.2 | 333.4 | 51.3 | 333.4 | 51.3 | 7.5 |
| JBJ01a | 400.0 | Gh | 0 | 0.14175 | 146.7 | 17.4 | 333.3 | 50.3 | 333.3 | 50.3 | 7.5 |
| JBJ01a | 500.0 | Gh | 0 | 0.12253 | 147.8 | 16.5 | 335.5 | 50.2 | 335.5 | 50.2 | 7.0 |
| JBJ01a | 525.0 | Gh | 0 | 0.10704 | 142.8 | 14.8 | 331.2 | 45.9 | 331.2 | 45.9 | 7.0 |
| JBJ01a | 550.0 | Gh | 0 | 0.10252 | 143.2 | 14.2 | 332.1 | 45.7 | 332.1 | 45.7 | 7.0 |
| JBJ01a | 575.0 | Gh | 0 | 0.09443 | 144.3 | 15.2 | 332.5 | 47.1 | 332.5 | 47.1 | 14.0 |

| | | | | | | | | | | | |
|---|---|---|---|---|---|---|---|---|---|---|---|
| JBJ01a | 600.0 | Gh | 0 | 0.08928 | 144.0 | 13.5 | 333.6 | 45.6 | 333.6 | 45.6 | 21.5 |
| JBJ01a | 625.0 | Gh | 1 | 0.09433 | 144.7 | 14.0 | 334.0 | 46.4 | 334.0 | 46.4 | 162.0 |
| JBJ01a | 650.0 | Gh | 0 | 0.08750 | 143.3 | 15.8 | 330.9 | 47.0 | 330.9 | 47.0 | 189.0 |
| JBJ01a | 660.0 | Gh | 0 | 0.06916 | 147.9 | 20.3 | 332.0 | 53.3 | 332.0 | 53.3 | 218.0 |
| JBJ01a | 670.0 | Gh | 2 | 0.01578 | 168.2 | 45.6 | 296.9 | 81.8 | 296.9 | 81.8 | 237.0 |
| JBJ01a | 675.0 | Gh | 1 | 0.02088 | 165.1 | 42.3 | 312.2 | 78.7 | 312.2 | 78.7 | 240.5 |
| | | | | | | | | | | | |
| JBJ03a | 0.0 | Gh | 0 | 0.25021 | 160.6 | 13.3 | 349.4 | 59.1 | 349.4 | 59.1 | 8.0 |
| JBJ03a | 100.0 | Gh | 0 | 0.23897 | 161.1 | 14.2 | 349.3 | 60.1 | 349.3 | 60.1 | 7.0 |
| JBJ03a | 200.0 | Gh | 0 | 0.22494 | 159.3 | 13.2 | 347.4 | 58.4 | 347.4 | 58.4 | 8.0 |
| JBJ03a | 300.0 | Gh | 0 | 0.20727 | 156.1 | 13.4 | 342.3 | 56.8 | 342.3 | 56.8 | 8.0 |
| JBJ03a | 400.0 | Gh | 0 | 0.19377 | 154.8 | 12.9 | 341.0 | 55.7 | 341.0 | 55.7 | 8.0 |
| JBJ03a | 500.0 | Gh | 0 | 0.12962 | 154.7 | 12.3 | 341.5 | 55.1 | 341.5 | 55.1 | 7.5 |
| JBJ03a | 525.0 | Gh | 0 | 0.12333 | 154.8 | 12.7 | 341.2 | 55.5 | 341.2 | 55.5 | 7.0 |
| JBJ03a | 550.0 | Gh | 0 | 0.10434 | 152.2 | 10.9 | 339.5 | 52.6 | 339.5 | 52.6 | 12.5 |
| JBJ03a | 575.0 | Gh | 0 | 0.09959 | 152.1 | 11.8 | 338.5 | 53.2 | 338.5 | 53.2 | 12.5 |
| JBJ03a | 600.0 | Gh | 0 | 0.09635 | 150.8 | 9.9 | 338.7 | 50.9 | 338.7 | 50.9 | 47.0 |
| JBJ03a | 625.0 | Gh | 1 | 0.09097 | 153.4 | 8.1 | 343.7 | 51.0 | 343.7 | 51.0 | 82.0 |
| JBJ03a | 650.0 | Gh | 3 | 0.07874 | 164.4 | 8.5 | 359.6 | 56.4 | 359.6 | 56.4 | 346.5 |
| JBJ03a | 660.0 | Gh | 3 | 0.07808 | 157.8 | 18.2 | 339.3 | 61.7 | 339.3 | 61.7 | 456.5 |
| JBJ03a | 670.0 | Gh | 3 | 0.05938 | 161.2 | 17.2 | 346.2 | 62.7 | 346.2 | 62.7 | 509.5 |
| JBJ03a | 675.0 | Gh | 3 | 0.05637 | 151.9 | 17.8 | 331.4 | 57.7 | 331.4 | 57.7 | 528.0 |
| | | | | | | | | | | | |
| JBJ05a | 0.0 | Gh | 0 | 0.33992 | 159.5 | 13.3 | 345.4 | 60.0 | 345.4 | 60.0 | 9.5 |
| JBJ05a | 100.0 | Gh | 0 | 0.32566 | 158.4 | 13.7 | 343.1 | 59.8 | 343.1 | 59.8 | 10.0 |
| JBJ05a | 200.0 | Gh | 0 | 0.29610 | 157.9 | 13.8 | 342.3 | 59.6 | 342.3 | 59.6 | 10.0 |
| JBJ05a | 300.0 | Gh | 0 | 0.27683 | 156.4 | 14.1 | 339.6 | 58.9 | 339.6 | 58.9 | 9.0 |
| JBJ05a | 400.0 | Gh | 0 | 0.24856 | 156.1 | 15.1 | 338.0 | 59.5 | 338.0 | 59.5 | 9.5 |
| JBJ05a | 500.0 | Gh | 0 | 0.18699 | 155.9 | 15.4 | 337.3 | 59.6 | 337.3 | 59.6 | 10.5 |
| JBJ05a | 525.0 | Gh | 0 | 0.17861 | 155.6 | 16.0 | 336.1 | 59.9 | 336.1 | 59.9 | 11.0 |
| JBJ05a | 550.0 | Gh | 0 | 0.14825 | 155.5 | 17.2 | 334.3 | 60.7 | 334.3 | 60.7 | 17.0 |
| JBJ05a | 575.0 | Gh | 0 | 0.14242 | 154.0 | 16.4 | 333.3 | 59.2 | 333.3 | 59.2 | 18.0 |
| JBJ05a | 600.0 | Gh | 0 | 0.12239 | 154.4 | 17.7 | 332.1 | 60.4 | 332.1 | 60.4 | 47.5 |
| JBJ05a | 625.0 | Gh | 0 | 0.12872 | 150.7 | 16.0 | 329.6 | 56.7 | 329.6 | 56.7 | 104.5 |
| JBJ05a | 650.0 | Gh | 2 | 0.12291 | 164.9 | 14.1 | 354.0 | 63.4 | 354.0 | 63.4 | 437.0 |
| JBJ05a | 660.0 | Gh | 3 | 0.15908 | 151.2 | 9.1 | 338.1 | 51.8 | 338.1 | 51.8 | 702.5 |
| JBJ05a | 670.0 | Gh | 5 | 0.13890 | 176.7 | 10.3 | 21.2 | 63.1 | 21.2 | 63.1 | 891.0 |
| JBJ05a | 675.0 | Gh | 7 | 0.12452 | 138.6 | 9.6 | 324.0 | 43.7 | 324.0 | 43.7 | 1035 |
| | | | | | | | | | | | |
| JBK01 | 0.0 | Gh | 0 | 0.02438 | 159.3 | 6.3 | 331.3 | 62.8 | 331.3 | 62.8 | 7.0 |
| JBK01 | 100.0 | Gh | 0 | 0.02249 | 159.7 | 5.6 | 333.0 | 62.5 | 333.0 | 62.5 | 6.0 |
| JBK01 | 200.0 | Gh | 0 | 0.02186 | 158.2 | 4.0 | 332.9 | 60.3 | 332.9 | 60.3 | 7.0 |
| JBK01 | 300.0 | Gh | 0 | 0.02136 | 155.6 | 0.8 | 333.4 | 56.2 | 333.4 | 56.2 | 7.0 |
| JBK01 | 400.0 | Gh | 0 | 0.02066 | 154.2 | 1.3 | 331.0 | 55.6 | 331.0 | 55.6 | 6.0 |
| JBK01 | 500.0 | Gh | 0 | 0.01928 | 156.8 | -0.8 | 336.9 | 55.8 | 336.9 | 55.8 | 7.0 |
| JBK01 | 525.0 | Gh | 0 | 0.01902 | 157.1 | 1.3 | 334.9 | 57.6 | 334.9 | 57.6 | 5.5 |
| JBK01 | 550.0 | Gh | 0 | 0.01856 | 157.7 | 0.5 | 336.7 | 57.4 | 336.7 | 57.4 | 6.0 |
| JBK01 | 575.0 | Gh | 0 | 0.01762 | 156.7 | 2.1 | 333.3 | 57.9 | 333.3 | 57.9 | 6.0 |
| JBK01 | 600.0 | Gh | 0 | 0.01795 | 157.0 | 2.5 | 333.2 | 58.4 | 333.2 | 58.4 | 13.5 |
| JBK01 | 625.0 | Gh | 1 | 0.01825 | 157.8 | 0.3 | 337.1 | 57.3 | 337.1 | 57.3 | 21.5 |
| JBK01 | 650.0 | Gh | 2 | 0.02019 | 154.3 | 1.8 | 330.5 | 56.0 | 330.5 | 56.0 | 43.0 |
| JBK01 | 660.0 | Gh | 1 | 0.01833 | 157.8 | 2.4 | 334.5 | 58.9 | 334.5 | 58.9 | 55.5 |
| JBK01 | 670.0 | Gh | 1 | 0.01863 | 156.2 | 3.4 | 330.9 | 58.5 | 330.9 | 58.5 | 62.5 |

| | | | | | | | | | | | |
|---|---|---|---|---|---|---|---|---|---|---|---|
| JBK01 | 675.0 | Gh | 1 | 0.01852 | 157.2 | 2.1 | 334.0 | 58.3 | 334.0 | 58.3 | 67.0 |
| | | | | | | | | | | | |
| JBK03a | 0.0 | Gh | 0 | 0.22783 | 160.0 | 0.0 | 358.3 | 54.5 | 358.3 | 54.5 | 9.0 |
| JBK03a | 100.0 | Gh | 0 | 0.22374 | 157.2 | 0.1 | 354.3 | 53.1 | 354.3 | 53.1 | 9.5 |
| JBK03a | 200.0 | Gh | 0 | 0.22137 | 156.7 | -0.2 | 353.8 | 52.5 | 353.8 | 52.5 | 9.0 |
| JBK03a | 300.0 | Gh | 0 | 0.21372 | 154.7 | -0.3 | 351.3 | 51.3 | 351.3 | 51.3 | 9.0 |
| JBK03a | 400.0 | Gh | 0 | 0.19845 | 155.0 | -0.8 | 352.1 | 51.1 | 352.1 | 51.1 | 9.0 |
| JBK03a | 500.0 | Gh | 0 | 0.16931 | 155.0 | -1.0 | 352.3 | 50.9 | 352.3 | 50.9 | 9.0 |
| JBK03a | 525.0 | Gh | 0 | 0.16018 | 154.1 | -1.7 | 351.8 | 49.8 | 351.8 | 49.8 | 9.0 |
| JBK03a | 550.0 | Gh | 0 | 0.15053 | 153.7 | -1.8 | 351.4 | 49.5 | 351.4 | 49.5 | 9.0 |
| JBK03a | 575.0 | Gh | 0 | 0.14468 | 153.3 | -0.9 | 350.1 | 50.0 | 350.1 | 50.0 | 13.0 |
| JBK03a | 600.0 | Gh | 0 | 0.13528 | 155.6 | -0.4 | 352.6 | 51.7 | 352.6 | 51.7 | 52.0 |
| JBK03a | 625.0 | Gh | 1 | 0.12658 | 155.6 | -3.8 | 355.5 | 48.9 | 355.5 | 48.9 | 106.0 |
| JBK03a | 650.0 | Gh | 1 | 0.11180 | 165.4 | 0.4 | 6.6 | 57.3 | 6.6 | 57.3 | 219.5 |
| JBK03a | 660.0 | Gh | 2 | 0.08389 | 146.2 | -7.4 | 347.9 | 40.5 | 347.9 | 40.5 | 338.0 |
| JBK03a | 670.0 | Gh | 3 | 0.10266 | 125.0 | 8.6 | 315.2 | 34.5 | 315.2 | 34.5 | 454.5 |
| JBK03a | 675.0 | Gh | 6 | 0.10252 | 132.4 | -7.5 | 335.8 | 30.9 | 335.8 | 30.9 | 607.0 |
| | | | | | | | | | | | |
| JBL01ai | 0.0 | Gh | 0 | 0.07361 | 331.5 | -24.6 | 88.0 | -58.7 | 88.0 | -58.7 | 8.5 |
| JBL01ai | 100.0 | Gh | 0 | 0.07467 | 338.2 | -25.0 | 81.1 | -63.8 | 81.1 | -63.8 | 8.0 |
| JBL01ai | 200.0 | Gh | 0 | 0.08956 | 341.5 | -19.1 | 90.0 | -69.4 | 90.0 | -69.4 | 8.0 |
| JBL01ai | 300.0 | Gh | 0 | 0.09419 | 341.2 | -15.7 | 99.5 | -70.5 | 99.5 | -70.5 | 9.0 |
| JBL01ai | 400.0 | Gh | 0 | 0.09122 | 343.4 | -11.8 | 110.2 | -73.4 | 110.2 | -73.4 | 7.0 |
| JBL01ai | 500.0 | Gh | 0 | 0.07035 | 340.7 | -11.6 | 111.9 | -70.8 | 111.9 | -70.8 | 7.0 |
| JBL01ai | 525.0 | Gh | 0 | 0.06329 | 338.8 | -17.5 | 96.8 | -67.7 | 96.8 | -67.7 | 6.5 |
| JBL01ai | 550.0 | Gh | 0 | 0.06537 | 341.7 | -17.4 | 94.3 | -70.3 | 94.3 | -70.3 | 7.5 |
| JBL01ai | 575.0 | Gh | 0 | 0.06207 | 339.8 | -16.9 | 97.5 | -68.8 | 97.5 | -68.8 | 6.5 |
| JBL01ai | 600.0 | Gh | 0 | 0.06063 | 339.1 | -10.8 | 114.6 | -69.3 | 114.6 | -69.3 | 7.0 |
| JBL01ai | 625.0 | Gh | 0 | 0.06027 | 334.8 | -11.5 | 113.5 | -65.1 | 113.5 | -65.1 | 7.5 |
| JBL01ai | 650.0 | Gh | 0 | 0.05943 | 336.9 | -14.5 | 105.5 | -66.7 | 105.5 | -66.7 | 7.0 |
| JBL01ai | 660.0 | Gh | 0 | 0.05743 | 337.5 | -16.0 | 101.5 | -67.0 | 101.5 | -67.0 | 7.0 |
| JBL01ai | 670.0 | Gh | 0 | 0.04731 | 334.0 | -14.7 | 106.3 | -63.9 | 106.3 | -63.9 | 8.0 |
| JBL01ai | 675.0 | Gh | 0 | 0.04343 | 336.5 | -13.2 | 108.9 | -66.6 | 108.9 | -66.6 | 7.5 |
| | | | | | | | | | | | |
| JBL01aii | 0.0 | Gh | 0 | 0.11801 | 322.7 | -15.1 | 108.2 | -53.1 | 108.2 | -53.1 | 8.0 |
| JBL01aii | 100.0 | Gh | 0 | 0.13325 | 327.2 | -13.1 | 111.1 | -57.6 | 111.1 | -57.6 | 8.0 |
| JBL01aii | 200.0 | Gh | 0 | 0.15212 | 331.8 | -11.0 | 114.9 | -62.2 | 114.9 | -62.2 | 8.5 |
| JBL01aii | 300.0 | Gh | 0 | 0.15449 | 329.0 | -11.8 | 113.4 | -59.4 | 113.4 | -59.4 | 7.0 |
| JBL01aii | 400.0 | Gh | 0 | 0.12455 | 329.7 | -9.1 | 118.8 | -60.1 | 118.8 | -60.1 | 8.0 |
| JBL01aii | 500.0 | Gh | 0 | 0.09306 | 328.8 | -9.6 | 117.7 | -59.2 | 117.7 | -59.2 | 7.0 |
| JBL01aii | 525.0 | Gh | 0 | 0.08985 | 329.8 | -9.7 | 117.6 | -60.2 | 117.6 | -60.2 | 7.0 |
| JBL01aii | 550.0 | Gh | 0 | 0.08780 | 327.2 | -12.0 | 113.2 | -57.6 | 113.2 | -57.6 | 7.0 |
| JBL01aii | 575.0 | Gh | 0 | 0.09421 | 329.2 | -11.2 | 114.6 | -59.6 | 114.6 | -59.6 | 6.5 |
| JBL01aii | 600.0 | Gh | 0 | 0.09275 | 324.3 | -12.1 | 113.1 | -54.8 | 113.1 | -54.8 | 6.5 |
| JBL01aii | 625.0 | Gh | 0 | 0.08514 | 327.7 | -9.2 | 118.4 | -58.1 | 118.4 | -58.1 | 7.0 |
| JBL01aii | 650.0 | Gh | 0 | 0.07685 | 327.9 | -6.3 | 123.9 | -58.1 | 123.9 | -58.1 | 7.0 |
| JBL01aii | 660.0 | Gh | 0 | 0.07290 | 327.3 | -7.3 | 121.9 | -57.6 | 121.9 | -57.6 | 6.0 |
| JBL01aii | 670.0 | Gh | 0 | 0.07053 | 326.5 | -11.1 | 114.9 | -57.0 | 114.9 | -57.0 | 7.0 |
| JBL01aii | 675.0 | Gh | 0 | 0.06177 | 332.5 | -9.5 | 118.1 | -62.9 | 118.1 | -62.9 | 7.0 |
| | | | | | | | | | | | |
| JBM01a | 0.0 | Gh | 0 | 0.09679 | 204.8 | -5.7 | 80.7 | 56.6 | 80.7 | 56.6 | 10.5 |
| JBM01a | 100.0 | Gh | 0 | 0.07185 | 196.1 | -11.3 | 61.8 | 57.5 | 61.8 | 57.5 | 10.0 |
| JBM01a | 200.0 | Gh | 0 | 0.03249 | 199.5 | -23.8 | 57.0 | 45.0 | 57.0 | 45.0 | 11.5 |

| | | | | | | | | | | | |
|---|---|---|---|---|---|---|---|---|---|---|---|
| JBM01a | 300.0 | Gh | 0 | 0.01691 | 157.2 | -30.2 | 6.3 | 37.9 | 6.3 | 37.9 | 11.0 |
| JBM01a | 400.0 | Gh | 0 | 0.01117 | 168.2 | 18.0 | 294.6 | 78.7 | 294.6 | 78.7 | 9.5 |
| JBM01a | 500.0 | Gh | 0 | 0.02079 | 17.1 | -51.2 | 13.5 | -53.2 | 13.5 | -53.2 | 9.0 |
| JBM01a | 525.0 | Gh | 0 | 0.01902 | 2.3 | -26.6 | 19.3 | -80.2 | 19.3 | -80.2 | 8.5 |
| JBM01a | 550.0 | Gh | 0 | 0.03103 | 342.8 | -38.6 | 62.8 | -63.7 | 62.8 | -63.7 | 8.0 |
| JBM01a | 575.0 | Gh | 0 | 0.02006 | 354.7 | -21.0 | 82.0 | -83.6 | 82.0 | -83.6 | 7.5 |
| JBM01a | 600.0 | Gh | 0 | 0.02861 | 345.8 | -37.2 | 60.4 | -66.2 | 60.4 | -66.2 | 9.0 |
| JBM01a | 625.0 | Gh | 0 | 0.02392 | 349.3 | -16.7 | 121.5 | -79.8 | 121.5 | -79.8 | 8.0 |
| JBM01a | 650.0 | Gh | 0 | 0.02859 | 335.5 | -23.9 | 100.6 | -66.1 | 100.6 | -66.1 | 7.5 |
| JBM01a | 660.0 | Gh | 0 | 0.02747 | 344.7 | -22.2 | 99.1 | -74.7 | 99.1 | -74.7 | 8.5 |
| JBM01a | 670.0 | Gh | 0 | 0.02427 | 341.4 | 0.1 | 162.6 | -64.9 | 162.6 | -64.9 | 9.0 |
| JBM01a | 675.0 | Gh | 0 | 0.02011 | 349.4 | -17.7 | 115.9 | -79.9 | 115.9 | -79.9 | 8.0 |
| | | | | | | | | | | | |
| JBM03a | 0.0 | Gh | 0 | 0.01631 | 183.4 | -52.3 | 32.5 | 13.6 | 32.5 | 13.6 | 9.5 |
| JBM03a | 100.0 | Gh | 0 | 0.02605 | 339.9 | -34.7 | 84.3 | -69.5 | 84.3 | -69.5 | 9.5 |
| JBM03a | 200.0 | Gh | 0 | 0.02624 | 338.2 | -33.9 | 87.9 | -68.6 | 87.9 | -68.6 | 9.5 |
| JBM03a | 300.0 | Gh | 0 | 0.03601 | 338.7 | -17.5 | 134.5 | -69.1 | 134.5 | -69.1 | 9.0 |
| JBM03a | 400.0 | Gh | 0 | 0.04883 | 346.5 | -19.9 | 135.9 | -76.8 | 135.9 | -76.8 | 8.5 |
| JBM03a | 500.0 | Gh | 0 | 0.02918 | 8.2 | -19.0 | 268.7 | -80.9 | 268.7 | -80.9 | 7.0 |
| JBM03a | 525.0 | Gh | 0 | 0.03188 | 7.3 | -25.4 | 313.8 | -83.2 | 313.8 | -83.2 | 7.0 |
| JBM03a | 550.0 | Gh | 0 | 0.03816 | 359.2 | -23.0 | 174.0 | -88.8 | 174.0 | -88.8 | 8.5 |
| JBM03a | 575.0 | Gh | 0 | 0.03689 | 11.0 | -24.2 | 303.8 | -80.0 | 303.8 | -80.0 | 8.0 |
| JBM03a | 600.0 | Gh | 0 | 0.04372 | 340.1 | -16.2 | 139.4 | -69.8 | 139.4 | -69.8 | 7.0 |
| JBM03a | 625.0 | Gh | 0 | 0.03643 | 343.6 | -29.2 | 97.3 | -74.5 | 97.3 | -74.5 | 8.0 |
| JBM03a | 650.0 | Gh | 0 | 0.03115 | 341.0 | -15.3 | 142.9 | -70.1 | 142.9 | -70.1 | 8.0 |
| JBM03a | 660.0 | Gh | 0 | 0.03256 | 346.1 | -9.1 | 166.4 | -70.0 | 166.4 | -70.0 | 10.5 |
| JBM03a | 670.0 | Gh | 0 | 0.03210 | 337.9 | -14.5 | 140.9 | -67.1 | 140.9 | -67.1 | 12.5 |
| JBM03a | 675.0 | Gh | 0 | 0.02020 | 330.7 | -18.8 | 125.5 | -62.3 | 125.5 | -62.3 | 13.0 |
| | | | | | | | | | | | |
| JBN01a | 0.0 | Gh | 0 | 0.23841 | 181.0 | 49.6 | 189.4 | 87.3 | 189.4 | 87.3 | 13.5 |
| JBN01a | 100.0 | Gh | 0 | 0.16743 | 190.0 | 46.1 | 109.6 | 83.1 | 109.6 | 83.1 | 14.0 |
| JBN01a | 200.0 | Gh | 0 | 0.15973 | 190.1 | 48.2 | 127.1 | 83.1 | 127.1 | 83.1 | 14.5 |
| JBN01a | 300.0 | Gh | 0 | 0.11683 | 206.2 | 53.2 | 143.5 | 72.2 | 143.5 | 72.2 | 13.0 |
| JBN01a | 400.0 | Gh | 0 | 0.09899 | 222.3 | 52.4 | 140.5 | 62.5 | 140.5 | 62.5 | 12.0 |
| JBN01a | 500.0 | Gh | 0 | 0.06210 | 220.4 | 56.9 | 150.4 | 63.7 | 150.4 | 63.7 | 8.0 |
| JBN01a | 525.0 | Gh | 0 | 0.05261 | 245.8 | 57.8 | 154.1 | 50.2 | 154.1 | 50.2 | 8.0 |
| JBN01a | 550.0 | Gh | 0 | 0.05198 | 266.9 | 56.7 | 158.4 | 39.2 | 158.4 | 39.2 | 8.5 |
| JBN01a | 575.0 | Gh | 0 | 0.03959 | 259.3 | 51.3 | 149.5 | 40.5 | 149.5 | 40.5 | 7.5 |
| JBN01a | 600.0 | Gh | 0 | 0.06525 | 295.5 | 51.2 | 165.6 | 22.7 | 165.6 | 22.7 | 7.0 |
| JBN01a | 625.0 | Gh | 0 | 0.04859 | 300.8 | 54.3 | 170.4 | 23.0 | 170.4 | 23.0 | 8.0 |
| JBN01a | 650.0 | Gh | 0 | 0.05930 | 325.1 | 57.1 | 184.3 | 18.1 | 184.3 | 18.1 | 8.0 |
| JBN01a | 660.0 | Gh | 0 | 0.05398 | 307.6 | 52.6 | 172.8 | 19.2 | 172.8 | 19.2 | 8.0 |
| JBN01a | 670.0 | Gh | 0 | 0.03320 | 303.8 | 59.0 | 175.1 | 25.6 | 175.1 | 25.6 | 8.5 |
| JBN01a | 675.0 | Gh | 0 | 0.03305 | 311.4 | 44.7 | 170.5 | 11.2 | 170.5 | 11.2 | 8.5 |
| | | | | | | | | | | | |
| JBN03 | 0.0 | Gh | 0 | 1.27829 | 174.5 | 17.9 | 15.0 | 62.5 | 15.0 | 62.5 | 42.0 |
| JBN03 | 100.0 | Gh | 0 | 0.43786 | 168.8 | 15.7 | 5.0 | 59.2 | 5.0 | 59.2 | 51.5 |
| JBN03 | 200.0 | Gh | 0 | 0.38508 | 168.7 | 16.2 | 4.5 | 59.7 | 4.5 | 59.7 | 53.0 |
| JBN03 | 300.0 | Gh | 0 | 0.24646 | 168.8 | 11.3 | 7.0 | 55.0 | 7.0 | 55.0 | 53.5 |
| JBN03 | 400.0 | Gh | 0 | 0.10809 | 189.8 | 23.3 | 49.9 | 66.9 | 49.9 | 66.9 | 43.0 |
| JBN03 | 500.0 | Gh | 0 | 0.06960 | 251.8 | 83.5 | 197.4 | 46.7 | 197.4 | 46.7 | 35.5 |
| JBN03 | 525.0 | Gh | 0 | 0.04610 | 166.3 | 67.5 | 219.5 | 66.4 | 219.5 | 66.4 | 31.5 |
| JBN03 | 550.0 | Gh | 0 | 0.01498 | 162.4 | -7.3 | 4.8 | 35.4 | 4.8 | 35.4 | 27.0 |

| | | | | | | | | | | | |
|---|---|---|---|---|---|---|---|---|---|---|---|
| JBN03 | 575.0 | Gh | 0 | 0.01404 | 61.5 | 65.9 | 231.0 | 30.5 | 231.0 | 30.5 | 24.0 |
| JBN03 | 600.0 | Gh | 0 | 0.03978 | 286.3 | 13.0 | 137.0 | -2.0 | 137.0 | -2.0 | 18.0 |
| JBN03 | 625.0 | Gh | 0 | 0.04225 | 332.1 | 8.1 | 173.6 | -31.3 | 173.6 | -31.3 | 15.0 |
| JBN03 | 650.0 | Gh | 0 | 0.03978 | 295.1 | -6.7 | 129.9 | -22.4 | 129.9 | -22.4 | 11.0 |
| JBN03 | 660.0 | Gh | 0 | 0.04292 | 272.3 | 19.0 | 131.6 | 11.7 | 131.6 | 11.7 | 10.5 |
| JBN03 | 670.0 | Gh | 0 | 0.05531 | 258.3 | 15.0 | 119.1 | 18.8 | 119.1 | 18.8 | 9.0 |
| JBN03 | 675.0 | Gh | 0 | 0.02358 | 299.8 | 37.9 | 162.5 | 9.0 | 162.5 | 9.0 | 9.0 |
| | | | | | | | | | | | |
| JBO01 | 0.0 | Gh | 0 | 1.10609 | 173.2 | 0.4 | 9.9 | 71.2 | 9.9 | 71.2 | 37.0 |
| JBO01 | 100.0 | Gh | 0 | 0.37001 | 174.1 | 2.2 | 10.6 | 73.2 | 10.6 | 73.2 | 46.0 |
| JBO01 | 200.0 | Gh | 0 | 0.33224 | 176.4 | 4.6 | 16.2 | 76.1 | 16.2 | 76.1 | 48.5 |
| JBO01 | 300.0 | Gh | 0 | 0.17949 | 179.7 | 15.4 | 25.0 | 87.4 | 25.0 | 87.4 | 47.0 |
| JBO01 | 400.0 | Gh | 0 | 0.09469 | 178.1 | 45.7 | 214.3 | 62.3 | 214.3 | 62.3 | 37.0 |
| JBO01 | 500.0 | Gh | 0 | 0.05529 | 93.6 | 62.8 | 240.0 | 17.6 | 240.0 | 17.6 | 31.5 |
| JBO01 | 525.0 | Gh | 0 | 0.05474 | 350.1 | 85.9 | 210.7 | 14.0 | 210.7 | 14.0 | 27.5 |
| JBO01 | 550.0 | Gh | 0 | 0.03351 | 10.2 | 73.3 | 214.3 | 1.5 | 214.3 | 1.5 | 23.5 |
| JBO01 | 575.0 | Gh | 0 | 0.05383 | 356.5 | 72.3 | 210.3 | 0.3 | 210.3 | 0.3 | 21.0 |
| JBO01 | 600.0 | Gh | 0 | 0.05946 | 313.0 | 31.6 | 168.8 | -23.0 | 168.8 | -23.0 | 17.0 |
| JBO01 | 625.0 | Gh | 0 | 0.06379 | 339.0 | 45.0 | 195.3 | -24.2 | 195.3 | -24.2 | 14.0 |
| JBO01 | 650.0 | Gh | 0 | 0.06497 | 336.4 | 42.8 | 192.4 | -25.4 | 192.4 | -25.4 | -9.9 |
| JBO01 | 660.0 | Gh | 0 | 0.07396 | 324.2 | 45.8 | 185.9 | -18.4 | 185.9 | -18.4 | 11.0 |
| JBO01 | 670.0 | Gh | 0 | 0.05463 | 298.7 | 45.1 | 172.9 | -5.9 | 172.9 | -5.9 | 10.0 |
| JBO01 | 675.0 | Gh | 0 | 0.03922 | 343.8 | 31.8 | 193.9 | -37.8 | 193.9 | -37.8 | 9.5 |
| | | | | | | | | | | | |
| JBO03a | 0.0 | Gh | 0 | 0.60726 | 183.8 | 1.0 | 42.5 | 71.6 | 42.5 | 71.6 | 21.5 |
| JBO03a | 100.0 | Gh | 0 | 0.32818 | 191.6 | -2.8 | 59.2 | 65.4 | 59.2 | 65.4 | 24.0 |
| JBO03a | 200.0 | Gh | 0 | 0.31833 | 194.9 | -2.6 | 66.1 | 63.9 | 66.1 | 63.9 | 25.5 |
| JBO03a | 300.0 | Gh | 0 | 0.26643 | 193.5 | -2.0 | 64.1 | 65.2 | 64.1 | 65.2 | 26.5 |
| JBO03a | 400.0 | Gh | 0 | 0.18891 | 209.8 | -2.9 | 86.8 | 53.4 | 86.8 | 53.4 | 23.0 |
| JBO03a | 500.0 | Gh | 0 | 0.11174 | 217.1 | 1.5 | 99.1 | 49.7 | 99.1 | 49.7 | 19.0 |
| JBO03a | 525.0 | Gh | 0 | 0.11309 | 204.4 | 2.0 | 87.9 | 60.7 | 87.9 | 60.7 | 16.5 |
| JBO03a | 550.0 | Gh | 0 | 0.09257 | 197.7 | -4.2 | 69.1 | 61.0 | 69.1 | 61.0 | 15.0 |
| JBO03a | 575.0 | Gh | 0 | 0.05985 | 228.3 | -11.8 | 91.4 | 33.3 | 91.4 | 33.3 | 13.0 |
| JBO03a | 600.0 | Gh | 0 | 0.04795 | 224.2 | 8.9 | 113.4 | 46.1 | 113.4 | 46.1 | 11.0 |
| JBO03a | 625.0 | Gh | 0 | 0.01543 | 249.7 | 56.1 | 174.5 | 26.9 | 174.5 | 26.9 | 9.5 |
| JBO03a | 650.0 | Gh | 0 | 0.01778 | 259.5 | -3.1 | 114.0 | 8.9 | 114.0 | 8.9 | 8.0 |
| JBO03a | 660.0 | Gh | 0 | 0.02116 | 238.2 | 26.1 | 139.3 | 36.2 | 139.3 | 36.2 | 9.0 |
| JBO03a | 670.0 | Gh | 0 | 0.01775 | 236.1 | 38.0 | 154.3 | 38.0 | 154.3 | 38.0 | 8.5 |
| JBO03a | 675.0 | Gh | 0 | 0.02840 | 261.4 | 48.4 | 166.2 | 19.7 | 166.2 | 19.7 | 9.0 |
| | | | | | | | | | | | |
| JBP01a | 0.0 | Gh | 0 | 0.05149 | 184.5 | 8.3 | 40.4 | 77.5 | 40.4 | 77.5 | 7.5 |
| JBP01a | 100.0 | Gh | 0 | 0.01454 | 221.3 | 10.4 | 102.1 | 49.1 | 102.1 | 49.1 | 15.0 |
| JBP01a | 200.0 | Gh | 0 | 0.01481 | 220.9 | 11.1 | 102.9 | 49.7 | 102.9 | 49.7 | 7.0 |
| JBP01a | 300.0 | Gh | 0 | 0.01096 | 225.0 | 28.8 | 130.6 | 48.3 | 130.6 | 48.3 | 7.5 |
| JBP01a | 400.0 | Gh | 0 | 0.01026 | 223.9 | 16.6 | 112.2 | 48.3 | 112.2 | 48.3 | 7.5 |
| JBP01a | 500.0 | Gh | 0 | 0.00700 | 224.2 | 15.6 | 110.8 | 47.8 | 110.8 | 47.8 | 6.5 |
| JBP01a | 525.0 | Gh | 0 | 0.00532 | 263.6 | -0.9 | 106.4 | 5.7 | 106.4 | 5.7 | 7.0 |
| JBP01a | 550.0 | Gh | 0 | 0.00322 | 243.3 | 70.9 | 180.2 | 27.5 | 180.2 | 27.5 | 8.0 |
| JBP01a | 575.0 | Gh | 1 | 0.00346 | 302.0 | 4.9 | 126.6 | -27.8 | 126.6 | -27.8 | 9.0 |
| JBP01a | 600.0 | Gh | 1 | 0.00358 | 238.4 | 5.7 | 103.7 | 31.6 | 103.7 | 31.6 | 13.5 |
| JBP01a | 625.0 | Gh | 1 | 0.00563 | 132.9 | 21.2 | 279.2 | 46.1 | 279.2 | 46.1 | 17.0 |
| JBP01a | 650.0 | Gh | 1 | 0.00484 | 153.1 | 4.8 | 316.0 | 59.7 | 316.0 | 59.7 | 19.0 |
| JBP01a | 660.0 | Gh | 2 | 0.00351 | 122.4 | 78.5 | 210.2 | 25.8 | 210.2 | 25.8 | 21.0 |

| | | | | | | | | | | | |
|---|---|---|---|---|---|---|---|---|---|---|---|
| JBP01a | 670.0 | Gh | 2 | 0.00482 | 148.3 | -24.2 | 343.0 | 36.1 | 343.0 | 36.1 | 22.0 |
| JBP01a | 675.0 | Gh | 7 | 0.00115 | 318.6 | -47.9 | 59.6 | -46.6 | 59.6 | -46.6 | 22.0 |
| | | | | | | | | | | | |
| JBP03a | 0.0 | Gh | 0 | 0.03543 | 199.6 | -2.9 | 77.0 | 66.1 | 77.0 | 66.1 | 14.0 |
| JBP03a | 100.0 | Gh | 0 | 0.02027 | 213.6 | -1.8 | 92.5 | 54.2 | 92.5 | 54.2 | 14.5 |
| JBP03a | 200.0 | Gh | 0 | 0.01985 | 214.5 | -2.5 | 91.9 | 53.1 | 91.9 | 53.1 | 14.5 |
| JBP03a | 300.0 | Gh | 0 | 0.01049 | 189.3 | -5.8 | 50.7 | 70.8 | 50.7 | 70.8 | 14.0 |
| JBP03a | 400.0 | Gh | 0 | 0.00808 | 255.3 | 43.4 | 153.7 | 18.2 | 153.7 | 18.2 | 14.0 |
| JBP03a | 500.0 | Gh | 0 | 0.00811 | 237.3 | 36.4 | 147.8 | 32.7 | 147.8 | 32.7 | 15.5 |
| JBP03a | 525.0 | Gh | 0 | 0.00566 | 245.7 | 34.9 | 145.0 | 26.1 | 145.0 | 26.1 | 16.0 |
| JBP03a | 550.0 | Gh | 0 | 0.00902 | 252.4 | 27.3 | 136.6 | 20.6 | 136.6 | 20.6 | 15.0 |
| JBP03a | 575.0 | Gh | 0 | 0.00831 | 211.7 | 53.6 | 177.2 | 40.5 | 177.2 | 40.5 | 17.0 |
| JBP03a | 600.0 | Gh | 0 | 0.00214 | 305.1 | -77.6 | 32.0 | -17.9 | 32.0 | -17.9 | 19.5 |
| JBP03a | 625.0 | Gh | 2 | 0.00199 | 289.4 | 66.6 | 179.4 | 2.6 | 179.4 | 2.6 | 21.5 |
| JBP03a | 650.0 | Gh | 1 | 0.00332 | 61.7 | -32.8 | 323.0 | -29.6 | 323.0 | -29.6 | 23.0 |
| JBP03a | 660.0 | Gh | 0 | 0.00969 | 170.7 | 6.4 | 317.2 | 79.7 | 317.2 | 79.7 | 25.5 |
| JBP03a | 670.0 | Gh | 1 | 0.00696 | 124.5 | -9.9 | 310.1 | 31.0 | 310.1 | 31.0 | 28.5 |
| JBP03a | 675.0 | Gh | 1 | 0.00434 | 121.5 | -33.8 | 333.0 | 18.7 | 333.0 | 18.7 | 31.0 |
| | | | | | | | | | | | |
| JBQ01a | 0.0 | Gh | 0 | 0.02849 | 164.1 | 8.9 | 355.5 | 71.6 | 355.5 | 71.6 | 16.5 |
| JBQ01a | 100.0 | Gh | 0 | 0.01938 | 168.5 | -7.3 | 30.0 | 61.4 | 30.0 | 61.4 | 12.0 |
| JBQ01a | 200.0 | Gh | 0 | 0.01912 | 169.5 | -8.9 | 33.1 | 60.2 | 33.1 | 60.2 | 12.5 |
| JBQ01a | 300.0 | Gh | 0 | 0.01959 | 163.9 | -18.1 | 30.4 | 49.7 | 30.4 | 49.7 | 12.0 |
| JBQ01a | 400.0 | Gh | 1 | 0.00731 | 142.5 | 2.0 | 344.7 | 49.6 | 344.7 | 49.6 | 17.0 |
| JBQ01a | 500.0 | Gh | 0 | 0.00951 | 154.7 | 4.1 | 352.3 | 61.2 | 352.3 | 61.2 | 17.0 |
| JBQ01a | 525.0 | Gh | 1 | 0.00808 | 174.1 | -47.5 | 50.1 | 23.3 | 50.1 | 23.3 | 17.0 |
| JBQ01a | 550.0 | Gh | 1 | 0.01060 | 159.3 | 33.4 | 282.3 | 66.6 | 282.3 | 66.6 | 17.0 |
| JBQ01a | 575.0 | Gh | 1 | 0.00805 | 161.4 | 15.9 | 331.4 | 72.0 | 331.4 | 72.0 | 18.0 |
| JBQ01a | 600.0 | Gh | 0 | 0.00847 | 115.9 | 19.4 | 312.4 | 29.8 | 312.4 | 29.8 | 18.5 |
| JBQ01a | 625.0 | Gh | 1 | 0.00085 | 302.7 | 56.4 | 206.6 | -0.7 | 206.6 | -0.7 | 18.0 |
| JBQ01a | 650.0 | Gh | 1 | 0.00400 | 231.2 | 37.6 | 178.3 | 41.9 | 178.3 | 41.9 | 18.5 |
| JBQ01a | 660.0 | Gh | 1 | 0.00355 | 190.3 | 32.8 | 202.7 | 73.4 | 202.7 | 73.4 | 18.5 |
| JBQ01a | 670.0 | Gh | 1 | 0.00278 | 286.9 | -32.3 | 116.7 | -24.0 | 116.7 | -24.0 | 19.0 |
| JBQ01a | 675.0 | Gh | 2 | 0.00367 | 171.9 | 18.8 | 324.6 | 82.3 | 324.6 | 82.3 | 19.0 |
| | | | | | | | | | | | |
| JBQ03a | 0.0 | Gh | 0 | 0.03205 | 169.7 | 26.7 | 267.3 | 72.4 | 267.3 | 72.4 | 10.5 |
| JBQ03a | 100.0 | Gh | 0 | 0.01522 | 195.3 | 54.3 | 222.6 | 46.0 | 222.6 | 46.0 | 12.0 |
| JBQ03a | 200.0 | Gh | 0 | 0.01480 | 198.5 | 53.5 | 219.6 | 46.0 | 219.6 | 46.0 | 11.5 |
| JBQ03a | 300.0 | Gh | 0 | 0.01691 | 191.8 | 75.7 | 232.2 | 26.0 | 232.2 | 26.0 | 14.5 |
| JBQ03a | 400.0 | Gh | 4 | 0.00494 | 207.0 | 23.8 | 173.9 | 61.8 | 173.9 | 61.8 | 24.0 |
| JBQ03a | 500.0 | Gh | 3 | 0.00503 | 258.0 | -31.4 | 112.2 | 3.7 | 112.2 | 3.7 | 24.5 |
| JBQ03a | 525.0 | Gh | 2 | 0.00776 | 317.1 | -32.8 | 110.3 | -45.6 | 110.3 | -45.6 | 24.5 |
| JBQ03a | 550.0 | Gh | 1 | 0.00845 | 228.2 | 27.9 | 172.4 | 42.3 | 172.4 | 42.3 | 25.0 |
| JBQ03a | 575.0 | Gh | 1 | 0.01510 | 227.0 | 6.6 | 143.2 | 43.4 | 143.2 | 43.4 | 25.0 |
| JBQ03a | 600.0 | Gh | 0 | 0.02474 | 42.3 | -47.2 | 18.7 | -40.1 | 18.7 | -40.1 | 26.0 |
| JBQ03a | 625.0 | Gh | 0 | 0.01034 | 310.0 | 17.7 | 175.6 | -32.4 | 175.6 | -32.4 | 25.0 |
| JBQ03a | 650.0 | Gh | 1 | 0.00688 | 339.6 | -54.9 | 71.6 | -44.2 | 71.6 | -44.2 | 25.5 |
| JBQ03a | 660.0 | Gh | 0 | 0.01155 | 133.5 | 13.1 | 318.8 | 44.7 | 318.8 | 44.7 | 25.0 |
| JBQ03a | 670.0 | Gh | 0 | 0.00414 | 92.8 | -32.4 | 357.7 | -4.1 | 357.7 | -4.1 | 24.0 |
| JBQ03a | 675.0 | Gh | 1 | 0.00763 | 119.3 | 21.7 | 307.2 | 31.4 | 307.2 | 31.4 | 24.5 |
| | | | | | | | | | | | |
| JBR01 | 0.0 | Gh | 0 | 0.03594 | 165.7 | 7.6 | 10.4 | 70.8 | 10.4 | 70.8 | 16.0 |
| JBR01 | 100.0 | Gh | 0 | 0.01523 | 155.1 | 5.6 | 357.4 | 61.4 | 357.4 | 61.4 | 15.5 |

```
JBR01      200.0  Gh  0 0.01499 153.7   1.3    2.5  57.7    2.5  57.7  15.0
JBR01      300.0  Gh  0 0.00585 167.0  27.2  298.3  76.6  298.3  76.6  16.0
JBR01      400.0  Gh  0 0.00405  78.4 -26.0  349.8 -19.0  349.8 -19.0  14.5
JBR01      500.0  Gh  1 0.00303 242.4 -63.2   82.1  -7.2   82.1  -7.2  15.5
JBR01      525.0  Gh  1 0.00392 171.1  62.2  244.6  48.3  244.6  48.3  16.5
JBR01      550.0  Gh  0 0.00844 261.3  17.6  162.2  14.1  162.2  14.1  16.0
JBR01      575.0  Gh  1 0.00733 107.4 -44.3   15.3  -2.9   15.3  -2.9  22.0
JBR01      600.0  Gh  1 0.00736 143.1  10.0  339.9  52.9  339.9  52.9  26.0
JBR01      625.0  Gh  1 0.01140 194.5   6.9  105.3  70.1  105.3  70.1  34.0
JBR01      650.0  Gh  1 0.00739  68.1  79.8  248.3  16.9  248.3  16.9  40.5
JBR01      660.0  Gh  2 0.00517 163.2   5.3   10.0  67.4   10.0  67.4  48.0
JBR01      670.0  Gh  3 0.00497  47.0 -11.6  324.3 -44.1  324.3 -44.1  54.0
JBR01      675.0  Gh  3 0.00870 350.0  71.0  235.2   2.3  235.2   2.3  58.0

JBR03        0.0  Gh  0 0.03626 151.1  36.4  343.4  65.9  343.4  65.9  16.0
JBR03      100.0  Gh  0 0.01747 119.5  23.3  330.5  36.6  330.5  36.6  17.0
JBR03      200.0  Gh  0 0.01744 119.2  23.7  329.9  36.7  329.9  36.7  16.5
JBR03      300.0  Gh  0 0.01534 108.6   5.0  336.1  16.1  336.1  16.1  16.0
JBR03      400.0  Gh  0 0.00488 157.3  51.1  305.0  75.0  305.0  75.0  16.0
JBR03      500.0  Gh  0 0.00676  84.8  -9.0  327.6 -10.1  327.6 -10.1  17.0
JBR03      525.0  Gh  1 0.00278 154.1  -4.9   24.4  32.4   24.4  32.4  17.5
JBR03      550.0  Gh  0 0.00670   9.5  18.1  245.2 -23.4  245.2 -23.4  18.0
JBR03      575.0  Gh  1 0.00926 292.3  57.4  200.5  29.3  200.5  29.3  25.0
JBR03      600.0  Gh  1 0.01281   0.3  -5.8  235.8 -47.8  235.8 -47.8  30.0
JBR03      625.0  Gh  8 0.00155 156.8 -39.7   37.8  -0.1   37.8  -0.1  39.0
JBR03      650.0  Gh  1 0.00402 225.3  21.3  125.2  45.1  125.2  45.1  47.0
JBR03      660.0  Gh  6 0.00477 127.1  -9.0    0.2  16.4    0.2  16.4  54.5
JBR03      670.0  Gh  5 0.00454 201.2  38.1  120.5  71.7  120.5  71.7  61.5
JBR03      675.0  Gh  4 0.01081 146.9  19.3    0.8  50.8    0.8  50.8  65.0
!_____________________________END OF FILE_____________________________________
```

Table S3. ‘B’ component PCA directions from samples from the Lower and Upper Morrison Fm.

LAT: 38.13  LON:  251.79
!  Principal component analysis (PCA) on Morrison TH data

Lamont datafile format
ID = sample identification (J=Jurassic, M=Morrison, A to L are sampling sites
     followed by drillcore sample number and specimen with 'a' at the bottom if
     more than one.
comp = magnetization component estimated by PCA analysis.
N = number of demagnetization steps analyzed.
F/A = demagnetization trajectory free (F) or anchored (A) to the origin.
MAD = maximum angular deviation (°).
%VAR = percentage variance accounted for by best-fit line.
CDECL, CINCL = declination and inclination in core coordinates.
GDECL, GINCL = declination and inclination in geographic (in-situ) coordinates.
BDECL, BINCL = declination and inclination in tilt-corrected coordinates.
TR1, TR2 = thermal demagnetization step interval analyzed.
Jcomp = component magnetization (10E-4 emu, equivalent to 10E-2 A/m for 10 cc
   volume).

| ID | comp | N | F/A | MAD | %VAR | CDECL | CINCL | GDECL | GINCL | BDECL | BINCL | TR1 | TR2 | Jcomp |
|---|---|---|---|---|---|---|---|---|---|---|---|---|---|---|
| Lower Morrison Fm. (sites JMA-JML): | | | | | | | | | | | | | | |
| JMA01a | B | 6 | F | 17.7 | 90.8 | 189.5 | -26.3 | 15.9 | 34.9 | 15.9 | 34.9 | 500.0 | 660.0 | 0.0699 |
| JMA03a | B | 4 | F | 7.7 | 98.2 | 154.4 | -9.8 | 321.2 | 53.8 | 321.2 | 53.8 | 400.0 | 600.0 | 0.0741 |
| JMA05a | B | 4 | F | 11.7 | 95.9 | 179.2 | -8.5 | 3.3 | 68.4 | 3.3 | 68.4 | 100.0 | 400.0 | 0.0434 |
| JMA11a | B | 5 | F | 21.2 | 87.0 | 148.0 | -14.6 | 333.4 | 44.6 | 333.4 | 44.6 | 200.0 | 600.0 | 0.0525 |
| JMA14a | B | 5 | F | 16.6 | 91.9 | 141.8 | -24.3 | 322.3 | 38.6 | 322.3 | 38.6 | 100.0 | 500.0 | 0.0407 |
| JMA15a | B | 4 | F | 11.0 | 96.3 | 140.2 | -16.6 | 310.6 | 44.1 | 310.6 | 44.1 | 200.0 | 500.0 | 0.0458 |
| JMA16a | B | 7 | F | 6.4 | 98.8 | 196.5 | -8.2 | 27.9 | 61.1 | 27.9 | 61.1 | 100.0 | 600.0 | 0.0705 |
| JMA18a | B | 8 | F | 10.1 | 96.9 | 175.9 | -27.4 | 4.4 | 50.6 | 4.4 | 50.6 | 0.0 | 650.0 | 0.0531 |
| JMA19a | B | 5 | F | 10.2 | 96.9 | 175.8 | -3.8 | 12.8 | 70.7 | 12.8 | 70.7 | 100.0 | 500.0 | 0.0359 |
| JMA20a | B | 7 | F | 19.4 | 89.0 | 168.8 | -7.2 | 5.3 | 70.9 | 5.3 | 70.9 | 0.0 | 550.0 | 0.0624 |
| JMA22a | B | 9 | F | 11.7 | 95.9 | 195.1 | 2.4 | 32.5 | 65.3 | 32.5 | 65.3 | 100.0 | 650.0 | 0.0808 |
| JMA23a | B | 5 | F | 9.6 | 97.2 | 192.2 | -17.7 | 9.6 | 52.4 | 9.6 | 52.4 | 100.0 | 500.0 | 0.0672 |
| JMA25a | B | 10 | F | 9.5 | 97.3 | 184.3 | -9.0 | 26.8 | 59.7 | 26.8 | 59.7 | 0.0 | 650.0 | 0.1113 |
| JMA26a | B | 10 | F | 13.5 | 94.6 | 192.2 | -11.9 | 23.0 | 53.4 | 23.0 | 53.4 | 0.0 | 650.0 | 0.0892 |
| JMA27a | B | 6 | F | 17.5 | 90.9 | 190.4 | -6.7 | 46.2 | 69.5 | 46.2 | 69.5 | 100.0 | 670.0 | 0.0428 |
| JMA28a | B | 5 | F | 6.7 | 98.6 | 185.8 | -2.9 | 30.1 | 69.3 | 30.1 | 69.3 | 100.0 | 500.0 | 0.0409 |
| JMA30a | B | 5 | F | 13.9 | 94.2 | 165.1 | -2.2 | 331.0 | 70.1 | 331.0 | 70.1 | 100.0 | 500.0 | 0.0410 |
| JMA31a | B | 5 | F | 14.4 | 93.8 | 165.9 | -14.1 | 349.6 | 50.4 | 349.6 | 50.4 | 100.0 | 500.0 | 0.0565 |
| JMA34a | B | 4 | F | 13.0 | 94.9 | 205.4 | 2.2 | 44.2 | 37.5 | 44.2 | 37.5 | 100.0 | 400.0 | 0.0481 |
| JMA35a | B | 5 | F | 14.9 | 93.4 | 175.8 | -5.0 | 7.2 | 75.4 | 7.2 | 75.4 | 0.0 | 400.0 | 0.0300 |
| JMA39a | B | 5 | F | 8.8 | 97.6 | 191.0 | -34.9 | 27.8 | 30.2 | 27.8 | 30.2 | 0.0 | 400.0 | 0.0810 |
| JMA40a | B | 4 | F | 13.9 | 94.2 | 174.9 | 0.5 | 3.6 | 66.1 | 3.6 | 66.1 | 0.0 | 300.0 | 0.0630 |
| JMA41a | B | 5 | F | 7.6 | 98.2 | 189.6 | 2.8 | 46.7 | 68.5 | 46.7 | 68.5 | 0.0 | 400.0 | 0.0460 |
| JMA42a | B | 4 | F | 5.4 | 99.1 | 187.3 | 2.7 | 40.6 | 70.4 | 40.6 | 70.4 | 0.0 | 300.0 | 0.0752 |
| JMA43a | B | 4 | F | 19.5 | 88.9 | 203.4 | -35.7 | 34.5 | 26.4 | 34.5 | 26.4 | 300.0 | 550.0 | 0.0522 |
| JMA44a | B | 4 | F | 6.0 | 98.9 | 162.6 | -1.9 | 332.4 | 62.1 | 332.4 | 62.1 | 100.0 | 500.0 | 0.0366 |
| JMA46a | B | 5 | F | 19.6 | 88.8 | 133.8 | -0.8 | 304.0 | 39.4 | 304.0 | 39.4 | 100.0 | 500.0 | 0.0715 |
| JMA50a | B | 4 | F | 11.2 | 96.2 | 143.1 | -19.5 | 323.7 | 37.9 | 323.7 | 37.9 | 200.0 | 500.0 | 0.0408 |
| JMB01a | B | 7 | F | 8.2 | 98.0 | 162.6 | 15.7 | 353.6 | 68.6 | 353.6 | 68.6 | 0.0 | 550.0 | 0.1241 |
| JMB02a | B | 6 | F | 4.8 | 99.3 | 176.3 | 6.1 | 17.1 | 75.8 | 17.1 | 75.8 | 0.0 | 500.0 | 0.0455 |
| JMB03a | B | 6 | F | 6.4 | 98.8 | 176.8 | 5.1 | 3.9 | 81.4 | 3.9 | 81.4 | 0.0 | 500.0 | 0.0891 |
| JMB04a | B | 6 | F | 7.5 | 98.3 | 172.8 | 0.2 | 7.7 | 69.0 | 7.7 | 69.0 | 0.0 | 500.0 | 0.0763 |

| | | | | | | | | | | | | | | |
|---|---|---|---|---|---|---|---|---|---|---|---|---|---|---|
| JMB05a | B | 12 | F | 7.4 | 98.3 | 181.5 | -12.3 | 27.9 | 65.7 | 27.9 | 65.7 | 0.0 | 670.0 | 0.2374 |
| JMB06a | B | 4 | F | 4.1 | 99.5 | 173.9 | -7.3 | 10.6 | 63.9 | 10.6 | 63.9 | 0.0 | 300.0 | 0.0412 |
| JMB07a | B | 8 | F | 6.0 | 98.9 | 194.6 | -6.9 | 24.4 | 55.1 | 24.4 | 55.1 | 0.0 | 600.0 | 0.1639 |
| JMB09ai | B | 9 | F | 8.6 | 97.8 | 185.0 | 2.8 | 2.7 | 63.7 | 2.7 | 63.7 | 0.0 | 625.0 | 0.1911 |
| JMB09aii | B | 5 | F | 17.8 | 90.7 | 203.1 | 4.0 | 37.5 | 57.5 | 37.5 | 57.5 | 500.0 | 650.0 | 0.0508 |
| JMB10a | B | 6 | F | 8.1 | 98.0 | 191.4 | -10.2 | 18.9 | 52.2 | 18.9 | 52.2 | 0.0 | 500.0 | 0.1122 |
| JMB11a | B | 8 | F | 4.7 | 99.3 | 195.6 | -6.1 | 18.2 | 53.6 | 18.2 | 53.6 | 0.0 | 600.0 | 0.1884 |
| JMB12a | B | 6 | F | 7.3 | 98.4 | 186.3 | -1.5 | 9.0 | 67.7 | 9.0 | 67.7 | 0.0 | 500.0 | 0.1106 |
| JMB13a | B | 5 | F | 4.9 | 99.3 | 195.7 | -11.6 | 16.5 | 59.1 | 16.5 | 59.1 | 0.0 | 400.0 | 0.0999 |
| JMB14a | B | 9 | A | 2.8 | 99.8 | 169.2 | -11.6 | 3.5 | 66.9 | 3.5 | 66.9 | 0.0 | 625.0 | 0.2908 |
| JMB15a | B | 5 | F | 4.3 | 99.4 | 192.2 | 14.6 | 26.8 | 61.6 | 26.8 | 61.6 | 100.0 | 500.0 | 0.0973 |
| JMB16a | B | 4 | F | 4.4 | 99.4 | 177.7 | -0.9 | 358.1 | 65.0 | 358.1 | 65.0 | 200.0 | 500.0 | 0.0726 |
| JMB17a | B | 12 | A | 2.7 | 99.8 | 185.2 | -1.9 | 10.5 | 64.6 | 10.5 | 64.6 | 0.0 | 680.0 | 0.2816 |
| JMB18a | B | 9 | A | 4.0 | 99.5 | 190.1 | -0.1 | 24.7 | 62.1 | 24.7 | 62.1 | 100.0 | 650.0 | 0.3004 |
| JMB19a | B | 10 | F | 4.2 | 99.5 | 174.1 | 1.3 | 355.9 | 65.6 | 355.9 | 65.6 | 0.0 | 650.0 | 0.1163 |
| JMB20a | B | 8 | A | 2.6 | 99.8 | 178.2 | -4.7 | 357.7 | 63.3 | 357.7 | 63.3 | 200.0 | 650.0 | 0.3275 |
| JMB21a | B | 7 | F | 5.0 | 99.3 | 188.7 | -4.7 | 22.4 | 63.8 | 22.4 | 63.8 | 0.0 | 550.0 | 0.1573 |
| JMB23a | B | 9 | A | 3.4 | 99.7 | 184.0 | -4.7 | 14.0 | 68.0 | 14.0 | 68.0 | 0.0 | 680.0 | 0.4052 |
| JMB24a | B | 6 | F | 6.1 | 98.9 | 180.5 | 42.4 | 7.3 | 79.4 | 7.3 | 79.4 | 0.0 | 500.0 | 0.0944 |
| JMB25a | B | 7 | F | 7.6 | 98.2 | 179.3 | 8.4 | 10.6 | 67.4 | 10.6 | 67.4 | 0.0 | 550.0 | 0.1419 |
| JMB26a | B | 6 | F | 3.3 | 99.7 | 181.9 | 5.9 | 10.0 | 69.8 | 10.0 | 69.8 | 0.0 | 500.0 | 0.1553 |
| JMB27a | B | 13 | A | 3.0 | 99.7 | 191.5 | 2.2 | 30.1 | 65.5 | 30.1 | 65.5 | 0.0 | 680.0 | 0.3106 |
| JMB28a | B | 6 | F | 4.9 | 99.3 | 184.5 | -9.2 | 10.3 | 63.7 | 10.3 | 63.7 | 0.0 | 550.0 | 0.1523 |
| JMB29 | B | 4 | F | 6.8 | 98.6 | 176.9 | 17.5 | 346.8 | 67.4 | 346.8 | 67.4 | 400.0 | 600.0 | 0.0717 |
| JMB30 | B | 7 | F | 4.0 | 99.5 | 190.4 | 39.4 | 25.7 | 70.9 | 25.7 | 70.9 | 100.0 | 600.0 | 0.1570 |
| JMB31a | B | 11 | F | 3.1 | 99.7 | 160.2 | -1.5 | 351.6 | 66.7 | 351.6 | 66.7 | 0.0 | 660.0 | 0.2614 |
| JMB32a | B | 9 | F | 3.6 | 99.6 | 158.3 | 6.9 | 348.7 | 66.7 | 348.7 | 66.7 | 0.0 | 625.0 | 0.3170 |
| JMB33a | B | 11 | F | 2.2 | 99.9 | 163.9 | 3.7 | 359.5 | 68.1 | 359.5 | 68.1 | 0.0 | 670.0 | 0.3021 |
| JMB34 | B | 10 | F | 3.6 | 99.6 | 160.3 | 6.1 | 2.3 | 66.3 | 2.3 | 66.3 | 0.0 | 650.0 | 0.2534 |
| JMB35a | B | 9 | F | 3.1 | 99.7 | 159.6 | 6.6 | 359.4 | 65.0 | 359.4 | 65.0 | 0.0 | 625.0 | 0.2226 |
| JMB36a | B | 10 | F | 3.7 | 99.6 | 160.1 | 9.8 | 349.5 | 66.3 | 349.5 | 66.3 | 0.0 | 650.0 | 0.1541 |
| JMB37 | B | 4 | F | 14.3 | 93.9 | 170.2 | 15.2 | 357.3 | 78.0 | 357.3 | 78.0 | 200.0 | 500.0 | 0.0302 |
| JMB38a | B | 10 | F | 2.9 | 99.7 | 157.8 | 9.8 | 353.9 | 66.4 | 353.9 | 66.4 | 0.0 | 650.0 | 0.3214 |
| JMB39a | B | 10 | F | 3.3 | 99.7 | 158.6 | -0.1 | 9.9 | 62.3 | 9.9 | 62.3 | 300.0 | 680.0 | 0.2868 |
| JMB40a | B | 8 | F | 4.9 | 99.3 | 170.7 | 4.3 | 352.1 | 74.9 | 352.1 | 74.9 | 0.0 | 650.0 | 0.1489 |
| JMB41a | B | 11 | F | 5.3 | 99.1 | 174.9 | 10.2 | 12.2 | 75.3 | 12.2 | 75.3 | 0.0 | 670.0 | 0.1672 |
| JMB42a | B | 6 | F | 5.9 | 98.9 | 174.1 | -9.4 | 19.5 | 66.9 | 19.5 | 66.9 | 0.0 | 500.0 | 0.1117 |
| JMB43a | B | 6 | F | 7.2 | 98.4 | 183.9 | 3.3 | 44.0 | 69.9 | 44.0 | 69.9 | 0.0 | 500.0 | 0.1211 |
| JMB44a | B | 6 | F | 5.9 | 99.0 | 173.7 | 1.9 | 18.5 | 72.7 | 18.5 | 72.7 | 0.0 | 500.0 | 0.1317 |
| JMB45a | B | 4 | F | 8.6 | 97.8 | 164.2 | -10.7 | 2.6 | 46.8 | 2.6 | 46.8 | 100.0 | 550.0 | 0.0797 |
| JMB46a | B | 6 | F | 5.4 | 99.1 | 185.8 | 4.1 | 24.8 | 61.6 | 24.8 | 61.6 | 0.0 | 500.0 | 0.1067 |
| JMB47a | B | 6 | F | 9.5 | 97.3 | 175.6 | -9.6 | 5.6 | 65.9 | 5.6 | 65.9 | 0.0 | 500.0 | 0.1148 |
| JMB48a | B | 6 | F | 7.4 | 98.4 | 173.6 | 14.2 | 359.7 | 70.3 | 359.7 | 70.3 | 0.0 | 500.0 | 0.1038 |
| JMB49a | B | 6 | F | 8.1 | 98.0 | 171.7 | 14.3 | 352.6 | 70.6 | 352.6 | 70.6 | 0.0 | 500.0 | 0.0843 |
| JMB50a | B | 6 | F | 6.3 | 98.8 | 180.0 | 18.1 | 17.2 | 77.1 | 17.2 | 77.1 | 0.0 | 500.0 | 0.0815 |
| JMC01a | B | 5 | F | 4.7 | 99.3 | 155.0 | 15.1 | 2.8 | 62.6 | 2.8 | 62.6 | 100.0 | 500.0 | 0.0975 |
| JMC02 | B | 15 | F | 5.7 | 99.0 | 157.0 | 18.2 | 357.8 | 67.4 | 357.8 | 67.4 | 0.0 | 675.0 | 0.1846 |
| JMC03a | B | 12 | F | 6.1 | 98.9 | 151.2 | 17.4 | 356.2 | 61.7 | 356.2 | 61.7 | 0.0 | 650.0 | 0.1785 |
| JMC04a | B | 7 | F | 5.4 | 99.1 | 160.4 | 18.2 | 6.1 | 69.1 | 6.1 | 69.1 | 0.0 | 525.0 | 0.1021 |
| JMC05a | B | 10 | F | 2.9 | 99.7 | 155.7 | 12.4 | 352.8 | 65.6 | 352.8 | 65.6 | 0.0 | 600.0 | 0.1893 |
| JMD01a | B | 12 | F | 8.4 | 97.9 | 175.8 | -16.0 | 8.3 | 55.8 | 8.3 | 55.8 | 0.0 | 650.0 | 0.0945 |
| JMD02a | B | 8 | F | 6.9 | 98.6 | 192.5 | -14.6 | 36.8 | 53.2 | 36.8 | 53.2 | 0.0 | 550.0 | 0.1002 |
| JMD03a | B | 4 | F | 4.9 | 99.3 | 177.2 | 2.5 | 7.8 | 68.3 | 7.8 | 68.3 | 0.0 | 400.0 | 0.0637 |
| JMD04a | B | 9 | F | 7.0 | 98.5 | 177.3 | -1.7 | 12.3 | 63.2 | 12.3 | 63.2 | 0.0 | 575.0 | 0.1352 |
| JMD05a | B | 6 | F | 5.8 | 99.0 | 195.5 | -0.9 | 44.1 | 57.5 | 44.1 | 57.5 | 100.0 | 525.0 | 0.0951 |
| JMD06a | B | 4 | F | 8.0 | 98.1 | 183.2 | 24.7 | 21.9 | 77.5 | 21.9 | 77.5 | 0.0 | 300.0 | 0.0588 |
| JME01a | B | 7 | F | 31.0 | 73.4 | 175.8 | -9.7 | 8.9 | 66.0 | 8.9 | 66.0 | 0.0 | 525.0 | 0.0621 |
| JME02a | B | 6 | F | 7.3 | 98.4 | 170.8 | -12.5 | 3.6 | 55.3 | 3.6 | 55.3 | 0.0 | 500.0 | 0.0912 |
| JME04a | B | 5 | F | 8.3 | 97.9 | 170.8 | 5.3 | 354.6 | 68.5 | 354.6 | 68.5 | 0.0 | 400.0 | 0.0532 |
| JMF01a | B | 12 | F | 6.7 | 98.7 | 170.5 | -13.2 | 0.3 | 54.6 | 0.3 | 54.6 | 300.0 | 675.0 | 0.2207 |

| | | | | | | | | | | | | | | |
|---|---|---|---|---|---|---|---|---|---|---|---|---|---|---|
| JMF03a | B | 12 | F | 9.2 | 97.4 | 160.2 | 25.3 | 341.6 | 66.1 | 341.6 | 66.1 | 0.0 | 650.0 | 0.1547 |
| JMG01a | B | 11 | F | 5.8 | 99.0 | 208.4 | 2.8 | 19.6 | 59.5 | 19.6 | 59.5 | 0.0 | 625.0 | 0.2368 |
| JMG02a | B | 11 | F | 4.6 | 99.4 | 209.4 | -4.6 | 5.3 | 53.8 | 5.3 | 53.8 | 100.0 | 650.0 | 0.2004 |
| JMG03a | B | 10 | F | 4.8 | 99.3 | 206.0 | -3.0 | 12.0 | 59.1 | 12.0 | 59.1 | 100.0 | 625.0 | 0.2406 |
| JMH02a | B | 14 | F | 15.2 | 93.2 | 151.5 | 15.8 | 13.8 | 60.2 | 13.8 | 60.2 | 0.0 | 670.0 | 0.1893 |
| JMH03a | B | 6 | F | 6.6 | 98.7 | 154.6 | 36.8 | 23.4 | 64.9 | 23.4 | 64.9 | 100.0 | 525.0 | 0.0670 |
| JMI05a | B | 9 | F | 33.9 | 69.0 | 183.0 | -4.3 | 16.8 | 68.5 | 16.8 | 68.5 | 300.0 | 660.0 | 0.0598 |
| JMJ01a | B | 12 | F | 6.9 | 98.6 | 192.4 | 4.9 | 1.6 | 71.4 | 1.6 | 71.4 | 300.0 | 675.0 | 0.2717 |
| JMJ03a | B | 4 | F | 13.6 | 94.5 | 230.8 | 9.2 | 46.2 | 39.9 | 46.2 | 39.9 | 300.0 | 525.0 | 0.0935 |
| JMJ05 | B | 3 | F | 8.4 | 97.9 | 239.5 | -9.1 | 32.1 | 27.0 | 32.1 | 27.0 | 0.0 | 200.0 | 0.0285 |
| JML04a | B | 7 | F | 10.1 | 97.0 | 163.2 | 11.7 | 341.9 | 63.0 | 341.9 | 63.0 | 100.0 | 550.0 | 0.1504 |
| JML05a | B | 13 | A | 7.2 | 98.4 | 172.9 | 10.6 | 1.6 | 66.6 | 1.6 | 66.6 | 200.0 | 675.0 | 0.2597 |
| JML06a | B | 14 | F | 16.9 | 91.5 | 171.2 | 15.0 | 348.0 | 73.0 | 348.0 | 73.0 | 0.0 | 670.0 | 0.1780 |
| JML07a | B | 8 | F | 7.6 | 98.2 | 163.3 | -16.0 | 355.8 | 41.3 | 355.8 | 41.3 | 550.0 | 675.0 | 0.0874 |
| JML09a | B | 12 | F | 11.3 | 96.2 | 180.9 | 2.1 | 18.8 | 51.1 | 18.8 | 51.1 | 300.0 | 675.0 | 0.1658 |
| JML10a | B | 12 | F | 10.5 | 96.7 | 178.7 | 12.6 | 12.6 | 62.5 | 12.6 | 62.5 | 200.0 | 670.0 | 0.1946 |
| JML12a | B | 11 | F | 12.9 | 95.0 | 169.3 | 17.8 | 349.6 | 65.9 | 349.6 | 65.9 | 400.0 | 675.0 | 0.1908 |
| JML14a | B | 9 | F | 9.8 | 97.1 | 165.7 | 15.4 | 10.9 | 71.8 | 10.9 | 71.8 | 100.0 | 600.0 | 0.0977 |
| JML16a | B | 15 | F | 16.6 | 91.8 | 157.4 | 1.2 | 17.0 | 59.1 | 17.0 | 59.1 | 0.0 | 675.0 | 0.1451 |
| JML17a | B | 9 | F | 19.0 | 89.4 | 149.1 | 17.1 | 341.9 | 60.4 | 341.9 | 60.4 | 0.0 | 600.0 | 0.0729 |
| JML18a | B | 13 | F | 24.5 | 82.8 | 146.3 | -5.0 | 9.8 | 47.9 | 9.8 | 47.9 | 0.0 | 660.0 | 0.0969 |
| | | | | | | | | | | | | | | |
| Upper Morrison Fm. (sites JBA–JBR): | | | | | | | | | | | | | | |
| JBA01 | B | 10 | F | 13.8 | 94.3 | 169.0 | 21.1 | 332.7 | 77.9 | 332.7 | 77.9 | 0.0 | 600.0 | 0.0520 |
| JBA02 | B | 10 | F | 10.4 | 96.7 | 156.7 | -1.3 | 343.1 | 57.4 | 343.1 | 57.4 | 0.0 | 600.0 | 0.0945 |
| JBA03a | B | 13 | F | 12.7 | 95.2 | 177.1 | -7.3 | 25.1 | 62.5 | 25.1 | 62.5 | 100.0 | 670.0 | 0.0951 |
| JBB01 | B | 12 | F | 19.4 | 89.0 | 153.2 | 1.6 | 326.7 | 58.5 | 326.7 | 58.5 | 0.0 | 650.0 | 0.0441 |
| JBB03a | B | 11 | F | 8.8 | 97.7 | 165.8 | 10.5 | 349.8 | 67.2 | 349.8 | 67.2 | 0.0 | 625.0 | 0.0196 |
| JBC01a | B | 11 | F | 2.4 | 99.8 | 166.5 | -1.5 | 345.4 | 67.2 | 345.4 | 67.2 | 0.0 | 625.0 | 0.1451 |
| JBC03 | B | 9 | F | 4.3 | 99.4 | 179.6 | -4.9 | 20.3 | 71.1 | 20.3 | 71.1 | 100.0 | 600.0 | 0.0726 |
| JBD01 | B | 12 | F | 5.2 | 99.2 | 169.3 | -8.0 | 10.1 | 64.7 | 10.1 | 64.7 | 100.0 | 670.0 | 0.2105 |
| JBD03a | B | 12 | F | 4.3 | 99.4 | 168.7 | 14.1 | 358.7 | 64.9 | 358.7 | 64.9 | 0.0 | 650.0 | 0.2457 |
| JBE01a | B | 9 | F | 3.1 | 99.7 | 173.4 | 21.2 | 20.2 | 67.5 | 20.2 | 67.5 | 0.0 | 575.0 | 0.1724 |
| JBF01a | B | 4 | F | 2.0 | 99.9 | 162.2 | 15.3 | 344.8 | 70.3 | 344.8 | 70.3 | 0.0 | 300.0 | 0.1011 |
| JBF03a | B | 5 | F | 1.2 | 100.0 | 181.7 | 10.2 | 53.2 | 70.2 | 53.2 | 70.2 | 0.0 | 400.0 | 0.1218 |
| JBG01a | B | 15 | F | 2.6 | 99.8 | 162.9 | -0.5 | 3.7 | 62.0 | 3.7 | 62.0 | 0.0 | 675.0 | 0.4404 |
| JBG03a | B | 12 | F | 2.9 | 99.7 | 158.1 | -3.4 | 0.1 | 59.7 | 0.1 | 59.7 | 0.0 | 650.0 | 0.3214 |
| JBH01a | B | 14 | F | 3.7 | 99.6 | 169.2 | -1.8 | 19.0 | 67.5 | 19.0 | 67.5 | 100.0 | 675.0 | 0.2188 |
| JBH03a | B | 12 | F | 2.2 | 99.9 | 161.5 | 7.4 | 357.6 | 66.4 | 357.6 | 66.4 | 0.0 | 650.0 | 0.3582 |
| JBI01 | B | 9 | F | 2.3 | 99.8 | 176.7 | -10.3 | 21.4 | 57.5 | 21.4 | 57.5 | 100.0 | 600.0 | 0.2198 |
| JBI03 | B | 6 | F | 5.7 | 99.0 | 164.9 | -1.2 | 352.1 | 60.8 | 352.1 | 60.8 | 0.0 | 500.0 | 0.1009 |
| JBJ01a | B | 13 | F | 8.6 | 97.8 | 146.9 | 14.9 | 335.7 | 48.4 | 335.7 | 48.4 | 200.0 | 675.0 | 0.1462 |
| JBJ03a | B | 14 | F | 8.0 | 98.1 | 159.9 | 13.7 | 347.8 | 59.1 | 347.8 | 59.1 | 100.0 | 675.0 | 0.1832 |
| JBJ05a | B | 12 | F | 5.2 | 99.2 | 162.2 | 12.1 | 351.1 | 60.4 | 351.1 | 60.4 | 0.0 | 660.0 | 0.1835 |
| JBK01 | B | 15 | F | 20.4 | 87.8 | 164.2 | 17.7 | 314.7 | 73.6 | 314.7 | 73.6 | 0.0 | 675.0 | 0.0061 |
| JBK03a | B | 10 | F | 5.9 | 98.9 | 158.8 | 2.7 | 354.1 | 56.2 | 354.1 | 56.2 | 100.0 | 625.0 | 0.0979 |
| JBL01ai | B | 3 | F | 6.6 | 98.7 | 170.9 | -13.1 | 9.1 | 66.2 | 9.1 | 66.2 | 100.0 | 300.0 | 0.0241 |
| JBN03 | B | 4 | F | 6.3 | 98.8 | 162.9 | 14.0 | 355.9 | 55.8 | 355.9 | 55.8 | 100.0 | 400.0 | 0.3393 |
| JBO01 | B | 4 | F | 1.7 | 99.9 | 172.1 | -1.8 | 9.2 | 68.7 | 9.2 | 68.7 | 0.0 | 300.0 | 0.9351 |
| JBO03a | B | 5 | F | 4.0 | 99.5 | 173.8 | 3.0 | 9.0 | 72.8 | 9.0 | 72.8 | 0.0 | 400.0 | 0.4458 |

!_____END OF FILE_____

Table S4. ‘Ch’ component PCA directions from samples from the Lower and Upper Morrison Fm.

LAT: 38.13  LON:  251.79
!  Principal component analysis on Morrison TH data
!
Lamont datafile format
ID = sample identification (J=Jurassic, M=Morrison, A to L are sampling sites followed by
      drillcore sample number and specimen with 'a' at the bottom if more than one.
comp = magnetization component estimated by PCA analysis.
N = number of demagnetization steps analyzed.
F/A = demagnetization trajectory free (F) or anchored (A) to the origin.
MAD = maximum angular deviation (°).
%VAR = percentage variance accounted for by best-fit line.
CDECL, CINCL = declination and inclination in core coordinates.
GDECL, GINCL = declination and inclination in geographic (in-situ) coordinates.
BDECL, BINCL = declination and inclination in tilt-corrected coordinates.
TR1, TR2 = thermal demagnetization step interval analyzed.
Jcomp = component magnetization (10E-4 emu, equivalent to 10E-2 A/m for 10 cc volume).

| ID | comp | N | F/A | MAD | %VAR | CDECL | CINCL | GDECL | GINCL | BDECL | BINCL | TR1 | TR2 | Jcomp |
|---|---|---|---|---|---|---|---|---|---|---|---|---|---|---|
| Lower Morrison Fm. (sites JMA-JML): | | | | | | | | | | | | | | |
| JMA05a | C | 7 | A | 17.7 | 90.7 | 294.0 | -27.0 | 71.5 | -27.1 | 71.5 | -27.1 | 550.0 | 680.0 | 0.0601 |
| JMA09a | C | 6 | A | 6.0 | 98.9 | 339.6 | -26.1 | 82.9 | -67.4 | 82.9 | -67.4 | 500.0 | 660.0 | 0.1580 |
| JMA10a | C | 5 | A | 6.3 | 98.8 | 305.0 | -14.2 | 100.8 | -37.1 | 100.8 | -37.1 | 500.0 | 650.0 | 0.1433 |
| JMA19a | C | 6 | A | 6.6 | 98.7 | 333.5 | -33.9 | 72.3 | -59.5 | 72.3 | -59.5 | 500.0 | 660.0 | 0.0887 |
| JMA31a | C | 5 | A | 17.3 | 91.1 | 302.6 | -6.4 | 108.6 | -32.5 | 108.6 | -32.5 | 600.0 | 670.0 | 0.0504 |
| JMA33a | C | 6 | F | 21.0 | 87.2 | 306.8 | 10.3 | 116.5 | -29.5 | 116.5 | -29.5 | 300.0 | 625.0 | 0.0491 |
| JMA37a | C | 8 | A | 6.9 | 98.6 | 282.9 | -12.8 | 103.5 | -16.3 | 103.5 | -16.3 | 400.0 | 670.0 | 0.1556 |
| JMA38a | C | 7 | A | 12.2 | 95.5 | 273.5 | -23.6 | 86.6 | -10.1 | 86.6 | -10.1 | 200.0 | 650.0 | 0.0694 |
| JMA39a | C | 7 | F | 23.4 | 84.2 | 321.5 | 36.5 | 165.4 | -19.4 | 165.4 | -19.4 | 550.0 | 680.0 | 0.1105 |
| JMA40a | C | 6 | A | 8.2 | 98.0 | 295.2 | 0.3 | 112.2 | -22.7 | 112.2 | -22.7 | 400.0 | 650.0 | 0.2417 |
| JMA46a | C | 3 | A | 3.9 | 99.5 | 302.6 | 2.2 | 108.3 | -28.6 | 108.3 | -28.6 | 600.0 | 650.0 | 0.1356 |
| JMA49a | C | 5 | A | 7.9 | 98.1 | 297.2 | -14.6 | 97.3 | -30.2 | 97.3 | -30.2 | 550.0 | 660.0 | 0.0903 |
| JMB01a | C | 7 | A | 3.5 | 99.6 | 286.3 | -44.7 | 98.7 | -31.6 | 98.7 | -31.6 | 550.0 | 680.0 | 0.1669 |
| JMB02a | C | 3 | A | 1.2 | 100.0 | 309.1 | -4.8 | 121.9 | -38.2 | 121.9 | -38.2 | 600.0 | 650.0 | 0.1345 |
| JMB04a | C | 3 | A | 3.2 | 99.7 | 319.2 | -8.7 | 118.0 | -49.0 | 118.0 | -49.0 | 600.0 | 650.0 | 0.1642 |
| JMB06a | C | 3 | A | 1.4 | 99.9 | 304.8 | 10.1 | 126.9 | -28.6 | 126.9 | -28.6 | 600.0 | 650.0 | 0.2287 |
| JMB10a | C | 4 | A | 1.8 | 99.9 | 317.4 | 28.3 | 129.9 | -22.0 | 129.9 | -22.0 | 550.0 | 650.0 | 0.1799 |
| JMB11a | C | 6 | A | 7.4 | 98.4 | 286.0 | 36.9 | 121.0 | 4.4 | 121.0 | 4.4 | 600.0 | 680.0 | 0.1444 |
| JMB13a | C | 4 | A | 4.2 | 99.5 | 301.6 | 38.1 | 121.8 | -13.8 | 121.8 | -13.8 | 650.0 | 680.0 | 0.1654 |
| JMB42a | C | 3 | A | 1.5 | 99.9 | 324.5 | -6.1 | 121.7 | -54.4 | 121.7 | -54.4 | 600.0 | 650.0 | 0.1661 |
| JMB43a | C | 4 | A | 6.9 | 98.6 | 312.9 | -0.7 | 141.6 | -39.1 | 141.6 | -39.1 | 600.0 | 670.0 | 0.0936 |
| JMB44a | C | 4 | F | 9.3 | 97.4 | 308.4 | -37.8 | 85.0 | -40.8 | 85.0 | -40.8 | 550.0 | 650.0 | 0.0366 |
| JMB45a | C | 7 | A | 3.2 | 99.7 | 317.1 | -34.5 | 96.8 | -53.8 | 96.8 | -53.8 | 550.0 | 680.0 | 0.2707 |
| JMB46a | C | 3 | A | 3.5 | 99.6 | 336.4 | -22.6 | 110.2 | -67.1 | 110.2 | -67.1 | 600.0 | 650.0 | 0.1321 |
| JMB47a | C | 6 | A | 2.5 | 99.8 | 329.0 | -15.7 | 99.0 | -60.0 | 99.0 | -60.0 | 600.0 | 680.0 | 0.3514 |
| JMB49a | C | 2 | A | 2.9 | 99.8 | 301.1 | 11.0 | 134.6 | -19.2 | 134.6 | -19.2 | 670.0 | 680.0 | 0.1098 |
| JMB50a | C | 4 | A | 4.6 | 99.4 | 330.6 | 9.1 | 147.0 | -41.0 | 147.0 | -41.0 | 550.0 | 650.0 | 0.1279 |
| JMC01a | C | 2 | A | 5.6 | 99.1 | 289.6 | -38.9 | 126.0 | -32.7 | 126.0 | -32.7 | 670.0 | 675.0 | 0.0434 |
| JMD03a | C | 7 | A | 5.4 | 99.1 | 288.2 | -10.6 | 102.7 | -20.9 | 102.7 | -20.9 | 575.0 | 675.0 | 0.2144 |
| JMD04a | C | 4 | A | 8.6 | 97.8 | 311.5 | -25.0 | 97.6 | -46.3 | 97.6 | -46.3 | 650.0 | 675.0 | 0.0984 |
| JMD05a | C | 7 | A | 3.6 | 99.6 | 323.8 | -3.9 | 132.7 | -48.0 | 132.7 | -48.0 | 575.0 | 675.0 | 0.1296 |
| JMD06a | C | 5 | A | 8.5 | 97.8 | 310.1 | 4.7 | 129.0 | -27.6 | 129.0 | -27.6 | 625.0 | 675.0 | 0.1443 |
| JME02a | C | 10 | A | 7.6 | 98.2 | 323.6 | 34.1 | 166.7 | -24.9 | 166.7 | -24.9 | 500.0 | 675.0 | 0.1364 |
| JME03a | C | 5 | A | 6.7 | 98.6 | 320.5 | -2.2 | 128.9 | -48.4 | 128.9 | -48.4 | 500.0 | 670.0 | 0.1062 |
| JMH01a | C | 10 | A | 2.2 | 99.9 | 95.5 | 50.3 | 304.8 | 30.1 | 304.8 | 30.1 | 500.0 | 675.0 | 0.4271 |
| JMI01a | C | 10 | A | 9.2 | 97.4 | 142.5 | 1.3 | 303.7 | 46.7 | 303.7 | 46.7 | 300.0 | 675.0 | 0.0700 |
| JMI02a | C | 8 | A | 5.2 | 99.2 | 115.1 | -23.5 | 308.8 | 10.1 | 308.8 | 10.1 | 550.0 | 675.0 | 0.0854 |

```
JMJ02a     C    3 A  2.7  99.8  177.4 -40.1  316.1  31.8  316.1  31.8 625.0 660.0  0.1130
JML11a     C    6 A  5.5  99.1  132.7 -15.4  327.9  21.3  327.9  21.3 575.0 670.0  0.1282
JML15a     C    4 F  4.8  99.3  117.7  12.0  332.8  30.0  332.8  30.0 575.0 650.0  0.0771

Upper Morrison Fm. (sites JBA-JBR):
JBF01a     C    4 A  2.4  99.8  294.9  -6.2  140.9 -25.1  140.9 -25.1 650.0 675.0  0.1067
JBF03a     C    4 A  3.0  99.7  330.4 -15.2  160.3 -59.1  160.3 -59.1 650.0 675.0  0.0611
JBI01      C    4 A  4.6  99.4  302.5   1.6  132.4 -29.2  132.4 -29.2 650.0 675.0  0.0710
JBI03      C    6 A  3.5  99.6  290.6   9.7  132.1 -14.4  132.1 -14.4 600.0 675.0  0.0849
JBL01ai    C   10 A  3.4  99.7  338.4 -14.4  104.9 -68.2  104.9 -68.2 500.0 675.0  0.0702
JBL01aii   C   11 A  2.5  99.8  328.3  -9.8  117.2 -58.7  117.2 -58.7 400.0 675.0  0.1245
!_____________________________________END OF FILE_____________________________________
```

## Supporting Information 3

**Text S2. Litho-magneto-biostratigraphic data from parauthocthonous Adria.**

Litho-magneto-biostratigraphic data from sections in Adria discussed in the main text with Elongation/Inclination (E/I) test (*Tauxe and Kent*, 2004) and bootstrap reversal test (*Tauxe*, 2010) on the characteristic remanent magnetization component (ChRM) directions are described below in a series of figures and tables: **Fig. S3** is for Bombatierle pole 158Bomb, **Fig. S4** is for Foza pole 158Foz, **Fig. S5** is for Colme di Vignola pole 154Vig, **Fig. S6** is for Sciapala pole 150Sci, **Fig. S7** is for Passo del Branchetto pole 150Branch (**Table 1** of main text). Note that E/I tests of poles 238Dol, 147VFF, 143BVFF, 128Mai, and 50Sca (**Table 1** of main text) have been performed in Muttoni et al. (2013) and are not reported here.

In all figures, panel A shows the litho-magneto-biostratigraphic data from *Channell et al.* (2010) (**Fig. S7** does not include panel A because the Passo del Branchetto section is only 5.5 m-thick and all ChRM directions have been considered for analyses). The gray shaded box in panel A indicates the portion of the section that was considered for E/I test and bootstrap reversal test and pole definition for this study.

Panel B shows a stereoplot of the ChRM directions from the considered stratigraphic interval (gray shaded box in panel A). ChRM directions are listed in **Table S5** (Bombatierle pole 158Bomb), **Table S6** (Foza pole 158Foz), **Table S7** (Colme di Vignola pole 154Vig), **Table S8** (Sciapala pole 150Sci), and **Table S9** (Passo del Branchetto pole 150Branch). Panel C shows the results of the E/I test and derived flattening factor (f). Panel D reports the cumulative distribution of the ChRM inclinations with indication of the mean, minimum, and maximum E/I-corrected inclination values. Panel D is the results of the bootstrap reversal test on the x, y, and z ChRM axes.

E/I test and reversal test made with PmagPy (*Tauxe et al.*, 2016).

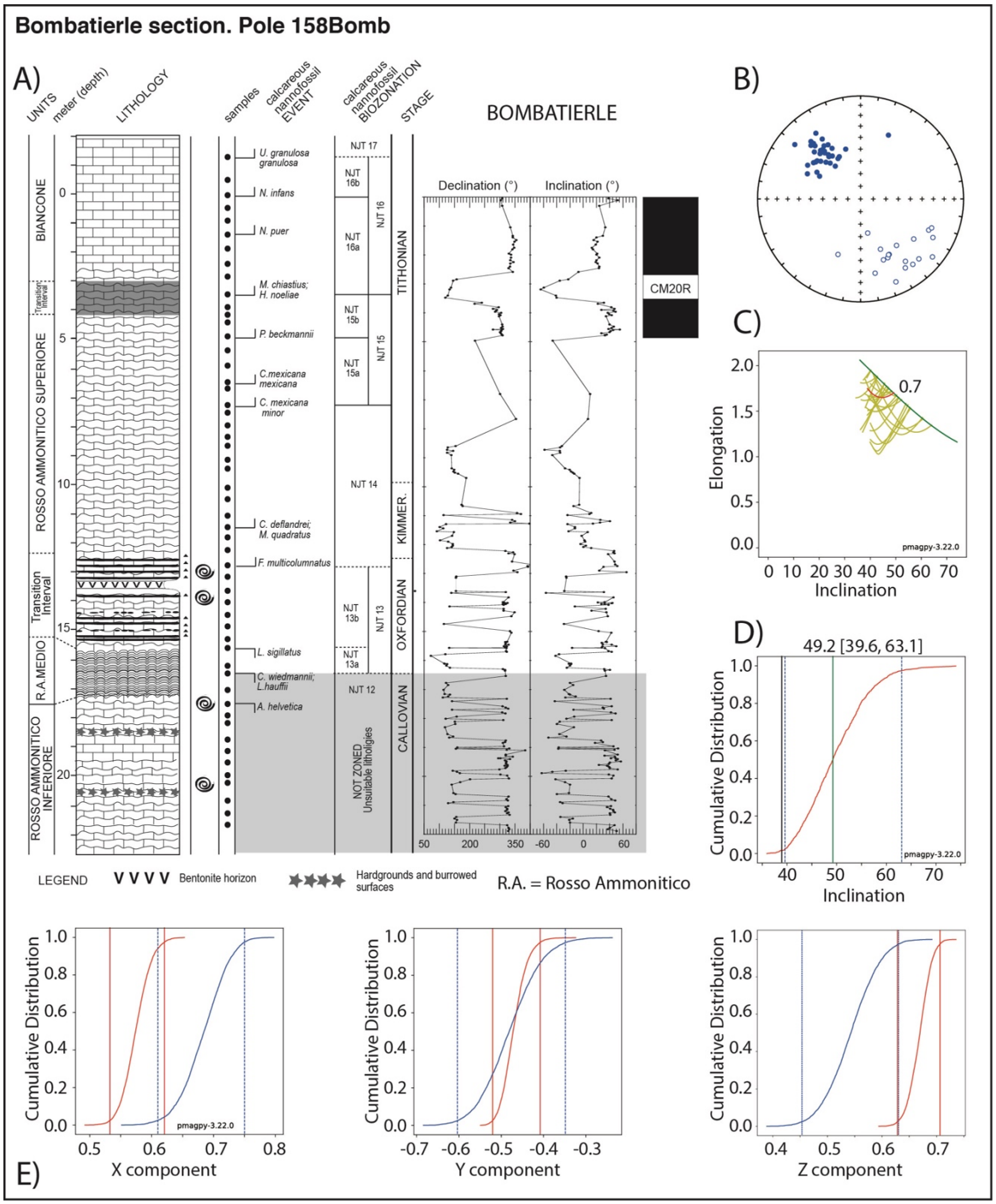


**Figure S3.** Litho-magneto-biostratigraphic data from the Bombatierle section. Pole 158Bomb is derived from data from gray-shaded interval.

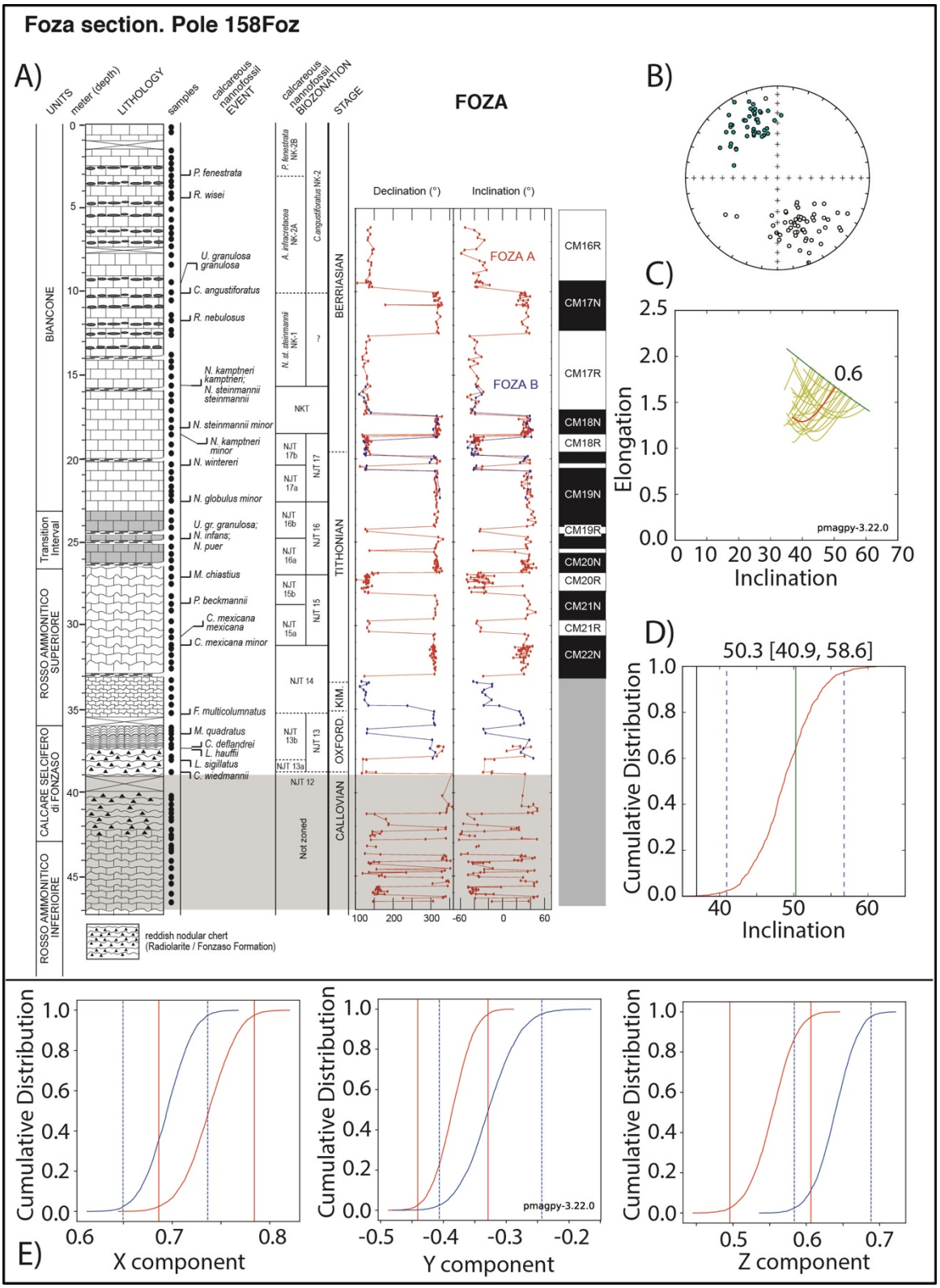


**Figure S4.** Litho-magneto-biostratigraphic data from the Foza section. Pole 158Foz is derived from data from gray-shaded interval.

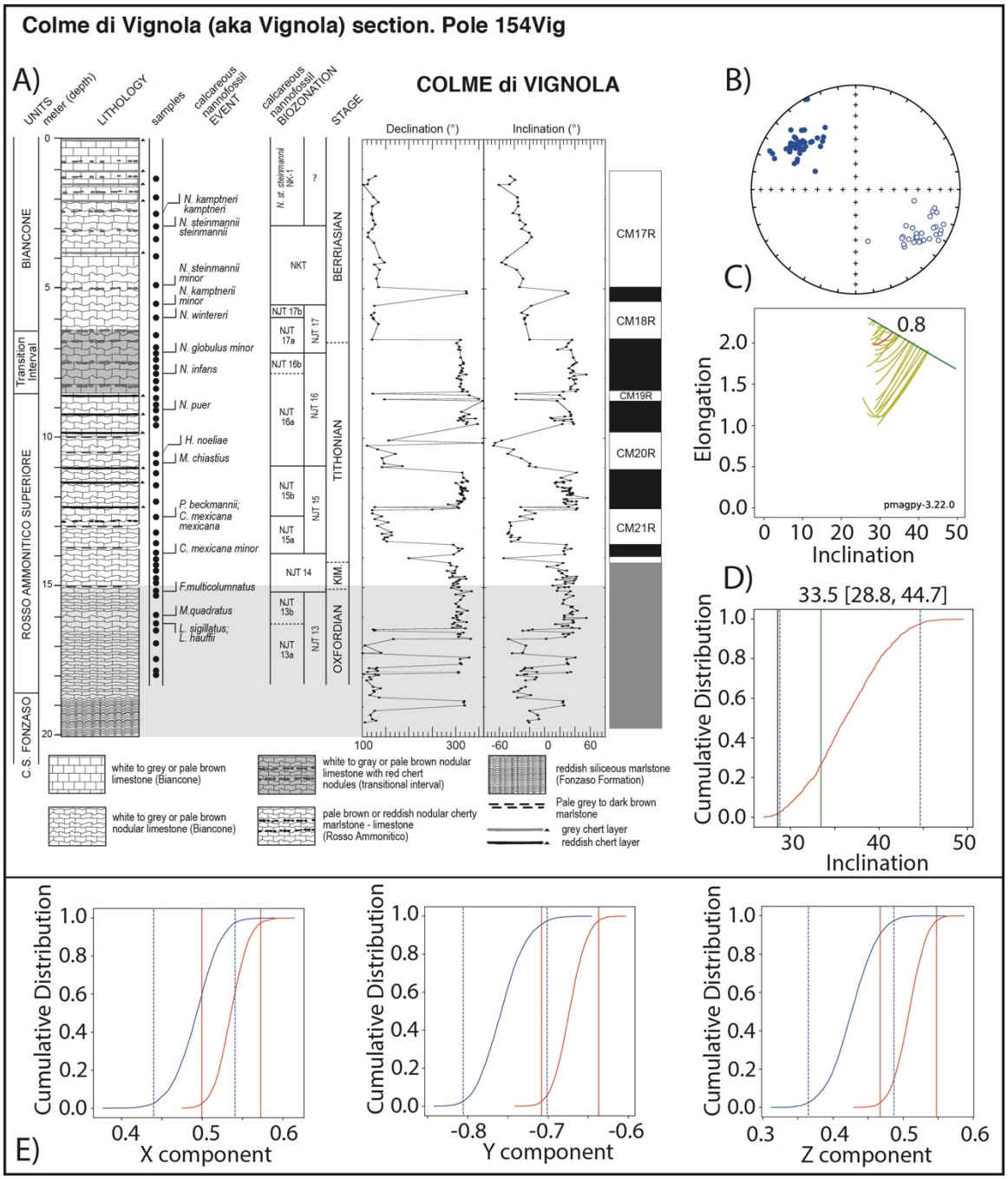


**Figure S5.** Litho-magneto-biostratigraphic data from the Colme di Vignola section. Pole 154Vig is derived from data from gray-shaded interval.

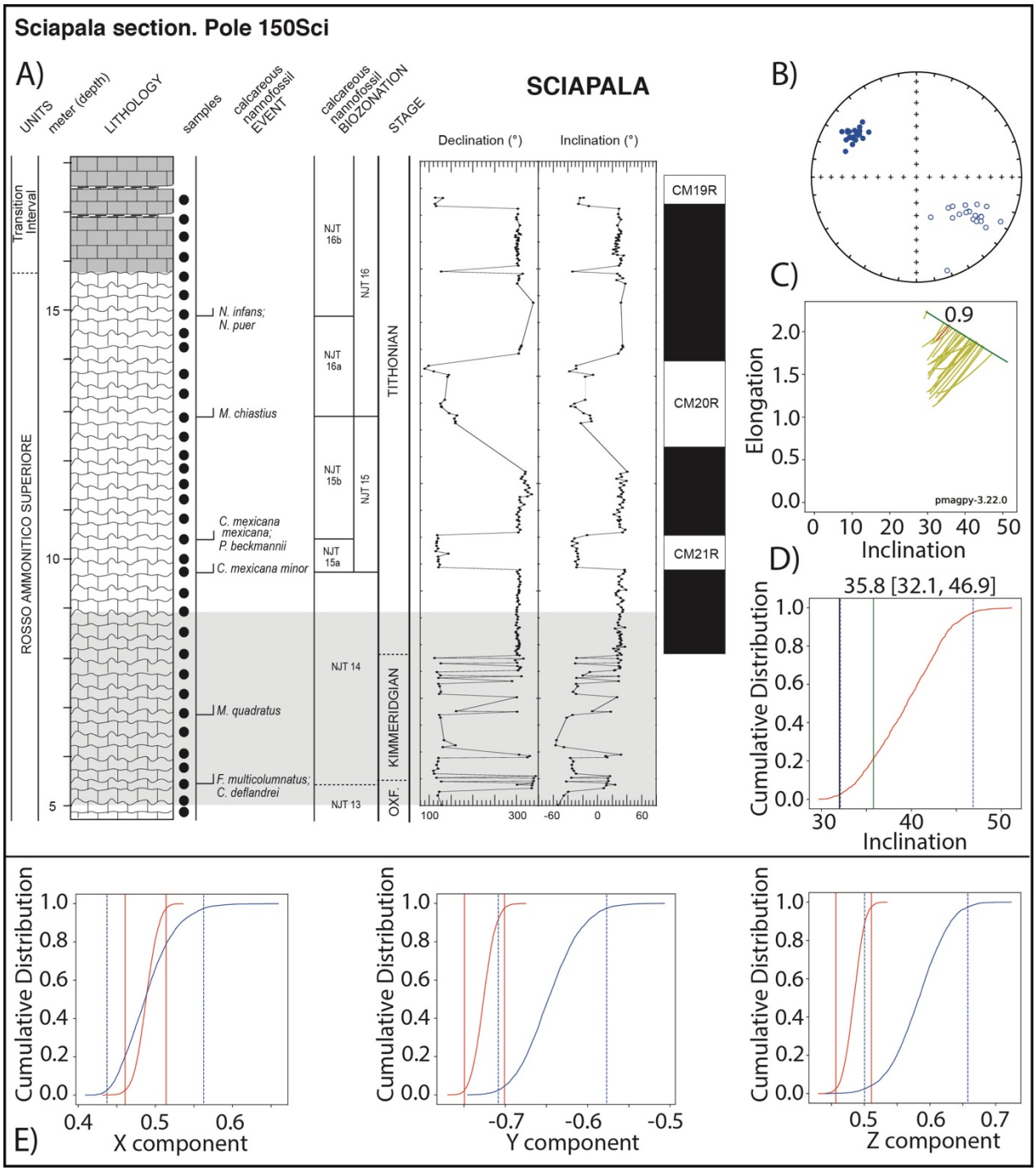


**Figure S6.** Litho-magneto-biostratigraphic data from the Sciapala section. Pole 150Sci is derived from data from gray-shaded interval.

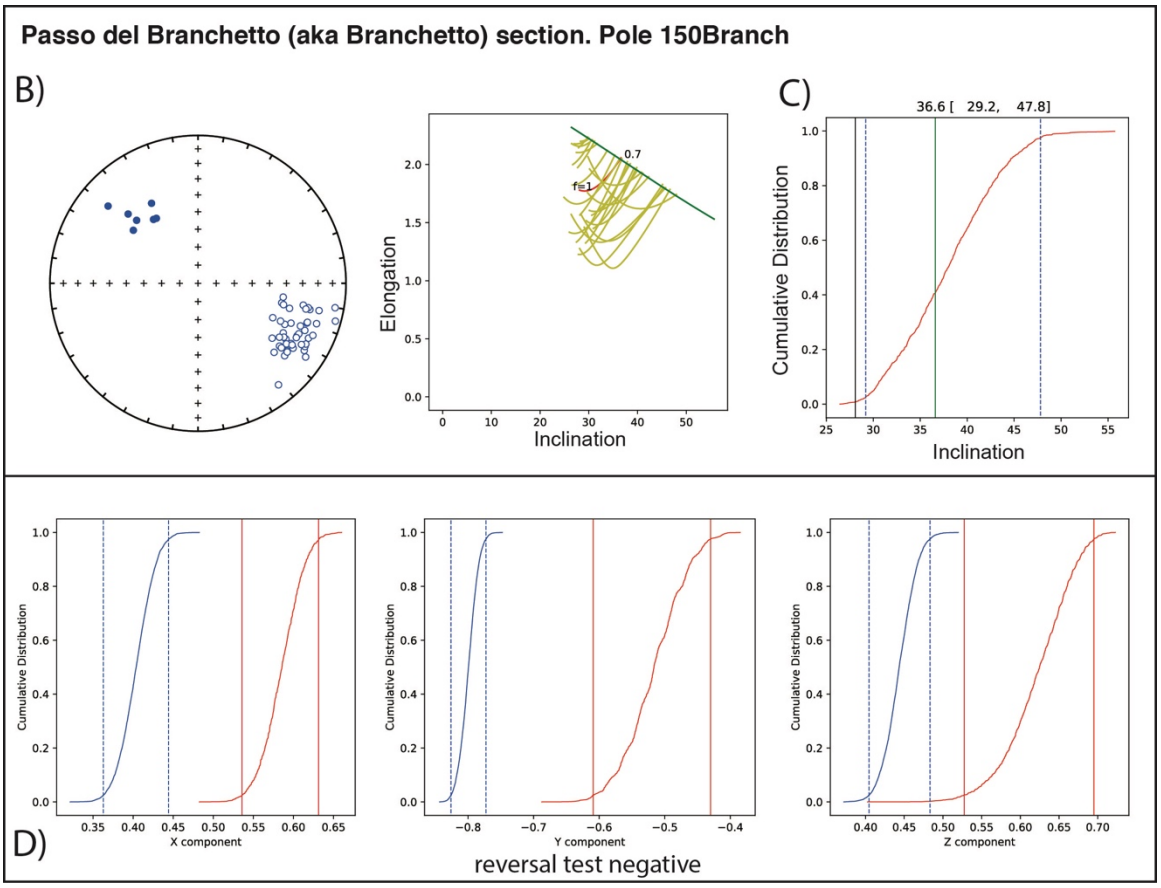


**Figure S7.** Magnetostratigraphic data from the Passo del Branchetto section used to define pole 150Branch. Panel A) with litho-biostratigraphy is not reported because the section is only 5.5 m-thick and all ChRM directions have been considered for analyses. Note that ChRM data fail the bootstrap reversal test but yield an *I*-corrected pole consistent with broadly coeval poles from Adria (see text for discussion).

Table S5
Ch component directions from the pre-CM30 (pre-C. wiedmanni LO) interval of the Bombatierle section (45.85°N, 11.51°E)

Dec = Declination of Ch component
Inc = inclination of Ch component

Data generated at U Florida paleomagnetics laboratory [Channell et al., 2010]

| Dec | Inc |
|---|---|
| 114.60 | -28.100 |
| 118.10 | -21.500 |
| 135.80 | -19.900 |
| 128.90 | -11.300 |
| 112.20 | -26.400 |
| 322.90 | 41.500 |
| 142.30 | -42.400 |
| 309.50 | 43.000 |
| 319.70 | 30.100 |
| 327.40 | 31.600 |
| 307.60 | 41.900 |
| 156.90 | -13.500 |
| 311.30 | 43.300 |
| 152.70 | -39.200 |
| 127.00 | -35.600 |
| 319.20 | 27.200 |
| 317.20 | 29.900 |
| 309.60 | 18.300 |
| 313.40 | 45.800 |
| 159.40 | -36.900 |
| 330.80 | 53.000 |
| 155.10 | -37.200 |
| 323.20 | 47.500 |
| 23.600 | 32.900 |
| 319.70 | 52.400 |
| 319.40 | 32.600 |
| 343.40 | 48.200 |
| 295.30 | 42.400 |
| 301.50 | 48.900 |
| 333.30 | 52.100 |
| 316.70 | 49.500 |
| 322.40 | 57.000 |
| 321.20 | 40.700 |
| 320.50 | 38.900 |
| 325.80 | 23.900 |
| 315.50 | 36.200 |
| 325.50 | 37.500 |
| 322.60 | 39.400 |
| 318.20 | 40.700 |
| 299.00 | 52.500 |
| 144.30 | -26.300 |
| 158.40 | -46.400 |

168.20  -62.300
302.50  39.000
324.00  45.800
330.60  43.000
202.10  -41.400
168.90  -27.400
141.40  -19.800
147.00  -21.300
153.40  -39.200
329.00  38.600
322.10  42.800
326.70  48.700

Non E/I corrected mean Dec 322.3, Inc 38.9, k=21, a95=4.3, n=54
E/I estimated flattening factor f=0.7
E/I corrected mean Inc= 49.2 (39.6, 63.1)

Table S6
Ch component directions from the pre-CM30 (pre-C. wiedmanni LO) interval of the of the Foza section (45.89°N, 11.60°E)

Dec = Declination of Ch component
Inc = inclination of Ch component

Data generated at U Florida paleomagnetics laboratory [Channell et al., 2010]

| Dec | Inc |
|---|---|
| 303.70 | 38.400 |
| 322.30 | 14.700 |
| 319.50 | 25.300 |
| 317.50 | 25.500 |
| 334.00 | 40.600 |
| 297.70 | 30.200 |
| 330.40 | 5.9000 |
| 311.80 | 26.200 |
| 316.10 | 31.500 |
| 305.20 | 44.200 |
| 120.10 | -25.300 |
| 129.60 | -11.400 |
| 128.70 | -14.700 |
| 154.70 | -27.800 |
| 117.00 | -15.600 |
| 363.40 | 32.300 |
| 330.30 | 28.700 |
| 348.00 | 44.200 |
| 345.70 | 27.400 |
| 357.10 | 37.400 |
| 342.50 | 49.700 |
| 342.30 | 49.700 |
| 340.80 | 36.400 |
| 324.00 | 43.100 |
| 129.50 | -29.500 |
| 151.10 | -50.200 |
| 181.00 | -40.100 |
| 188.50 | -56.000 |
| 187.00 | -35.600 |
| 340.00 | 23.300 |
| 338.80 | 20.300 |
| 339.60 | 12.400 |
| 318.70 | 23.900 |
| 170.30 | -25.900 |
| 145.30 | -57.800 |
| 166.10 | -58.200 |
| 144.80 | -60.500 |
| 151.80 | -47.100 |
| 139.40 | -39.200 |
| 340.10 | 27.500 |
| 286.00 | 49.300 |
| 141.30 | -62.100 |

130.70  -33.700
154.50  -37.300
125.00  -49.400
166.20  -59.200
335.50  27.300
340.10  32.900
340.70  25.900
331.00  46.100
332.60  42.700
329.90  28.300
341.80  16.800
342.00  22.200
352.00  27.200
149.00  -48.700
162.80  -18.500
134.90  -43.200
142.10  -27.200
138.60  -41.900
351.60  -13.800
156.00  -26.100
337.60  45.700
329.30  35.900
136.10  -26.000
234.70  -31.400
119.00  -41.600
170.40  -49.300
162.50  -34.700
178.40  -33.100
331.00  29.400
345.20  26.000
341.10  33.100
347.80  49.200
304.60  44.700
344.70  45.300
163.10  -48.500
159.80  -2.1000
156.30  -49.200
156.80  -42.600
160.00  -37.400
165.10  -43.200
153.30  -34.300
153.40  -37.200
162.00  -37.800
168.30  -41.400
185.20  -46.800
159.70  -46.100
147.10  -46.200
145.90  -42.200
159.80  -44.400
157.10  -12.400
177.40  -37.900

151.40  -23.800
339.50  50.300
333.90  44.100
331.80  45.000
226.60  -39.000
306.40  37.300
146.70  -15.100

Non E/I corrected mean Dec 333.6, Inc 36.8, n=100, k=16, a95=3.7
E/I estimated flattening factor f=0.6
E/I corrected mean Inc= 50.3 (40.9, 56.8)

Table S7
Ch component directions from the CM25-CM30 (pre-F. multicolumnatus FO) interval of the Colme di Vignola (aka Vignola) section (45.77°N 10.95°E)

Dec = Declination of Ch component
Inc = inclination of Ch component

Data generated at U Florida paleomagnetics laboratory [Channell et al., 2010]

| Dec | Inc |
|---|---|
| 301.40 | 27.200 |
| 295.40 | 37.900 |
| 304.90 | 27.000 |
| 294.20 | 10.800 |
| 307.70 | 32.200 |
| 305.00 | 26.900 |
| 290.90 | 17.900 |
| 312.60 | 16.800 |
| 333.80 | 34.100 |
| 299.80 | 28.100 |
| 317.70 | 37.900 |
| 310.50 | 25.600 |
| 300.30 | 23.900 |
| 307.60 | 36.600 |
| 305.80 | 34.600 |
| 325.60 | 43.200 |
| 303.00 | 36.300 |
| 312.80 | 33.800 |
| 310.70 | 36.900 |
| 301.10 | 26.200 |
| 302.70 | 25.900 |
| 294.30 | 55.000 |
| 304.10 | 25.700 |
| 307.50 | 37.200 |
| 323.40 | 38.400 |
| 297.50 | 37.200 |
| 293.40 | 14.200 |
| 304.40 | 30.800 |
| 310.60 | 23.700 |
| 293.00 | 36.400 |
| 320.80 | 45.700 |
| 123.70 | -16.100 |
| 128.00 | -21.200 |
| 125.90 | -28.900 |
| 316.40 | 37.500 |
| 305.60 | 24.500 |
| 309.80 | 32.000 |
| 306.30 | 27.100 |
| 331.90 | 2.1000 |
| 166.60 | -47.800 |
| 105.70 | -24.400 |
| 139.60 | -28.700 |

100.90  -42.400
328.50  40.700
309.70  29.500
309.70  30.100
312.60  31.500
132.20  -25.600
115.00  -16.700
128.60  -27.300
133.10  -31.000
111.60  -10.300
306.10  34.700
306.20  29.900
103.20  -23.400
127.90  -26.500
135.10  -36.300
115.60  -10.400
119.30  -12.600
109.80  -25.100
123.60  -25.100
138.70  -30.800
124.00  -34.600
125.70  -40.300
116.20  -18.000
136.50  -35.800
318.00  24.500
317.60  24.200
319.30  25.700
126.60  -19.800
117.70  -9.3000
121.60  -7.7000
129.60  -22.100
105.80  -20.400

Non E/I corrected mean Dec 306.3, Inc 28.5 n=74 k=33, a95=2.9
E/I estimated flattening factor f=0.8
E/I corrected mean Inc= 33.5 (28.8, 44.7)

Table S8
Ch component directions from the CM22-CM25 (post-F. multicolumnatus FO and pre-C. mexicana minor FO) interval of the Sciapala section (45.85°N 11.58°E)

Dec = Declination of Ch component
Inc = inclination of Ch component

Data generated at U Florida paleomagnetics laboratory [Channell et al., 2010]

| Dec | Inc |
|---|---|
| 138.50 | -47.000 |
| 313.30 | 37.700 |
| 123.10 | -40.100 |
| 114.30 | -36.900 |
| 129.00 | -53.500 |
| 119.90 | -45.400 |
| 123.10 | -39.600 |
| 305.70 | 32.100 |
| 130.90 | -45.10 |
| 160.40 | -56.70 |
| 134.10 | -55.30 |
| 125.50 | -41.60 |
| 123.20 | -33.50 |
| 301.40 | 18.100 |
| 161.80 | -7.100 |
| 300.80 | 26.800 |
| 123.70 | -29.00 |
| 126.60 | -33.20 |
| 124.40 | -26.50 |
| 121.40 | -28.80 |
| 289.90 | 29.000 |
| 121.50 | -28.50 |
| 311.40 | 28.800 |
| 126.00 | -19.50 |
| 117.90 | -10.30 |
| 303.20 | 22.800 |
| 304.10 | 23.900 |
| 307.80 | 30.300 |
| 309.10 | 31.000 |
| 302.20 | 29.500 |
| 126.40 | -29.70 |
| 301.60 | 28.900 |
| 297.00 | 32.200 |
| 315.60 | 27.500 |
| 112.70 | -28.40 |
| 307.00 | 27.200 |
| 301.30 | 32.700 |
| 301.60 | 30.300 |
| 297.90 | 25.300 |
| 301.50 | 28.600 |
| 304.00 | 22.100 |
| 305.90 | 37.200 |

300.60  27.200
305.60  30.700
306.70  32.700

Non E/I corrected mean Dec 305.3, Inc 32.0 n=45 k=41 a95=3.4

E/I estimated flattening factor f=0.9
E/I corrected mean Inc= 35.8 (32.1, 46.9)

Table S9
Ch component directions from the CM22-CM25 (~post-F. multicolumnatus FO and pre-C. mexicana minor FO) interval of the
Passo del Branchetto section (45.6°N/11°E)

Dec = Declination of Ch component
Inc = inclination of Ch component

Data generated at U Florida paleomagnetics laboratory [Channell et al., 2010]

| Dec | Inc |
|---|---|
| 327.4 | 46.7 |
| 309.4 | 42.9 |
| 325.2 | 46.3 |
| 329.9 | 37.5 |
| 124.3 | -23.3 |
| 310.7 | 21.0 |
| 127.1 | -25.4 |
| 129.9 | -24.7 |
| 127.6 | -24.9 |
| 127.5 | -29.2 |
| 120.2 | -33.8 |
| 122.9 | -26.1 |
| 127.6 | -31.1 |
| 122.4 | -30.4 |
| 314.8 | 33.9 |
| 315.8 | 40.3 |
| 126.5 | -37.7 |
| 117.9 | -25.2 |
| 113.2 | -32.2 |
| 115.3 | -35.4 |
| 122.1 | -32.1 |
| 103.1 | -41.5 |
| 105.4 | -4.2 |
| 113.8 | -22.2 |
| 124.4 | -12.9 |
| 141.6 | -13.5 |
| 116.4 | -17.8 |
| 110.0 | -22.7 |
| 124.4 | -28.4 |
| 123.2 | -25.0 |
| 122.3 | -16.2 |
| 99.2 | -41.3 |
| 100.1 | -6.6 |
| 105.3 | -36.1 |
| 114.7 | -43.7 |
| 108.8 | -16.5 |
| 127.7 | -29.5 |
| 120.6 | -17.2 |
| 119.4 | -17.5 |
| 116.6 | -24.8 |
| 132.2 | -31.2 |

102.7 -17.3
103.2 -23.4
102.5 -24.7
101.7 -28.2
103.4 -26.0
109.6 -22.6
114.4 -15.9
120.6 -19.9
104.0 -40.2
118.9 -25.1
123.5 -34.4
114.6 -38.6
112.6 -26.0

Non E/I corrected mean Dec 299.3, Inc 28.1, k=32, a95=3.5, n=54
E/I estimated flattening factor f=0.72
E/I corrected mean Inc= 36.6 (29.0, 48.0)

Corresponding to entry #43 of Table 1 of Muttoni et al. [2013]